



BINDING SERVICES
Tel +44 (0)29 2087 4949
Fax +44 (0)29 20371921
e-mail bindery@cardiff.ac.uk

**BIOMECHANICAL ANALYSIS OF FALLS ONTO THE
OUTSTRETCHED HAND.**

A thesis submitted for the degree of
Doctor of Philosophy.

by

Nicola Jane Gittens MEng (Hons)

September 2005

University of Wales, Cardiff

UMI Number: U584838

All rights reserved

INFORMATION TO ALL USERS

The quality of this reproduction is dependent upon the quality of the copy submitted.

In the unlikely event that the author did not send a complete manuscript and there are missing pages, these will be noted. Also, if material had to be removed, a note will indicate the deletion.



UMI U584838

Published by ProQuest LLC 2013. Copyright in the Dissertation held by the Author.
Microform Edition © ProQuest LLC.

All rights reserved. This work is protected against
unauthorized copying under Title 17, United States Code.



ProQuest LLC
789 East Eisenhower Parkway
P.O. Box 1346
Ann Arbor, MI 48106-1346

ACKNOWLEDGEMENTS

Firstly I would like to thank my supervisor Dr. Mike Jones for all his support and encouragement. I only hope that one day I will have as much knowledge and understanding of biomechanics as you do.

Extended thanks go to Dr. Corrina Cory who has also supported me during the past 3 years, not just in a professional role but a personal one as well. Also to all the lecturers who have given up their time to provide help when I needed it.

To the 'research girls' and Fiona who have always had a smile on their face and words of encouragement whenever I have needed help, or just wanted a chat, especially Chris for all her hard work and laughter.

My life would not be complete without my partner Rach, you have been with me throughout my PhD and been there for whatever life has thrown at me. I love you so much and thank you immensely for giving me the support and encouragement I have needed to help me through the last three years. I also know that you will be glad it is now over!

I would like to thank my brother and friends for believing in me and putting up with my everlasting student days, but most importantly I thank my mum. You have done a fantastic job in raising my brother and I and always supported us in whatever we chose to do, I hope I have made you proud, I love you.

SUMMARY

Research has shown that the installation of Impact Absorbing Playground Surfaces (IAPS) in play areas in Cardiff has reduced the amount of serious head injuries. However, even though head injuries have been greatly reduced in severity, arm fractures have not reduced in severity or frequency. This confirms that the current strategies for the assessment and prevention of head injury potential have been shown to be highly successful, yet totally ineffective for preventing upper limb fractures. A need therefore exists to develop a method for the assessment of playground surfaces for their ability to alleviate arm fractures. The force required to fracture the arm during a fall in a playground is currently unknown. The overall aims of the study were to investigate the forces that are produced in the arm during a fall onto the outstretched hand at a non-injurious level and to then utilize the data to aid in the development of a mechanical arm fracture model that could be used, alongside a British Standard head impact testing device, to additionally test IAPS for their ability to alleviate arm fractures. A study was conducted, using motion analysis equipment, to investigate the forces produced during a fall onto the outstretched hand. Thirty-five volunteers of mixed gender, age and weight were dropped through a height of 3 and 5 cm onto force plates, and from 5 cm onto a domestic surface and a playground surface. A further study was conducted to assess the mechanism of the arm prior to and during impact using high-speed video (HSV) equipment. Electromyography (EMG) equipment was also used to record the activation of certain muscles throughout the falls. These tests were completed with five volunteers at heights of 1 and 5 cm onto force plates, and further tests were conducted on one volunteer at heights of 10 and 20 cm, and two volunteers from standing height. The results showed that falls onto the outstretched hand produce an impact force characterised by an initial force peak, F1, followed by two further force peaks, F2 and F3. The magnitude of force peak F1 was found to be generally higher than the subsequent force peaks F2 and F3. Force peak F3 was not prevalent in all force time curves and it was suggested from the results that when it did occur it was not significantly different to force peak F2. A positive linear relationship was found between force peaks F1 and F2 (as F1 increases, F2 increases). The increase of force peak F2 was not as great as the increase of force peak F1, confirming the suggestion that the magnitude of force peak F1 is generally greater than F2. Gender, fall height and effective mass were found to be important factors when assessing the impact forces found during a fall onto the outstretched hand. The mechanism of the arm prior to and during impact was found to be similar regardless of the fall height and falls were found to not generally occur onto a fully extended elbow. A shock wave was produced in the arm on impact with a surface and the initiation of arm muscles in response to a fall was found to be due to motor vestibular reflexes and not an intentional cerebral decision as to when was best to arrest the fall. Using the information from the experimental fall studies, a computer model was developed to enable falls from a higher height, such as those that occur during a playground fall, to be investigated. The model was developed and a series of simulations were performed at heights of 1 and 2 cm. Despite an overestimation of the magnitude of force peak F1, the computer model was found to correlate well with the results found from the experimental studies. Force peak F1 was influenced by fall height and force peak F2 was influenced by effective mass (in male volunteers). Data from the experimental falls and computer modelling conducted in this study, along with data from a playground injury study can be used to further develop and validate an arm fracture model to investigate playground injuries and also for application to domestic falls and non-accidental injury investigation for a range of ages.

CONTENTS

	PAGE
ACKNOWLEDGEMENTS	
DECLARATION	I
SUMMARY	II
TABLE OF CONTENTS	III
LIST OF FIGURES	VII
LIST OF TABLES	XIII
CHAPTER 1 INTRODUCTION	
1.1 Introduction	1 - 3
1.2 Aims of this study	1 - 4
1.3 Anatomy	1 - 5
1.3.1 Anatomical terminology	1 - 6
1.3.2 Terminology for describing movement	1 - 7
1.3.2.1 Flexion-extension	1 - 7
1.3.2.2 Abduction-adduction	1 - 8
1.3.2.3 Pronation-supination	1 - 9
1.3.3 Structure and function of bones	1 - 10
1.3.3.1 Long bones	1 - 12
1.3.3.2 Short bones	1 - 14
1.3.3.3 Flat bones	1 - 14
1.3.3.4 Sesamoid	1 - 14
1.3.3.5 Irregular bones	1 - 14
1.3.4 Skeletal structure of the upper extremity	1 - 15
1.3.4.1 Shoulder and upper arm	1 - 15
1.3.4.2 Elbow and lower arm	1 - 17
1.3.4.3 Wrist and hand	1 - 19
1.3.5 Muscular structure of the upper extremity	1 - 20
1.3.5.1 Shoulder and upper arm	1 - 20
1.3.5.2 Elbow and lower arm	1 - 23
1.3.5.3 Wrist and hand	1 - 24
1.3.6 Motor vestibular system	1 - 24
1.3.6.1 Visual information	1 - 24
1.3.6.2 Proprioceptive information	1 - 25
1.3.6.3 Vestibular information	1 - 26
1.3.7 Motor vestibular reflexes	1 - 26
1.4 Trauma Mechanics	1 - 27
1.4.1 Soft tissue injuries	1 - 27
1.4.2 Fracture mechanics	1 - 28
1.4.2.1 The causation of the fracture	1 - 29

	1.4.2.2 The relationship of the fracture to the surrounding tissues	1 - 29
	1.4.2.3 The pattern of the fracture	1 - 29
1.5	Literature review	1 - 32
	1.5.1 Fracture forces	1 - 32
	1.5.2 Falls onto the outstretched hand	1 - 34
	1.5.2.1 Falls due to trips and slips	1 - 34
	1.5.2.2 Sideways falls	1 - 37
	1.5.2.3 Forward falls	1 - 39
	1.5.3 Other studies assessing forces in the arm during a fall	1 - 55
	1.5.4 Falls onto different impact surfaces	1 - 60
	1.5.5 Biomechanical models investigating falls from playground equipment	1 - 65
	1.5.6 Electromyography	1 - 71
1.6	Objectives	1 - 76

CHAPTER 2 MATERIALS AND METHODS

2.1	Introduction	2 - 1
2.2	Observational study	2 - 2
	2.2.1 Equipment	2 - 3
	2.2.2 Methodology	2 - 5
2.3	Materials	2 - 7
	2.3.1 Drop rig	2 - 7
	2.3.2 Drop mechanism	2 - 10
	2.3.2 Harness	2 - 10
2.4	Motion analysis study	2 - 11
	2.4.1 Equipment	2 - 12
	2.4.2 Methodology	2 - 12
2.5	Surface study	2 - 14
	2.5.1 Equipment	2 - 14
	2.5.2 Methodology	2 - 15
2.6	HSV study	2 - 15
	2.6.1 Equipment	2 - 16
	2.6.2 Methodology	2 - 23
2.7	Computer modelling	2 - 25
	2.7.1 Model 1	2 - 27
	2.7.2 Model 2	2 - 28
	2.7.3 Model 3	2 - 29
	2.7.4 Model 4	2 - 30
	2.7.5 Model 5	2 - 31

CHAPTER 3 RESULTS

3.1	Introduction	3 - 1
3.2	Observational study	3 - 1
3.3	Motion analysis study	3 - 3
	3.3.1 Analysis of arm angles	3 - 5
	3.3.2 Typical force-time impact curves	3 - 6
	3.3.3 Analysis of left and right hand impact forces	3 - 8
	3.3.4 Analysis of impact forces	3 - 9

3.3.4.1	Analysis of force peaks	3 - 12
3.3.4.2	Analysis of gender	3 - 14
3.3.4.3	Analysis of fall height	3 - 18
3.3.4.4	Analysis of effective mass	3 - 20
3.3.4.5	Analysis of age	3 - 22
3.4	Surface study using motion analysis	3 - 25
3.4.1	Analysis of force-time impact curves	3 - 25
3.4.2	Impact forces	3 - 27
3.5	Time duration study	3 - 28
3.6	Statistical analysis	3 - 31
3.6.1	Statistical analysis of impact forces	3 - 31
3.6.2	Statistical analysis on the factors affecting a fall onto the outstretched hand	3 - 32
3.6.3	Statistical analysis on the time duration of force peak F1	3 - 36
3.6	High-speed video study	3 - 38
3.6.1	Typical force-time impact curves	3 - 38
3.6.2	Fall and impact mechanism	3 - 41
3.6.3	Electromyography results.	3 - 51
3.7	Computer modelling results	3 - 61

CHAPTER 4 DISCUSSION

4.1	Introduction	4 - 1
4.2	Observational study	4 - 2
4.3	Motion analysis study	4 - 3
4.3.1	Analysis of arm angles at 3 and 5 cm fall heights	4 - 3
4.3.2	Analysis of falls at 3 and 5 cm fall heights onto force plates	4 - 4
4.3.3	Hand dominance	4 - 5
4.3.4	Impact forces at 3 and 5 cm	4 - 6
4.3.4.1	Force Peaks	4 - 8
4.3.4.2	Gender	4 - 10
4.3.4.3	Height	4 - 13
4.3.4.4	Effective mass	4 - 15
4.3.4.5	Age	4 - 16
4.4	Surface study using motion analysis	4 - 19
4.4.1	Force time curves onto surfaces	4 - 19
4.4.2	Impact forces	4 - 20
4.5	Analysis of time duration of force peak F1	4 - 21
4.6	Summary of main results and discussion from motion analysis studies	4 - 24
4.7	High-speed video (HSV) Study	4 - 26
4.7.1	Force time curves for falls at 1, 5, 10 and 20 cm fall heights	4 - 28
4.7.2	Force time curves from standing height	4 - 28
4.7.3	Fall and impact mechanism	4 - 29
4.7.3.1	Falls from 1 cm	4 - 30
4.7.3.2	Falls from 5 cm	4 - 31
4.7.3.3	Falls from 10 and 20 cm	4 - 31
4.7.3.4	Falls from a standing height	4 - 32
4.7.4	Shock wave	4 - 35
4.7.4.1	Relationship between shock wave and force time curves	4 - 37
4.8	Electromyography study	4 - 38

4.8.1	Analysis of EMG data during falls from the drop rig, from heights of 1, 5, 10 and 20 cm	4 - 39
4.8.2	Analysis of EMG data during falls from standing height	4 - 40
4.9	Summary of main results and discussion from HSV and EMG studies	4 - 41
4.10	Computer modelling	4 - 44
4.10.1	Introduction	4 - 44
4.10.2	Progression of models	4 - 45
4.10.3	Simulated response	4 - 48
4.11	Discussion of fall studies and computer simulations	4 - 50
4.12	Problems and limitations of study	4 - 50

CHAPTER 5 CONCLUSIONS

5.1	Introduction	5 - 1
5.2.	Conclusions	5 - 3
5.2.1	General conclusions	5 - 3
5.2.2	Factors affecting the impact forces	5 - 3
5.2.3	Mechanism of fall arrest and impact	5 - 4
5.2.4	Computer modelling	5 - 6
5.3	Summary of conclusions	5 - 7

CHAPTER 6 FURTHER WORK

6.1	Introduction	6 - 1
6.2	Fall experiments	6 - 2
6.3	Modelling	6 - 4

REFERENCES

APPENDICES

- Appendix A: Technical drawings for drop mechanism
- Appendix B: Arm angle data
- Appendix C: Statistical Analysis
- Appendix D: HASS/LASS data
- Appendix E: HSV files (CD)

LIST OF FIGURES

Chapter 1

- Figure 1.1: Diagram showing the anatomical terms used to describe relative position or direction (Hamill and Knutzen, 2003).
- Figure 1.2: Flexion-extension movements in the arm and forearm (Hamill and Knutzen, 2003).
- Figure 1.3: Flexion-extension movements in the hand and fingers (Hamill and Knutzen, 2003).
- Figure 1.4: Abduction-adduction movements in the arm, hand and fingers (Hamill and Knutzen, 2003).
- Figure 1.5: Pronation-supination in the forearm (Hamill and Knutzen, 2003).
- Figure 1.6: Examples of the different types of bone in the human skeleton (Hamill and Knutzen, 2003).
- Figure 1.7: Diagram showing the long bone (Hamill and Knutzen, 2003)
- Figure 1.8: (a) Anterior view (b) Posterior view of the shoulder (Moore and Augur, 1995).
- Figure 1.9: (a) Anterior view (b) Posterior view of the Humerus (Moore and Augur, 1995).
- Figure 1.10: (a) Anterior view (b) Posterior view of the forearm (Moore and Augur, 1995).
- Figure 1.11: (a) Anterior view (b) Posterior view of the wrist and hand (Moore and Augur, 1995).
- Figure 1.12: Anterior view of the muscles that move the shoulder. Superficial muscles are shown on left, deep muscles on the right (Carola et al, 1990).
- Figure 1.13: Posterior view of the muscles that move the shoulder. Superficial muscles are shown on left, deep muscles on the right (Carola et al, 1990).
- Figure 1.14: (a) Anterior and (b) posterior view of the superficial muscles that move the arm (Carola et al, 1990).
- Figure 1.15: (a) Anterior and (b) posterior view of superficial muscles of the forearm and hand (Carola et al, 1990).
- Figure 1.16: Examples of a non-comminuted fracture (a) transverse (b) oblique and (c) spiral (Levine, 1993).
- Figure 1.17: (a) A comminuted fracture, examples of which are (b) butterfly fragment and (c) segmental (Levine, 1993).
- Figure 1.18: (a) displaced fracture (b) undisplaced fracture (Levine, 1993).
- Figure 1.19: Impact force for fall onto floor (90° from vertical) (Dietz et al, 1981).
- Figure 1.20: Impact force for fall onto platform inclined 70° to the vertical. (Dietz et al, 1981).
- Figure 1.21: (a) Impact response of the body during forward fall onto the outstretched hand showing force peaks F_{max1} and F_{max2} (b) Two-degree-of-freedom lumped-parameter mathematical model (Chiu and Robinovitch, 1998).

- Figure 1.22: (a) Cable released fall experiment set up (Kim and Ashton Miller, 2003) (b) Diagram showing ankle movement (Kreighbaum and Barthels, 1996).
- Figure 1.23: Diagram showing the different positions of the arm during falls at two distances from vertically positioned force plate.
- Figure 1.24: Tabulated results from Chou et al, 2001.
- Figure 1.26: The fall simulator with description of parts (Maki and Fernie, 1990).
- Figure 1.27: Graph showing the effect of peak impact forces applied to the hand during experimental falls from a height of 5 cm, onto foam padding. (Robinovitch and Chiu, 1998).
- Figure 1.28: Rheological two-mass model of arm impact (Davidson et al, 2005).
- Figure 1.29: Photographs showing (a) Impact dummy and (b) portable drop rig (Sherker et al, 2003).
- Figure 1.30: Typical EMG traces for the right triceps brachii during a fall (a) with and (b) without visual control. (At platform angles of 50-80°) (Dietz and Noth, 1978).
- Figure 1.31: Typical EMG profiles of the forearm flexors (upper trace) and forearm extensors (lower trace) during an 80° fall (Dietz et al, 1981).

Chapter 2

- Figure 2.1: Photo showing two Bertec force plates situated flush with the floor in the Human Movement Laboratory in Cardiff University.
- Figure 2.2: (a) Retro-reflective markers (b) Marker placements for initial study.
- Figure 2.3: Pro Reflex camera.
- Figure 2.4: Calibration kit consisting of a reference structure and wand.
- Figure 2.5: Observational study, fall onto 30 cm thick crash mat.
- Figure 2.6: (a) Drop rig constructed from scaffolding (b) Manufactured drop rig feet.
- Figure 2.7: Steel box section drop rig.
- Figure 2.8: Engine hoist.
- Figure 2.9: Mechanical drop mechanism (a) closed and (b) open.
- Figure 2.10: Harness in (a) open position and (b) closed position.
- Figure 2.11: Retro-reflective marker positions.
- Figure 2.12: Volunteer suspended in harness from drop rig with each hand positioned over the force plates.
- Figure 2.13: MOTIONeer camera (a) full view (b) rear panel.
- Figure 2.14: Static calibration frame positioned in the centre of the test space.
- Figure 2.15: Hedlar 1250-Watt lantern.
- Figure 2.16: High-speed video study equipment set up.
- Figure 2.17: Main amplifier unit showing front (top) and rear (bottom) views.
- Figure 2.18: Data acquisition box.
- Figure 2.19: Patient unit with waist belt and battery pack.
- Figure 2.20: Pre-amplifiers connected to the patient at one end and the electrode at the other.
- Figure 2.21: Silver/Silver Chloride (Ag/AgCl) electrode, front and back views.
- Figure 2.22: Electrodes placed on the skin with pre-amplifiers connecting electrodes to the patient unit.
- Figure 2.23: Black circular markers.
- Figure 2.24: Volunteer suspended in rig with EMG equipment.

- Figure 2.25: Model 1.
- Figure 2.26: Model 2.
- Figure 2.27: Model 3.
- Figure 2.28: Model 4.
- Figure 2.29: Model 5.

Chapter 3

- Figure 3.1: Series of photographs showing a fall from standing height onto a 2.5 cm foam surface with associated stick figures from QTM and time of fall.
- Figure 3.2: Series of photographs showing a fall from the drop rig, at a height of 5 cm, onto the force plates with associated stick figures from QTM and time of fall.
- Figure 3.3: Graph showing arm angles immediately prior to impact, for left and right hands at fall heights of 3 and 5 cm.
- Figure 3.4: Graph showing typical force-time impact curve at a fall height of 3 cm.
- Figure 3.5: Graph showing typical force-time impact curve at a fall height of 5 cm.
- Figure 3.6: Graph showing a typical force-time curve, introducing terminology of the force peaks used throughout the study.
- Figure 3.7: Graph showing a comparison of left and right hand impact forces at a fall height of 3 cm.
- Figure 3.8: Graph showing a comparison of left and right hand impact forces at a fall height of 5 cm.
- Figure 3.9: Graph showing a comparison of impact force peaks at a fall height of 3 cm.
- Figure 3.10: Graph showing a comparison of impact force peaks at a fall height of 5 cm.
- Figure 3.11: Graph showing a comparison of impact force peak F1 at fall heights of 3 and 5 cm.
- Figure 3.12: Graph showing a comparison of impact force peak F2 at fall heights of 3 and 5 cm.
- Figure 3.13: Graph showing a comparison of impact force peaks for females at fall heights of 3 and 5 cm.
- Figure 3.14: Graph showing a comparison of impact force peaks for males at fall heights of 3 and 5 cm.
- Figure 3.15: Graph showing a comparison of impact force peaks F1 and F2 at a fall height of 3 cm.
- Figure 3.16: Graph showing a comparison of impact force peaks F1 and F2 at a fall height of 5 cm.
- Figure 3.17: Graph showing a comparison of impact force peak F1 for females and males at a fall height of 3 cm.
- Figure 3.18: Graph showing a comparison of impact force peak F1 for females and males at a fall height of 5 cm.
- Figure 3.19: Graph showing a comparison of impact force peak F2 for females and males at a fall height of 3 cm.
- Figure 3.20: Graph showing a comparison of impact force peak F2 for females and males at a fall height of 5 cm.
- Figure 3.21: Graph showing a comparison of impact force peaks F1 and F2 for females and males at a fall height of 3 cm.

- Figure 3.22: Graph showing a comparison of impact force peaks F1 and F2 for females and males at a fall height of 5 cm.
- Figure 3.23: Graph showing a comparison of impact force peak F1 at fall heights of 3 and 5 cm for females and males.
- Figure 3.24: Graph showing a comparison of impact force peak F2 at fall heights of 3 and 5 cm for females and males.
- Figure 3.25: Graph showing a comparison of impact force peak F1 against effective mass for females and males at a fall height of 3 cm.
- Figure 3.26: Graph showing a comparison of impact force peak F1 against effective mass for females and males at a fall height of 5 cm.
- Figure 3.27: Graph showing a comparison of impact force peak F2 against effective mass for females and males at a fall height of 3 cm.
- Figure 3.28: Graph showing a comparison of impact force peak F2 against effective mass for females and males at a fall height of 5 cm.
- Figure 3.29: Graph showing a comparison of impact force peaks F1 and F2 against age for females at a fall height of 3 cm.
- Figure 3.30: Graph showing a comparison of impact force peaks F1 and F2 against age for females at a fall height of 5 cm.
- Figure 3.31: Graph showing a comparison of impact force peaks F1 and F2 against age for males at a fall height of 3 cm.
- Figure 3.32: Graph showing a comparison of impact force peaks F1 and F2 against age for males at a fall height of 5 cm.
- Figure 3.33: Graph showing a typical force-time impact curve at a fall height of 5 cm onto the domestic surface.
- Figure 3.34: Graph showing a typical force-time impact curve at a fall height of 5 cm onto the playground surface.
- Figure 3.35: Graph showing a comparison of impact force peaks F1 and F2 at different surfaces for females at a fall height of 5 cm.
- Figure 3.36: Graph showing a comparison of impact force peaks F1 and F2 at different surfaces for males at a fall height of 5 cm.
- Figure 3.37: Graph showing the time duration of impact force peak F1 for females and males onto force plates at a fall height of 3 cm.
- Figure 3.38: Graph showing the time duration of impact force peak F1 for females and males onto force plates at a fall height of 5 cm.
- Figure 3.39: Graph showing the time duration of impact force peak F1 for females and males onto the domestic surface at a fall height of 5 cm.
- Figure 3.40: Graph showing the time duration of impact force peak F1 for females and males onto the playground surface at a fall height of 5 cm.
- Figure 3.41: Graph showing typical force-time impact curve at a fall height of 1 cm.
- Figure 3.42: Graph showing typical force-time impact curve at a fall height of 5 cm.
- Figure 3.43: Graph showing typical force-time impact curve at a fall height of 10 cm.
- Figure 3.44: Graph showing typical force-time impact curve at a fall height of 20 cm.
- Figure 3.45: Graph showing typical force-time impact curve from a standing fall height.
- Figure 3.46: Series of still photographs taken from high-speed video footage, showing the hand mechanism prior to impact during a fall onto the force plates from a 10 cm fall height

- Figure 3.47a: Series of still photographs taken from high-speed video footage, showing a fall onto the force plates from standing height.
- Figure 3.47b: Series of still photographs taken from high-speed video footage, showing a fall onto the force plates from standing height.
- Figure 3.48: Series of still photographs taken from high-speed video footage, showing a fall onto the force plates from kneeling height (female volunteer).
- Figure 3.49: Series of still photographs taken from high-speed video footage, showing a fall onto the force plates from kneeling height (male volunteer).
- Figure 3.50: Series of still photographs taken from high-speed video footage, showing shock wave travelling up through the lower arm with the associated time, during a fall from kneeling height.
- Figure 3.51: Still photographs taken from high-speed video footage showing a comparison between skin and soft tissues (a) immediately prior to and (b) during impact with the force plates, from a fall from standing height.
- Figure 3.52: Typical EMG trace of the triceps brachii muscle showing the raw and filtered data for a fall height from 1 cm.
- Figure 3.53: Typical filtered EMG trace for the thenar eminence, from a fall height of 5 cm.
- Figure 3.54: Typical filtered EMG trace for the forearm flexors, from a fall height of 5 cm.
- Figure 3.55: Typical filtered EMG trace for the forearm extensors, from a fall height of 5 cm.
- Figure 3.56: Typical filtered EMG trace for the biceps brachii, from a fall height of 5 cm.
- Figure 3.57: Typical filtered EMG trace for the triceps brachii, from a fall height of 5 cm.
- Figure 3.58: Typical filtered EMG trace for the anterior deltoid, from a fall height of 5 cm.
- Figure 3.59: Typical filtered EMG trace for the pectoralis major, from a fall height of 5 cm.
- Figure 3.60: Typical filtered EMG trace for the trapezius, from a fall height of 5 cm.
- Figure 3.61: Typical filtered EMG trace for the thenar eminence, for a fall from standing height.
- Figure 3.62: Typical filtered EMG trace for the forearm flexors, for a fall from standing height.
- Figure 3.63: Typical filtered EMG trace for the forearm extensors, for a fall from standing height.
- Figure 3.64: Typical filtered EMG trace for the biceps brachii, for a fall from standing height.
- Figure 3.65: Typical filtered EMG trace for the triceps brachii, for a fall from standing height.
- Figure 3.66: Typical filtered EMG trace for the anterior deltoid, for a fall from standing height.
- Figure 3.67: Typical filtered EMG trace for the pectoralis major, for a fall from standing height.

- Figure 3.68: Typical filtered EMG trace for the trapezius, for a fall from standing height.
- Figure 3.69: Graph showing force-time curve of hand to ground contact of model 5, from a fall height of 1 and 2 cm.
- Figure 3.70: Graph showing force-time curve of hand to ground contact of model 5, with masses of 15 and 30 kg.

LIST OF TABLES

Chapter 1

- Table 1.1: Fracture forces from studies using cadaveric material.
Table 1.2: Means, standard deviations and ranges of the impact forces, fracture forces and FR for the case and control groups at both peaks (Davidson et al, 2005).

Chapter 3

- Table 3.1: Results from the observational study showing the angle of the arm during a fall from standing height.
Table 3.2: Table showing significance (P) values from Mann-Whitney tests, to assess if there was a significant difference between the magnitude of the impact force peaks produced in the right and left hand during a fall onto the outstretched hand.
Table 3.3: Table showing significance (P) values from Mann-Whitney tests, to assess if there was a significant difference between the magnitude of the impact force peaks during a fall onto the outstretched hand.
Table 3.4: Table showing significance (P) values from Mann Whitney tests, to assess if gender significantly affects the magnitude of the impact force peaks during a fall onto the outstretched hand.
Table 3.5: Table showing significance (P) values from Mann Whitney tests, to assess if the fall height significantly affects the magnitude of the impact force peaks during a fall onto the outstretched hand.
Table 3.6: Table showing significance (P) values from Mann Whitney tests, to assess if effective mass significantly affects the magnitude of the impact force peaks during a fall onto the outstretched hand.
Table 3.7: Table showing significance (P) values from Mann Whitney tests, to assess if age significantly affects the magnitude of the impact force peaks during a fall onto the outstretched hand.
Table 3.8: Table showing significance (P) values from Mann Whitney tests, to assess if the impact surface significantly affects the magnitude of the impact force peaks during a fall onto the outstretched hand.
Table 3.9: Table showing significance (P) values from Mann Whitney tests, to assess if the time duration of impact force peak F1 is significantly affected by fall height or impact surface during a fall onto the outstretched hand.

CHAPTER 1

INTRODUCTION

1.1 INTRODUCTION

Playground injuries account for approximately 5-6% of all childhood injuries (Altman *et al*, 1996, Macarthur *et al*, 2000). Although this is a small percentage of all injuries they are important because they result in a greater proportion of fractures and hospital admissions than many other types of injury (Mott *et al*, 1994, Mowat *et al*, 1998).

Although the risk of serious head injury due to a playground fall is not as great as the risk of a serious limb fracture (Illingworth *et al*, 1975, King and ball, 1991, Mott *et al*, 1994, Stathakis, 1999 in Ozanne-Smith, 2001, Norton *et al*, 2004) playground safety has predominantly been directed at preventing head injury.

Hard playground surfaces (concrete and tarmac) have been phased out and replaced with Impact Absorbing Playground Surfaces (IAPS). These surfaces consist of synthetic surfaces (prefabricated rubber tiles or wet pour elastomers) and loose fill surfaces (tree bark, woodchip, sand, pea gravel or loose rubber crumb).

The shock absorbing properties of IAPS are tested, for their ability to alleviate serious head injury, using an instrumented metal head form. (The head form is described in ASTM F 355-78, 1978). The head form is dropped onto a sample of the playground material and outputs the acceleration/time pulse during impact, from which a Head Injury Model is calculated (Cory, 1998).

Any IAPS that is installed under playground equipment in Britain will have been tested using this head form and will comply with the method laid out in British

Standards (BS 7188, 1989). (Other countries use the same head form, but the method may differ to that of British Standards).

Research has shown that installation of IAPS in the play areas of Cardiff has indeed reduced the amount of serious head injuries (Mott *et al*, 1994, Mott *et al* 1997, Norton *et al*, 2004). However, even though head injuries have been greatly reduced in severity, arm fractures have not reduced in severity or frequency.

This confirms that the current strategies for the assessment and prevention of head injury potential have been shown to be highly successful, yet totally ineffective for preventing upper limb fractures. A need therefore exists to develop a method for the assessment of playground surfaces for their ability to alleviate arm fractures and subsequently to assist in the development of 'arm friendly' surfaces.

1.2 AIMS OF THIS STUDY

It has been shown previously that approximately 60-80% of playground injuries are the direct result of a fall (Illingworth *et al*, 1975, Goss, 1992, Bond and Peck, 1993, Routley, 1993, Mott *et al*, 1994, Mott *et al*, 1997, Altman *et al*, 1996, Chalmers *et al* 1996) and that the most common injury due to a fall in children aged 5 to 14 years is a fracture to the upper extremity (King and Ball, 1991, Goss, 1992, Routley, 1993, Mott *et al*, 1994, Altman *et al*, 1996, Chalmers *et al* 1996, Ashby and Corbo, 2000, Macarthur *et al*, 2000, Ozanne-smith, 2001, Clapperton *et al*, 2003, Norton *et al*, 2004).

However, the force required to fracture the arm during a fall in a playground is currently unknown. The aims of this study are:

- to investigate the forces that are produced in the arm during a fall onto the outstretched hand at a non-injurious level.
- to utilize the data for non-injurious impact forces, during a fall onto the outstretched hand, to aid in the development of a mechanical arm fracture model that could be used, alongside the British Standard head impact testing device, to test IAPS for their ability to alleviate arm fractures.

Previous research has investigated upper extremity fractures and falls onto the outstretched hand both epidemiology and experimentally. A review of the literature is discussed in section 1.5. However, due to the content of this thesis and the reported literature, it is important to first have an understanding of the medical terminology and anatomy of the upper extremity. This is therefore described before the literature review in section 1.3. Section 1.4 describes trauma mechanics, detailing the types of injuries associated with a fall onto the outstretched hand.

1.3 ANATOMY

The following sections 1.3.1 to 1.3.5 describes the terminology for anatomical referencing, movement descriptions and anatomy of the upper extremity that will be referred to throughout this thesis. Sections 1.3.6 and 1.3.7 describe the motor vestibular system and reflexes.

1.3.1 ANATOMICAL TERMINOLOGY

The position of a segment or joint movement is usually described relative to a designated starting position. This reference position is referred to as the anatomical position. In this position the body is standing erect with the head facing forward, arms at the side of the trunk with palms facing forward, and the legs together with the feet pointing forward. The anatomical terms describing the relative position or direction are shown in figure 1.1 and these are explained briefly below.

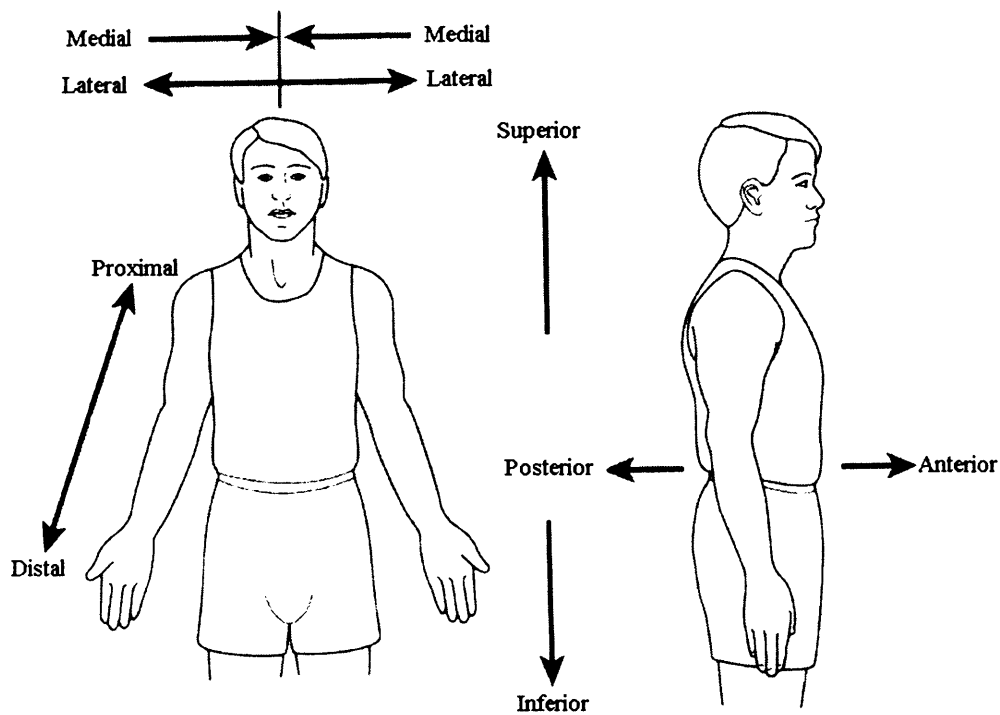


Figure 1.1: Diagram showing the anatomical terms used to describe relative position or direction (Hamill and Knutzen, 2003).

Medial – A position that is relatively close to the midline of the body or movement towards it.

Lateral – A position that is relatively far from the midline of the body or movement away from it.

Proximal – A position that is close to the reference point.

Distal – A position that is farther from the reference point.

Superior – A position that is above a particular reference point or closer to the top of the head.

Inferior – A position that is below a particular reference point.

Anterior – A position that is relative to the front of the body.

Posterior – A position that is relative to the back of the body.

1.3.2 TERMINOLOGY FOR DESCRIBING MOVEMENT

The joints of the body move using varying combinations of six basic movements – flexion-extension, abduction-adduction, rotation and circumduction. The particular movements relative to the upper extremity that will be referred to in this thesis are described below.

1.3.2.1 FLEXION-EXTENSION

Flexion occurs when the relative angle of the joint between two adjacent segments decreases (bending movement). Extension occurs when the relative angle of the joint between two adjacent segments increases (straightening movement) as the joint returns to the zero or reference position. If either of these movements go beyond the normal range of motion it is referred to as hyperflexion and hyperextension respectively. These movements can be seen in figure 1.2 for the arm (shoulder joint) and forearm (elbow joint) and in figure 1.3 for the hand (wrist joint) and fingers (metacarpophalanx joint).

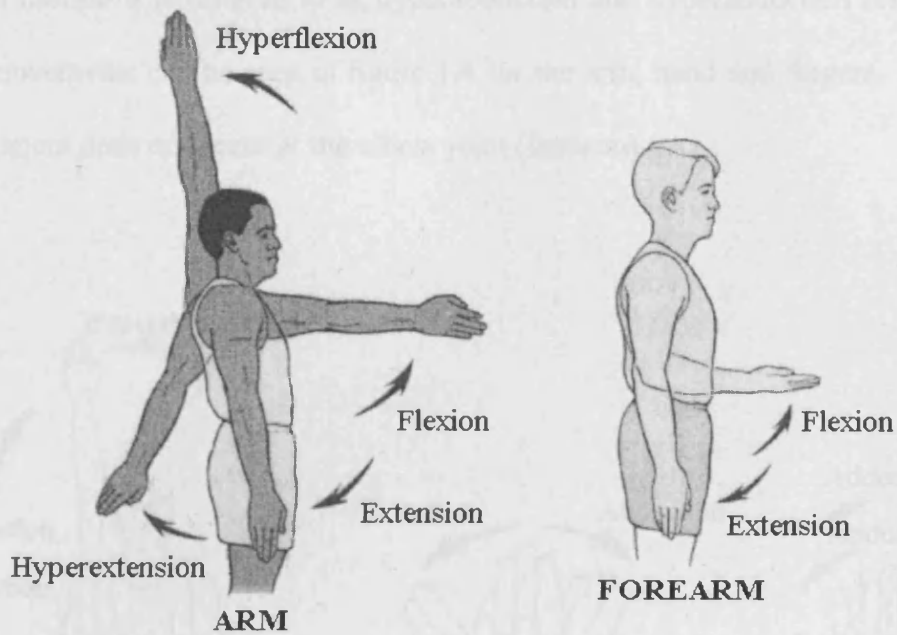


Figure 1.2: Flexion-extension movements in the arm and forearm (Hamill and Knutzen, 2003).

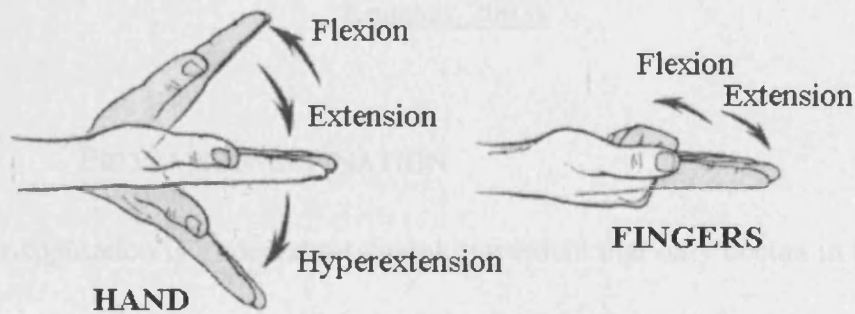


Figure 1.3: Flexion-extension movements in the hand and fingers (Hamill and Knutzen, 2003).

1.3.2.2 ABDUCTION-ADDUCTION

Abduction occurs when a movement is performed that moves the segment away from the midline. Adduction occurs when a movement is performed that moves the segment towards the midline. If either of these movements go beyond the normal

range of motion it is referred to as hyperabduction and hyperadduction respectively. These movements can be seen in figure 1.4 for the arm, hand and fingers. This type of movement does not occur at the elbow joint (forearm).

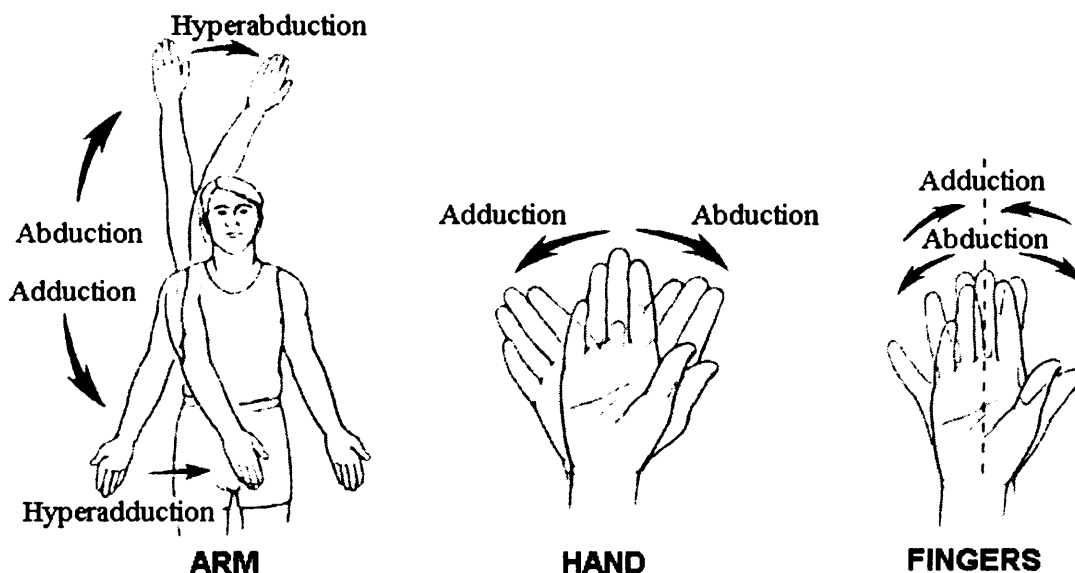


Figure 1.4: Abduction-adduction movements in the arm, hand and fingers (Hamill and Knutzen, 2003).

1.3.2.3 PRONATION-SUPINATION

Pronation-supination is a special rotational movement that only occurs in the forearm. Pronation is the movement in which the palm faces backward. Supination is when the palm faces forward (figure 1.5).

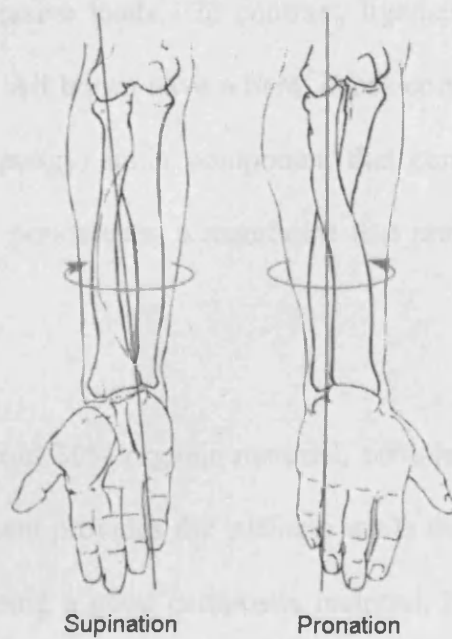


Figure 1.5: Pronation-supination in the forearm (Hamill and Knutzen, 2003).

1.3.3 STRUCTURE AND FUNCTION OF BONES

Bone is the hard and rigid tissue that is the main structural component of the adult skeleton. The skeleton has two main functions:

Biomechanical:

- Support - maintains shape of the body and provides attachments for muscles and tendons
- Movement - articulated system of stiff levers
- Protection - the brain and spinal cord, the thoracic organs and the bone marrow

Metabolic:

- Contains substantial amount of calcium and phosphate

Bone is stiff, strong, tough, and resilient. Its primary function is that of load carrying and because of its higher compressive (as compared to tensile) properties it is capable

of carrying large compressive loads. In contrast, ligaments, tendons, and muscles carry only tensile loads. All bones have a hard, dense cortical (compact) shell and a less dense cancellous (spongy) inner component that contains marrow. The bone surface is surrounded by periosteum, a membrane that provides a network of nerves and blood vessels.

Bone is composed of about 30% organic material, 60% inorganic material and 10% water. The mineral content provides the stiffness while the fibrous content produces the toughness. Bone, being a good composite material, has a greater strength than either of its two main components: the softer component prevents the stiff one from cracking, while the stiff component prevents the soft one from yielding.

The mechanical properties of bone are greatly dependent on the condition of the bone, which is related to the age, sex, and health of the individual. Its mechanical properties are also time dependent because bone is a visco-elastic material. This means that if you were to load a bone at a higher loading rate the bone will be stiffer than if it were loaded slowly. The behavior of the bone will also vary with the direction of the load application, as bone is an anisotropic material. (Panjabi and White, 2001)

Bones are classified according to their shape (figure 1.6). The shape and features of each bone reflect its biomechanical role, each of which are described below.

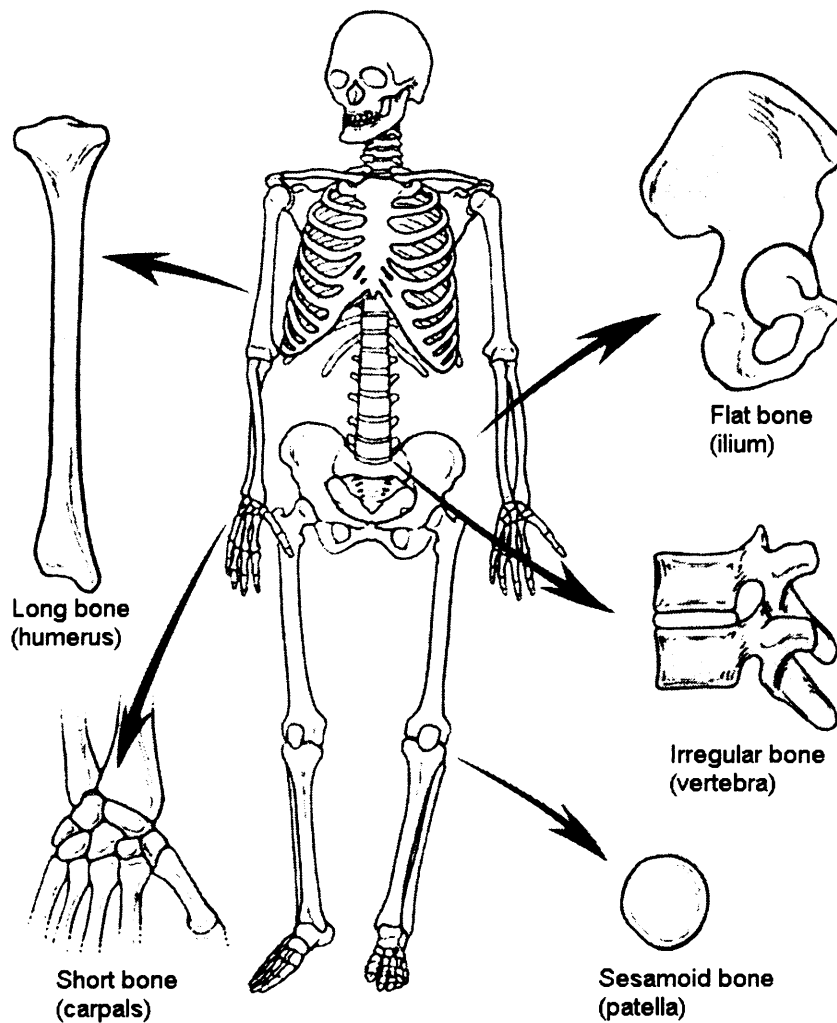


Figure 1.6: Examples of the different types of bone in the human skeleton (Hamill and Knutzen, 2003).

1.3.3.1 LONG BONES

Long bones (as their name would suggest) are longer than they are wide (e.g. humerus, radius and ulna). The long bone (figure 1.7) has a shaft (diaphysis) consisting of a thick layer of compact bone surrounding a bone marrow cavity. The shaft widens towards the ends of the bone (metaphysis) where the compact bone becomes a thin layer covering spongy inner bone. In children, the end of the long bone, the epiphysis, is separated from the metaphysis by cartilage (epiphyseal line).

The epiphysis consists of a thin outer layer of compact bone covering spongy inner bone, much the same as the metaphysis.

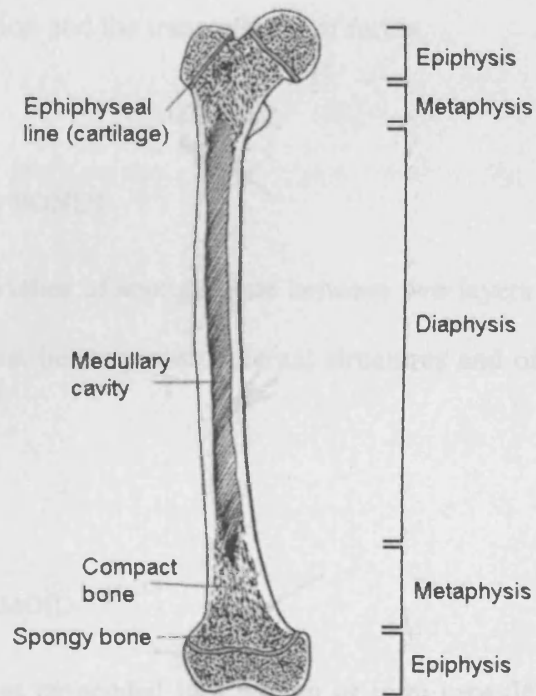


Figure 1.7: Diagram showing the long bone (Hamill and Knutzen, 2003).

Growth in length occurs in the epiphyseal plates. During bone growth and remodelling, the shape of the bone is maintained as it grows and the architecture of the bone is adapted to the bone's usage. Weak or damaged regions are removed and replaced with stronger bones. This continues in life in response to applied loads. Long bones offer the body support and provide an interconnected set of levers and linkages that allow us to move.

1.3.3.2 SHORT BONES

Short bones consist primarily of spongy bone with a thin layer of compact bone and tend to be cuboidal in shape (e.g. carpals and tarsals). These bones play an important role in shock absorption and the transmission of forces.

1.3.3.3 FLAT BONES

Flat bones are sandwiches of spongy bone between two layers of compact bone (e.g. ilium and ribs). Flat bones protect internal structures and offer broad surfaces for muscular attachment.

1.3.3.4 SESAMOID

These are small bones embedded in a tendon or joint capsule (e.g. patella). These bones usually occur where tendons pass over the joint of a long bone, and the role of a sesamoid bone is to alter the angle of insertion of the muscle.

1.3.3.5 IRREGULAR BONES

Any bones which don't fit these arbitrary categories and have various shapes (e.g. bones found in the skull and vertebrae) are referred to as irregular. Irregular bones consist of spongy bone with a thin exterior of compact bone. They have a wide variety of functions, including supporting weight, dissipating loads, protecting the spinal cord, contributing to movement and providing sites for muscular attachment.

1.3.4 SKELETAL STRUCTURE OF THE UPPER EXTREMITY

The human arm (often referred to as the upper extremity) is made up of three main sections; upper arm, lower arm and wrist and hand. These sections connect the three joints of the shoulder, elbow and wrist. The upper limb is characterised by considerable mobility and is adapted for grasping and manipulating. This section details the bones that make up the upper extremity (Moore and Augur, 1995).

1.3.4.1 SHOULDER AND UPPER ARM

The shoulder joint (figure 1.8) links the upper extremity to the trunk and acts in conjunction with the elbow to position the hand in space for efficient rotation. The clavicle connects the upper limb and trunk. Its medial end articulates with the manubrium of the sternum at the sternoclavicular joint. Its lateral end articulates with the acromion of the scapula at the acromioclavicular joint. The clavicle serves as a strut to keep the upper limb away from the thorax so that the arm has maximum freedom of movement and transmits shocks (impacts) from the upper limb to the axial skeleton.

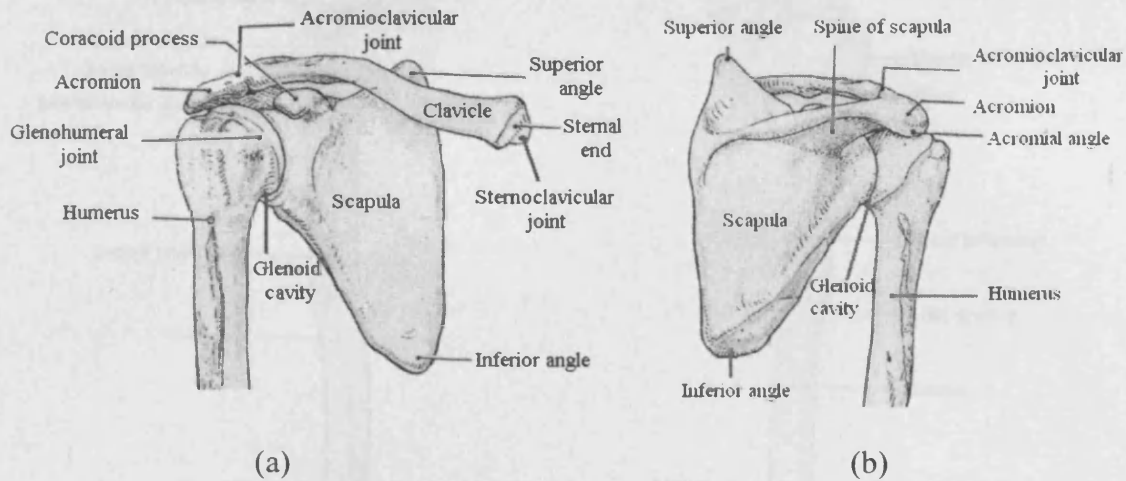


Figure 1.8: (a) Anterior view (b) Posterior view of the shoulder (Moore and Augur, 1995).

The scapula is a thin and translucent triangular body. The spine continues laterally as the acromion that forms the point of the shoulder and articulates with the clavicle. The lateral surface of the scapula forms the glenoid cavity, which articulates with the head of the humerus at the scapulohumeral (shoulder) joint.

The humerus (figure 1.9) has two prominent features, the deltoid tuberosity laterally and the radial groove posteriorly.

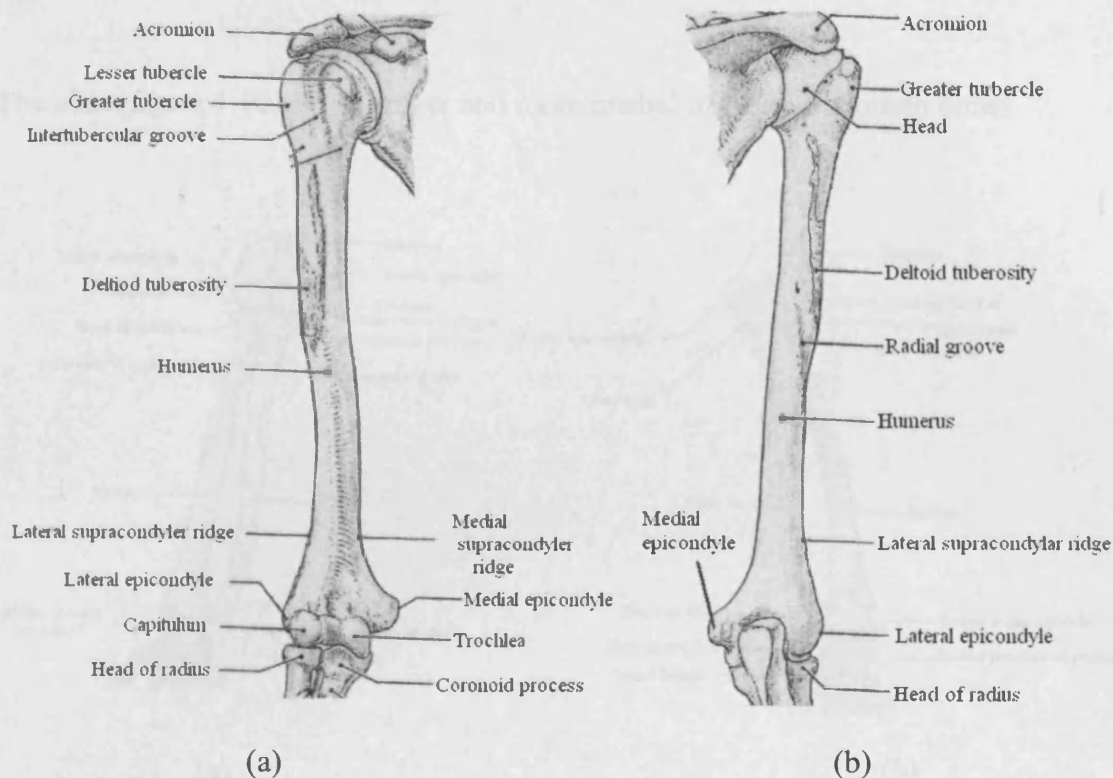


Figure 1.9: (a) Anterior view (b) Posterior view of the Humerus (Moore and Augur, 1995).

The sharp medial and lateral supracondylar ridges end distally in prominent medial and lateral epicondyles. The distal end of the humerus has two articular surfaces, a lateral capitulum for articulation with the head of the radius and a medial trochlea for the articulation with the ulna. This is the elbow joint.

1.3.4.2 ELBOW AND LOWER ARM

The elbow is a complex joint that functions as a fulcrum for the forearm lever system and is responsible for positioning the hand in space. The elbow allows two types of motion: Flexion-extension and pronation-supination. The humeroulnar and humeroradial articulations allow elbow flexion and extension and are classified as hinge joints. The proximal radioulnar articulation allows forearm pronation and supination and is classified as a trochoid joint.

The ulna (figure 1.10) is the longer and more medial of the two forearm bones.

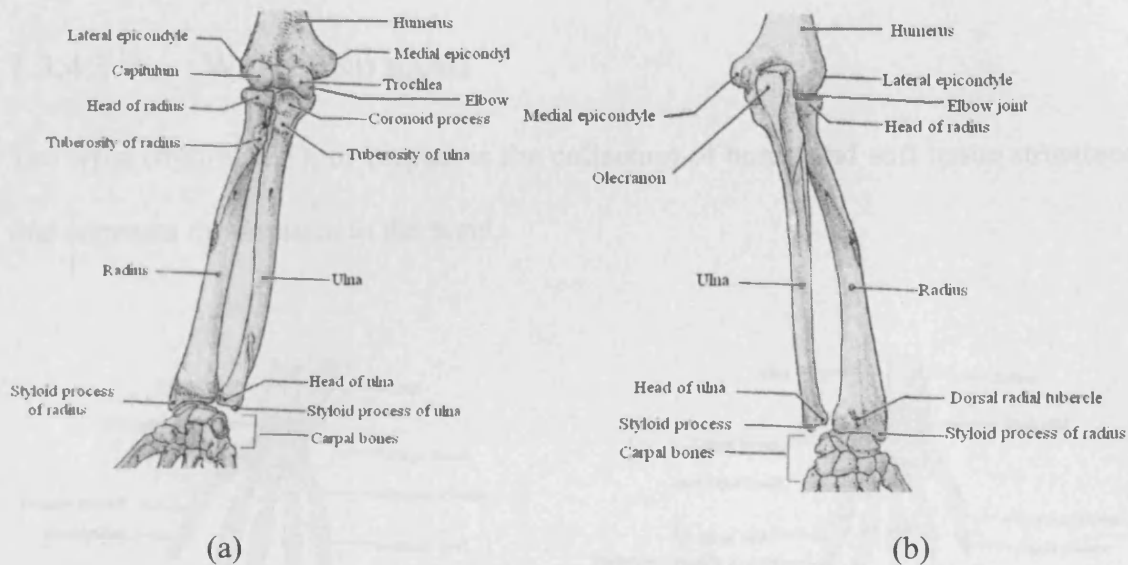


Figure 1.10: (a) Anterior view (b) Posterior view of the forearm (Moore and Augur, 1995).

Its proximal end includes the olecranon posteriorly and the coronoid process anteriorly. The anterior surface of the olecranon has the trochlea notch that receives the trochlea of the humerus. On the lateral side of the coronoid process is the radial notch, and inferior to this process is the tuberosity of the ulna. Initially the body is thick, but it becomes narrow at its distal end, which has a large rounded head and a small conical styloid process.

The radius (figure 1.10) is the shorter and more lateral of the two forearm bones. Its proximal end consists of a disc-like head, a short neck, and tuberosity. Proximally the smooth head is concave for articulation with the capitulum of the humerus. The neck is the constriction distal to the head. The tuberosity of the radius, just distal to the neck, separates the proximal end of the radius from the body. The distal end of the

radius had an ulna notch medially, a styloid process laterally, and a dorsal tubercle dorsally.

1.3.4.3 WRIST AND HAND

The wrist (figure 1.11), or carpus, is the collection of bones and soft tissue structures that connects the forearm to the hand.

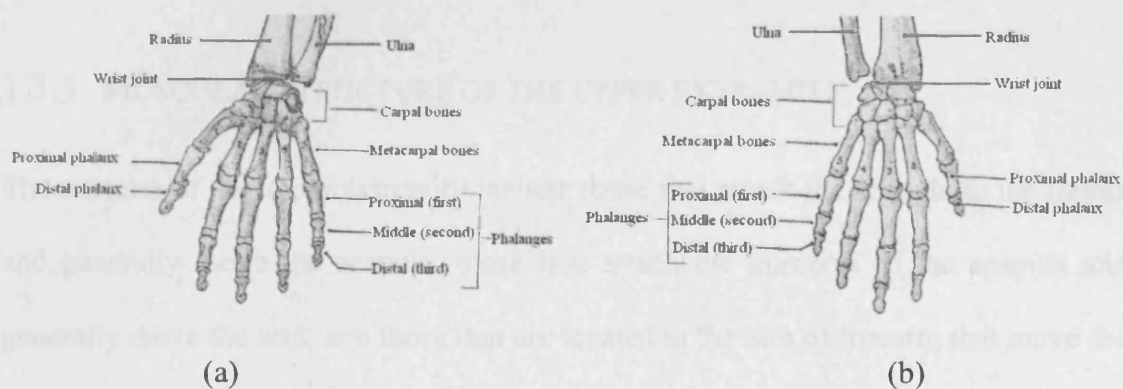


Figure 1.11: (a) Anterior view (b) Posterior view of the wrist and hand (Moore and Augur, 1995).

This joint complex is capable of a substantial arc of motion that augments hand and finger function, yet it possesses a considerable degree of stability. The eight carpals forming the carpus and the skeleton of the wrist are arranged in two rows. From lateral to medial, the three large bones in the proximal row are the scaphoid, the lunate and the triquetrum; the pisiform lies on the palmer surface of the triquetrum.

The distal row, from lateral to medial, consists of the trapezium, the trapezoid, the capitate and the hamate, which has a hook like process called the hook of the hamate. The carpus is markedly convex from side to side posteriorly and concave anteriorly.

The five metacarpals forming the metacarpus and the skeleton of the hand connect the carpus with the phalanges in the digits. Each metacarpal consists of a body and two ends. The distal ends or heads articulate with the phalanges and form the knuckles of the fist (metacarpophalanx joint); the proximal ends or bases articulate with the carpal bones. Each digit has three phalanges except the first one, the thumb, which has only two. Each phalanx has a base proximally, a head distally, and a body between the base and the head.

1.3.5 MUSCULAR STRUCTURE OF THE UPPER EXTREMITY

The muscles of the upper extremity include those that attach the scapula to the thorax and generally move the scapula, those that attach the humerus to the scapula and generally move the arm, and those that are located in the arm or forearm that move the forearm, wrist and hand. This section details the muscles of the upper extremity that enable movement of the arm (Carola *et al*, 1990).

1.3.5.1 SHOULDER AND UPPER ARM

Muscles in the shoulder act together to perform certain movements, such as lifting a heavy object in the hand. During elevation the muscles active include the trapezius, levator scapulae and the rhomboids. Those acting during depression include the pectoralis major, pectoralis minor and latissimus dorsi. Upward rotation uses the trapezius and serratus anterior whilst downward rotation uses the levator scapulae, rhomboids major and minor, pectoralis major and minor, and the latissimus dorsi.

The shoulder joint is stabilised by the four SITS muscles – supraspinatus, infraspinatus, teres minor, and subscapularis (figures 1.12 to 1.14).

Muscles that contribute to the flexion motion of the arm include the pectoralis major, deltoid, coracobrachialis and biceps brachii. Extension motion uses latissimus dorsi, teres major, pectoralis major, deltoid and triceps. Muscles that contribute to abduction are the supraspinatus and the deltoid whilst adduction uses the pectoralis major, latissimus dorsi, teres major, coracobrachialis, and the triceps (figures 1.12 to 1.14).

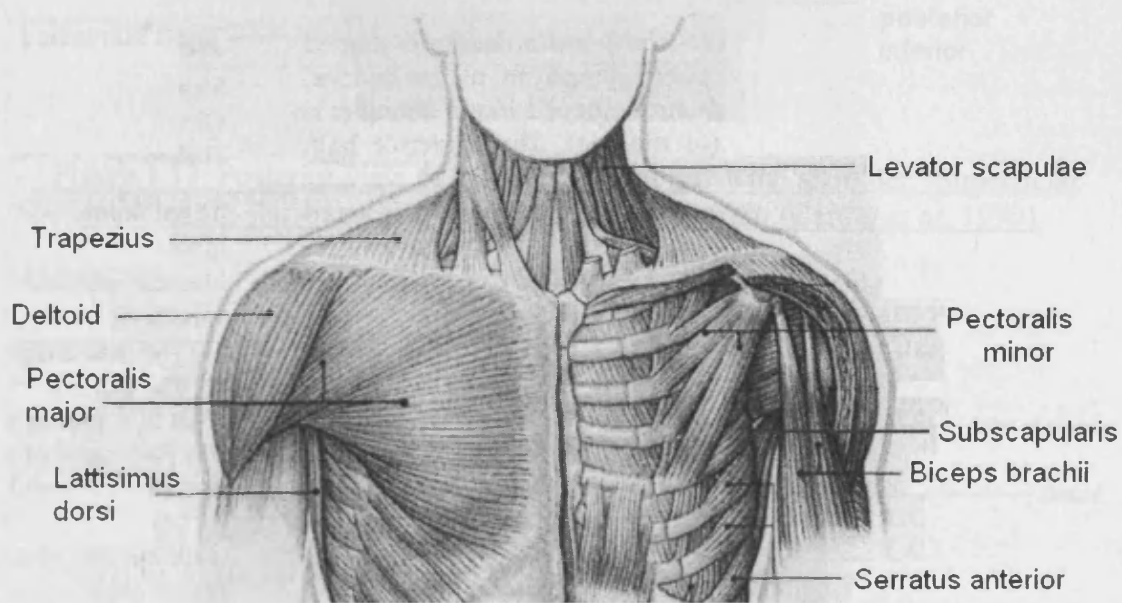


Figure 1.12: Anterior view of the muscles that move the shoulder. Superficial muscles are shown on left, deep muscles on the right (Carola *et al*, 1990).

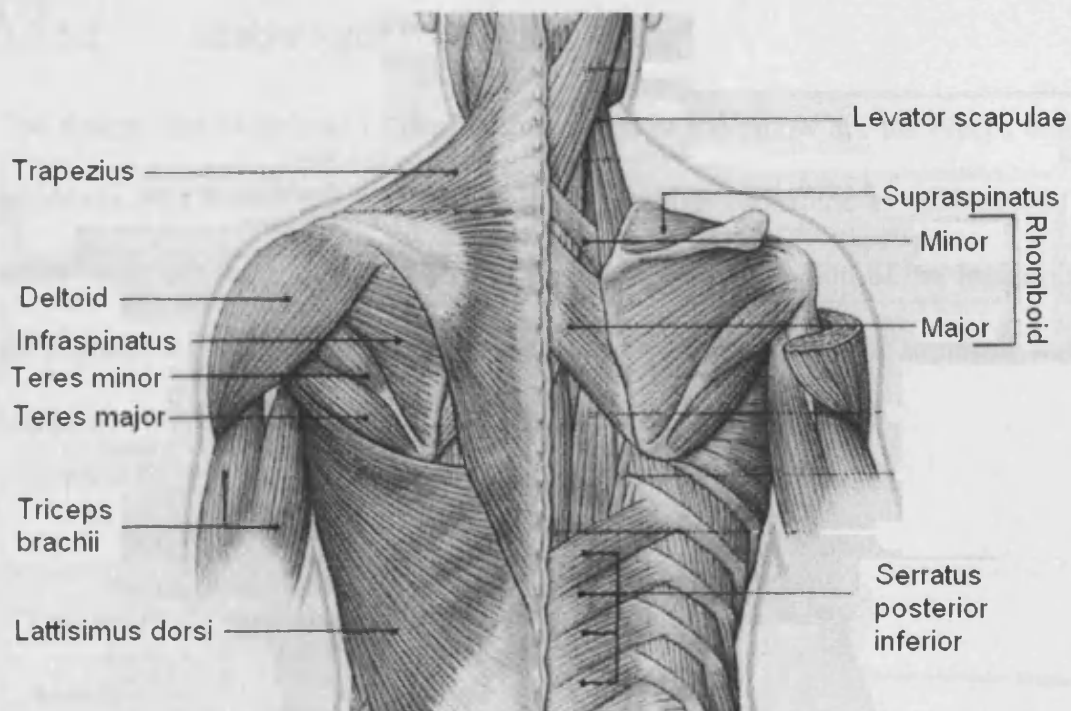


Figure 1.13: Posterior view of the muscles that move the shoulder. Superficial muscles are shown on left, deep muscles on the right (Carola *et al.*, 1990).

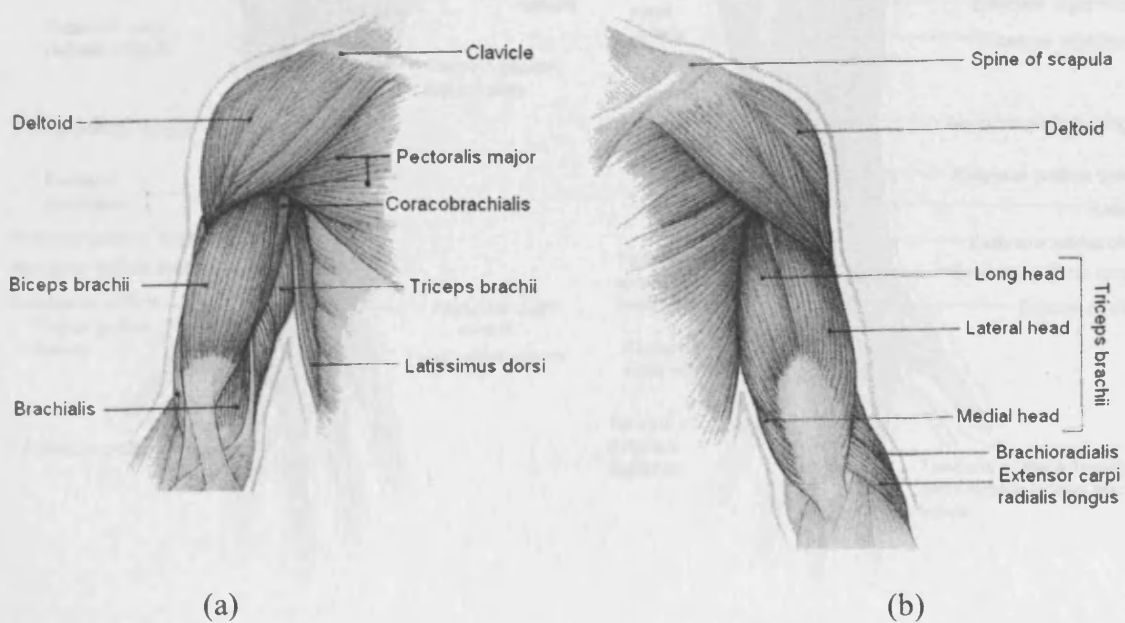


Figure 1.14: (a) Anterior and (b) posterior view of the superficial muscles that move the arm (Carola *et al.*, 1990).

1.3.5.2 ELBOW AND LOWER ARM

The flexors that contribute to flexion movement of the elbow are the biceps brachii, brachialis, and brachioradialis. The extensors, which contribute to extension of the elbow joint, are the triceps brachii and the anconeus. Pronation of the forearm uses the pronator teres and pronator quadratus whilst supination uses the supinator and the biceps brachii (figure 1.15).

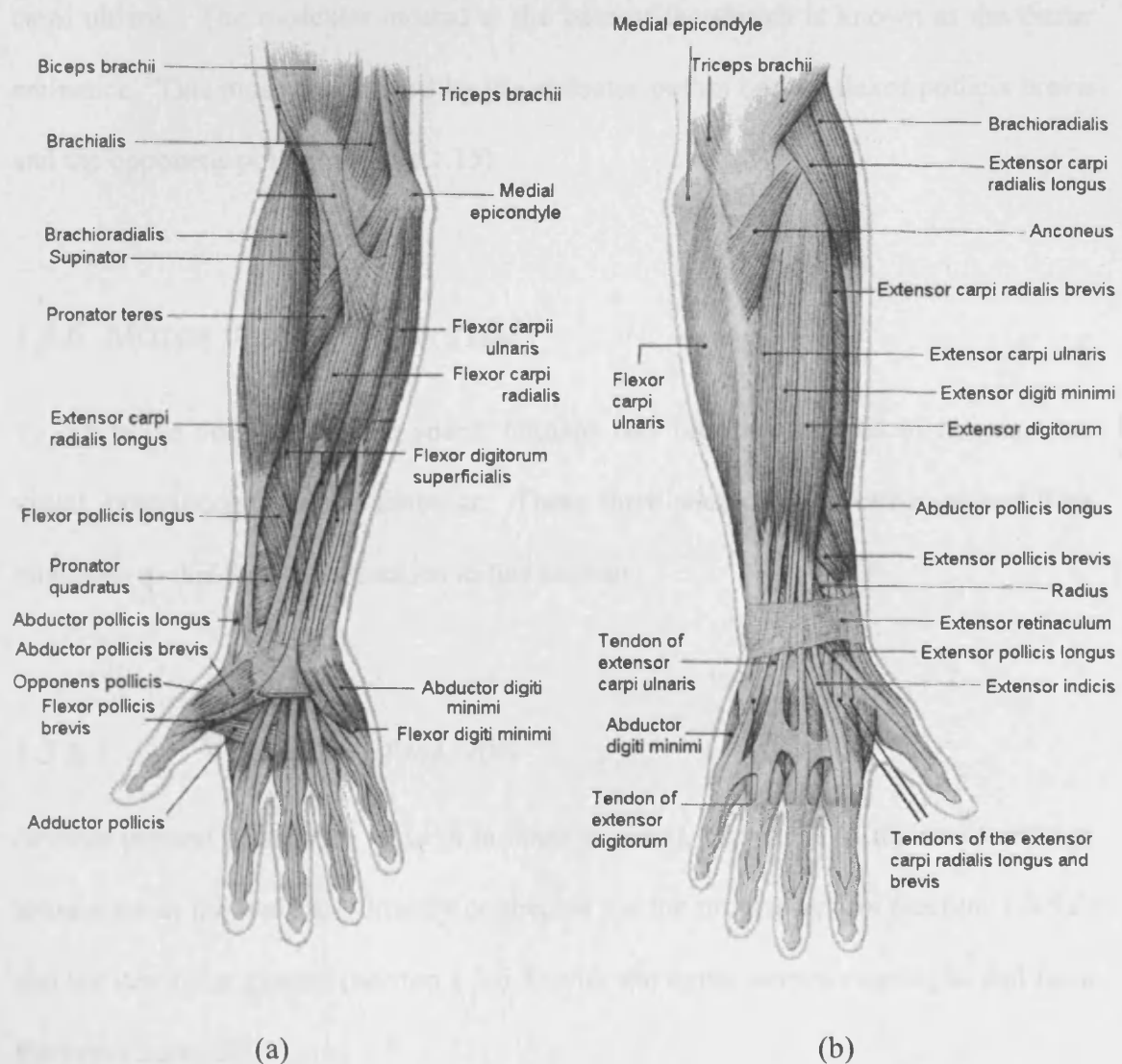


Figure 1.15: (a) Anterior and (b) posterior view of superficial muscles of the forearm and hand (Carola *et al.*, 1990).

1.3.5.3 WRIST AND HAND

Wrist flexion uses a group of muscles referred to as the forearm flexors. These are the flexor carpi ulnaris, flexor carpi radialis, and the palmaris longus. Similarly the forearm extensors, which perform wrist extension, are the extensor carpi radialis longus, extensor carpi radialis brevis, and the extensor carpi ulnaris. Abduction of the wrist uses the flexor carpi radialis, extensor carpi radialis longus and brevis, and the abductor pollicis longus. Adduction uses the extensor carpi ulnaris and the flexor carpi ulnaris. The muscular mound at the base of the thumb is known as the thenar eminence. This mound is formed by the abductor pollicis brevis, flexor pollicis brevis and the opponens pollicis (figure 1.15)

1.3.6 MOTOR VESTIBULAR SYSTEM

To determine ones position in space, humans rely on three sources of information: visual, proprioceptive and vestibular. These three sources of information and their relevance to this thesis are detailed in this section.

1.3.6.1 VISUAL INFORMATION

Seventy percent of sensory input in humans is visual, over 80% of the nerve endings to muscles in the body are directly connected via the proprioceptors (section 1.3.6.2) and the vestibular system (section 1.3.6.3) with the motor nerves running to and from the eyes (Boon, 2003).

When a person rapidly changes the direction of movement (for example during a fall), or even lean their head in a particular direction, they are not able to maintain a stable image unless they possess some automatic control mechanism to stabilise their direction of gaze of the eyes. Fortunately, when the head is suddenly rotated, signals from the semi-circular canals (section 1.3.6.3) cause the eyes to rotate in an equal but opposite direction to the rotation of the head. This enables, in the case of a fall, the eyes to gain a clear image of the surroundings even whilst moving rapidly towards the floor or surface (Guyton, 1991).

1.3.6.2 PROPRIOCEPTIVE INFORMATION

‘Proprioceptors are internal receptors located in and around the joints and muscles, in the skin, and in the inner ear. They respond to changes in the position and acceleration of body segments’ (Kreighbaum and Barthels, 1996).

The proprioceptors in the neck are particularly important. When the head is leaned to one side, by bending the neck, impulses from the neck proprioceptors keep the vestibular apparatus (section 1.3.6.3) in equilibrium. They do this by transmitting signals that equally oppose the signals transmitting from the vestibular apparatus. If they did not do this then the body would think it was falling over and try to compensate each time the head moved away from the centre line. However, if the entire body leans in one direction, the neck proprioceptors do not oppose the impulses from the vestibular apparatus and so the person will perceive a change in body equilibrium (Guyton, 1991).

Proprioceptors in other parts of the body are also important in the maintenance of equilibrium. For example, pressure sensations from the soles of the feet can tell a person if their weight is distributed equally between the two feet and whether the weight is more forward or backward on the feet (Guyton, 1991)

1.3.6.3 VESTIBULAR INFORMATION

The vestibular apparatus is an organ, which detects sensations of equilibrium. Part of this organ is called the semi-circular canals, which are located in the inner ear, and they provide information about gravity, balance and movement. These ducts, three in total, are filled with fluid and situated in different planes. At each end of the canals there is a wide opening with hundreds of tiny hair cells. When the head rotates in any direction the semi-circular canals rotate with the head causing the fluid to remain stationary. This causes the fluid to flow into the wide openings, which in turn moves the hair cells. These hair cells send signals to the central nervous system to tell it of any changes in the rate and direction of rotation of the head in the three planes of space.

1.3.7 MOTOR VESTIBULAR REFLEXES

When a person slips or stumbles, information from the sources discussed above (sections 1.3.6.1 to 1.3.6.3) is relayed quickly to the brain. The brain then sends signals, via the spinal cord, to stimulate motor neurones that, in turn, stimulate muscles to contract. The muscles that contract depend on the direction in which the person is falling, and act to re-establish the vertical orientation (balance) so as to avoid injury. Many of these corrective reactions are extremely fast and are

involuntary. These stereotypical involuntary postural adjustments are called reflexes. Postural reflexes are automatic and cannot easily be suppressed except with habituation or much training.

The collective term for the reflexes associated with the vestibular system are called motor vestibular reflexes, because the vestibular system, upon sensing a change in orientation of the head, signals to the motor (muscular) system to contract or “fire” certain muscles.

Motor vestibular reflexes during falling include ones that bend the trunk, others that raise the arms, and others that either flex or extend the forearm. The response time of these actions is very fast (in the order of 100 ms or less).

1.4 TRAUMA MECHANICS

This section details the types of injuries that are associated with a fall including injuries to the soft tissues (section 1.4.1) and fracture mechanics (section 1.4.2).

1.4.1 SOFT TISSUE INJURIES

Soft tissue injuries are those injuries affecting the joints and muscles of the limbs. Contusions, strains, sprains and dislocations are all considered to be soft tissue injuries. A brief description of each of these injuries are given below.

Contusion (or bruise) – Produced when a blunt impact ruptures small blood vessels, with bleeding into the adjacent tissues.

Abrasion – Produced by a rough surface striking the body tangentially and removing part of the outer layer of the skin

Laceration – Produced when a blunt object strikes the skin with sufficient force to stretch and tear it.

Strain – A strain involves the over-stretching of the major muscles of the limb. If a muscle is forced to stretch excessively then the tendons, which attach the muscle to the bone, will tear.

Sprain – This involves the over-extension of a joint, usually with partial rupture of the ligaments. There may also be blood vessel, nerve and tendon damage.

Dislocation – This is the complete displacement of 2 bones in a joint so that they are no longer in contact. Tearing of the joint ligaments may also occur and an injury severe enough to cause dislocation may also cause fracture.

1.4.2 FRACTURE MECHANICS

An understanding of how bones respond to loads that cause fracture is important in helping us to understand the forces that cause the damage. There are many classifications of injuries but unfortunately the same group of injuries may have more than one classification associated with it. The same injuries may also be classified differently in different countries.

A fracture indicates a complete or partial break in the continuity of a bone. Although there are many different ways to classify fractures there are three main areas in which fractures can fall in. These are described below (Paton, 1992 and Levine, 1993).

1.4.2.1 THE CAUSATION OF THE FRACTURE

a) Traumatic fractures

The majority of fractures are as a result of a trauma; either directly (using the arm to block an object causing a fracture), indirectly (a fall onto the outstretched hand where the force is transmitted up the arm) or a muscular pull.

b) Stress or fatigue fractures

A fatigue failure of a bone resulting from repeated microtrauma (repetitive stress).

c) Pathological fractures

A fracture occurs through an area of abnormal or diseased bone.

1.4.2.2 THE RELATIONSHIP OF THE FRACTURE TO THE SURROUNDING TISSUES

a) Simple (or closed) fractures

The skin and soft tissues are intact.

b) Compound (or open) fractures

The skin and soft tissues are damaged and there is exposure of the bone to direct outside contamination. These fractures are generally classified by wound size.

c) Complicated fractures

In association with the fracture other important structures have been damaged e.g. nerves, vessels, viscera (organs) or joints.

1.4.2.3 THE PATTERN OF THE FRACTURE

a) Complete (or non-comminuted) fractures

The bone is completely divided into 2 separate fragments. The fracture itself may be transverse (figure 1.16a), oblique (figure 1.16b) or spiral (figure 1.16c).

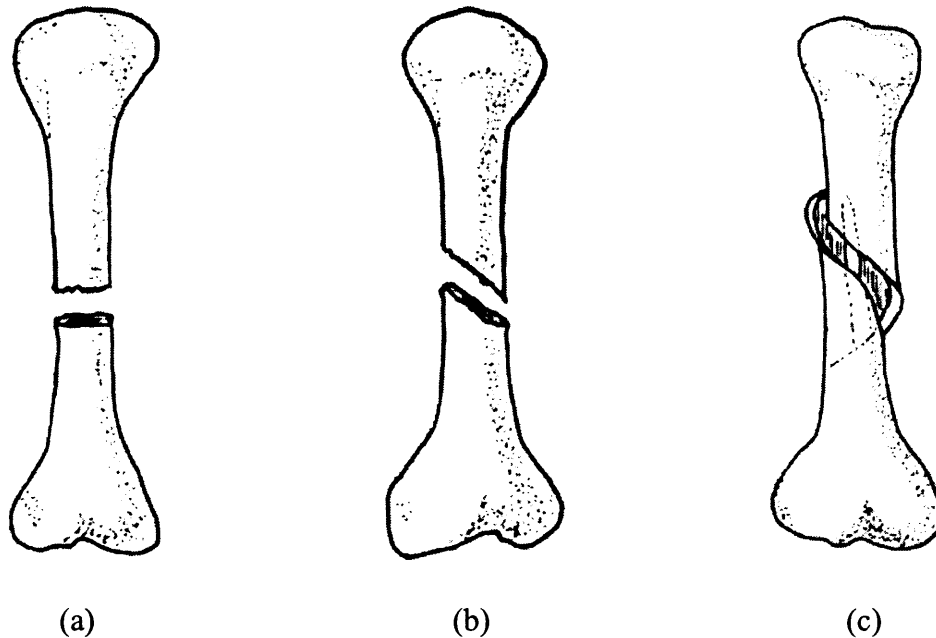


Figure 1.16: Examples of a non-comminuted fracture (a) transverse (b) oblique and (c) spiral (Levine, 1993).

b) Incomplete fractures

In children-only deformity is an angulation at the fracture site due to the elasticity of the bones. Known as a greenstick fracture.

In adults-the bone is compressed so fragments have been jammed together, slight bone shortening occurs but the fracture is stable.

c) Comminuted fractures

The bone is broken into more than two fragments (figure 1.17a). Specific examples of a comminuted fracture are a butterfly fragment (figure 1.17b) or segmental (figure 1.17c).

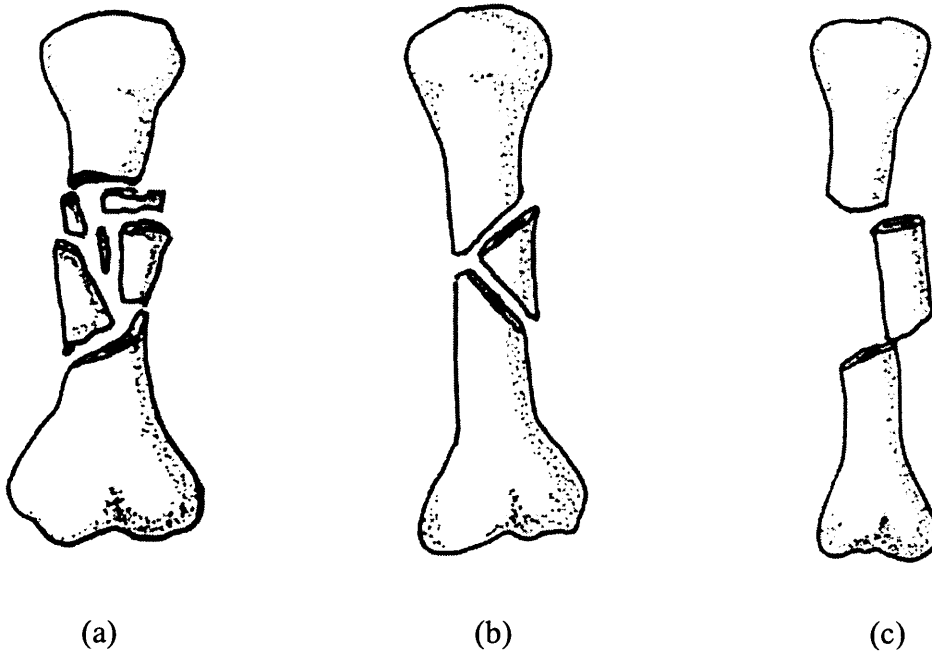


Figure 1.17: (a) A comminuted fracture, examples of which are (b) butterfly fragment and (c) segmental (Levine, 1993).

d) Compression or crush fractures

Usually occur in cancellous bone.

All fractures can also be described as either displaced or undisplaced. A displaced fracture is where one or more of the pieces of the bone has moved from its original position (figure 1.18a). An undisplaced fracture is where the bone fragments are still in their anatomical positions, there is simply a crack or cracks in the bone (figure 1.18b).

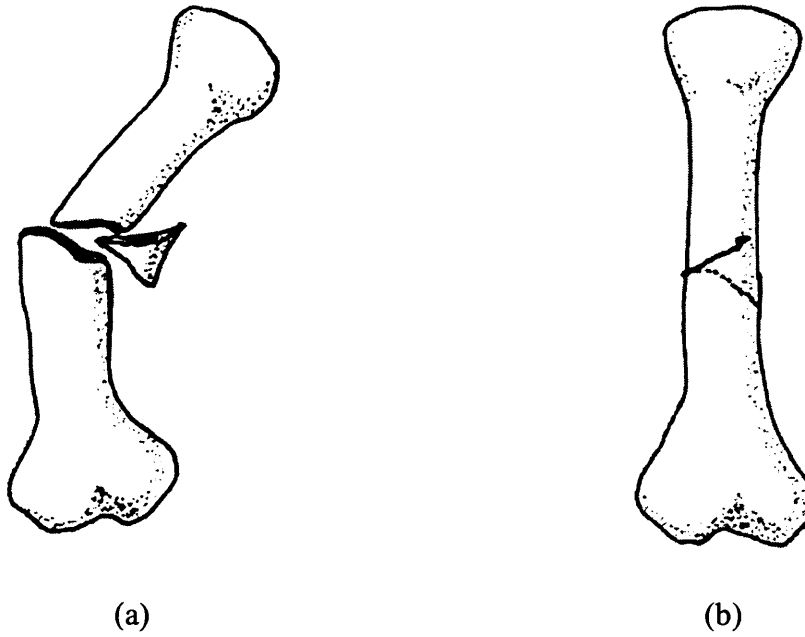


Figure 1.18: (a) displaced fracture (b) undisplaced fracture (Levine, 1993).

1.5 LITERATURE REVIEW

The distal radius is the most fractured bone in the human body. Over 90% of such fractures are caused by falls onto the outstretched hand. This section is a review of the current literature investigating the fracture forces of the distal radius and the assessment of falls onto the outstretched hand.

1.5.1 FRACTURE FORCES

The force required to fracture the distal radius has been investigated using cadaveric material (Frykman, 1967, Horsman and Currey, 1983, Myers *et al*, 1991, Myers *et al*, 1993, Spadaro *et al*, 1994). These fracture forces can be seen in table 1.1 below.

Table 1.1: Fracture forces from studies using cadaveric material.

STATIC LOADING STUDIES	Fracture Force (kN) (Mean fracture force shown in brackets)	
	Males	Females
Frykman, 1967	1.37 - 4.32 (2.84)	1.03 - 3.14 (2.08)
Horsman and Currey, 1983	N/A	1.72 and 6.52
Spadaro <i>et al</i> , 1994	0.66 - 2.62 (1.64).	

DYNAMIC LOADING STUDIES		
Frykman, 1967	3.43 and 4.31	1.86
Myers <i>et al</i> , 1991	3.21 - 4.27 (3.74)	2.18 - 4.18 (3.18)
Myers <i>et al</i> , 1993	1.95 - 2.79 (2.37)	0.98 - 2.18 (1.58)

Caution should be used when comparing these fracture forces with each other as there are many differences between the methodologies used in each study. These differences include; the age, condition and preparation of the cadaveric material, the position of the arm during loading, and the rate of loading used. All these factors would affect the amount of force required to fracture the arm. The sample sizes for each study also varied greatly.

A fall onto the outstretched hand is a dynamic event and while some studies did use dynamic loading, others used static loading. Bone is a visco-elastic material and therefore, its stiffness and amount of force required to fracture the arm will vary greatly depending on the rate of loading.

Caution should also be used when using the fracture force values found from these studies to assess fractures of the arm during falls onto the outstretched hand. During a fall onto the outstretched hand, neuromuscular and musculo-skeletal actions (motor vestibular reflexes) enable the fall to be arrested, attenuating the impact force to prevent a fracture from occurring. This would imply that the fracture forces found using cadaveric material may be below those that may occur during a fall onto the outstretched hand as neuromuscular and musculo-skeletal actions would not be present.

The fracture forces found from these studies should therefore, only be used as a guideline for investigating the forces required to fracture the arm and should not be used as threshold data for assessing the forces required to fracture the arm during a fall onto the outstretched hand. The following sections detail studies assessing falls onto the outstretched hand.

1.5.2 FALLS ONTO THE OUTSTRETCHED HAND

1.5.2.1 FALLS DUE TO TRIPS AND SLIPS

Hsiao and Robinovitch (1998) conducted studies to assess whether, in the event of an unexpected slip, young adults use common movement strategies to prevent falls and achieve safe landings. The authors hypothesised that; young subjects were less likely to fall after sideways perturbations to balance than backwards perturbations; young subjects impact their wrist before their hip to protect from hip fracture; regardless of direction of perturbation young subjects would avoid impact to the lateral aspect of the hip.

Three males and three females were subjected to a simulated slip scenario in which a gymnasium mattress, which they were standing on, was moved abruptly by means of a spring-actuated platform. The instruction given, was in the event that the platform moved they should 'try to prevent themselves from falling' and 'prior to platform movement, they should maintain their gaze directed forward and at eye level' (Hsiao and Robinovitch, 1998).

Hsiao and Robinovitch (1998) used a 6-camera motion analysis system with 20 markers placed at various anatomical landmarks [Motion analysis uses sophisticated kinematic motion capture and analysis equipment to accurately measure the kinematics of human movement in terms of displacement, velocity and acceleration. The co-ordinates of reflective marker sets, attached to a moving object, are measured using infrared video cameras.]. The trials were categorised by balance recovery and then only complete falls (where contact to the trunk and/or pelvis occurred) were further analysed to determine the time of contact and velocity of the wrist and pelvic markers.

Their results showed that perturbation direction strongly influenced the subjects ability to recover balance, with all subjects being more effective at recovering after a simulated forward and sideways falls as opposed to a backwards fall. Stepping was found to be the predominant balance recovery technique for all subjects. They found that wrist contact was observed in all the falls and was nearly as likely to occur at the pelvis before the wrist as vice versa.

The authors observed a consistent sequence of upper extremity movements to preventing the falls. 'This involved an immediate upward movement of the wrist, followed by a rapid downward movement, and a second upward acceleration just prior to impact. Head impact was observed in only five falls, three of which involved the same subject' (Hsiao and Robinovitch, 1998). They also found that trunk rotation occurred in falls to the side, which allowed subjects to break their falls with both hands and avoid impacting the lateral aspect of the hip.

Another study (Smeester *et al*, 2001) considered recovery from trips of increasing severity during gait on a level surface. 21 subjects (10 male, 11 female) volunteered for the study in which lower extremity strength, reaction time, step time, step distance and step velocity for a volitional stepping task was measured.

The disturbance threshold was defined as the magnitude of a disturbance that is just sufficient to provoke an uncontrollable fall, even if fall-arresting attempts were made. A four-camera motion analysis system was used with 12 markers. Trips were induced by suddenly interrupting the spooling of a cable, attached to an ankle cuff worn by the subject on the dominant leg, at mid swing.

They found that threshold trip duration for which recovery was no longer possible was significantly associated with lower extremity strength and volitional reaction time. This suggests that some trip related falls may be due to slower reaction times and/or reduced lower extremity strengths. Falls are likely to occur when the trip duration is greater than an individual's ability to recover.

Unfortunately, the authors were not able to record an accurate and precise measurement of the reaction time during the trip, due to technical limitations.

1.5.2.2 SIDEWAYS FALLS

Kroonenburg *et al* (1996) studied hip impact velocities and body configurations for a voluntary fall from standing height. One of the questions they addressed was, whether the use of an outstretched hand influenced the fall kinematics.

Six subjects (19-30 years) were instructed to launch themselves sideways onto a 0.6 m high crash mat (off a platform 0.12 m below the top of the crash mat) and subsequently to either fall as relaxed as possible, or to fall as naturally as possible. In the cases where the subjects were instructed to use their arm to break the fall, only two subjects were able to do so. The others impacted initially with their hip and then the hand.

A shortcoming with this methodology, is that the falls were not unintentional and because of this, volunteers were likely to have performed a predefined fall response, rather than a natural fall response, despite being instructed to fall naturally. Also, a fall onto a foam mattress may not induce the same reflexive response as a fall onto a hard floor as there is no immediate danger to the subject, if the fall is not fully arrested. This may explain why some subjects did not use their arm to arrest the fall.

The subjects used in this study were all young athletes, most of them active in sports in which falls are encountered regularly. This suggests that they may have already had some knowledge of how to arrest a fall efficiently.

Sabick *et al* (1999) conducted a similar study assessing the impact forces at the hip and shoulder during falls to the side. The subjects knelt beside a force plate array covered in foam padding, with their arms folded across their chest and were instructed to initiate a fall to the side. The subjects had to fall as relaxed as possible and if they heard a cue after the onset of the fall had to either perform a 'tensed fall' or a 'break fall' (depending on which set of falls was being tested). All of the subjects were from an Aikido club and therefore had experience in performing break falls.

The authors found that 'break falls' resulted in the lowest peak resultant hip and shoulder force values and that 'tensed falls' resulted in the largest resultant hip and shoulder force values.

The falls in this study were not unintentional but unlike the previous study by Kroonenburg *et al* (1996), the fall condition was unknown to the subject at fall initiation. Sabick *et al* (1999) stated that this 'eliminated any possibility that the initiation of the fall would be influenced by prior knowledge of the fall to be performed'.

However, the subjects knew that the fall would either be as relaxed as possible or one of the two pre-defined falling techniques. As the tensed falls and the break falls were tested separately, they would have already had a pre-determined response, depending on whether or not a cue was heard. Therefore, it could be argued that the subject did have prior knowledge of the fall to be performed.

Another limitation of this study by Sabick *et al* (1999) is the fact that all the subjects were from an Aikido club and therefore, knew how to effectively perform a break fall to the side. These break falls are intended to reduce the force imposed on the body at impact and it is of no surprise that the authors found this method of falling to produce the lowest resultant force values.

It is noteworthy, that in this study 'using the arm to break the fall' resulted in a somewhat different fall arrest strategy than might be seen in someone who is not trained in how to fall. Subjects who are trained in break falls tend to strike the impact surface with both the hand and forearm simultaneously rather than falling onto the outstretched hand. This was observed to happen in all of the break falls conducted in the study. The differences in these two fall arrest strategies may well affect the risk of upper extremity injuries.

1.5.2.3 FORWARD FALLS

Until recently few investigators have quantified the biomechanics of forward falls onto the outstretched hand, in an experimental context/laboratory setting. The first reported study by Dietz *et al* (1981) conducted forward falls on 27 healthy male subjects between 20 and 35 years. Subjects were asked to 'self-initiate forward falls with bodies straight and arms nearly extended, landing with both hands on a platform of variable height (standard falling angles between vertical and platform level were 50, 60, 70, 80 and 90°)'. Falls were conducted, first under visual control and then the subjects were blindfolded and the tests repeated. The fall height was varied at random.

The fall arrest strategy for a fall with visual control, compared to a fall without visual control, will vary due to the lack of visual information to the vestibular system. It is likely that during a fall without visual control, the muscles in the upper extremity will be firing from the start of the fall as the volunteer is unaware where the 'floor' is. During a fall with visual control, the visual information will be used in conjunction with the proprioceptors to enable the reflexes to initiate an appropriate fall arrest strategy.

The majority of the study was concerned with the electromyography (EMG) profile of proximal muscles, which are discussed in section 1.5.5. However, they also assessed the visual physiological aspects of the falls with the associated impact forces. To do this the falls were recorded using cinematography (capture rate 60 frames per second) and five piezo-electric force transducers were attached to the platform, one at each corner and one in the middle, to record the force exerted by each arm onto the platform.

The subjects were observed to impact the ground first, with their fingertips, before contact was made with the ball of the thumb. This impact force, shown in figure 1.19, showed a two-stage increase in the initial force peak, which was attributed to the fingertip impact followed by the ball of the thumb.

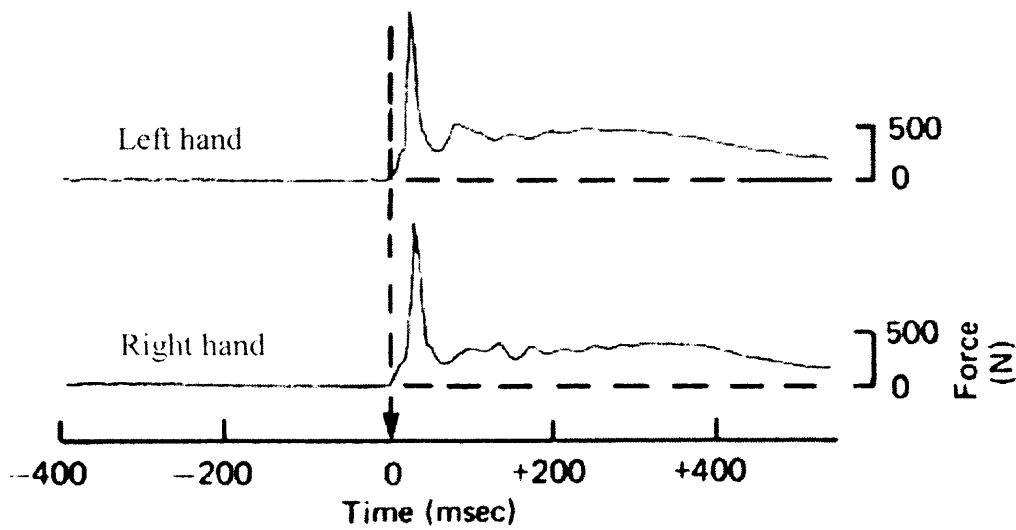


Figure 1.19: Impact force for fall onto floor (90° from vertical) (Dietz *et al*, 1981).

Other subjects were instructed to land directly onto the ball of the thumb with strong dorsiflexion of both hands, which produced the impact force shown in figure 1.20. Observations of this impact force show the initial force peak to rise quickly without initial creep.

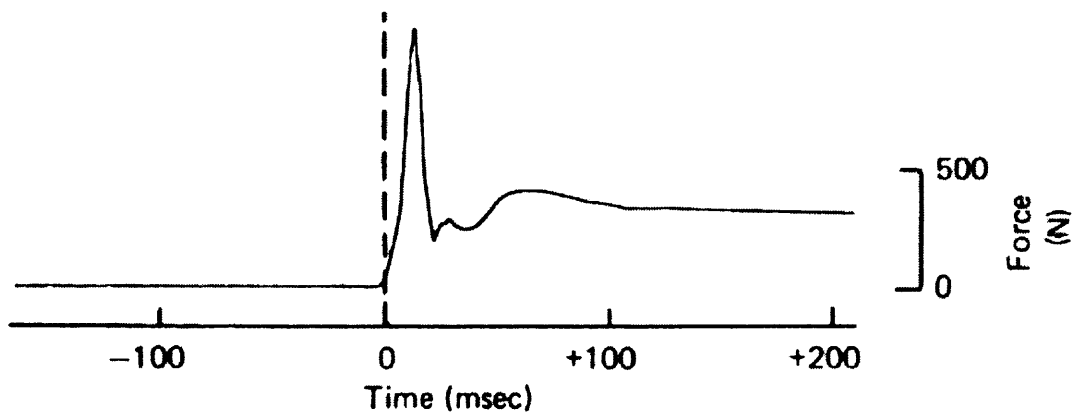


Figure 1.20: Impact force for fall onto platform inclined 70° to the vertical. (Dietz *et al*, 1981).

Unfortunately, they do not report the range of impact forces produced during their experiments. However, estimations from the force-time graphs shown in figures 1.19

and 1.20 show the impact force to be approximately 1100N for a fall onto the platform inclined at 70° from the vertical and approximately 1300 to 1400N for a fall onto the floor (90°).

Chiu and Robinovitch (1996, 1998) were the first reported researchers to conduct studies on human subjects to evaluate the forces produced in the upper extremity during low-level, non-injurious, forward falls (up to 5 cm) onto the outstretched hand. They conducted a series of experiments dropping human volunteers (8 male and 8 female) onto force plates.

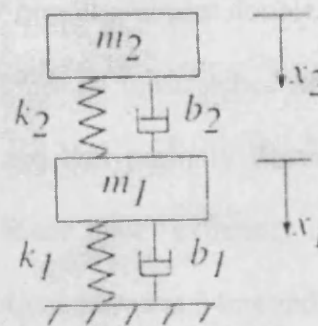
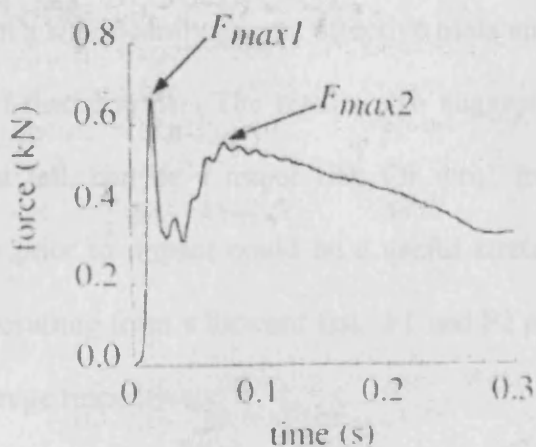
The volunteers assumed a 'one-handed push-up' position with the hand resting on a force plate and the knees on the ground. The forearm was orientated at 15° to the vertical, and the leg was orientated at 30° from the horizontal. This loading configuration was taken from Frykman (1967) as the most common configuration likely to produce Colles' fractures. However, it should be noted that the loading configuration in Frykmans (1967) study was used on cadavers of elderly subjects using static loading, whereas, the volunteers in Chiu and Robinovitch's (1996, 1998) study were all of a relatively young age and were subjected to a dynamic, and not a static, event.

It is also noteworthy, that Frykman's (1967) study did not take into account damping and stiffness values of the elbow and upper arm as the cadaver specimens were cut below the elbow before testing. In addition, there was an obvious lack of neuromuscular and musculo-skeletal physiological responses that would exist during a fall onto the outstretched hand in living subjects.

In the first set of experiments by Chiu and Robinovitch (1996, 1998), the torso rested on a rigid platform and the hand was lifted, via a cable attached to a glove, to decrease the contact force by approximately 50N. The next set of tests assumed an identical position, but with the torso support removed. Again the hand was raised off the force plate to decrease the contact force, this time by 50-100N. The final experiment was identical to the previous tests except the hand was raised off the force plate to a height of 1, 3 or 5cm. In all the tests the volunteers were instructed to maintain their elbows in a 'fully extended' position prior to, and during, impact.

Chiu and Robinovitch (1996, 1998) stated that common experience suggests that falling onto an extended elbow was not typical of actual falls but they used this position since they claimed it represented a 'worst-case falling scenario'. Practically speaking, however, if the position of a fully extended elbow is not typical of a physiological response to a fall, there seems little use in using it, even as a 'worst-case falling scenario'.

Their results show that 'falls onto the outstretched hand are governed by an initial high-frequency peak force [F_{max1}] and a subsequent, lower-frequency oscillation [F_{max2}]' (Chiu and Robinovitch 1996, 1998), which can be seen in figure 1.21 (a). F_{max1} and F_{max2} occur approximately 20 ms and 110 ms after impact respectively. The authors also simulated this using a two-degree-of-freedom lumped-parameter mathematical model as shown in figure 1.21 (b), assuming minimal elbow flexion during impact.



(a)

(b)

Figure 1.21: (a) Impact response of the body during forward fall onto the outstretched hand showing force peaks F_{max1} and F_{max2} (b) Two-degree-of-freedom lumped-parameter mathematical model (Chiu and Robinovitch, 1998).

The authors suggested that F_{max1} is influenced greatly by fall height and F_{max2} is affected by body mass, although both parameters will have an affect on both F_{max1} and F_{max2} .

Kim *et al* (1997) used force plates mounted on a wall (inclined at 10° to the vertical) and then used equations and least square estimates to predict peak ground reaction forces for a full fall to floor level. Testing the hypothesis ‘that elbow flexion angle does not affect hand impact forces when using both hands to arrest a forward fall’ they tested 11 young males, using two arm configurations; fully extended and half flexed. These arm configurations were held fixed throughout the fall, while the distance between the force plates and hands was kept at 20 cm for all the falls.

The authors state that the ground impact force always showed a *bimodal* shape with two characteristic peaks, maximum impact force (F_1) and maximum braking force

(F2). The results demonstrated that falls onto an outstretched arm (fully extended) result in a significantly greater effective mass and higher impulse, almost double those for half-flexed arms. The results also suggest that the use of outstretched arms to arrest a fall, can be a major risk for wrist fractures and that partially flexing the elbows prior to impact could be a useful strategy to reduce upper extremity impact loads resulting from a forward fall. F1 and F2 peak forces occurred at 34ms and 44ms on average respectively.

Following this study Kim and Ashton-Miller (2003) conducted a study to try and isolate critical biomechanical factors in fall arrests using the upper extremity, during simulated forward falls in both young and old age groups. They state that 'from a biomechanical point of view, falls from a standing height can generate enough energy and force to fracture the hip and wrist'. In their study they simulated 'bimanual forward falls in an attempt to understand the effects of various postural disturbances on the fallers protective response and the subsequent impact force at the hand' (Kim and Ashton-Miller, 2003).

Force plates, covered with a 1.9 cm thick wooden plate, were attached to the wall inclined at a 10° vertical angle. The subjects (10 healthy older males and 10 young males) stood on a narrow platform to prevent ankle plantar flexion during the fall and wore a safety harness attached to the waist.

In the first set of tests, the subject volitionally initiated the fall, arresting it with both hands. In the second set of tests, the subject was leaned at a 10° angle, via a cable

attached to the harness and was released after a random time delay, again arresting the fall with both hands.

The decision to stand the volunteers on a narrow platform was to prevent them from resisting the fall by plantar flexion of the ankle, i.e. they could not push back off the floor to resist being inclined at an angle of 10° to the vertical. This essentially ensures that the subjects are in free fall when the release mechanism is activated. The set up diagram for these falls is shown in figure 1.22.

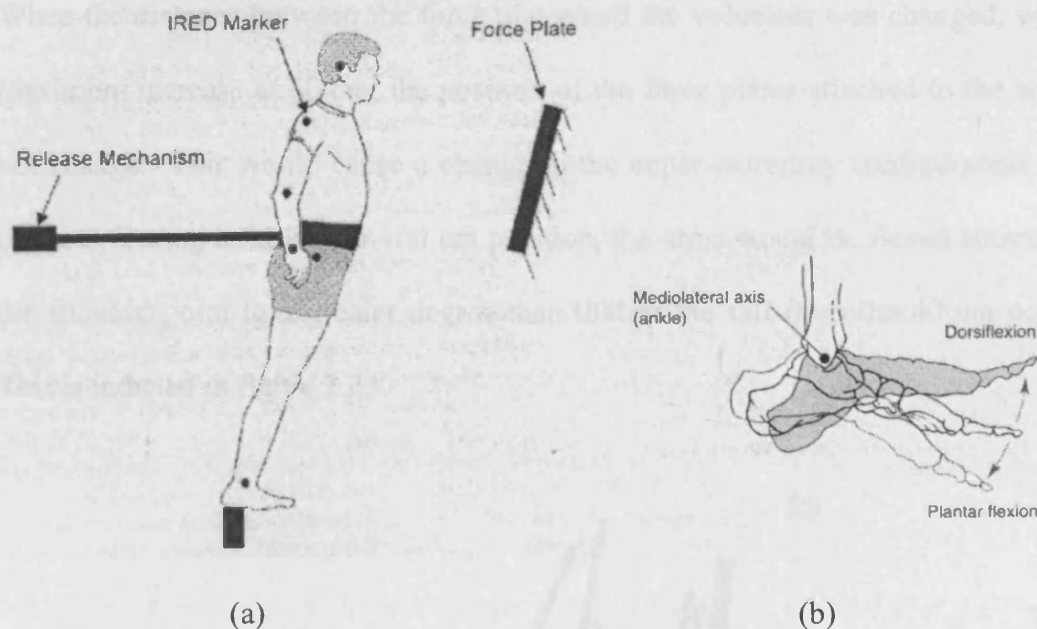


Figure 1.22: (a) Cable released fall experiment set up (Kim and Ashton Miller, 2003)
(b) Diagram showing ankle movement (Kreighbaum and Barthels, 1996).

Similar to the previous study, conducted by Kim *et al* (1997), this study had subjects falling onto force plates at an almost vertical angle. A shortcoming with this methodology is that the volunteer's response would be different in this falling scenario compared with a fall to the floor (even from short heights) due to the motor vestibular responses of the human body (see section 1.3.6). Combined with the visual

information, the 'perceived danger' of the fall would be less and may have affected the response time of the volunteers to arrest the fall.

The distance between the standing platform and the force plates was varied at intervals of 20 cm from 40 cm to 100 cm. An OPTOTRAK motion analysis system was used with 6 infrared-emitting diode markers. The kinematic and force plate data were synchronised externally and only force data for the right hand was reported, due to the bilateral symmetry of the measured force profiles.

When the distance between the force plates and the volunteer was changed, with the maximum increase at 60 cm, the position of the force plates attached to the wall did not change. This would cause a change in the upper extremity configuration during impact. During a fall in the 100 cm position, the arms would be flexed anteriorly at the shoulder joint to a greater degree than that of the fall from the 40 cm position. This is indicated in figure 1.23.

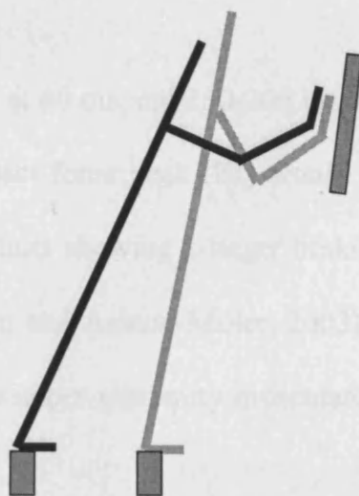


Figure 1.23: Diagram showing the different positions of the arm during falls at two distances from vertically positioned force plate.

The net result would be a change in shoulder position that would affect which muscles were used to arrest the fall.

In the 100 cm position the pectoralis muscle groups, anterior deltoid, trapezius and latissimus dorsi of the upper thoracic region would be used to a greater degree, than in the fall from 40 cm, where the majority of muscular response would occur in the bicep and tricep muscle groups of the upper arm. This would have an affect on the peak impact forces, response time and ability to fully arrest the fall. Extending the fall scenario to the floor (as performed in the previous study by Kim *et al* (1997) would result in an unrealistic fall arrest strategy.

Results showed that, once the arms had been elevated by flexing the elbow and shoulder joints, the subject extended the arm to position the hand before impact and further extended the arm during impact. After impact the subjects showed further increased wrist extension and elbow flexion and decreased shoulder flexion. Fall impact loading were approximately 50-80% of the body weight at each hand.

Force impact peaks occurred at 60 ms and 150-200 ms for F1 and F2 respectively. It was found that a higher impact force peak (F1) would cause a higher braking force peak (F2), with the young adults showing a larger braking force for the same degree of impact. The authors (Kim and Ashton-Miller, 2003) suggest that this indicates a higher activation level of the upper extremity musculature and this achieves a faster braking of the body motion.

Significant age differences were discovered in both joint kinematics and impact force parameters at close distances. Excessive reflexive responses of the upper extremity in cable-released falls for the older males resulted in 10-15 times higher peak impact forces and 2-3 times shorter body braking time than in self-initiated falls. The authors conclude that 'pre-impact activities of the upper extremity predispose the post-impact response during fall arrests. Suppressing excessive pre-impact reflexive activation of the arms could efficiently decrease the risk of fall related injuries, which calls for securing sufficient arm movement time' (Kim and Ashton-Miller, 2003). They suggest that increasing the arm movement time during a fall arrest strategy, could be effective against upper extremity injuries during falls in the older adult.

'The findings will help to understand underlying mechanisms of fall arrest using the upper extremity for prevention of fall related fractures'. (Kim and Ashton-Miller, 2003)

Chou *et al* (2001) investigated the effect of two different fall arrest strategies on upper extremity loading in a fall using three-dimensional motion analysis. The objective was to develop a biomechanical testing model for a simulated fall situation, incorporating two different fall heights and two elbow postures.

Using motion analysis equipment, volunteers were dropped onto force plates using one of two actions, either: (1) flexing the elbow slightly on impact or (2) maintaining elbow extension at impact. The authors were testing the hypothesis that fall height and fall arrest strategies would not significantly affect the ground reaction impact magnitude or the peak joint moments required to arrest the fall.

Eleven healthy male volunteers were asked to repeat each action twice, once at 3 cm and once at 6 cm. A force plate was used to measure vertical and two shear forces as well as the location of the centre of the palm and the moment about the axis normal to the force plate during the fall experiment.

Unfortunately the authors (Chou *et al*, 2001) do not explain the methodology for their study, so it is unclear what position the volunteers were in before the onset of the fall or how the fall was initiated. It is assumed that they followed the same methodology as Chiu and Robinovitch (1996, 1998) as that study is mentioned on numerous occasions throughout the paper.

It is noteworthy, that the findings of Chou *et al* (2001) were similar to that of Chiu and Robinovitch (1996, 1998) in that a high-frequency peak and a lower-frequency peak depicts the time history of the ground reaction forces of all the volunteers taking part in the extension experiments. Also, the fall height significantly affected the maximum impact force. As the fall height increased, the impact force increased.

The authors (Chou *et al*, 2001) also found that the first impact force peak (F_{max1}) decreased during tests where the volunteers flexed the elbow at impact and the time of the second impact force peak (F_{max2}) was delayed. They claim that this mechanism would significantly reduce upper extremity injury because the musculo-skeletal system would be able to absorb more of the impulse by delaying F_{max2} and decreasing F_{max1} .

In conclusion, the authors (Chou *et al*, 2001) state that flexing the elbow at impact results in less axial upper extremity force and delays the maximum ground reaction force therefore, providing enough time to adjust and avoid the injury.

The observations made from the tabulated results of their study, shown in figure 2.6, however, do not fully correlate with their conclusions.

Table 2
Mean (SD) measured (GRF) and calculated forces (in % body weight) for each fall height and arrest strategy

Fall height	Action			
	Extend elbow	Extend elbow	Flex Elbow	Flex Elbow
	3 cm	6 cm	3 cm	6 cm
GRF (vertical)	57.2 (8.8)	59.3 (13.2)	57.0 (11.6)	61.1 (11.3)
<i>Calculated joint force</i>				
<i>Wrist</i>				
Axial force	49.4 (12.8)	54.5 (11.8)	52.7 (11.4)	55.5 (10.9)
A/P shear force ^a	12.6 (10.3)	8.2 (3.4)	9.8 (3.9)	11.2 (3.6)
M/L shear force ^b	5.4 (2.2)	7.3 (1.5)	6.5 (3.7)	6.5 (2.4)
<i>Elbow</i>				
Axial force	49.2 (7.3)	50.4 (9.5)	48.6 (10.2)	52.1 (9.5)
A/P shear force ^a	8.3 (2.1)	6.3 (0.3)	4.7 (1.6)	5.5 (0.9)
M/L shear force ^b	6.2 (3.6)	7.2 (5.7)	10.3 (3.0)	10.1 (3.1)
<i>Shoulder</i>				
Axial force	38.9 (8.0)	38.7 (12.1)	38.2 (13.2)	42.6 (11.2)
A/P shear force ^a	24.1 (11.0)	20.6 (12.0)	32.6 (6.5)	33.1 (3.7)
M/L shear force ^b	7.5 (2.5)	8.3 (5.8)	13.1 (5.0)	13.1 (4.7)

^a Anterior/posterior. Positive values mean anterior force and negative values mean posterior force.

^b Medial/lateral. Positive values mean lateral force and negative values mean medial force.

Figure 1.24: Tabulated results from Chou *et al*, 2001.

The highlighted values in figure 1.24 are the only sections where a decrease between using the extended elbow and the flexed elbow occurs. The axial force appears to increase at the wrist, from a fall height of 3 cm, and in all areas of the arm from a fall height of 6 cm.

The results from the above study must therefore, be used with extreme caution when assessing the effect that elbow flexion has on the impact forces of the upper extremity, due to a fall onto the outstretched hand.

DeGoede and Ashton-Miller (2002) conducted a study to assess how fall arrest strategy affected the peak hand impact force during a forward fall. Subjects stood on a force platform and leaned forward against a supporting tether attached at the waist such that approximately 30% of their bodyweight (BW) was supported by the tether. Flexing at the hips lowered the shoulders to 1 m from the ground and the subjects were allowed to position the upper extremities in any configuration in preparation for the fall.

They were instructed to arrest their forward fall with their arms upon release of the supporting tether. Each hand contacted a force plate covered by 2.4-cm thick compact rubber foam and the kinematics of the left side body segments was measured using 11 infrared markers and an OPTOTRAK 3020 motion analysis system. Electrodes were also placed onto the skin to measure the electrical activity of the skeletal muscles by electromyography (EMG) of eight muscles in the upper arm, neck and chest areas. Unfortunately the results from the EMG tests are not fully reported so it is difficult to draw any valid conclusions from their results.

The results from this study (DeGoede and Ashton-Miller, 2002) do however, show that when subjects were instructed to minimise their impact force, they could significantly lower the peak force applied to their wrists upon impact with the floor. They demonstrated that they could voluntarily reduce the peak ground reaction forces

applied to the distal forearm during a fall arrest. Most of the reduction in force was achieved at impact by flexing the elbows slightly (11°), as well as by reducing the velocity of the hands relative to the torso to zero.

It is speculated that, if older adults could demonstrate the capacity to make these fall arrest strategy modifications, then the use of a minimum-impact strategy in falls could substantially reduce the risk of upper limb fracture in that population. The notable variability in fall arrest strategy can help explain the paradox of why, in a fall from the same height, healthy wrist bone may fracture, but osteoporotic bone may not.

Lo *et al* (2003) tested the hypothesis that after a brief 10-minute intervention young adults could volitionally reduce fall related wrist impact forces. Twenty-nine healthy young males were recruited and assigned to one of three groups. The three groups consisted of a 3-month intervention group, a 3-month control group and a baseline control group.

This study was a follow up of the aforementioned study by DeGoede and Ashton-Miller (2002), incorporating a control group into the study and therefore used the same equipment and methodology that was described above in the DeGoede and Ashton-Miller (2002) study.

When released, the subjects were instructed to 'arrest the fall with both hands'. All groups performed 5 falls, without instruction and then the 3-month intervention group were given a 10-minute instructional session on how to reduce the impact on the hands, by minimising the hand ground velocity at impact. Both the 3-month

intervention and 3-month control group were then asked to complete 5 more falls after a 10-minute rest break, (the baseline group did not take any further part in the study) and again, without further instruction, at 3 week and 12 week follow-up visits.

It was observed that after the 10-minute instructional session, the subjects demonstrated an 18% reduction in the magnitude of hand impact force while arresting a forward fall and led the authors to conclude that this reduction was due entirely to the educational instructions. However, in the absence of practice they could not retain their learning effects after 3 weeks, although at 3 months there was a significant reduction which may suggest that learning had occurred from the previous two visits.

The authors assume that Colles' fracture is associated with F_{max1} , the first peak in the wrist impact force, reaching the ultimate strength of the bone. They state that 'if this is true then even a 9% decrease in $F_{max}[1]$ can make the difference between fracture and no fracture when $F_{max}[1]$ nears the injury threshold' (Lo *et al*, 2003).

It is unclear how the authors claim that a 9% decrease in F_{max1} would reduce fractures considering that the fracture threshold of the arm due to falls onto the outstretched hand is at present, unknown.

The authors (Lo *et al*, 2003) suggest that repeated falls may lead to individuals teaching themselves to improve their fall-arrest techniques, which would therefore reduce their risk for a fall-related injury. They acknowledge that it is unknown whether these results could be extrapolated to other members of the population such as healthy young women or healthy older adults.

1.5.3 OTHER STUDIES ASSESSING FORCES IN THE ARM DURING A FALL

Other researchers have assessed the force in the arm during a fall onto the outstretched hand by assessing the time taken for adults to move their upper extremities into position to arrest a fall.

DeGoede *et al* (2001) considered the effect that age and gender had on the time required for healthy adults to move their upper extremities into a protective posture. 40 subjects volunteered, split equally into gender and age groups (young and old), to perform a seated movement task under three conditions perceived as no-threat, low-threat and high-threat. The tasks involved a swinging pendulum, which swung toward the subject in an antero-posterior direction.

In the no-threat task the pendulum was not swung toward them but subjects had to raise their hands forward (initially placed on the thighs) as quickly as possible to a stationary 'target' keeping an elbow angle of 120° with their fingers pointing upwards. In the low-threat task they had to arrest the swinging pendulum, but were cued as to its release. Similarly, in the high-threat task the swinging pendulum was released, but this time the subjects were asked to wait as long as possible before initiating the movement of their arms, thus getting into position "just in time".

The tests were measured using an OPTOTRAK system with markers placed on the arm, chair and impactor (pendulum) head. The movement time ranged from 226 to 292 milliseconds (ms), suggesting that a healthy adult should have sufficient time to deploy the hands properly to arrest a fall to the floor (a fall to the floor taking approximately 700 ms (Hiaso and Robinovitch, 1998)).

The authors (DeGoede *et al*, 2001) did comment however, that there is a speed-accuracy trade off which would mean that tasks involving greater accuracy, for example grabbing a support rail to arrest the fall, may take longer. They conclude that although they did observe significant slowing of movement time with age, it did not appear to be great enough to affect the biomechanics of fall arrests with the arms.

Further to this study DeGoede *et al* (2002) conducted a similar pendulum study, considering the effect of elbow flexion in a forward fall as well as gender and ageing-related declines in muscle strength, and relative velocity of the hands to the torso at impact. Their studies focused mainly on fall arrest strategies.

In the first study the authors tested the hypothesis, both experimentally and using a dynamic model, that neither initial elbow flexion angle, nor the velocity of impact of the mass relative to the hands at the time of impact, significantly alter impact forces on the hand. The second hypothesis tested was, at impact, hand and shoulder stiffness do not vary with age or gender and peak impact force does not significantly vary with age or gender for a given arm configuration and impact velocity.

Forty subjects were seated in a high-backed support chair and were then asked to arrest an oncoming pendulum with both hands. Their hands were to remain stationary before impact and when the pendulum struck their hands, to arrest it in a 'firm manner'. Three initial elbow angles (130°, 150° and 170°) and pendulum impact velocities (1.8, 2.3 and 3.0m/s) were used with each subject. Safety lines were used to prevent the pendulum from reaching the seated subject. The force components acting

on the hands were measured using load cells and arm segment and pendulum kinematic data was studied using motion analysis with light emitting diode (LED) markers placed on the arm, forearm, neck, impactor head and chair.

The advantage of this pendulum study was the ability to systematically control initial elbow angle and velocity before impact, in order to quantify each effect, however, the actual elbow angles varied slightly for each subject. Also, the experimental design allowed older subjects to be tested safely under a variety of impact severities, with impact velocities analogous to those of a fall from standing height.

‘A simple sagittally-symmetric biomechanical model of an equivalent arm arresting a moving mass was developed adapted from a two-link leg model’... ‘constructed and simulated using ADAMS[®] [Automatic Dynamic Analysis of Mechanical Systems] dynamics simulation software’ (DeGoede *et al*, 2002). This model and experimental results can be seen in figure 1.25. A model by Chiu and Robinovitch (1998) (figure 1.21b) was limited by the assumption of a locked elbow/arm configuration throughout the arrest whereas, this model takes into account elbow flexion.

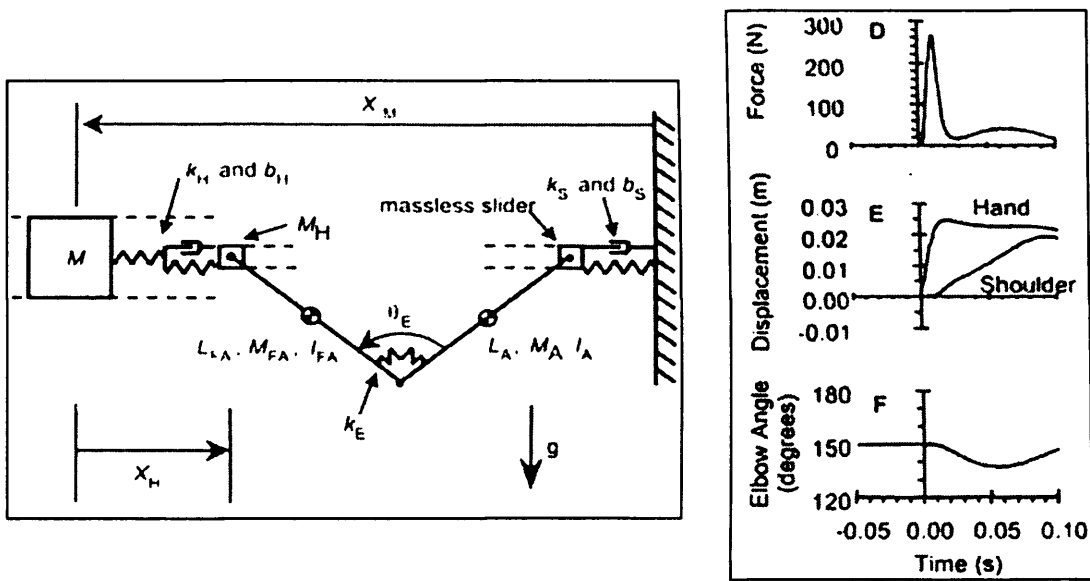


Figure 1.25: Dynamic model and graph showing simulation response (DeGoede *et al.*, 2002).

Their results showed that velocity, elbow angle and gender, but not age, significantly affected peak hand impact force. DeGoede *et al* (2002) found a decrease of 0.9 percent per degree in impact force. All subjects displayed increasing peak impact force magnitudes with more extended initial elbow angles. The force impulse lasted approximately 20 ms. The results from the biomechanical model correlated well with the experimental results. The effects of elbow angle and impact velocity were similar to the experimental results but the model tended to over predict the peak forces at higher impact velocities.

The authors acknowledge that the study was not without limitations. ‘First, the peak forces were significantly lower than those that must occur in actual falls. However, the primary trends from this study should hold in more severe impacts, since we expect the loads to be uniformly higher’ (DeGoede *et al*, 2002).

There will also be a difference in the kinematics and dynamics of a fall arrest when compared to this study. The hands were stationary prior to impact with the pendulum, which is not the case in an actual fall. The authors state however, that ‘in both cases the result of the collision is the arm being accelerated towards the torso, and the peak force in fall arrest occurs within the first 20 ms of the arrest’. [Therefore] ‘we believe the present analog provides conditions which are similar to a fall.’ (DeGoede *et al*, 2002)

A shortcoming of this study is that the conditions prior to impact are very different in their study compared to that of an actual fall and must be taken into account when comparing the two scenarios. Firstly, and acknowledged by the authors, the hands are not stationary before impact in an actual fall, they are accelerating towards the floor to arrest the fall, which would affect the subsequent acceleration towards the torso during impact.

Secondly, and more importantly, the ‘perceived danger’ of arresting a swinging pendulum (attached to a safety line) in a seated position is notably less than in an actual fall. The motor vestibular reflexes that occur when the vestibular system senses a change in orientation of the head would not be present. Therefore, the muscles that would usually contract to arrest the fall would not be ‘activated/fired’. This lack of reflexive action would result in a change in the reaction and position of the arm during impact with the pendulum compared to that that would occur during a fall.

1.5.4 FALLS ONTO DIFFERENT IMPACT SURFACES

The aforementioned studies have determined that fall height and arm responses are factors that should be taken into account when assessing falls. A further consideration is how a surface responds to the impact.

A few epidemiological studies have investigated the risk of arm injuries due to a fall from playground equipment and found that Impact Absorbing Playground Surfaces (IAPS) have little or no effect on the risk of injury to the upper limb (Mott *et al*, 1994, Mott *et al* 1997, Norton *et al*, 2004).

There is, however, little literature available of experimental studies that have quantified surface impact attenuation, due to falls onto the outstretched hand. The following two studies are the only studies found in the current literature to investigate experimentally how surfaces respond to an arm impact.

Maki and Fernie (1990) used a simple inverted-pendulum anthropomorphic fall simulator (figure 1.26) to assess what affect the floor covering had on the hand impact forces during a lateral fall.

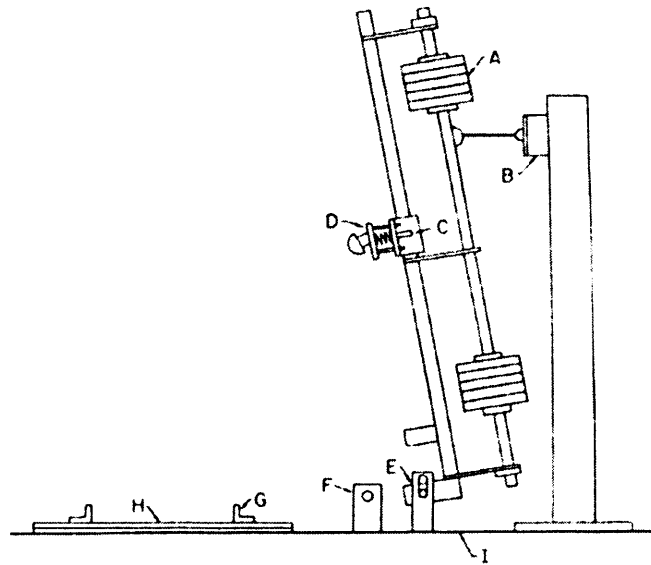


Fig. 1 The fall simulator: weights (A), electromagnet and cable (B), accelerometer (C), hip impactor (note springs and guide posts) (D), axis of rotation (note vertical slot in shaft support) (E), photocell (F), clamps (G), Plastazote (or silicon rubber) on top of flooring sample (H), terrazzo/concret slab floor (I)

Figure 1.26: The fall simulator with description of parts (Maki and Fernie, 1990).

The drop height simulated a fall from standing height and the impact deceleration was recorded by a piezoelectric accelerometer mounted on the mass supporting structure. Thirteen different floor coverings were used (commonly found in institutional and commercial settings), placed on top of a concrete slab floor, and were tested six times each. Equivalent impact forces, based on rigid-body analysis were calculated using the mean peak deceleration values.

A major shortcoming of this study by Maki and Fernie (1990) is that the simulator used for the hand impacts is not an accurate biomechanical model of the arm. In the same study, the simulator is used to represent a hip impact. During the hip study the impactor is hemispherical in shape, which is subsequently changed for a flat steel plate to represent the hand impacts.

The authors do not take into account the different segments of the arm (hand, forearm and upper arm) or the fact that the arm has three separate joints. All of which would attribute to the stiffness and damping of the arm during an impact. In fact, all of the internal body structures are represented by one spring, mounted between the impactor and the mass of the simulator. The spring stiffness was selected to yield an impact force of 10 kN, which was approximately the same magnitude as the bone failure strength for a fracture of the radius, ulna or humerus (Melvin and Evans, 1985 in Maki and Fernie, 1990).

Further it was assumed that the data used for the failure strength of bone was found by static loading as the authors allowed for an increase in strength under dynamic loading conditions. What this increase was, or how it was calculated, is not known but it should be noted, as previously discussed, that bone is a visco-elastic material and its stiffness therefore, would vary greatly in loading rate (e.g. static loading compared to dynamic loading).

It should also be noted that the bone failure strength quoted is for the fracture of three separate bones in the arm. The shape and structure of these three bones (radius, ulna and humerus) vary greatly and it could be suggested that the fracture rates of these bones would therefore, also vary greatly.

The results from this study by Maki and Fernie (1990) showed that floor covering had little effect on the impact forces produced by the hand impactor and would therefore not have a major effect on fractures of the arm. However, the number of problems,

shortcomings and assumptions within this study, that were discussed above, would indicate that any results found from this study would not give any meaningful data on which to base a study simulating hand impacts due to falling.

An acknowledged limitation of this study was a lack of human impact data on which to base their mechanical model, a later study by Robinovitch and Chiu (1998) attempted to study human impact data onto surfaces by conducting a study using four volunteers (three male and one female), to investigate whether the surface stiffness affects the impact force during a fall onto the outstretched hand.

The volunteers assumed a one-handed push-up position, with the hand placed on a force plate. The arm was oriented at 15° to the vertical, and the leg at 30° from the horizontal, with the elbow fully extended. This replicates the same methodology used in a previous study by the authors (Chiu and Robinovitch, 1996, 1998) that was discussed in detail in the previous section 1.5.2.3.

In addition to the methodology previously discussed, the volunteers fell onto different thickness' of foam pads (1.3, 2.5, 5.1 or 7.6 cm) from a height of 5 cm.

The results of their study suggests that the peak velocity generated across wrist damping elements is attenuated by compliant surfaces and thereby lowers F_{max1} forces (figure 1.27).

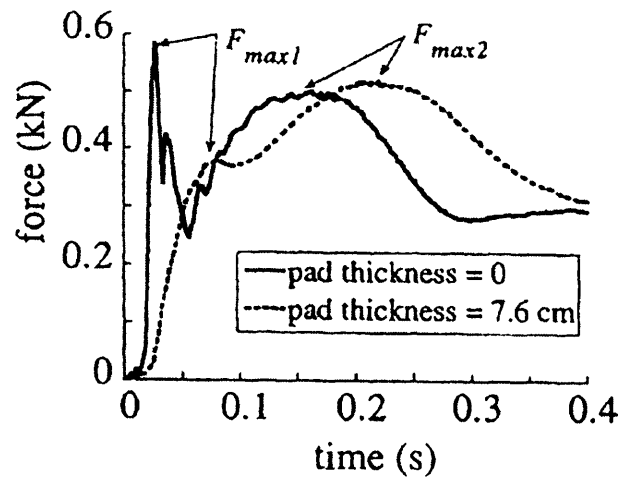


Figure 1.27: Graph showing the effect of peak impact forces applied to the hand during experimental falls from a height of 5 cm, onto foam padding. (Robinovitch and Chiu, 1998).

However, it may suggest that, to substantially reduce shoulder deformation and the associated low frequency peaks in hand and shoulder force, the surface stiffness has to be reduced to impractical levels. They only considered linear, spring-like surface materials so their results could not be used to assess force-attenuating capacity of non-linear surface materials.

This study only looked at falls from a low level, however, falls from playground equipment often involve a considerably greater fall height, leading Robinovitch and Chiu (1998) to conclude that ‘in these high-energy collisions, a compliant surface may attenuate F_{max1} to safe values but F_{max2} may rise to injurious levels and thereby initiate fracture’.

1.5.5 BIOMECHANICAL MODELS INVESTIGATING FALLS FROM PLAYGROUND EQUIPMENT

This section details current biomechanical models that have been developed to specifically investigate arm fractures due to falls from playground equipment.

A stochastic-rheological biomechanical model was developed to investigate the mechanics of impact fractures in the upper limbs of children falling from playground equipment (Davidson *et al*, 2004). The rheological aspect of the model characterises the musculo-skeletal tissues in terms of elastic, inertial and viscous parameters. The stochastic aspect of the model allows natural variation of these properties to be accounted for.

The model, shown in figure 1.28, which has been adapted from a model used by Chiu and Robinovitch (1998) to investigate arm injuries due to falls on adults, compares the impact force with the fracture force. The previous model (Chiu and Robinovitch, 1998) was discussed in section 1.5.2.3 and can be seen in figure 1.21b.

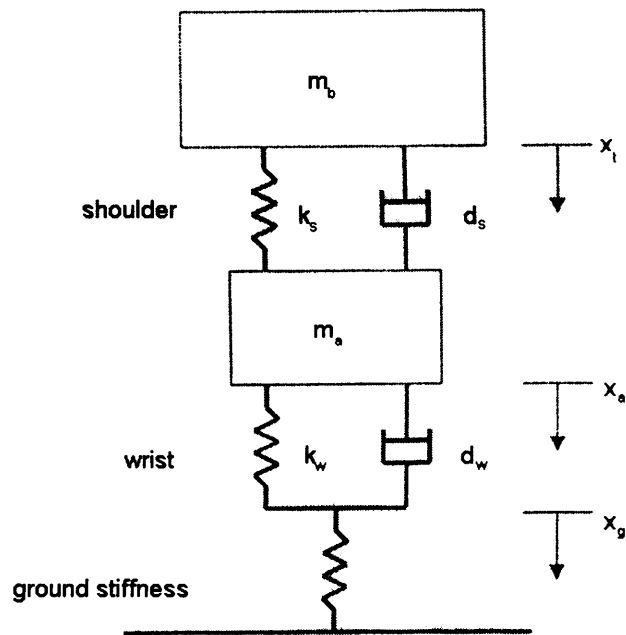


Fig. 1. Rheological two-mass spring-damper model used to represent arm impact from freefalls in children. Wrist stiffness and damping: k_w , d_w ; shoulder stiffness and damping: k_s , d_s ; displacement of ground, arm and torso: x_g , x_a , x_t ; mass of arm and suspended body: m_a , m_b .

Figure 1.28: Rheological two-mass model of arm impact (Davidson *et al*, 2005).

‘The ratio of the impact force over the fracture force is referred to as the Factor of Risk (FR)’ (Hayes, 1991, *in* Davidson *et al*, 2005). The higher the FR value, the higher the risk of fracture.

A further study by Davidson *et al* (2005) used data gathered from an epidemiological case-controlled study of falls from playground equipment (Chalmers *et al*, 1996) to validate the biomechanical model developed in their previous study (Davidson *et al*, 2004). The hypothesis was that ‘as FR increased, there would be an increased likelihood of fracture occurring’ (Davidson *et al*, 2005).

Chalmers *et al* (1996) collected data on children who fell from playground equipment. Cases involved children who had fractured their arm during a fall and controls were those who had fallen but not sustained an arm fracture. The data of 45 cases and 31

controls was then used in the study by Davidson *et al* (2005). The data used included gender, age, height, mass, fall height, impact surface and weather conditions.

Using the rheological model, impact forces (based on loading conditions, the mechanical properties of the impact surface, and the mechanical properties of the child) were estimated for each case and control and then a stochastic process was used to randomly vary these properties. Impact curves were then generated for each simulation and after a set number of simulations an output distribution was created.

The impact force curve found from the simulations had a high frequency force peak, and a lower frequency force peak. The authors (Davidson *et al*, 2005) attributed the force peaks to the initial hand impact and body deceleration respectively. The analyses were conducted on both peaks and considered separately.

The fracture force was estimated by multiplying the compressive strength of bone by the cross-sectional area. Both of these properties were calculated using data from bone mineral studies. (Goulding *et al*, 1998 in Davidson *et al*, 2005).

The model was then run through 1000 simulations for each child and the Factor of Risk (FR) was the mean impact force to fracture force ratios for the 1000 simulations.

Using logistic regression analyses the results showed a significant association between the probability of fracture and FR, showing that 'increased FR is a good predictor of increased likelihood of fracture' (Davidson *et al*, 2005). Table 1.2 shows

the values of impact force, fracture force and FR for the cases and controls used in the study.

Table 1.2: Means, standard deviations and ranges of the impact forces, fracture forces and FR for the case and control groups at both peaks (Davidson *et al.*, 2005).

Variable	Cases	Controls
1st peak impact force (N)	1415 ± 317 [912–2130]	1130 ± 229 [772–1757]
2nd peak impact force (N)	1162 ± 228 [791–1754]	964 ± 166 [712–1348]
1st peak fracture force (N)	2107 ± 545 [1697–3360]	2035 ± 374 [1691–2468]
2nd peak fracture force (N)	1689 ± 433 [1363–2683]	1634 ± 298 [1361–1979]
1st peak FR	0.69 ± 0.15 [0.74–1.11]	0.56 ± 0.09 [0.36–0.71]
2nd peak FR	0.71 ± 0.14 [0.41–1.08]	0.60 ± 0.08 [0.42–0.73]

The authors state that ‘validation of the model as an effective predictor of risk is important because the model is based on the mechanics of arm fracture’ (Davidson *et al.*, 2005). However, the model was found to underestimate the probability of fracture occurring. The authors state that this may be because ‘the actual impact forces experienced by the children falling from playground equipment were greater than those estimated by the biomechanical model and/or the actual fracture force for the distal radius of these children may be less than estimated by the model’ (Davidson *et al.*, 2005).

The main reasons why the actual impact forces may be higher than those estimated by the model could be due to the estimations made of loading conditions, playground surface stiffness and the joint properties of children. The reasons why the actual

fracture force may be less than estimated by the model could be due to the estimations made of the children's bone properties, as the majority of bone information was based on adult bones.

This further highlights the lack of data available on the impact forces and fracture forces of children's bones.

One point that the authors do not take into account is the limitation of their model to 'stiff-arm landings'. The addition of elbow flexion into the model could change the output values found in table 1.2 and may well alter the values of FR from the simulations performed. This model is the first one, however, that has attempted to investigate the fracture forces due to children falling from playground equipment.

Another study by Sherker *et al* (2003) has attempted to study the mechanism of children falling from playground equipment but their study concentrated on a physical impact model rather than a computer model.

Sherker *et al* (2003) first conducted an unmatched case-control study on children aged less than 13 years who fell from playground equipment located in primary schools and pre-schools and landed on their arm. Information such as the height fallen, the piece of equipment they fell from and where they landed was recorded, as well as the height and weight of the child.

Next, an impact arm load dummy was developed using anthropometric data of a 6 year old. The dummy (figure 1.29a) was made of steel, weighing 10 kg, and purpose

built plate weights were then added to the dummy to simulate a child up to 50 kg ('95th percentile for children <13 years' (Sherker *et al*, 2003)). The dummy was instrumented with load cells to record axial loads.

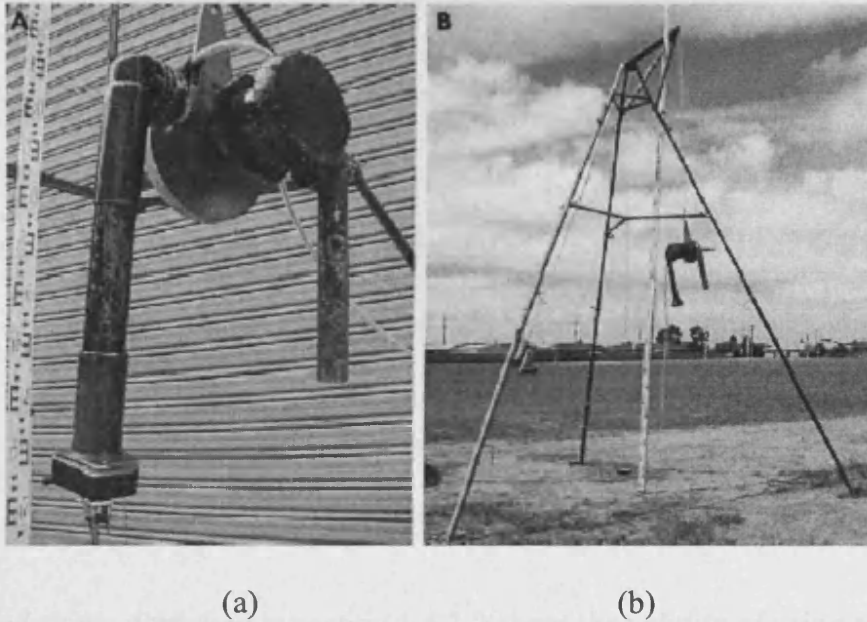


Figure 1.29: Photographs showing (a) Impact dummy and (b) portable drop rig (Sherker *et al*, 2003).

The dummy was validated using both a static compressive test and a dynamic pendulum test before it was then dropped, from a portable drop rig (figure 1.29b), using the fall height and surface type from the case-control study. From the drop tests arm load/time and deceleration/time traces were generated allowing peak load and peak deceleration to be calculated.

The results of this study are reported in a later study by Sherker *et al* (2005), who indicate that there is a 90% probability of arm fracture when arm loads exceed 3000 N.

These findings are similar to the upper end of the range of forces found in the aforementioned study by Davidson *et al* (2005), who reported fracture forces of 1363 to 3360 N (table 1.2). Unfortunately Sherker *et al* (2005) do not report the range of forces found from their studies either for the cases or controls.

Acknowledged limitations of the dummy are that it 'did not conform to the exact biofidelity of the human arm' (Sherker *et al*, 2003). This is because 'the model did not account for variable stiffness, nor damping of the joints and segments of the arm' (Sherker *et al*, 2005). 'The dummy did not have a wrist or elbow joint' [and so therefore] 'represented the worst case scenario of a fall onto the outstretched arm with joints locked and maximal loading on the long bones' (Sherker *et al*, 2003).

It has already been discussed in section 1.5.3.2 about the validity of using an extended arm as a 'worst-case falling scenario' and it remains to be seen if this is the case.

1.5.6 ELECTROMYOGRAPHY

The electrical activity in a muscle can be recorded using electromyography (EMG). Dietz and Noth (1978) and Dietz *et al* (1981) have used EMG to investigate the muscle activation of the upper extremity during falls onto the outstretched hand.

A series of experiments were conducted to investigate the interaction between pre-activity and stretch reflex in human triceps brachii during landing from forward falls, with and without visual control.

During the earlier study (Dietz and Noth, 1978) attached surface electrodes to both triceps brachii and assessed the muscle activity during self-initiated forward falls onto a platform (inclined at angles of 50, 60, 70 or 80°). In the first set of tests the subjects maintained visual control throughout the falls and in the second set of tests the subjects were blindfolded and the platform was randomly varied. The primary interest was to investigate the EMG activity just prior to, and immediately after, impact.

The results showed that, during falls with visual control, the EMG activity in both triceps brachii began 130-200 ms prior to impact, which was concomitant with an extension of the arms, and then built up continuously until impact occurred. The duration of the pre-innervation build up was roughly constant, 120 –130 ms, and was therefore, thought to be independent of the height fallen. The authors (Dietz and Noth, 1978) attribute the onset of pre-innervation to the point of impact rather than the onset of the fall and it was noted that the slope of the pre-activity became continuously steeper with fall height. The amplitude of the early peak after impact was also noted to rise with increasing fall height.

During the falls without visual control the pre-innervation was observed to be triggered by the start of the fall and increase continuously. This meant that the EMG curves were almost identical up to the moment of impact in relation to the start of the fall. The duration of pre-activity, 250-300 ms, was noted to be twice as long as that for the same fall height during falls with visual control.

A comparison of the EMG responses during falls with and without visual control can be seen in figure 1.30. (A1-A4 and B1-B4 signify the angle platform inclination, 50-80° respectively).

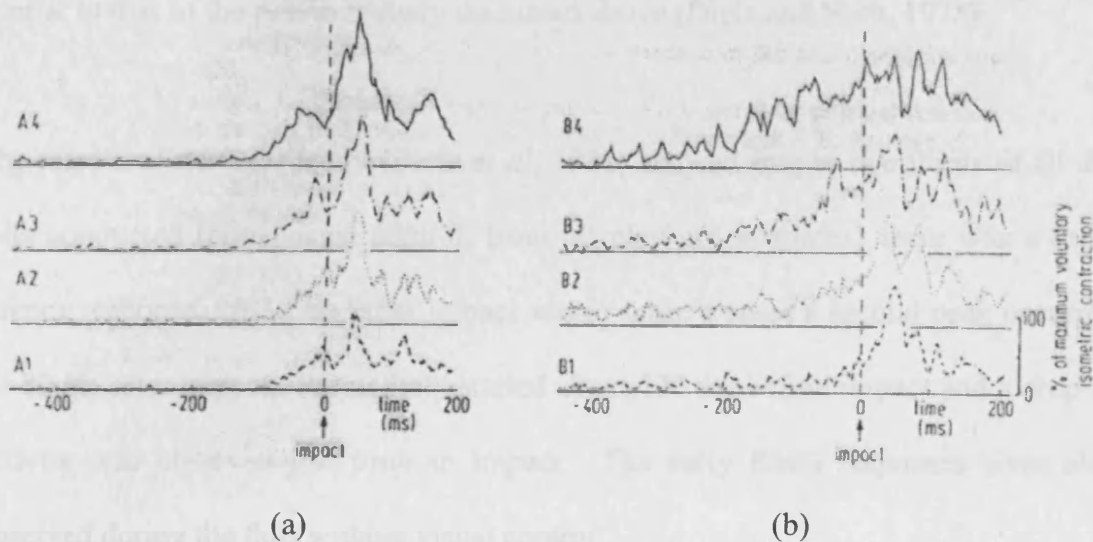


Figure 1.30: Typical EMG traces for the right triceps brachii during a fall (a) with and (b) without visual control. (At platform angles of 50-80°) (Dietz and Noth, 1978).

The results suggest that it is unlikely that pre-innervation depends on vestibular cues of the head movement during a fall, as activity was only observed 100-200 ms before impact, regardless of the time when the fall was initiated. The authors conclude that 'it is more likely that a central program is fed with visual and proprioceptive information and determines the onset and strength of the pre-innervation. However, in the absence of visual information, the pre-innervation begins at the start of the fall and increases continuously up to the moment of impact. This type of pre-innervation is much more likely to depend on the vestibular system [and] if so, this vestibular reflex is suppressed when the subject knows the falling height'. (Dietz and Noth, 1978).

Dietz and Noth (1978) only considered EMG activity at the triceps brachii, whereas the later study (Dietz *et al*, 1981) studied the EMG profiles of proximal arm muscles, which included the triceps brachii as well as the forearm flexors and extensors. The methodology for this study has been previously discussed in section 1.5.2.3 and was similar to that of the previous study discussed above (Dietz and Noth, 1978).

The results of the later study (Dietz *et al*, 1981) showed that in two thirds of all the falls conducted (with visual control, from all platform positions) there was a short latency response, 20-30 ms, after impact and in some a cases a second peak occurred 60-80 ms after impact. Pre-activity started about 130 ms before impact and a drop in activity was observed just prior to impact. The early EMG responses were also observed during the falls without visual control.

Their results suggest that ‘a large fraction of the EMG activity after impact is reactive rather than pre-programmed. Early EMG response is evoked by reflexes elicited at the moment of impact’ (Dietz *et al*, 1981).

Assessment of the forearm muscles showed that both flexors and extensors were pre-activated during the fall. The EMG profile of the forearm flexors mimicked the triceps but the extensor muscles declined rapidly before the fingers touched the platform, and approached zero shortly after impact. ‘The early onset of the decline argues against reflex inhibition as the only reason for this decay’ (Dietz *et al*, 1981). Typical EMG traces for the forearm muscles can be seen in figure 1.31.

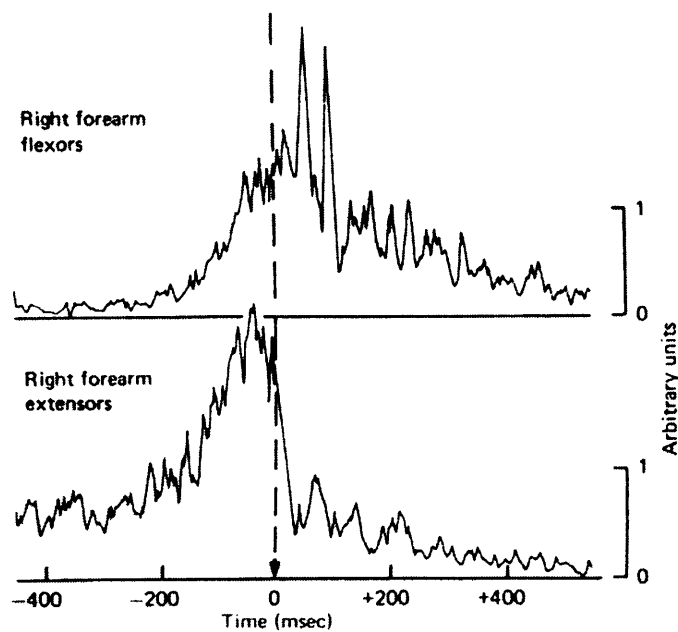


Figure 1.31: Typical EMG profiles of the forearm flexors (upper trace) and forearm extensors (lower trace) during an 80° fall (Dietz *et al*, 1981).

The early response of the forearm flexors were, in general, shorter than that of the triceps brachii and consisted of only one or two peaks.

The authors claim that 'subjects who are able to land smoothly on their fingertips by strong pre-contraction of the finger flexors might use the stretch reflex without exhibiting the early increase in EMG activity' (Dietz *et al*, 1981). After the initial force peak, elbow flexion begins and deceleration of the body lasts for about 200-300 ms (for deep falls). During the deceleration phase, the spinal stretch reflex may serve to provide full activation of the triceps brachii. This would ensure that the muscle is fully activated as soon as the high initial muscle stiffness is reduced after impact.

The authors conclude that 'both the pre-existing activity and the spinal stretch reflex contribute significantly to the over-all activity of the triceps during stretch after impact' (Dietz *et al*, 1981).

1.6 OBJECTIVES

The literature review in section 1.5 detailed relevant studies investigating falls onto the outstretched hand. A summary of the main shortcomings of these studies is detailed below:

- Quotation of fracture forces from cadaver studies – The only quantitative data presently available on the fracture forces of the arm are from cadaver studies. These studies have obvious limitations in that the cadaveric material is often from elderly subjects and potentially have poor bone stock quality, and there is a lack of neuromuscular and musculo-skeletal responses that would be present during a fall. Despite this, many researchers take the fracture forces found from cadaver studies as the threshold fracture force of the arm due to a fall onto the outstretched hand.
- Small sample sizes – The majority of the studies reported in the literature review used a volunteer cohort size of between 4 and 16 people. Generally speaking, any sample size below 30 is considered to be small.
- Lack of female and male data – All but one of the studies assessing falls onto the outstretched hand used only male volunteers in their study.
- Small age range – Most of the fall studies only used volunteers between 20 and 30 years of age.
- Use of extended arm – Many researchers used the methodology of an extended arm during their fall studies as it was claimed to represent a ‘worst-case falling scenario’. It is not actually known if falls commonly occur onto the extended arm or not.

- Lack of different impact surfaces – There were very few studies that used different impact surfaces when assessing falls onto the outstretched hand.
- Lack of motor vestibular responses – The methodologies used in some of the studies did not allow the type of motor vestibular responses that would generally occur in fall. These methodologies therefore, are not an accurate representation of a fall, even from low fall heights.

The aims of this study, as laid out in section 1.2, are:

- to investigate the forces that are produced in the arm during a fall onto the outstretched hand at a non-injurious level.
- to utilize the data for non-injurious impact forces, during a fall onto the outstretched hand, to aid in the development of a mechanical arm fracture model that could be used, alongside the British Standard head impact testing device, to test IAPS for their ability to alleviate arm fractures.

It is important to gain an understanding of what forces are produced during a fall onto the outstretched hand at a non-injurious level, to be able to understand the magnitude of forces required to fracture the arm during a fall. To do this, a better understanding of the factors that affect the impact forces, produced during a fall onto the outstretched hand and the mechanism in which the arm responds to a fall is required. Shortcomings found from previous studies should also be addressed to ensure the problems found from those studies are not repeated.

The objectives of this study are therefore:

- to obtain impact data for a fall from a non-injurious height, using adult volunteers falling onto the outstretched hand
- to assess what factors are influential on the forces produced during the experimental falls. These factors include the fall height, the effective mass, gender and age of the volunteer, the impact surface, and the angle of the elbow prior to and during impact
- to investigate the mechanism of the arm prior to and during impact
- to assess the activation of the muscles in the arm in response to a fall
- to develop a computational arm model to enable falls from higher (injurious) heights to be investigated.

It was decided to first develop a computational arm model rather than the physical arm model due to the advantage of being able to change the parameters of the model quickly and easily. The data from the computational arm model can then be used to develop the physical model.

This study will investigate falls in the forward direction only, as this is the mechanism in which the majority of falls occur onto the outstretched hand (DeGoede *et al*, 2003).

The next chapter details the materials and methodology used in this study.

CHAPTER 2

MATERIALS AND METHODS

2.1 INTRODUCTION

All of the experimental studies detailed in this chapter were carried out in the Human Movement Laboratory in Cardiff University. The studies involved dropping volunteers onto an outstretched arm onto two Bertec force plates (figure 2.1) and recording the drops using cameras detailed in the following pages. The force plates were set at a sampling frequency of 2040 Hz for the motion analysis studies and 300 Hz for the high-speed video study.

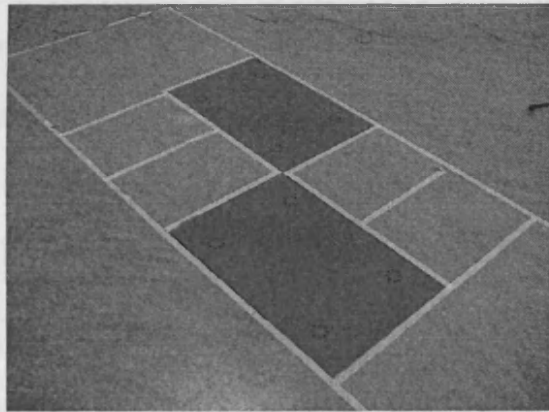


Figure 2.1: Photo showing two Bertec force plates situated flush with the floor in the Human Movement Laboratory in Cardiff University.

Each volunteer read and signed a written statement of informed consent and the Local Ethical Committee approved all test procedures. All the volunteers had previously read an information sheet containing the procedure before signing their consent forms and had the opportunity to ask any questions before agreeing to volunteer for the study.

The objectives of the study are:

- to obtain impact data for a fall from a non-injurious height using adult volunteers falling onto the outstretched hand
- to assess what factors are influential on the forces produced during the experimental falls. These factors include the fall height, the effective mass, gender and age of the volunteer, the impact surface, and the angle of the elbow prior to and during impact
- to investigate the mechanism of the arm prior to and during impact
- to assess the activation of the muscles in the arm in response to a fall
- to develop a computational arm model to enable falls from higher (injurious) heights to be investigated.

Four studies were conducted; an observational study, two further studies using a motion analysis system, and a study using high-speed video (HSV) and electromyography (EMG) equipment. Each study will be detailed fully in this chapter.

2.2 OBSERVATIONAL STUDY

An observational study was conducted to assess the position of the arm, specifically the angle of the elbow, during a fall and subsequent impact with a surface. A volunteer was subjected to a series of experiments involving falls from a standing height, to assess if there was a difference between the reaction and position of the arm during a self initiated fall and an unexpected fall.

2.2.1 EQUIPMENT

Retro-reflective markers (20 mm cork balls covered in reflective tape) were placed on the volunteer at the forehead, shoulders, elbows, wrists, hips, knees and feet using adhesive tape. The markers and their placement on the volunteer are shown in figure 2.2. The markers were used in conjunction with a Qualisys motion analysis system with five 120 Hz Pro Reflex cameras.

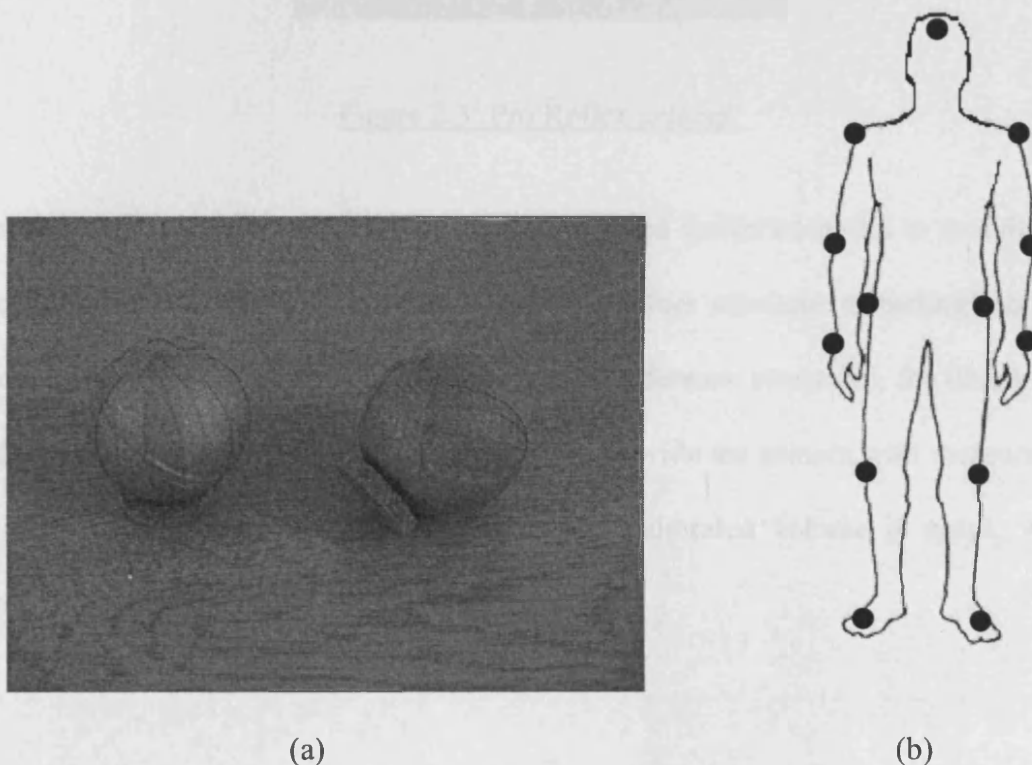


Figure 2.2: (a) Retro-reflective markers (b) Marker placements for initial study.

The Pro Reflex cameras, shown in figure 2.3, emit infrared light, which reflects back off the retro-reflective markers. It is important therefore, that the cameras are positioned in such a way that the infrared emissions from one camera are not mistaken as light reflected off a marker by another camera. The cameras measure the 3D coordinates of each marker, provided that two or more cameras can see a marker at any one time, using the software program Qualisys Track Manager (QTM).



Figure 2.3: Pro Reflex camera.

The Pro Reflex system was calibrated using a wand (calibration) kit to establish the global co-ordinate system within the laboratory before subsequent readings could be taken. The wand kit (figure 2.4) consisted of a 'reference structure', for defining the calibration co-ordinate system, and a 'wand', to provide the camera with measurement points to use for the calibration and provide a calibrated volume in space, within which measurements would be taken.

2.2.2 METHODOLOGY

The volunteer was requested (in their own time) to donate a forearm (10 cm thick) to be used as a reference structure. The forearm was positioned in a fixed position and was instructed to stand upright as best as possible.

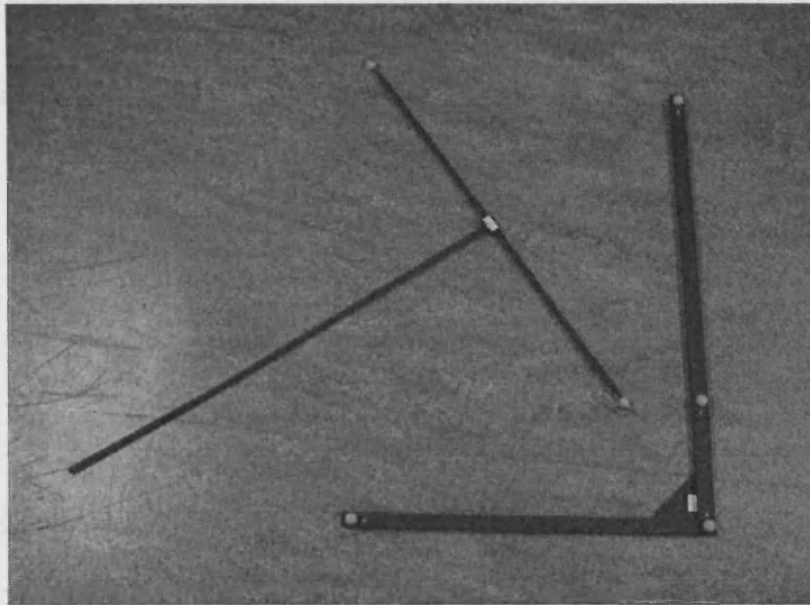


Figure 2.4: Calibration kit consisting of a reference structure and wand.

The 'reference structure' is an L-shaped steel frame that consists of four markers in a fixed configuration, which was placed on the floor in the centre of where the measurements would be taken. The cameras were adjusted so that the 'reference structure' was in the field of view of all five cameras. The 'wand' is a T-shaped structure consisting of two markers a fixed distance apart (750.9mm). The 'wand' was "waved around" so as to move the two markers in all directions (x,y,z) within the space in which the tests would be conducted. The cameras would have needed to be calibrated again if any of them had moved, otherwise the global co-ordinate system would not be correct and would have given incorrect 3D co-ordinates of the markers.

2.2.2 METHODOLOGY

The volunteer was requested (in their own time) to initiate a forward fall onto a 30 cm thick gymnasium-crash mat and was instructed to arrest their fall as best as possible

(figure 2.5). The purpose was to assess how the volunteer used their arms to arrest a controlled fall to the 'floor'.



Figure 2.5: Observational study, fall onto 30 cm thick crash mat.

These falls were then repeated with the volunteer standing on a moveable platform. The platform was pulled out from underneath the volunteer causing an unexpected forward fall onto the same crash mat used in the previous test. The purpose of this test was to discover, if there was a difference in the reaction and position of the arm when the timing of the fall was unexpected and/or out of the volunteers control.

Finally the volunteer volitionally fell, again from a standing height, onto a 2.5 cm foam surface. This was to assess if an increase in perceived danger, due to falling onto a less padded surface, would affect the reaction and positioning of the arm.

All the fall scenarios were repeated three times each.

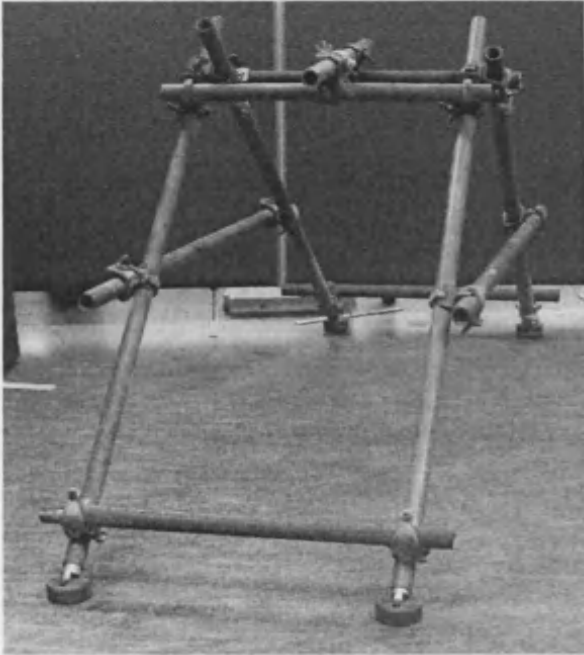
Assessment of the observational study suggested that in none of the fall scenarios did the volunteer attempt to break the fall using a fully extended arm, instead the arm was always flexed slightly during descent and extended marginally prior to impact with the surface.

From this observational study it was decided that falling onto an extended arm in an experimental context would not be consistent with falling in a physiological context and volunteers should therefore be able to assume a natural arm angle, rather than a pre-defined position, prior to falling. These findings were used as the methodology for further tests.

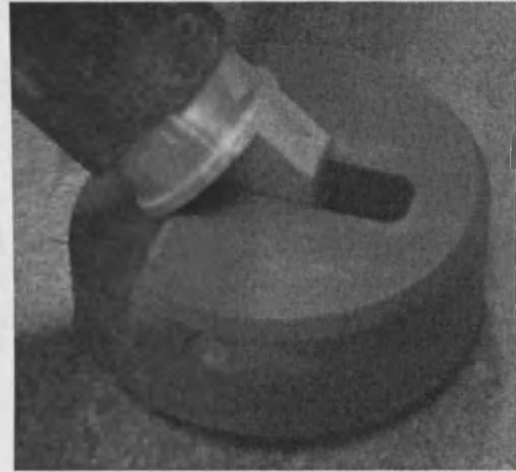
2.3 MATERIALS

2.3.1 DROP RIG

An important aspect of the fall studies was the safety of the volunteers. For this reason a rig had to be constructed to enable volunteers to be safely dropped, from different heights, onto the force plates. An initial rig was constructed from scaffolding (figure 2.6a), with specially designed feet (figure 2.6b), in the shape of an A-frame.



(a)



(b)

Figure 2.6: (a) Drop rig constructed from scaffolding (b) Manufactured drop rig feet.

The basic shape of the rig was a good supportive structure however, it was not stable and extremely heavy so it was remanufactured using steel box section and painted with non-toxic paint as shown in figure 2.7.

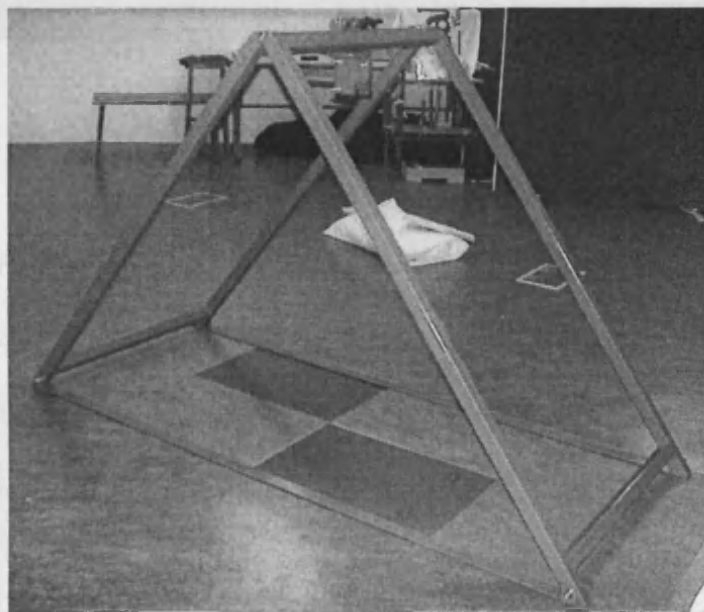


Figure 2.7: Steel box section drop rig.

Although this rig was much sturdier than the scaffolding, problems arose when trying to raise the volunteer off the floor to a specified drop height. Initially a ratchet was used, but it did not give a wide enough range of fall heights to incorporate the difference in arm length of the volunteers. It was also not accurate in raising the volunteers to the same height for each fall. It was decided that a simpler way of lifting the volunteers would be to use a hoist mechanism and so an engine hoist was bought, which can be seen in figure 2.8.

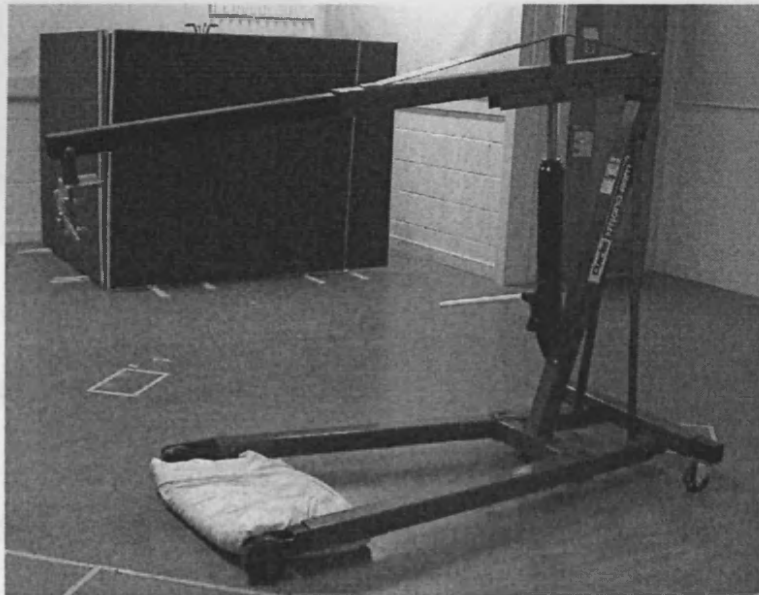


Figure 2.8: Engine hoist.

The hoist was capable of lifting 1000kg with its arm fully extended but to ensure the safety of the volunteers the hoist was used with the arm as short as possible. In this position the hoist was capable of lifting 250kg comfortably and could be lifted up almost to the nearest mm.

2.3.2 DROP MECHANISM

A mechanical drop mechanism was designed and manufactured, that was activated using a simple lever (figure 2.9). The back of the mechanism was a flat steel plate to enable attachments to be made to fit it onto any drop rig. Technical drawings for the drop mechanism can be seen in Appendix A.

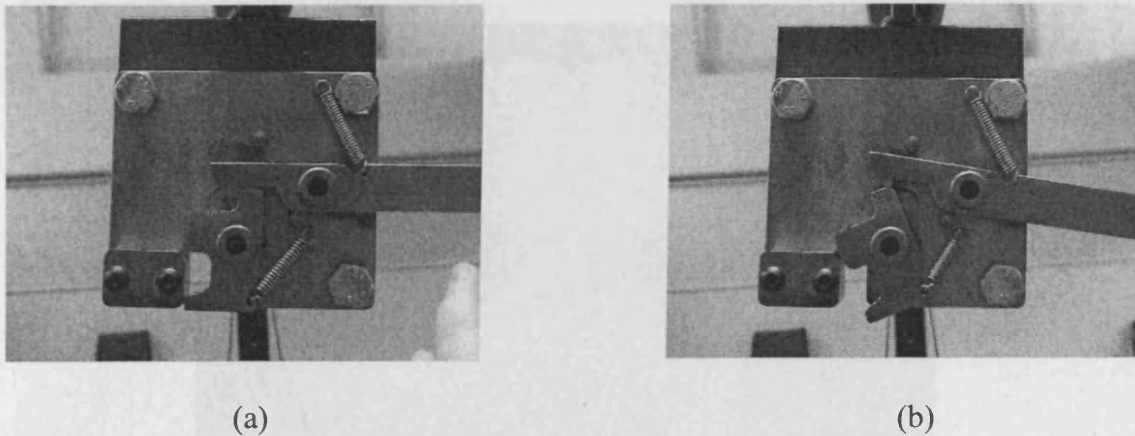
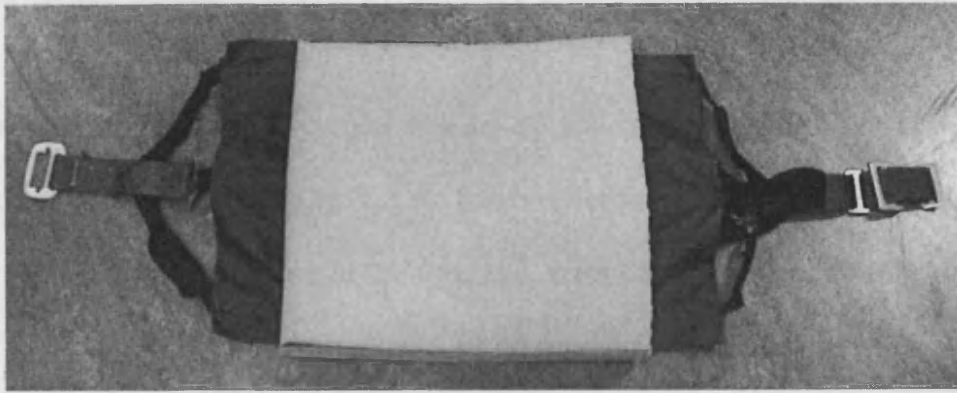


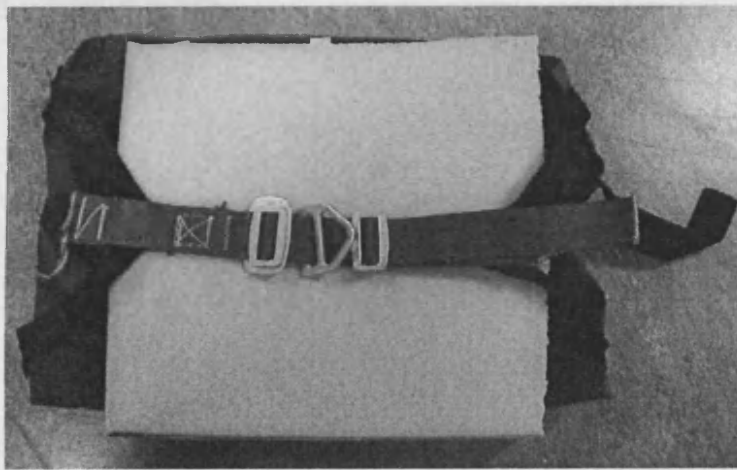
Figure 2.9: Mechanical drop mechanism (a) closed and (b) open.

2.3.2 HARNESS

A harness was designed (figure 2.10) to fit around the volunteer's torso, that would be strong enough to hold any volunteer safely before being dropped. The harness was manufactured using thick canvas and webbing, with a metal buckle to attach it to a volunteer. The harness was also fully adjustable. To ensure the volunteers comfort a 5 cm thick piece of foam was attached to the canvas onto which the torso of the volunteer would be positioned. The harness was tested in a tensile testing machine to ensure that it would not fail under heavy loading.



(a)



(b)

Figure 2.10: Harness in (a) open position and (b) closed position.

2.4 MOTION ANALYSIS STUDY

A study was conducted using 35 volunteers of mixed gender (11 female and 24 male), athletic ability and hand dominance. Each volunteer's height was measured and they were also weighed. A data sheet was completed for each volunteer that included gender, weight, age and height. The volunteers ranged in age between 22 and 51 years, weight between 55 and 106 kg, and height between 1.53 and 1.98 m.

2.4.1 EQUIPMENT

A Qualisys motion analysis system was set up and calibrated with five 120 Hz Pro Reflex cameras as described in 2.2.1. Retro-reflective markers were placed on the volunteer, using adhesive tape, at the forehead, acromion, the lateral epicondyle of the elbow and the styloid process of the ulna (figure 2.11) and the harness was placed around their torso. The hoist, with the mechanical drop mechanism attached to it, was positioned over the force plates.

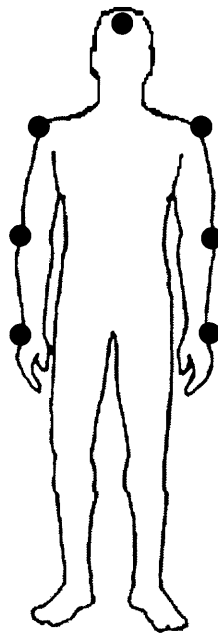


Figure 2.11: Retro-reflective marker positions.

2.4.2 METHODOLOGY

The effective mass of the volunteer was recorded by positioning the volunteer with each hand on a force plate, whilst laying on the floor. The volunteer was asked to perform a press-up, with their knees remaining on the floor, and hold the position so that a recording could be made of the force transmitted to the force plates by each

hand. The values at each force plate were then calculated and averaged to give the effective mass in each arm for each volunteer.

The volunteers were then asked to hold the same position but using a fully extended arm (no elbow flexion). This would be used to compare the angle of the arm in a natural fall arrest position to a fully extended position.

Drop tests were conducted at heights of 3 and 5 cm, directly onto the force plates. Volunteers were suspended by their torso from the drop rig (figure 2.12) via a metal buckle on the harness that clipped into the drop mechanism. Their hands were then hoisted off the force plates to either 3 or 5 cm, with their arms in a natural position to arrest their fall. Two blocks of wood (height, 3 cm and 5 cm) were used to ensure the volunteer's hands were the same distance from the floor. The knees of the volunteer remained on the floor at all times.



Figure 2.12: Volunteer suspended in harness from drop rig with each hand positioned over the force plates.

Volunteers were instructed to arrest the fall with both hands and were given no warning before the drop mechanism was activated, releasing them from the drop rig. A piece of 5 cm foam was placed on the floor in front of the volunteer to protect their head, should attempts to fully arrest the fall with the upper limbs fail. All falls were repeated three times, at 3 and 5 cm, and were recorded with the motion analysis cameras (capture rate 120 frames per second (fps)) and a digital camera (capture rate 60 fps). Volunteers were able to take a break from the testing at any time.

2.5 SURFACE STUDY

A further study was conducted, using the same volunteers as the previous study (section 2.4), to assess the effect the surface material properties had on the forces produced in the arm.

2.5.1 EQUIPMENT

The motion analysis cameras and markers, used in this study, were the same as those used in the previous study and are described in section 2.4.1.

Two impact surfaces were used in this study; a domestic surface and a playground surface, details of which are described below.

The domestic surface comprised of a natural wool carpet tile with a foam underlay. This was chosen because it was found to be the most compliant domestic surface, in a study by Cory (1998), to reduce head impacts in children. The force plates are a non-

compliant surface so using the domestic surface will enable the lower and upper range of compliant surfaces to be tested.

The playground surface was a 33 mm thick safety tile made from rubber shreds, which are graded and then bonded with a special polyurethane resin. The safety tile is designed to deform progressively on impact, absorbing energy from a fall. This surface was used as it has been proven to reduce head injuries in falls from playgrounds using the British standard head form drop test.

2.5.2 METHODOLOGY

The methodology for this study was the same as in the previous study and is described in section 2.4.2. In this study however, the volunteer fell onto the impact surface, which was positioned over the force plate, from a fall height of 5 cm. One hand impacted onto the impact surface whilst the other landed onto foam padding. All the drop tests were repeated three times, as in the previous study.

2.6 HSV STUDY

A study was conducted using a high-speed video (HSV) capture system, coupled with an electromyography (EMG) system, to investigate the mechanics of the arm and hand immediately prior to and during impact. Five volunteers were asked to participate in the study; a female and male each weighing 105 kg, a female and male weighing 60 kg and a male who weighed 80 kg.

2.6.1 EQUIPMENT

Two high-speed video (HSV) cameras and an 8-Channel Bortec Electromyography (EMG) system were used to analyse the impact onto the force plates.

The high-speed digital imaging system used in this study consisted of two MOTIONeer cameras, shown in figure 2.13, and VITcam software. The cameras were connected to a computer via fire wire and a binder connector synchronised the cameras and provided an external trigger source.



(a)



(b)

Figure 2.13: MOTIONeer camera (a) full view (b) rear panel.

The cameras were statically calibrated for 3D imaging using a standard calibration frame with 8 marker points, shown in figure 2.14, which was erected to occupy the space where the event/drop tests would take place.

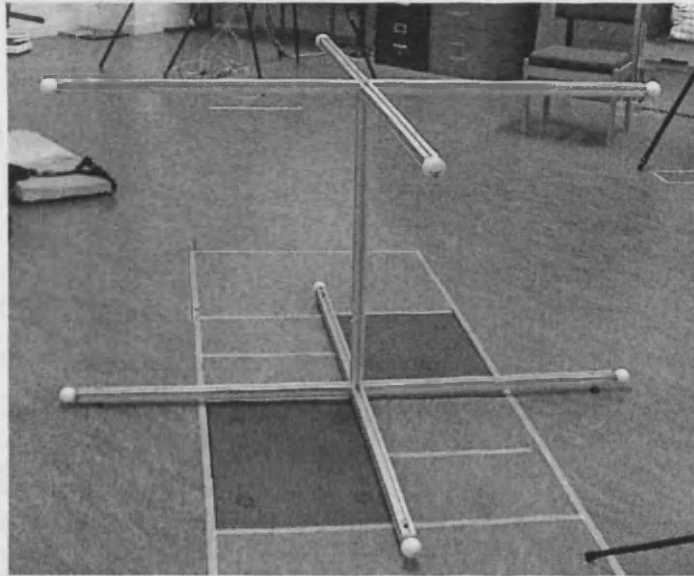


Figure 2.14: Static calibration frame positioned in the centre of the test space.

To ensure correct 3D calibration the two cameras had to be operating from different perspectives and all markers on the calibration frame had to be in the field of view of both cameras. The calibration frame was recorded for a period of four frames at a sampling rate of 62 fps (the slowest setting) and was removed once the image was captured. The cameras were calibrated for each new volunteer to ensure correct image recording.

Due to the fast capture rate of the HSV cameras, the time to capture each frame of the video is short and therefore, requires a higher intensity of light than would normally be used with standard digital video cameras. Two Hedlar 1250-Watt lights were used, shown in figure 2.15, which were positioned in front of the cameras about 1.83 m above the floor and approximately 1 m from the volunteer.

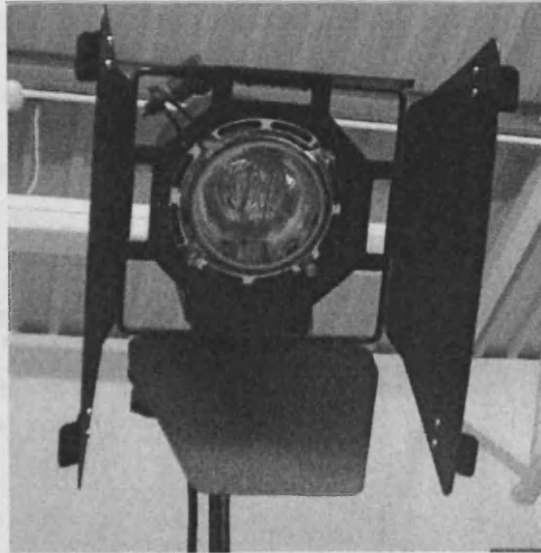


Figure 2.15: Hedlar 1250-Watt lantern.

The photograph below, figure 2.16, shows the HSV system set up in the laboratory.



Figure 2.16: High-speed video study equipment set up.

The EMG system was an 8-channel Analogue Multiplexed cable Telemetry, AMT-8, made by Bortec. This consisted of a main amplifier unit, a data acquisition box and a battery powered patient unit.

The main amplifier, shown in figure 2.17, receives the signals transmitted from the Patient Unit and provides necessary signal decoding, processing and further amplification.

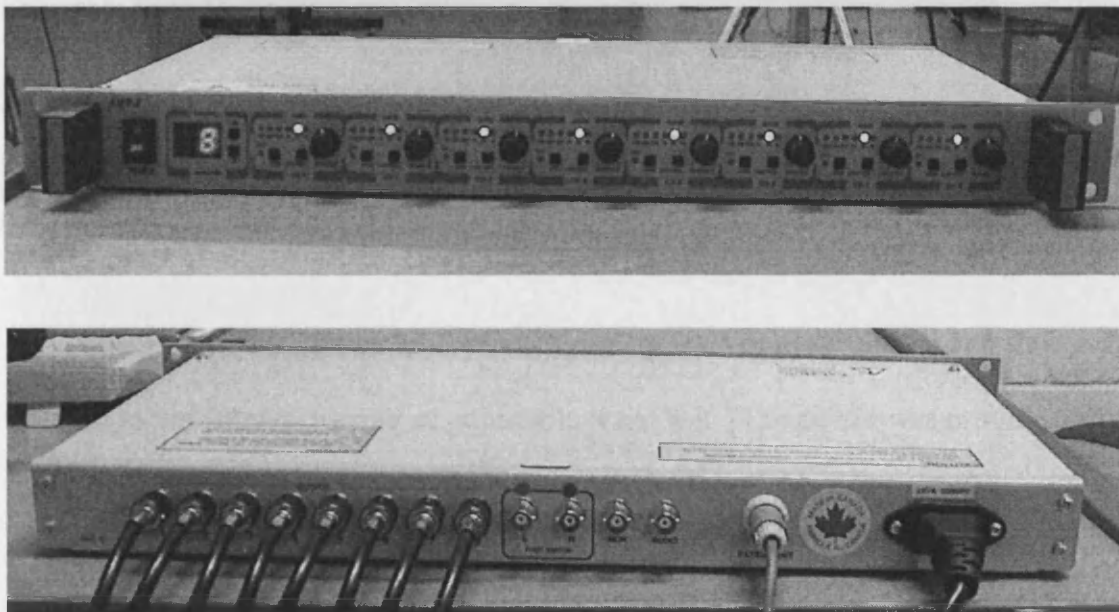


Figure 2.17: Main amplifier unit showing front (top) and rear (bottom) views.

The amplifier contains options for adjusting the number of channels used as well as fixed and variable gain controls, allowing the total gain range of the system to be between 100 and 15,000. All eight channels were used during the tests and the gain was set at 4000 (this value was chosen after initial observations were made of the output signals to ensure good readings).

Standard BNC connectors were used to attach the 8 analogue output channels into a data acquisition box, shown in figure 2.18. The information was then input into an analogue to digital PCI card, via a 50-pin connector, situated in a computer.



Figure 2.18: Data acquisition box.

The Patient Unit, which can be seen in figure 2.19, is a small plastic box that was fastened to the volunteer using an adjustable waist belt. The power was provided by a battery pack attached to the waist belt.



Figure 2.19: Patient unit with waist belt and battery pack.

The primary function of the Patient Unit is to provide connection for pre-amplifiers, distribute power to pre-amplifiers, encode incoming signals from the pre-amplifiers (APE-500) and to transmit these signals to the Main Amplifier unit via a Signal Transmission Cable. The APE-500 pre-amplifiers are a high impedance differential amplifier with a standard gain of 500, and can be seen connected to the patient unit in figure 2.20.

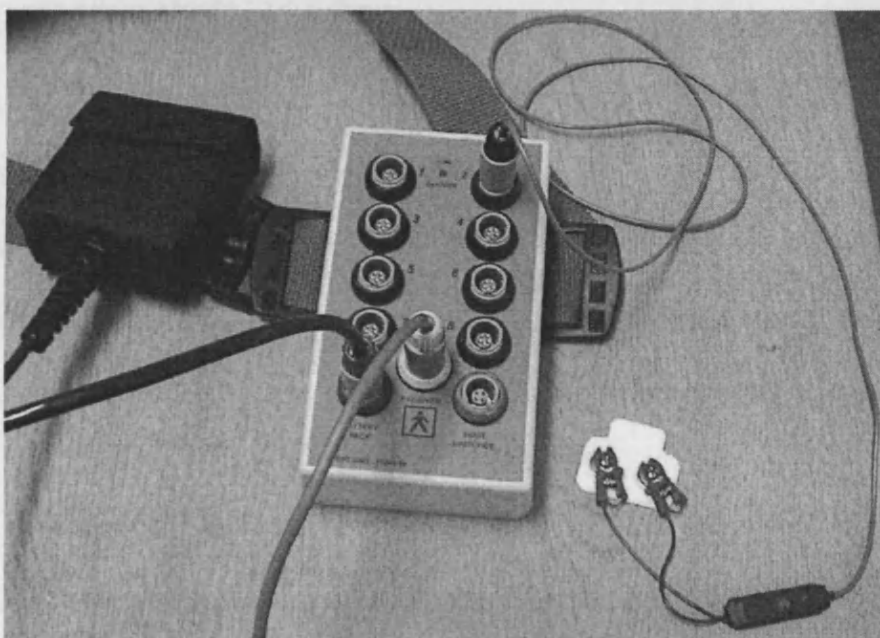


Figure 2.20: Pre-amplifiers connected to the patient at one end and the electrode at the other.

The pre-amplifiers amplify and condition the EMG signal by converting the signal from high impedance to low impedance, effectively eliminating cable noise in the transmission of the signal. One end of the lead connects to the patient unit and the other to electrodes attached at muscle sites on the volunteer. The electrodes used were self-adhesive wet electrodes with a silver/silver chloride (Ag/AgCl) gel, shown in figure 2.21 and each electrode occupied a separate channel on the main amplifier.

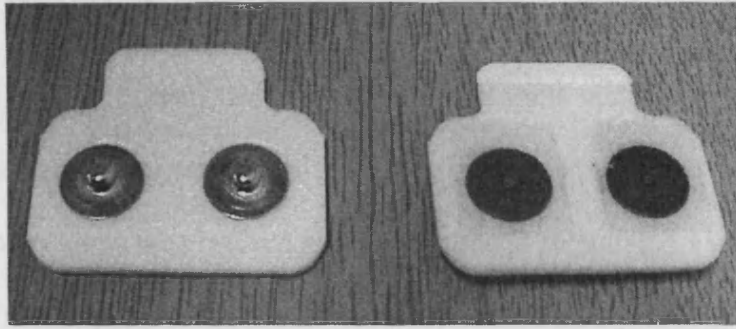


Figure 2.21: Silver/Silver Chloride (Ag/AgCl) electrode, front and back views.

These electrodes were chosen because the Ag/AgCl gel increases the conductive path between the skin and the electrode, enabling the quality of the EMG recording to be improved. Before attaching electrodes to the skin it is important that skin oils are removed, as these will also impede the conductive path between the skin and the electrode. Therefore, an alcohol wipe was used to clean the skin area of the dominant arm of the volunteer before the electrodes were placed on selected muscles (figure 2.22).

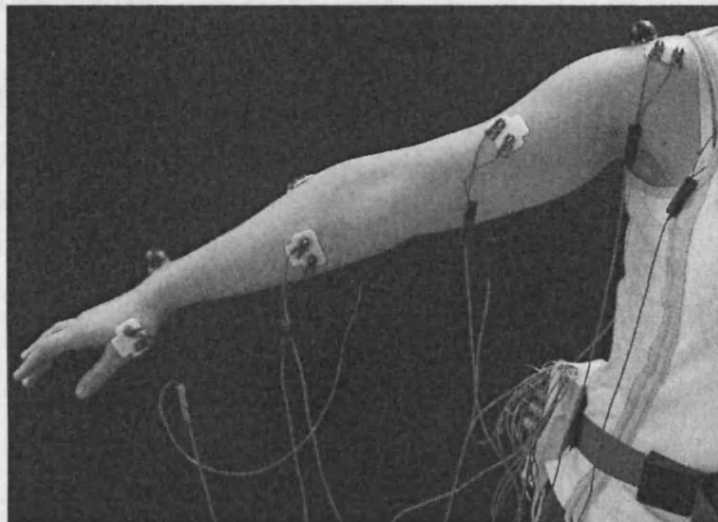


Figure 2.22: Electrodes placed on the skin with pre-amplifiers connecting electrodes to the patient unit.

The muscles used were the thenar eminence, forearm flexors, forearm extensors, biceps brachii, triceps brachii, anterior deltoid, pectoralis major and the trapezius in the neck. Black circular markers, shown in figure 2.23, were placed on the volunteer in the same positions as the previous study described in section 2.4.1 (figure 2.11).



Figure 2.23: Black circular markers.

2.6.2 METHODOLOGY

Volunteers were asked to kneel on a pillow under the drop rig and were suspended by their torso via a buckle and harness, which clipped into the drop mechanism (figure 2.24). In the first test their hands were hoisted off the force plates to a height of 1 cm, with their arms in a natural position to them in order to arrest their fall. Their knees remained on the floor at all times.

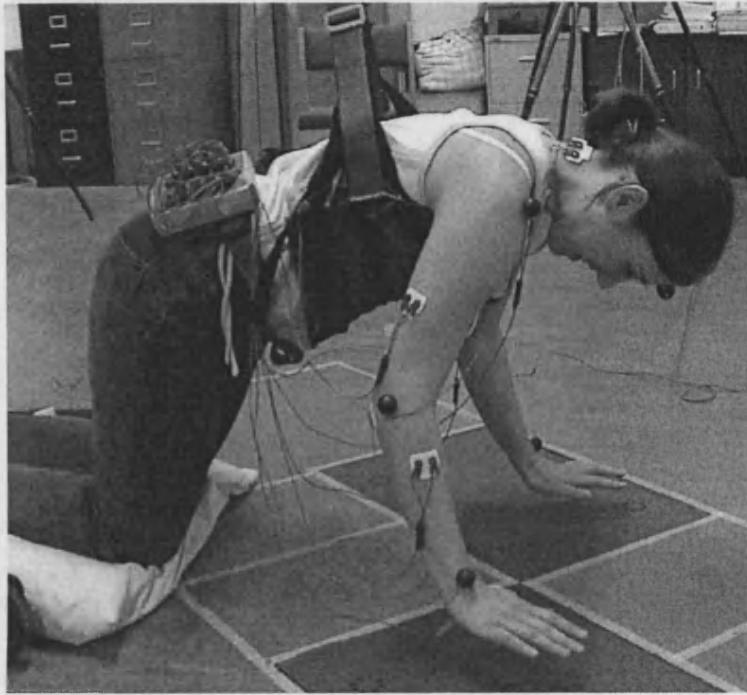


Figure 2.24: Volunteer suspended in rig with EMG equipment.

The HSV cameras were armed in VITcam (software for capturing high-speed video) and then both cameras and the EMG system were triggered from within SIMI Motion software so that they were synchronised with each other. The cameras were set to capture at 500 fps. The analogue data from both the force plates and the EMG system were captured in SIMI. The recording time was 2 seconds due to the short duration of the impact.

The sampling frequency of the force plates in this study was reduced from 2040 Hz to 300 Hz. This was due to an internal file in the SIMI Motion software that had been programmed to override the incoming sampling frequency and change it to a pre-defined one. This file was only discovered during analysis of the data but fortunately it was found that the sampling frequency of 300 Hz was fast enough to adequately capture the impact data.

After the 1 cm drop, the volunteer was dropped, using the same procedure, from a height of 5 cm. The drop from 5 cm was repeated once.

A male volunteer, who had previous training in how to fall during combat training, volunteered to do some extra falls at heights of 10 cm and 20 cm from the drop rig and also falls from standing height onto the force plates. The data was captured in the same way as the previous procedure and for the same time duration. To enable a comparison of the standing height falls to be made, another male volunteer, who had also had training in how to fall during combat training, completed falls from a standing height using the same procedure.

2.7 COMPUTER MODELLING

A series of biomechanical arm models were developed using the ADAMS[®] (Automatic Dynamic Analysis of Mechanical Systems) software. ADAMS[®] enables the user to build any mechanical model in the interface and then simulate that model dynamically, statically or kinematically.

ADAMS[®] contains a number of simple tools containing rigid bodies that can be joined to each other using joints (e.g. revolute and translational) and connectors (e.g. springs, bushings and beams) in order to build a full model. Motions and contacts can then be added to these parts and joints to produce dynamic models. ADAMS[®] simulations are used to evaluate the model performance characteristics and its response to a set of operating conditions.

The model under development in this thesis is not intended as an exact model of the human arm but a tool to aid in the building of a mechanical assessment device for use on IAPS (Impact Absorbing Playground Surfaces). Therefore, the muscles, joint surfaces, ligaments and tendons in the arm, that are very complex, are represented using spring damper systems. Also, the complex bone structure in the arm is split into three very simple sections containing an upper arm (humerus), the lower arm (radius and ulna) and the hand that are joined to each other using simplified joints for the shoulder, elbow and wrist.

The following sections describe the development of the arm model through to the final model (Model 5). The progression of these models will be detailed in the discussion.

2.7.1 MODEL 1

Figure 2.25 shows the first model, that is a simple link model with a 15 kg mass representing the effective mass of the body (this mass is used throughout the models). Two links represented the upper and lower arms with a revolute joint for the elbow. There is no hand in this model as the wrist joint is fixed to the 'floor' using a revolute joint. A spring damper attaches the upper and lower arm to represent the resistance to the fall (muscle action). There are also contacts between the floor and the elbow and the floor and the body mass.

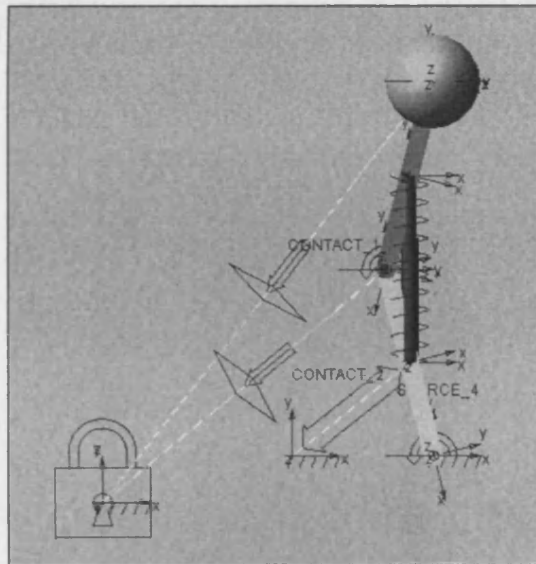


Figure 2.25: Model 1.

2.7.2 MODEL 2

Figure 2.26 shows Model 2. In this model the upper and lower arm and hand are represented using cylinders. Spheres and revolute joints represent the elbow, wrist and shoulder. A spring damper connects the upper to the lower arm.

This model is raised up off the floor, as in a fall situation, and the hand, lower arm and upper arm all possess contacts with the floor. Coulomb friction is added between floor and hand to prevent slipping when the hand hits the floor. A box is used to represent the floor to enable the contacts to be added. This is attached to ground using a fixed joint.

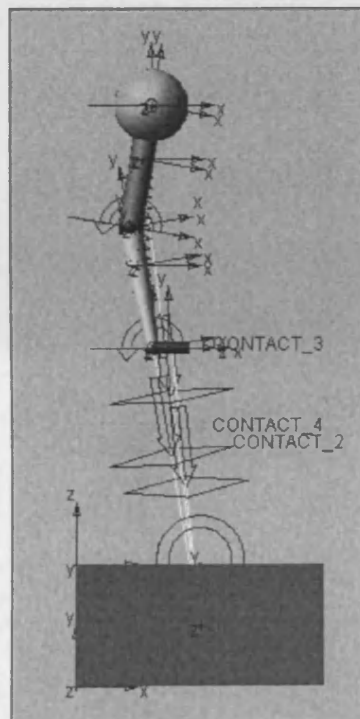


Figure 2.26: Model 2.

2.7.3 MODEL 3

Figure 2.27 shows a two handed model that contains a rectangle representing the torso of the body with shoulder joints as spheres on both sides. Cylinders represent the upper and lower arms and hands. Spheres and revolute joints represent the elbows, wrists and shoulders. A spring damper connects the upper arms to the lower arms. There is a *primitive joint* with a parallel axis added between the hand and floor in the x plane so that during the simulation the hand and floor are parallel throughout. Contacts have been added between the hand and floor and the body and floor.

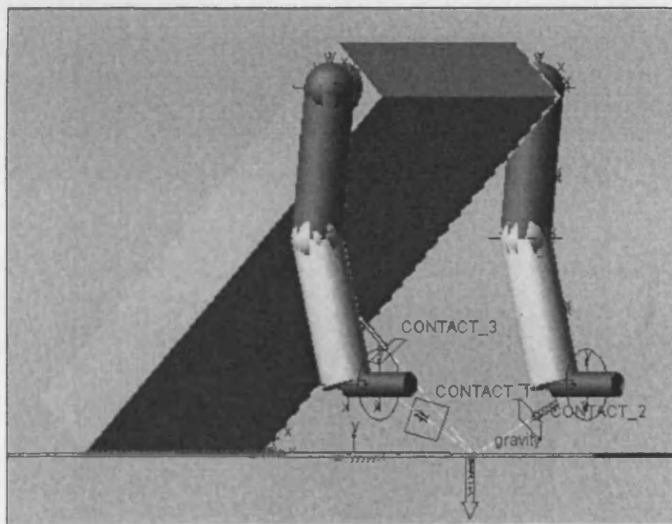


Figure 2.27: Model 3.

2.7.4 MODEL 4

Figure 2.28 shows Model 4. In this model the hand is represented by a cylinder that is locked to ground using a fixed joint. The lower and upper arms are made up of different sections of cylinders that are constrained with translational joints and a spring damper between shoulder and elbow and elbow and wrist. There is also a spring damper connected between the upper and lower arm. Spheres and revolute joints represent elbow and shoulder. The body mass and the elbow contain contacts with the floor.

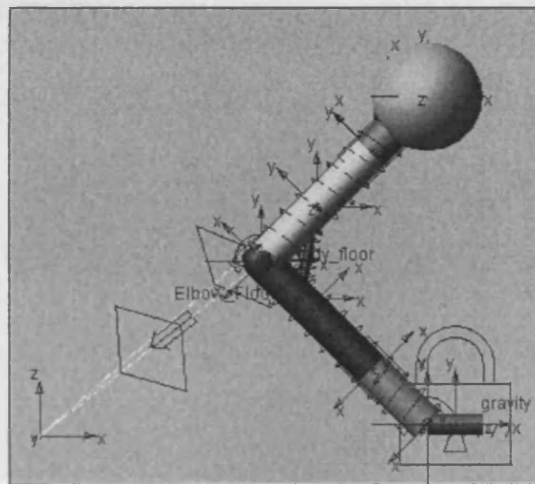


Figure 2.28: Model 4.

CHAPTER 3

RESULTS

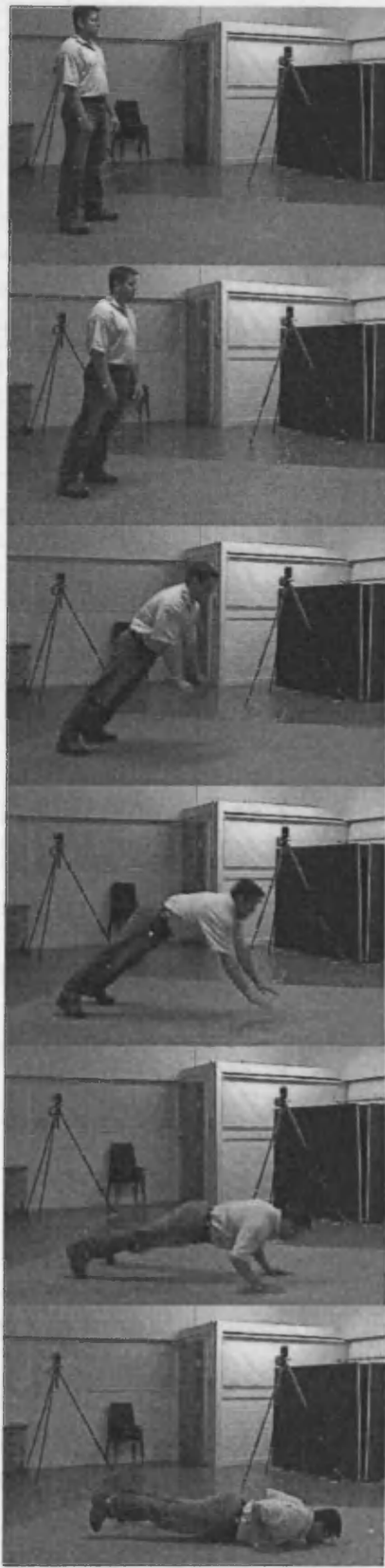
3.1 INTRODUCTION

A series of studies were conducted, using the materials and methodology detailed in Chapter 2, to assess falls onto the outstretched hand. The results of these studies are detailed in the relevant sections of this chapter and will be discussed in detail in Chapter 4.

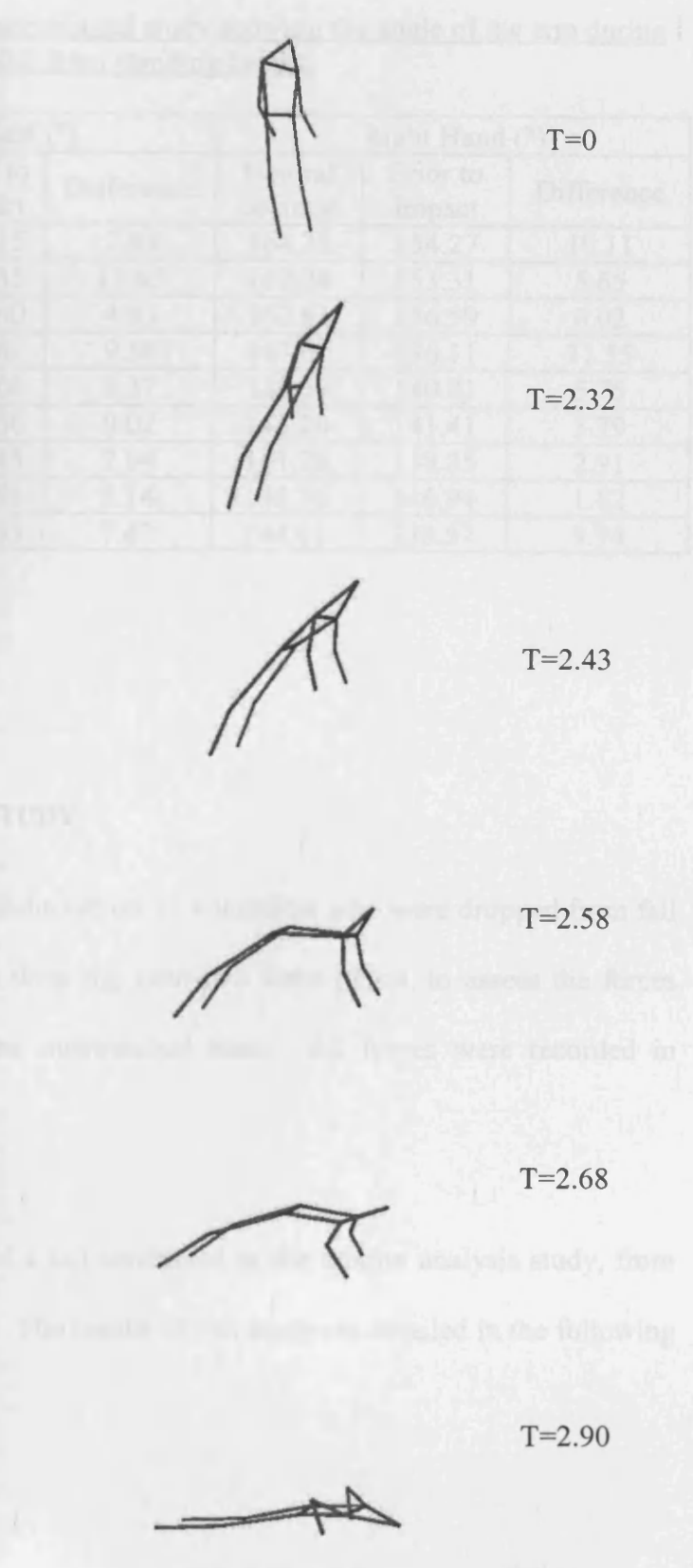
3.2 OBSERVATIONAL STUDY

An observational study was conducted to assess the position of the arm, specifically the angle of the elbow, during a fall and subsequent impact with a surface.

Figure 3.1 shows an example of a fall conducted in the observational study, from standing height onto a 2.5 cm foam surface. The results of the observational study can be seen in table 3.1, which shows the angle of the arms in an anatomically relaxed position and immediately prior to impact. The difference between these two values is also shown.



Real image photographs



QTM stick figures

Time (sec)

Figure 3.1: Series of photographs showing a fall from standing height onto a 2.5 cm foam surface with associated stick figures from QTM and time of fall.

Table 3.1: Results from the observational study showing the angle of the arm during a fall from standing height.

Test name	Left Hand (°)			Right Hand (°)		
	Neutral position	Prior to impact	Difference	Neutral position	Prior to impact	Difference
Standing 1	165	157.15	7.85	164.38	154.27	10.11
Standing 2	169	157.35	11.65	162.24	153.31	5.65
Standing 3	162.63	158.60	4.03	162.61	156.59	6.02
Crash mat 1	147.25	137.67	9.58	147.66	136.11	11.55
Crash mat 2	145.01	135.64	9.37	146.56	140.81	5.75
Crash mat 3	144.58	135.56	9.02	145.20	141.41	3.79
Platform 1	147.39	139.45	7.94	141.26	138.35	2.91
Platform 2	142.67	137.53	5.14	148.76	146.94	1.82
Platform 3	140.12	132.65	7.47	144.61	140.57	3.94

3.3 MOTION ANALYSIS STUDY

A series of experiments were conducted on 35 volunteers who were dropped from fall heights of 3 and 5 cms from a drop rig, onto two force plates, to assess the forces produced during a fall onto the outstretched hand. All forces were recorded in Newtons (N).

Figure 3.2 shows an example of a fall conducted in the motion analysis study, from the drop rig at a height of 5 cm. The results of this study are detailed in the following sections.

3.1.1 ANALYSIS OF FALLS

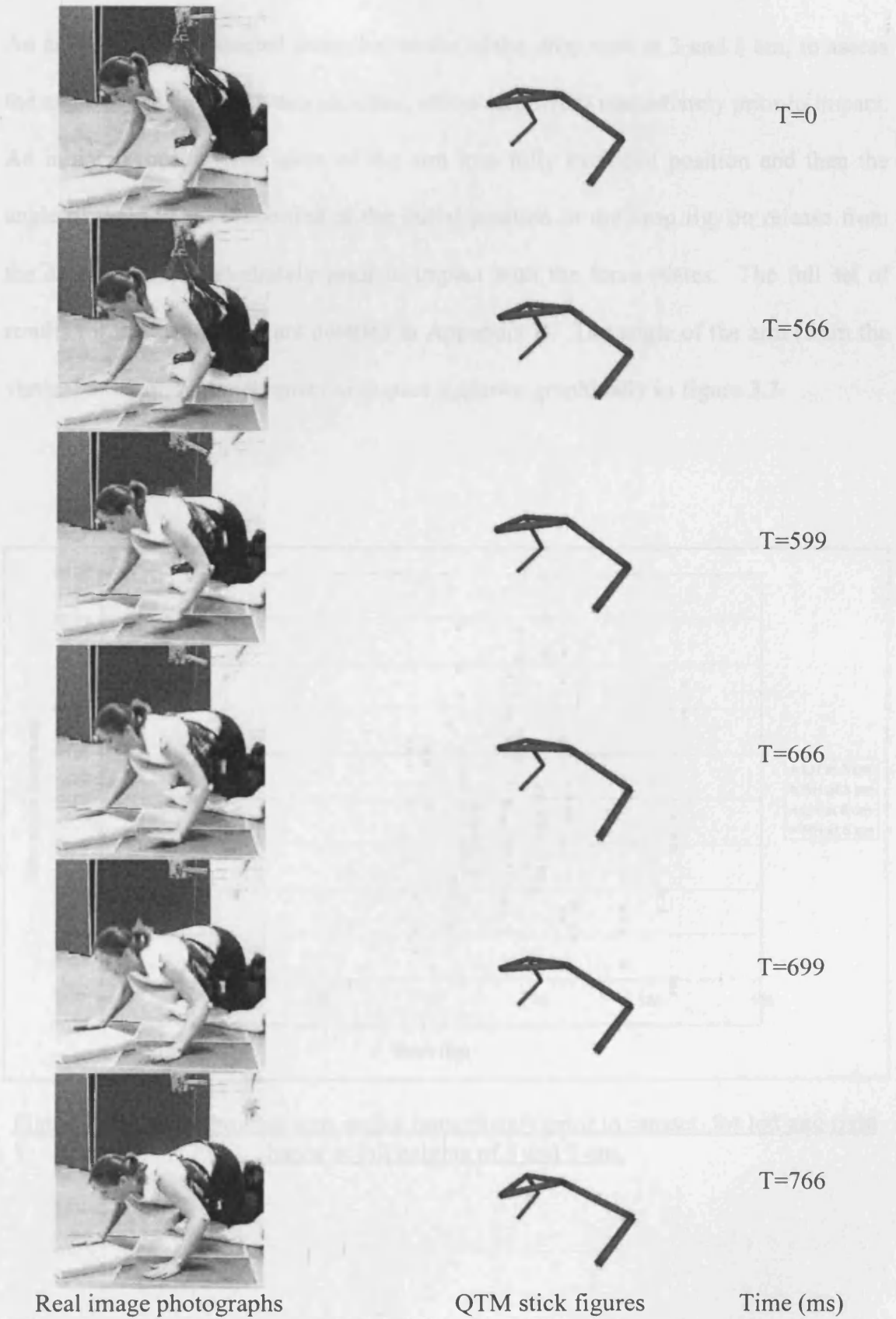


Figure 3.2: Series of photographs showing a fall from the drop rig, at a height of 5 cm, onto the force plates with associated stick figures from QTM and time of fall.

3.3.1 ANALYSIS OF ARM ANGLES

An analysis was conducted from the results of the drop tests at 3 and 5 cm, to assess the angle of the arm (between shoulder, elbow and wrist) immediately prior to impact. An initial recording was taken of the arm in a fully extended position and then the angle of the arm was recorded at the initial position in the drop rig, on release from the drop rig and immediately prior to impact with the force plates. The full set of results for the arm angles are detailed in Appendix B. The angle of the arm (from the vertical axis) immediately prior to impact is shown graphically in figure 3.3.

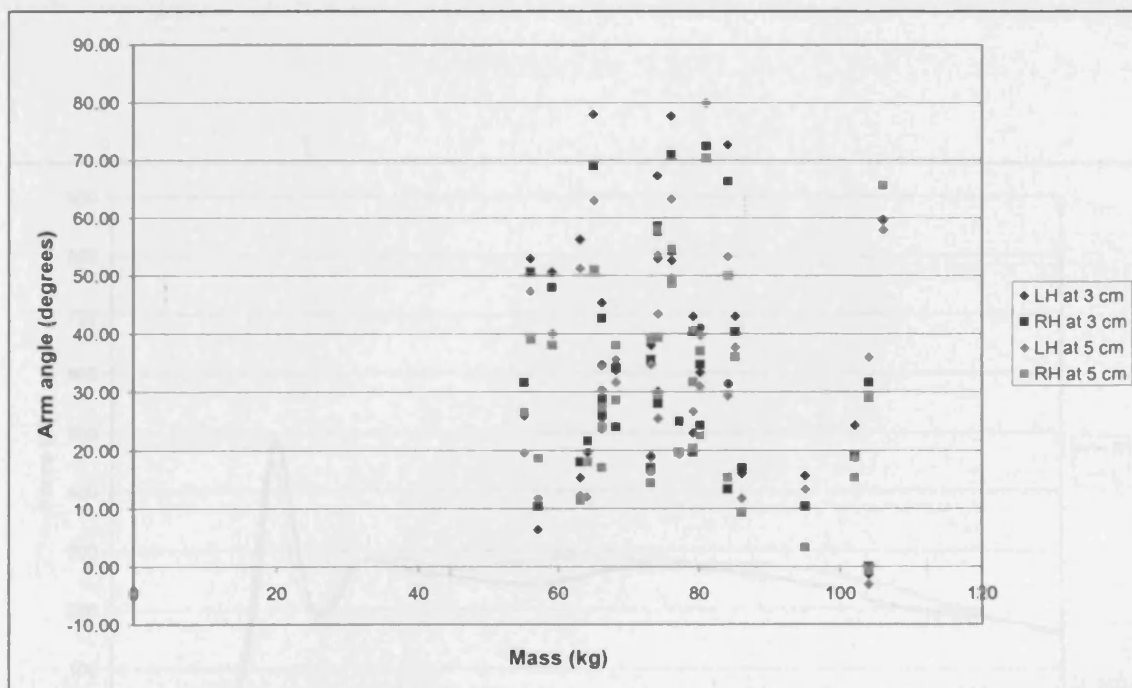


Figure 3.3: Graph showing arm angles immediately prior to impact, for left and right hands at fall heights of 3 and 5 cm.

3.3.2 TYPICAL FORCE-TIME IMPACT CURVES

Falls onto the outstretched hand, from fall heights of 3 and 5 cm, produced force-time impact curves with peak characteristics.

Figures 3.4 and 3.5 show typical force-time impact curves, for the right and left hand, at fall heights of 3 and 5 cm respectively.

Figure 3.6 shows a force-time impact curve, highlighting the characteristic force peaks. The terminology used in figure 3.6 will be used throughout the study when discussing the impact forces.

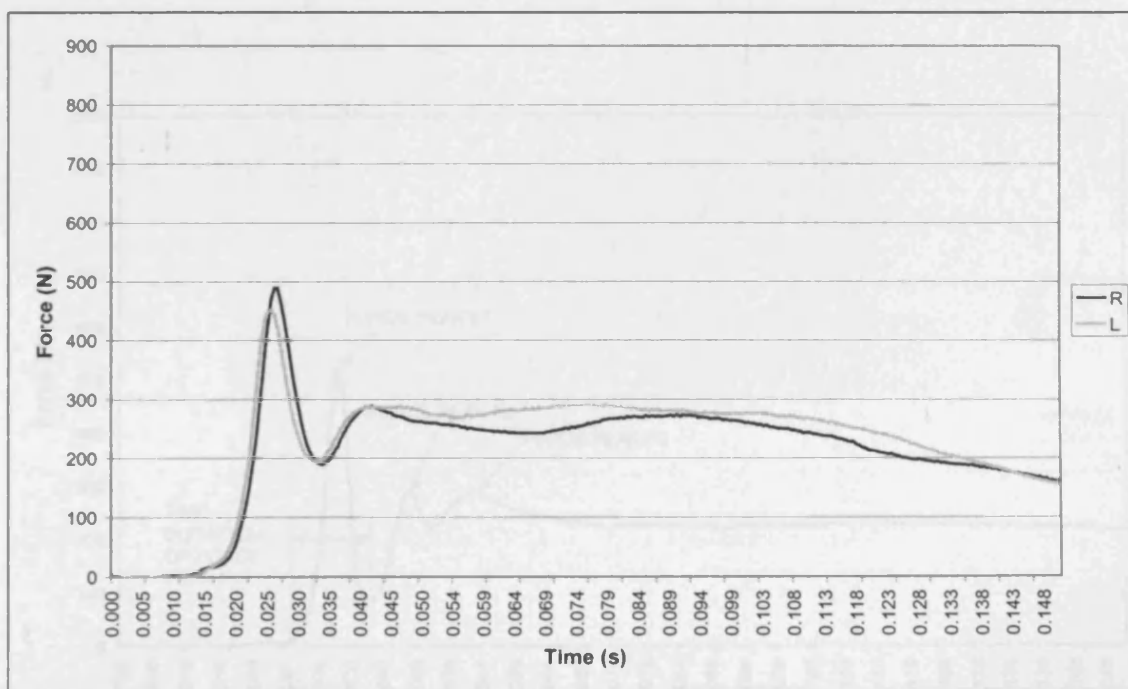


Figure 3.4: Graph showing typical force-time impact curve at a fall height of 3 cm.

3.3 ANALYSIS OF LEFT AND RIGHT HANDED IMPACT FORCES

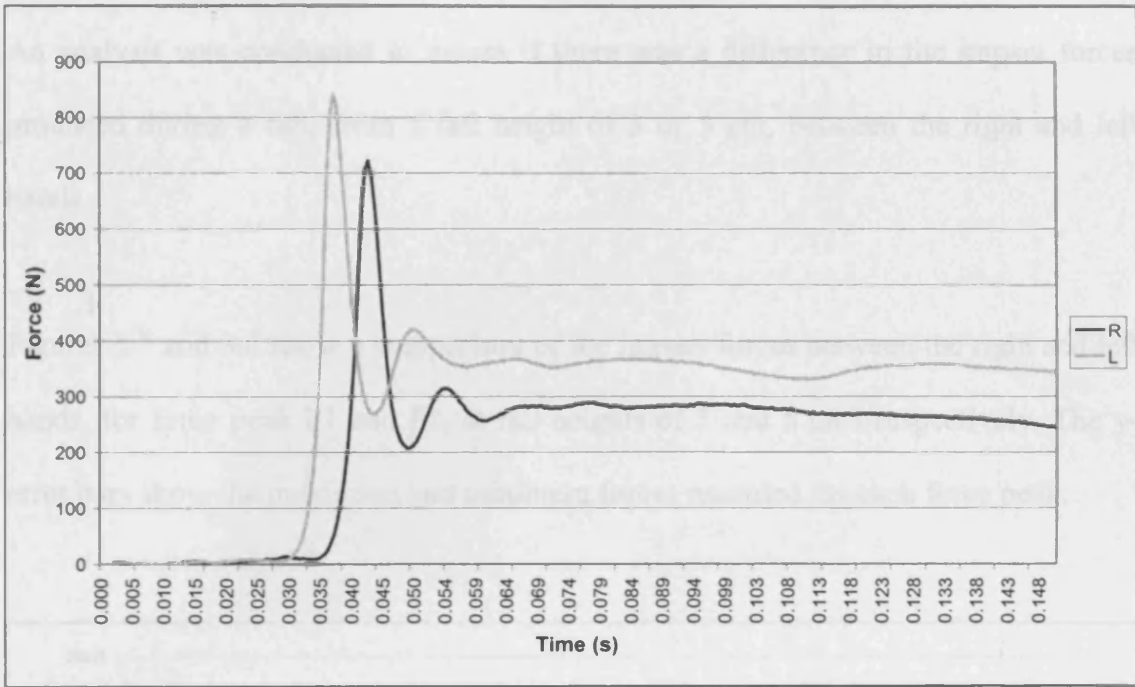


Figure 3.5: Graph showing typical force-time impact curve at a fall height of 5 cm.

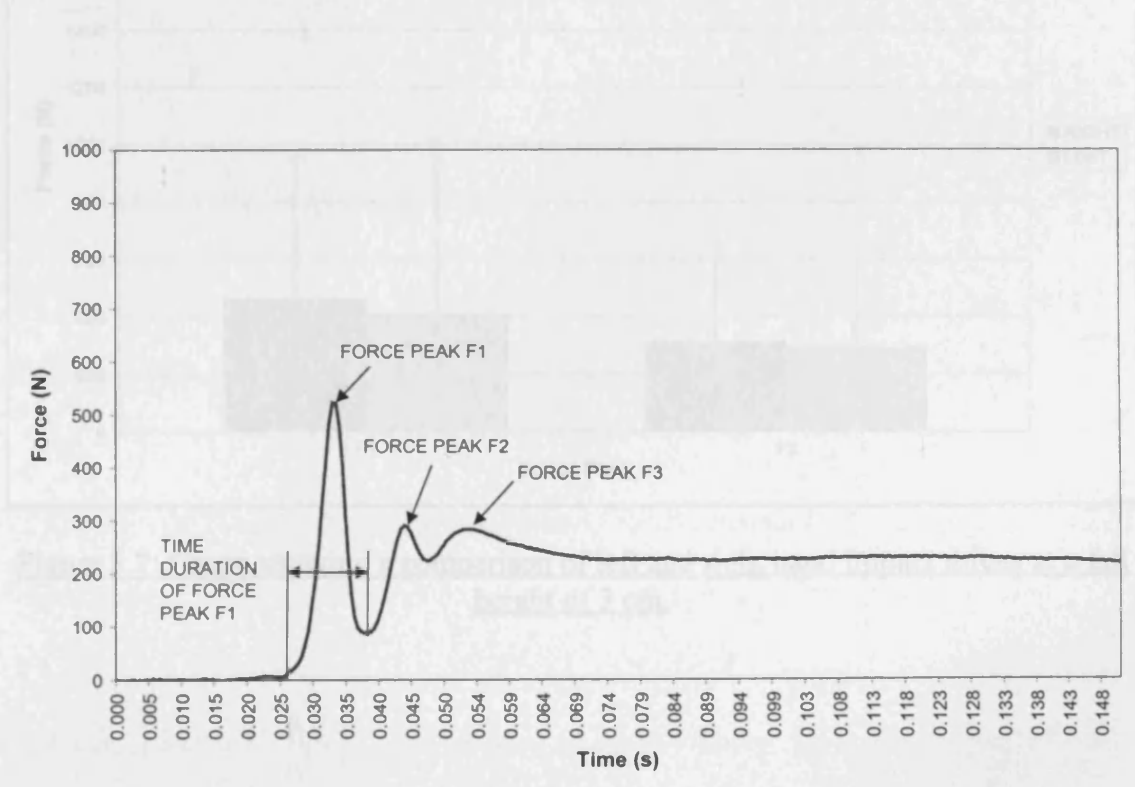


Figure 3.6: Graph showing a typical force-time curve, introducing terminology of the force peaks used throughout the study.

3.3.3 ANALYSIS OF LEFT AND RIGHT HAND IMPACT FORCES

An analysis was conducted to assess if there was a difference in the impact forces produced during a fall, from a fall height of 3 or 5 cm, between the right and left hands.

Figures 3.7 and 3.8 show a comparison of the impact forces between the right and left hands, for force peak F1 and F2, at fall heights of 3 and 5 cms respectively. The y-error bars show the maximum and minimum forces recorded for each force peak.

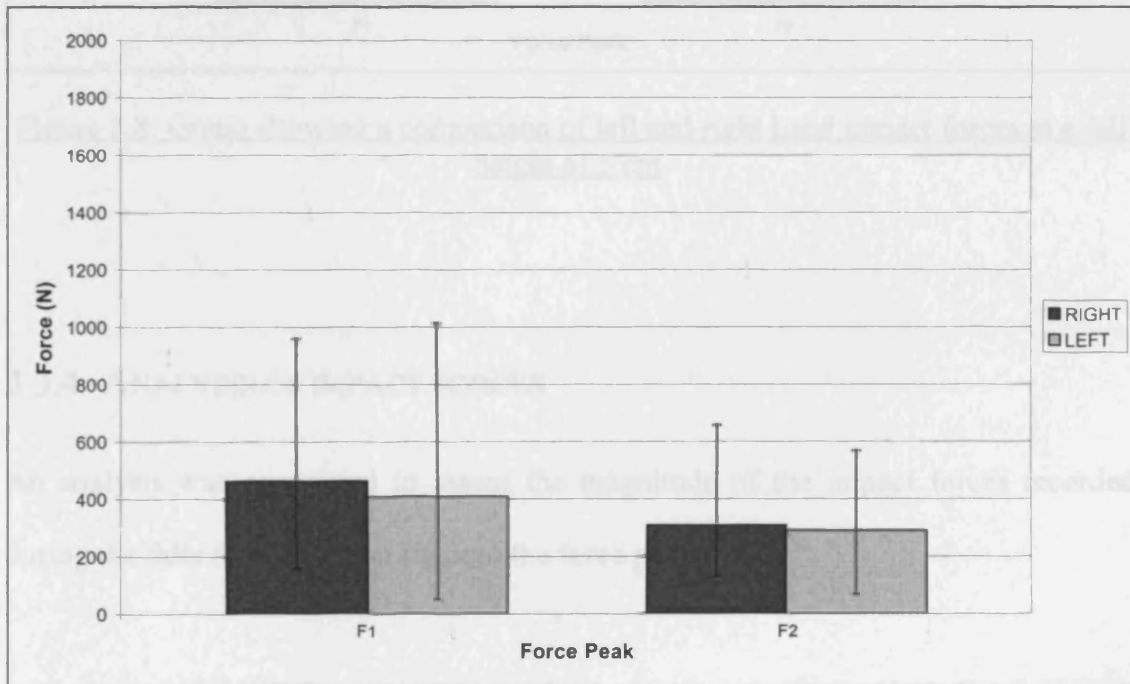


Figure 3.7: Graph showing a comparison of left and right hand impact forces at a fall height of 3 cm.

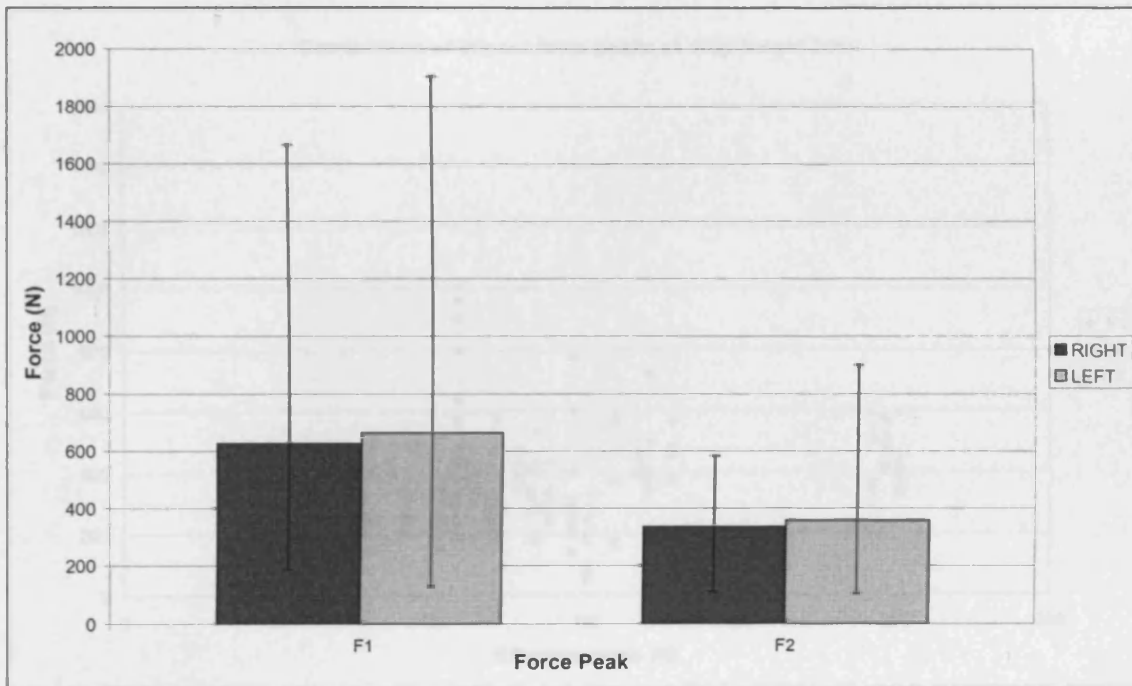


Figure 3.8: Graph showing a comparison of left and right hand impact forces at a fall height of 5 cm.

3.3.4 ANALYSIS OF IMPACT FORCES

An analysis was conducted to assess the magnitude of the impact forces recorded during the falls from the drop rig onto the force plates.

Figure 3.9 and 3.10 show the impact forces of the force peaks F1, F2 and F3 for all 35 volunteers (in terms of effective mass) at fall heights of 3 and 5 cm respectively.

Figure 3.11 and 3.12 show a comparison of impact forces, from falls heights of 3 and 5 cm, for force peak F1 and F2 respectively.

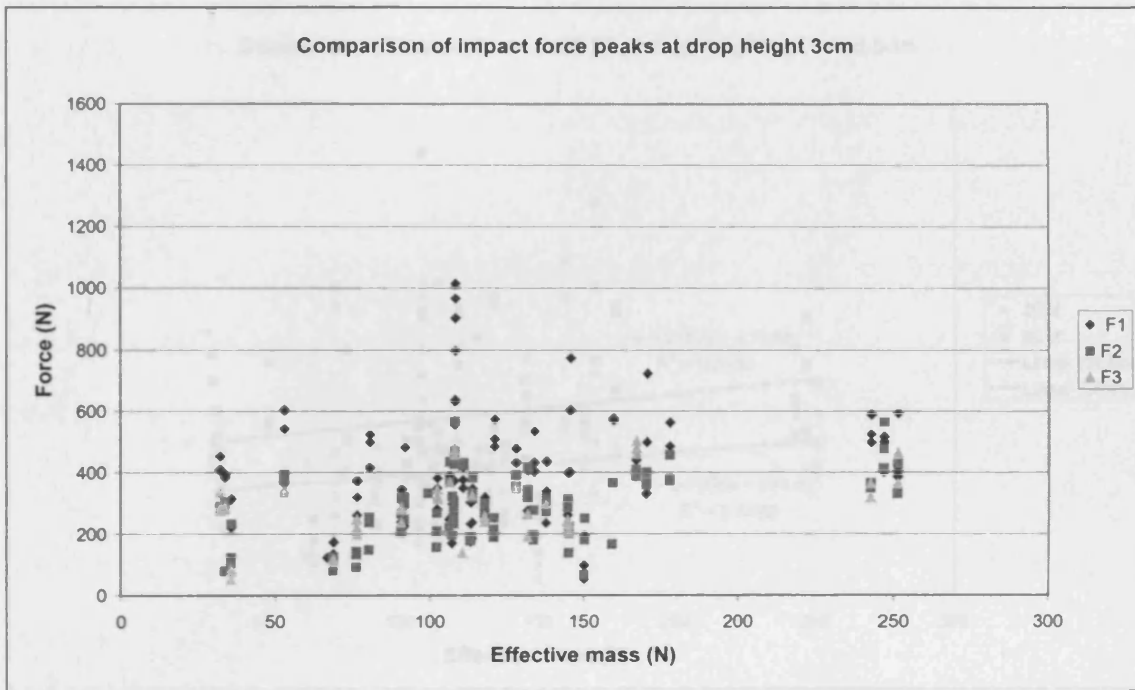


Figure 3.9: Graph showing a comparison of impact force peaks at a fall height of 3 cm.

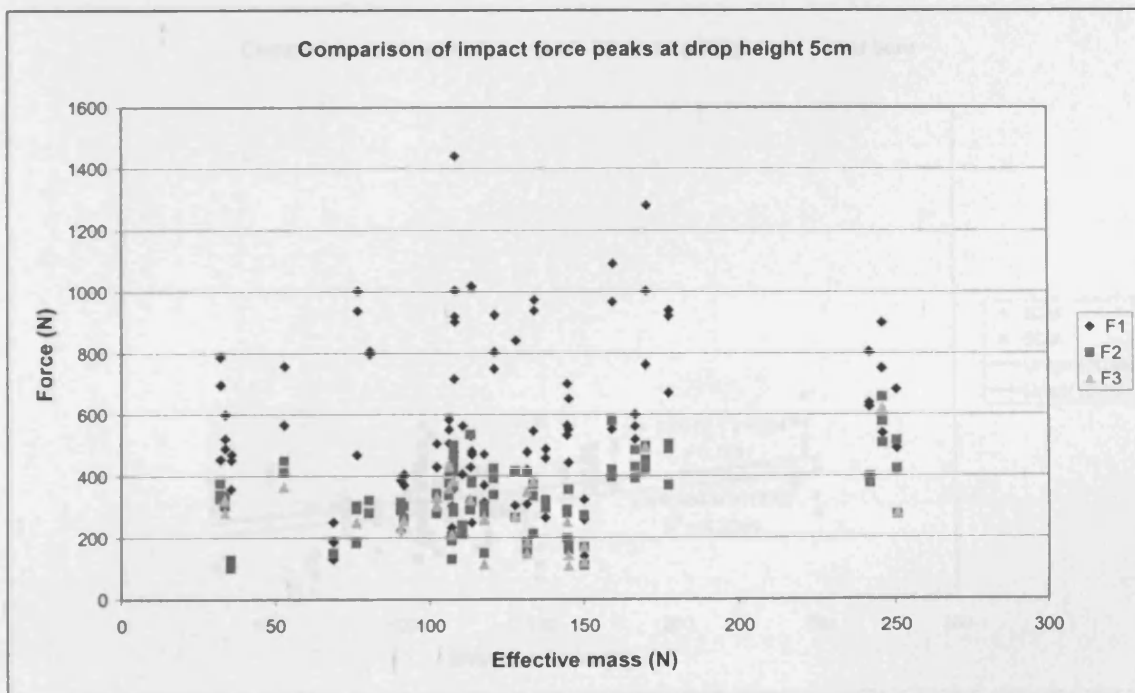


Figure 3.10: Graph showing a comparison of impact force peaks at a fall height of 5 cm.

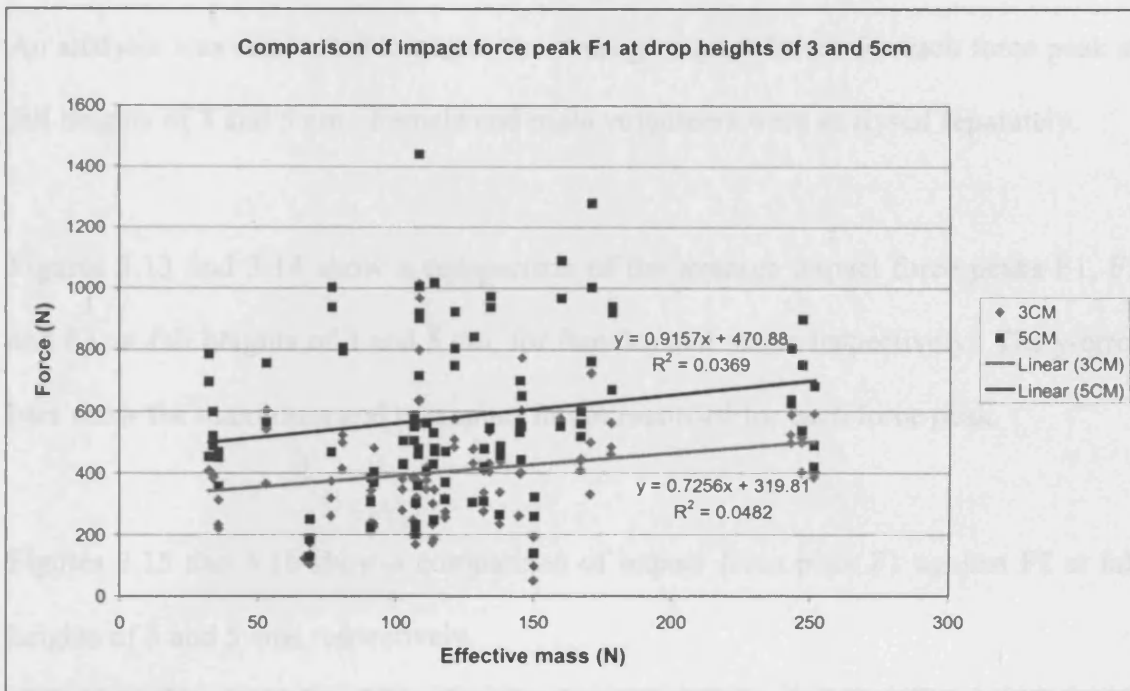


Figure 3.11: Graph showing a comparison of impact force peak F1 at fall heights of 3 and 5 cm.

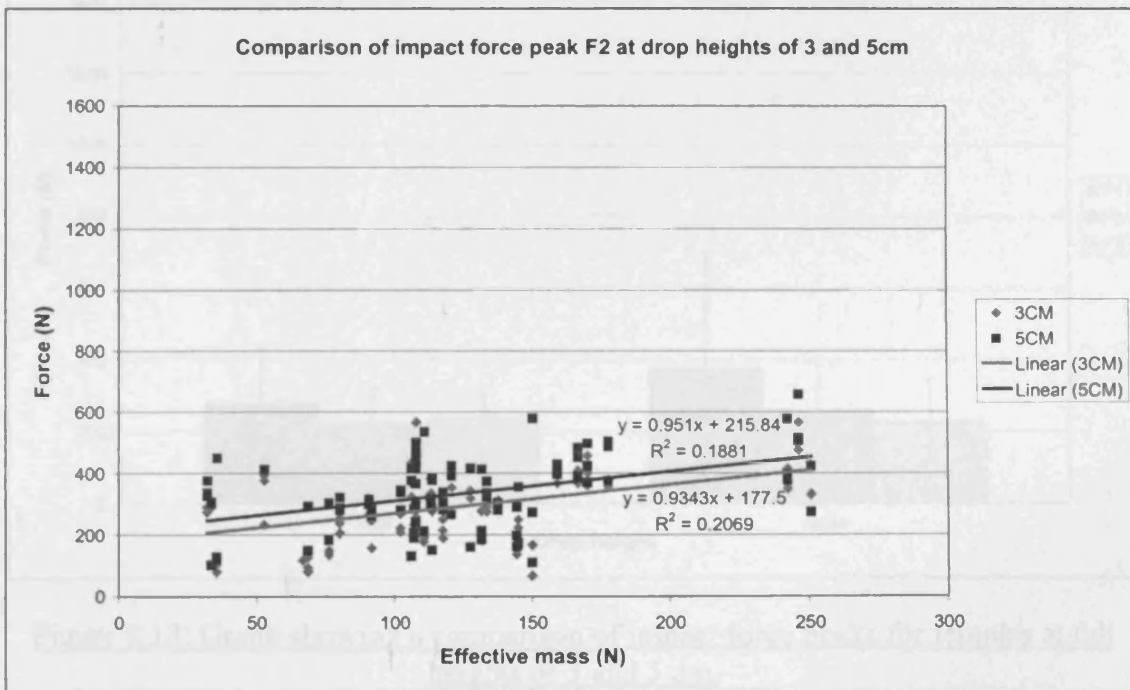


Figure 3.12: Graph showing a comparison of impact force peak F2 at fall heights of 3 and 5 cm.

3.3.4.1 ANALYSIS OF FORCE PEAKS

An analysis was conducted to assess the average impact forces for each force peak at fall heights of 3 and 5 cm. Female and male volunteers were analysed separately.

Figures 3.13 and 3.14 show a comparison of the average impact force peaks F1, F2 and F3, at fall heights of 3 and 5 cm, for females and males respectively. The y-error bars show the maximum and minimum forces recorded for each force peak.

Figures 3.15 and 3.16 show a comparison of impact force peak F1 against F2 at fall heights of 3 and 5 cms respectively.

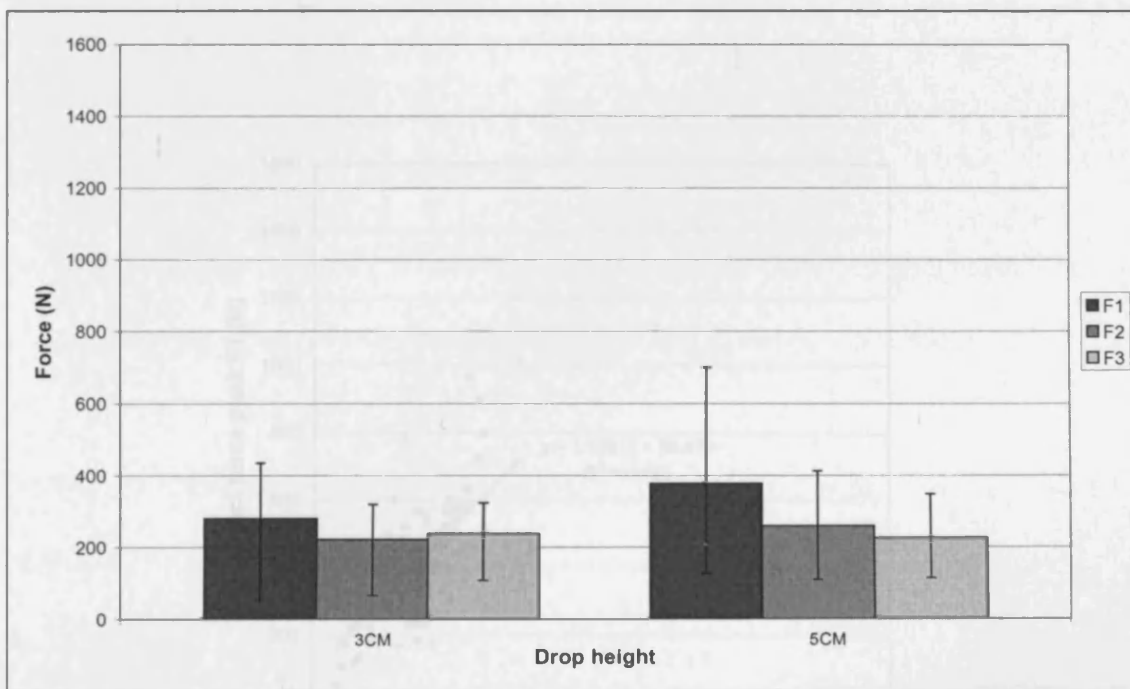


Figure 3.13: Graph showing a comparison of impact force peaks for females at fall heights of 3 and 5 cm.

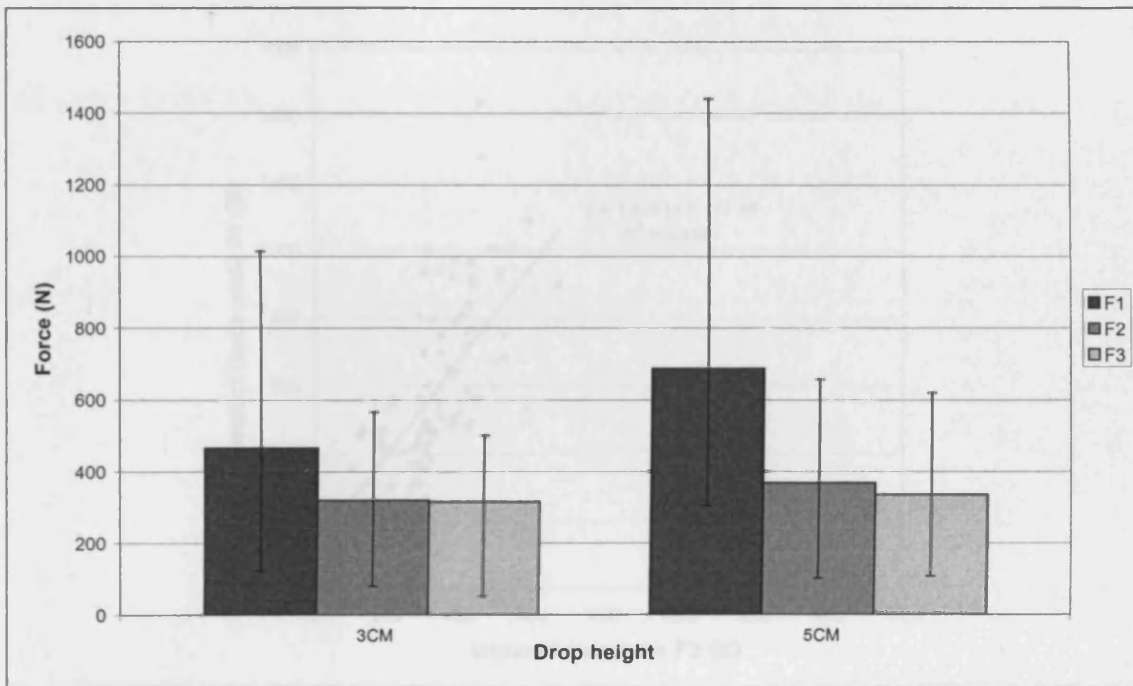


Figure 3.14: Graph showing a comparison of impact force peaks for males at fall heights of 3 and 5 cm.

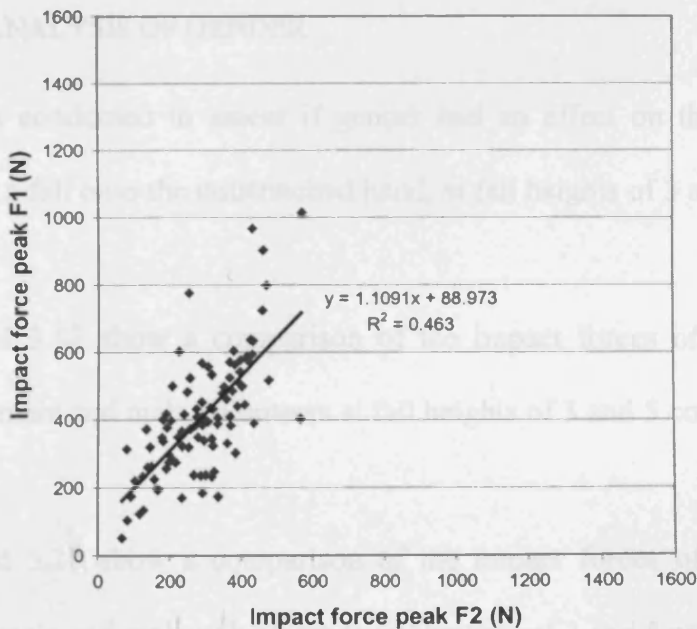


Figure 3.15: Graph showing a comparison of impact force peaks F1 and F2 at a fall height of 3 cm.

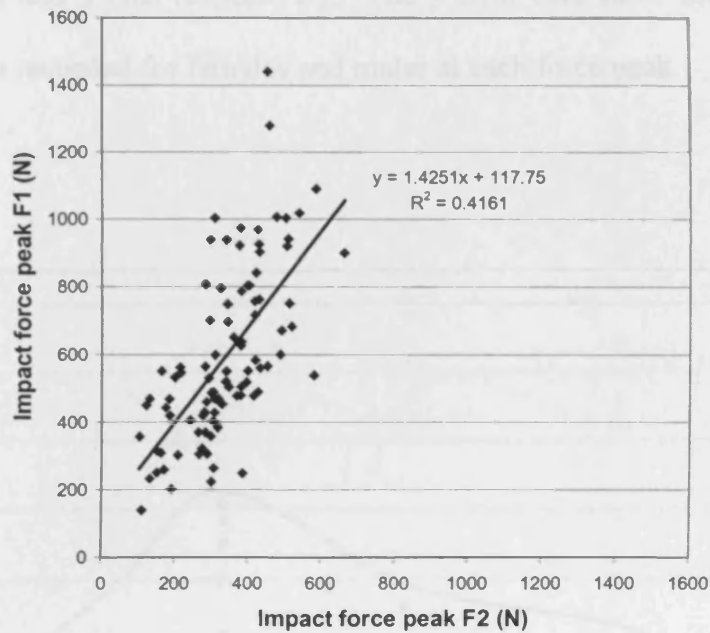


Figure 3.16: Graph showing a comparison of impact force peaks F1 and F2 at a fall height of 5 cm.

3.3.4.2 ANALYSIS OF GENDER

An analysis was conducted to assess if gender had an effect on the impact forces produced during a fall onto the outstretched hand, at fall heights of 3 and 5 cms.

Figures 3.17 and 3.18 show a comparison of the impact forces of force peak F1, separated into female and male volunteers at fall heights of 3 and 5 cm respectively.

Figures 3.19 and 3.20 show a comparison of the impact forces of force peak F2, separated into female and male volunteers at fall heights of 3 and 5 cm respectively.

Figures 3.21 and 3.22 show a comparison of the average impact forces for force peak F1 and F2, at 3 and 5 cms respectively. The y-error bars show the maximum and minimum forces recorded for females and males at each force peak.

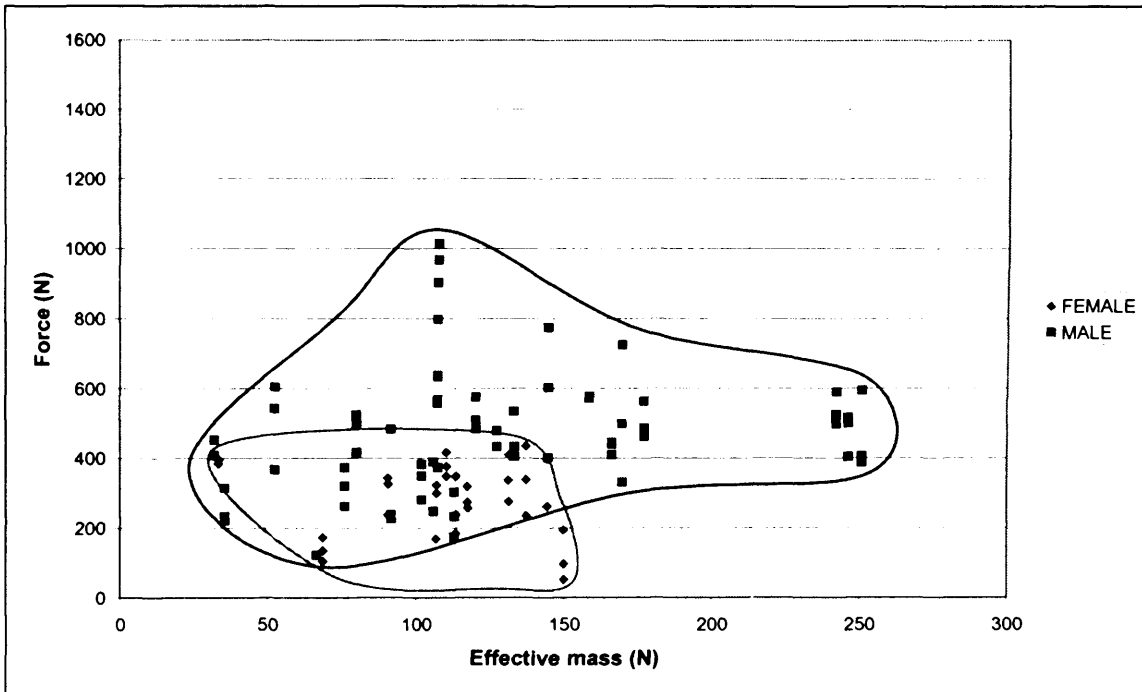


Figure 3.17: Graph showing a comparison of impact force peak F1 for females and males at a fall height of 3 cm.

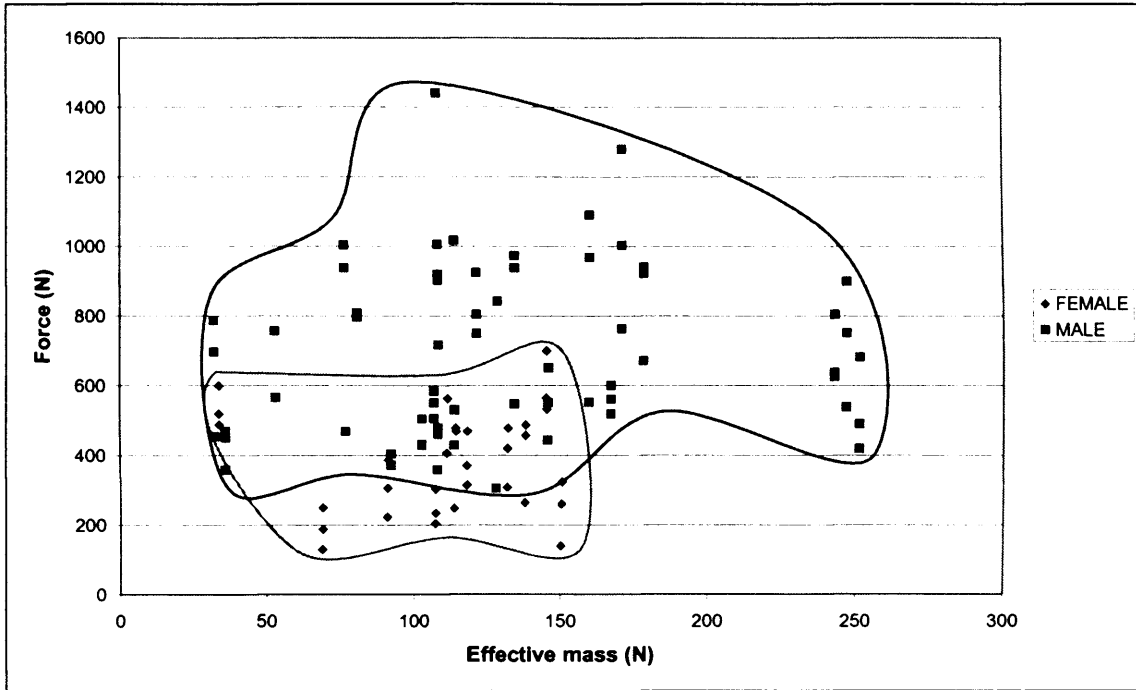


Figure 3.18: Graph showing a comparison of impact force peak F1 for females and males at a fall height of 5 cm.

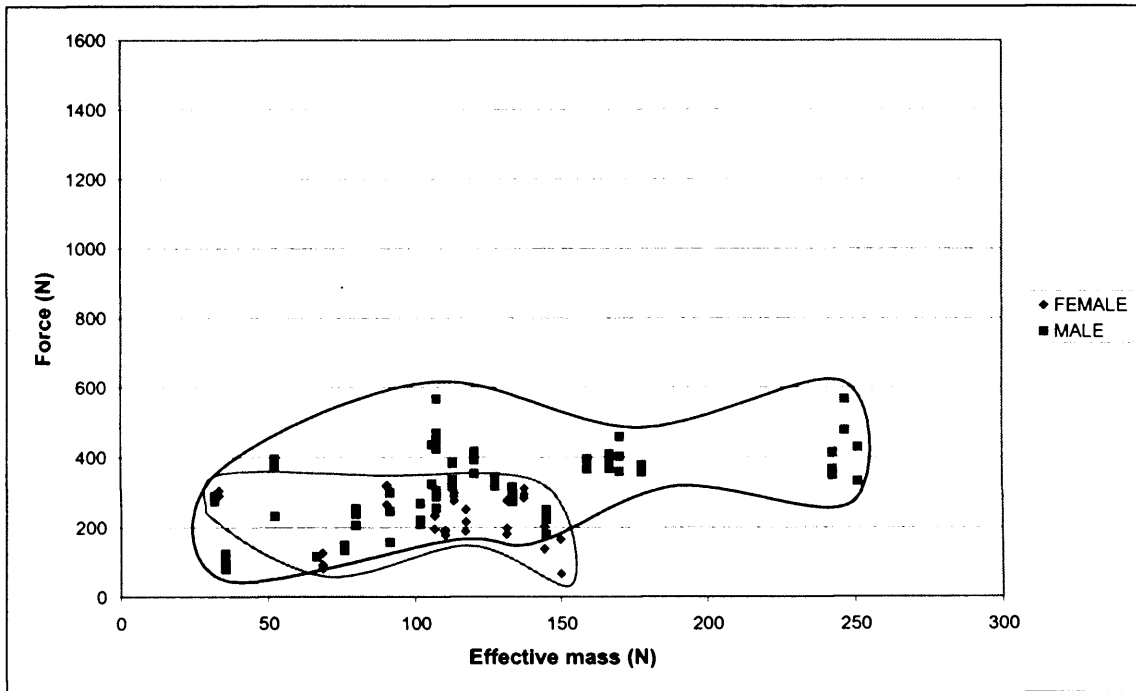


Figure 3.19: Graph showing a comparison of impact force peak F2 for females and males at a fall height of 3 cm.

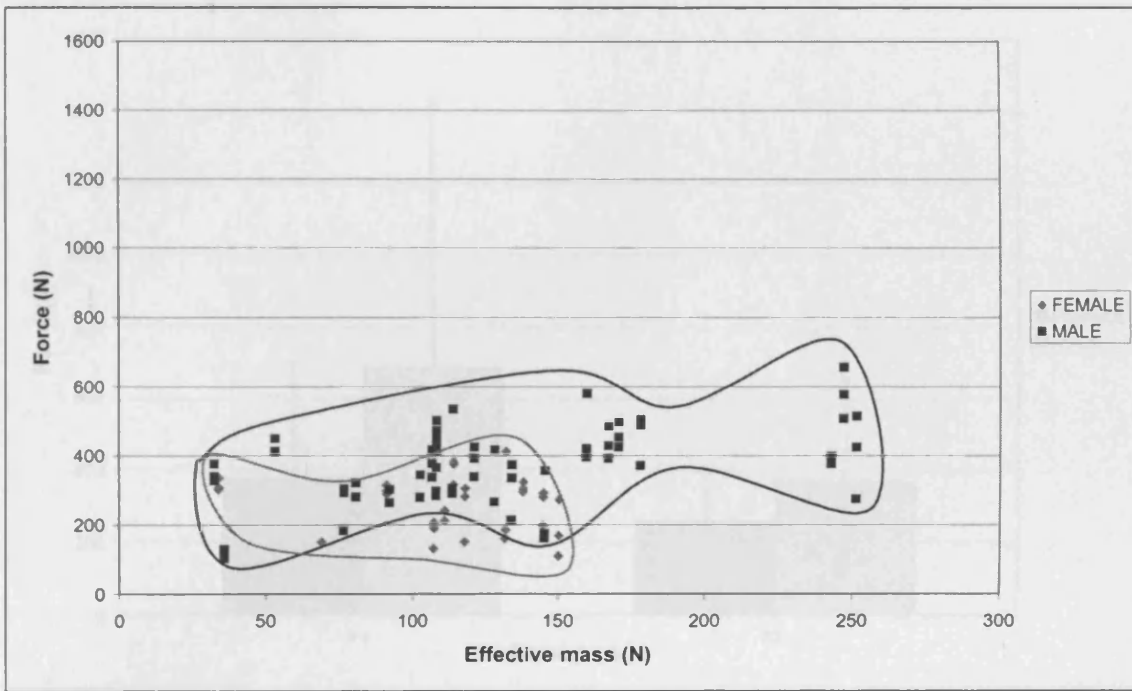


Figure 3.20: Graph showing a comparison of impact force peak F2 for females and males at a fall height of 5 cm.

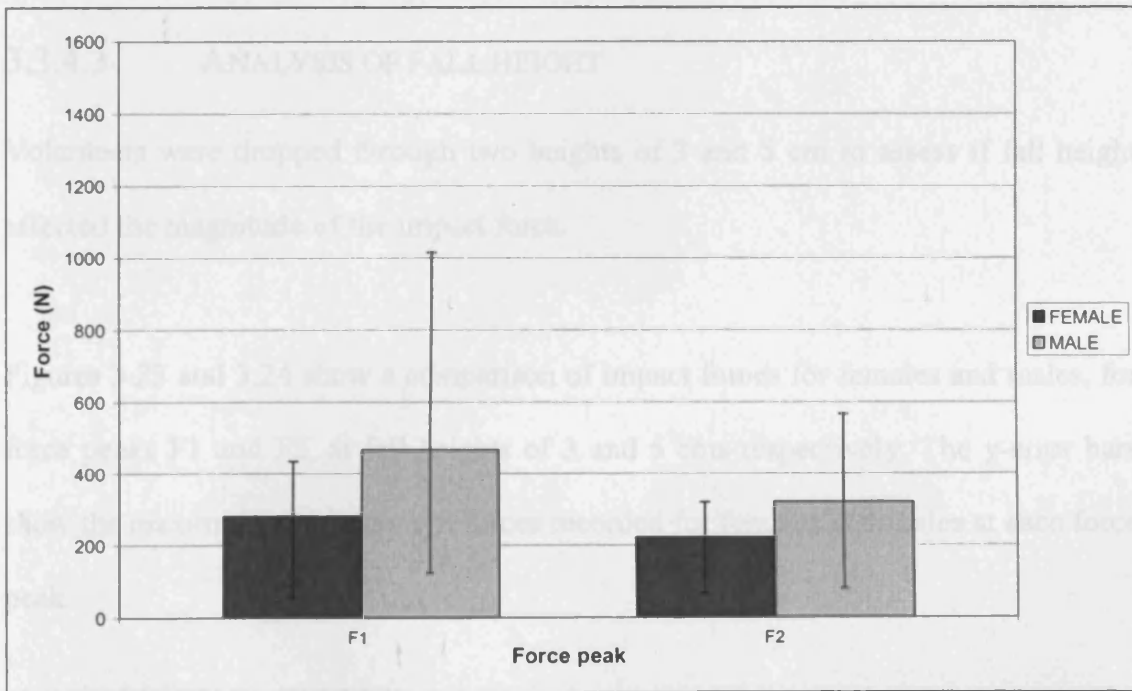


Figure 3.21: Graph showing a comparison of impact force peaks F1 and F2 for females and males at a fall height of 3 cm.

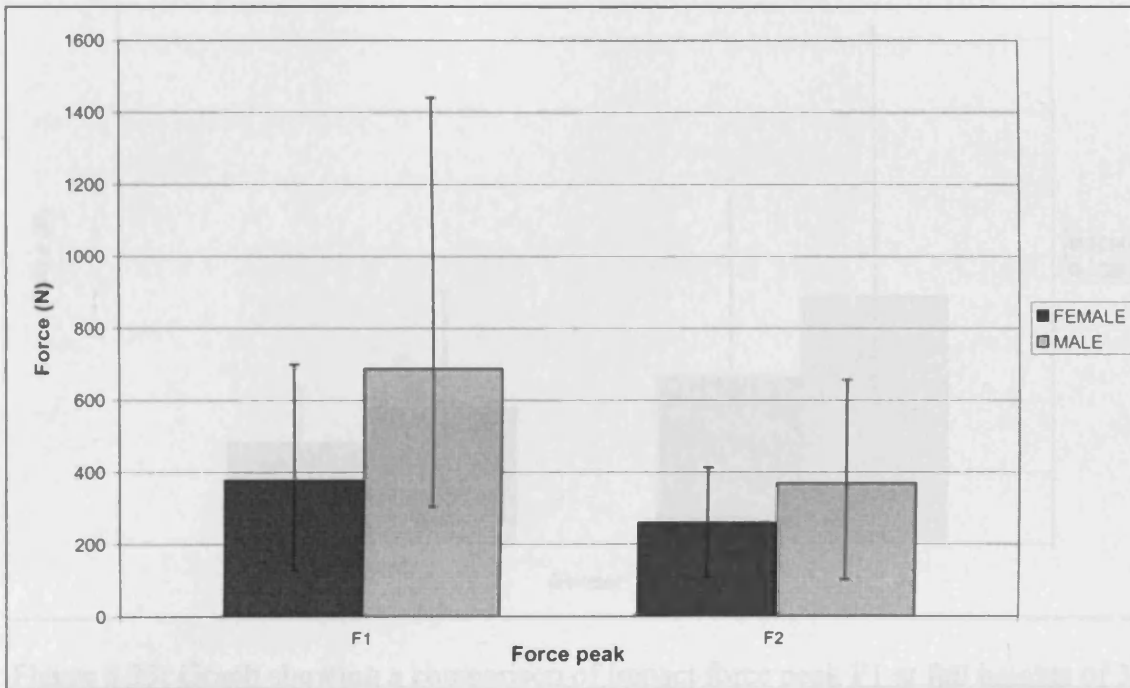


Figure 3.22: Graph showing a comparison of impact force peaks F1 and F2 for females and males at a fall height of 5 cm.

3.3.4.3 ANALYSIS OF FALL HEIGHT

Volunteers were dropped through two heights of 3 and 5 cm to assess if fall height affected the magnitude of the impact force.

Figures 3.23 and 3.24 show a comparison of impact forces for females and males, for force peaks F1 and F2, at fall heights of 3 and 5 cms respectively. The y-error bars show the maximum and minimum forces recorded for females and males at each force peak.

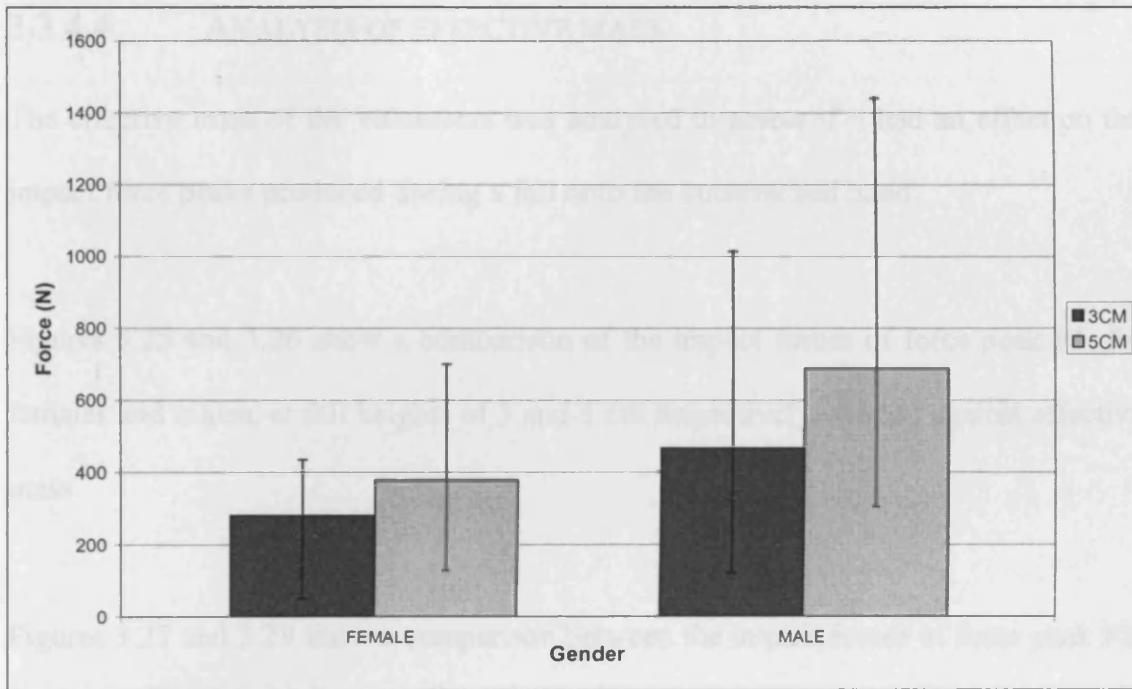


Figure 3.23: Graph showing a comparison of impact force peak F1 at fall heights of 3 and 5 cm for females and males.

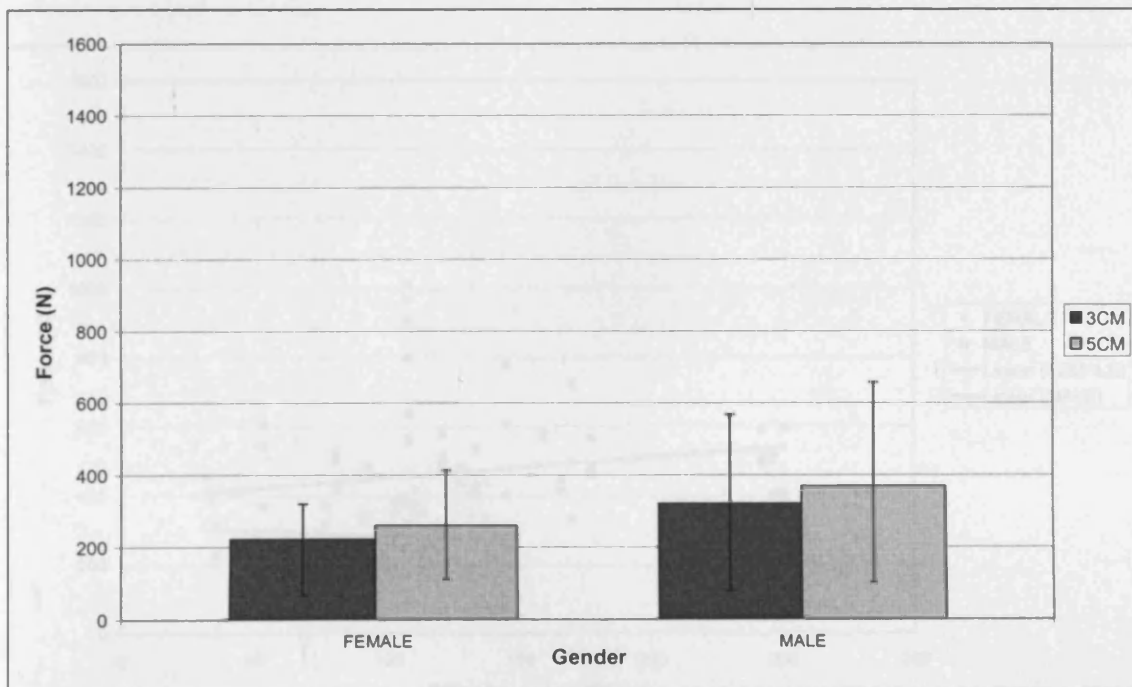


Figure 3.24: Graph showing a comparison of impact force peak F2 at fall heights of 3 and 5 cm for females and males.

3.3.4.4 ANALYSIS OF EFFECTIVE MASS

The effective mass of the volunteers was analysed to assess if it had an effect on the impact force peaks produced during a fall onto the outstretched hand.

Figures 3.25 and 3.26 show a comparison of the impact forces of force peak F1, for females and males, at fall heights of 3 and 5 cm respectively, plotted against effective mass.

Figures 3.27 and 3.28 show a comparison between the impact forces of force peak F2, for females and males, at fall heights of 3 and 5 cm respectively, plotted against effective mass

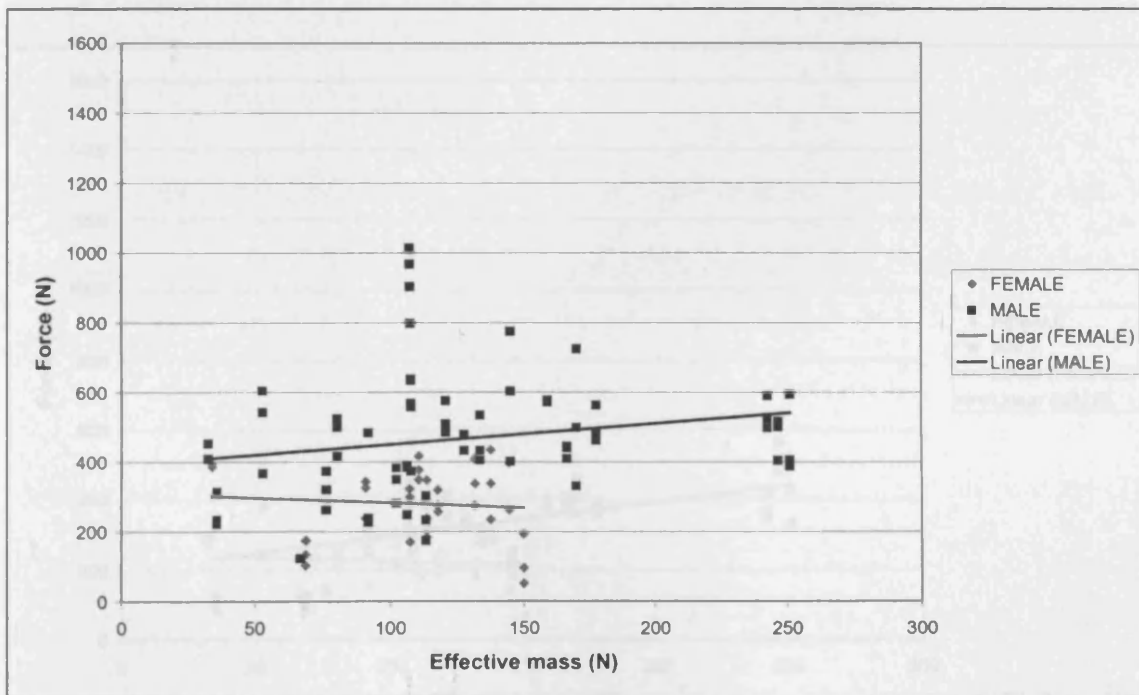


Figure 3.25: Graph showing a comparison of impact force peak F1 against effective mass for females and males at a fall height of 3 cm.

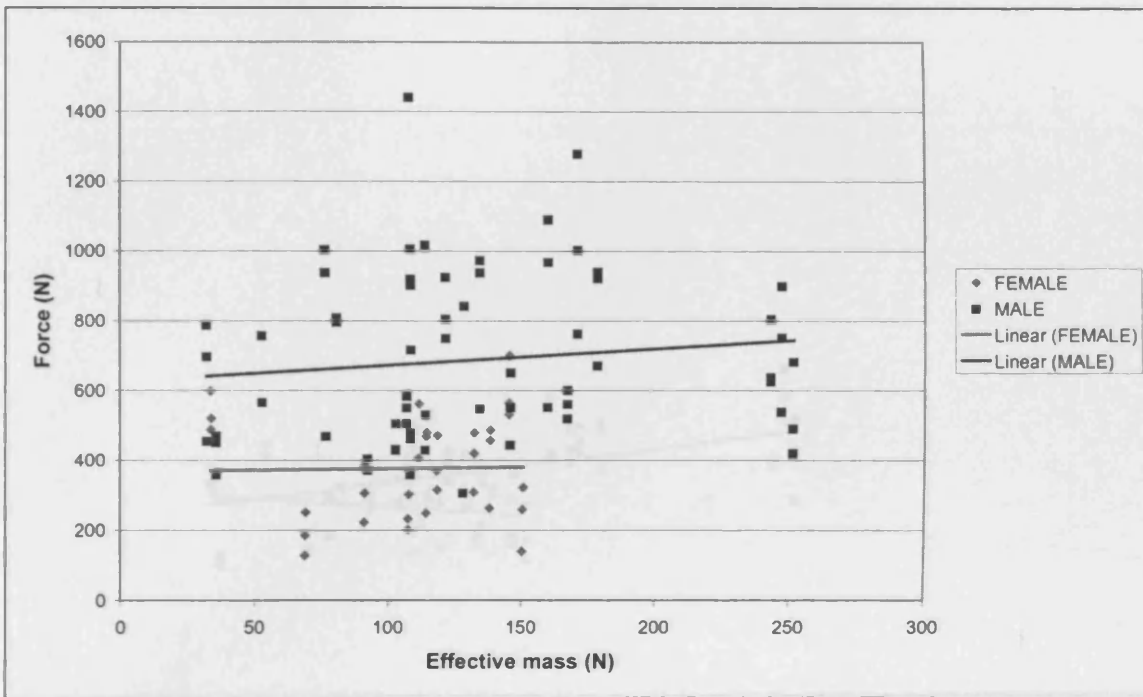


Figure 3.26: Graph showing a comparison of impact force peak F1 against effective mass for females and males at a fall height of 5 cm.

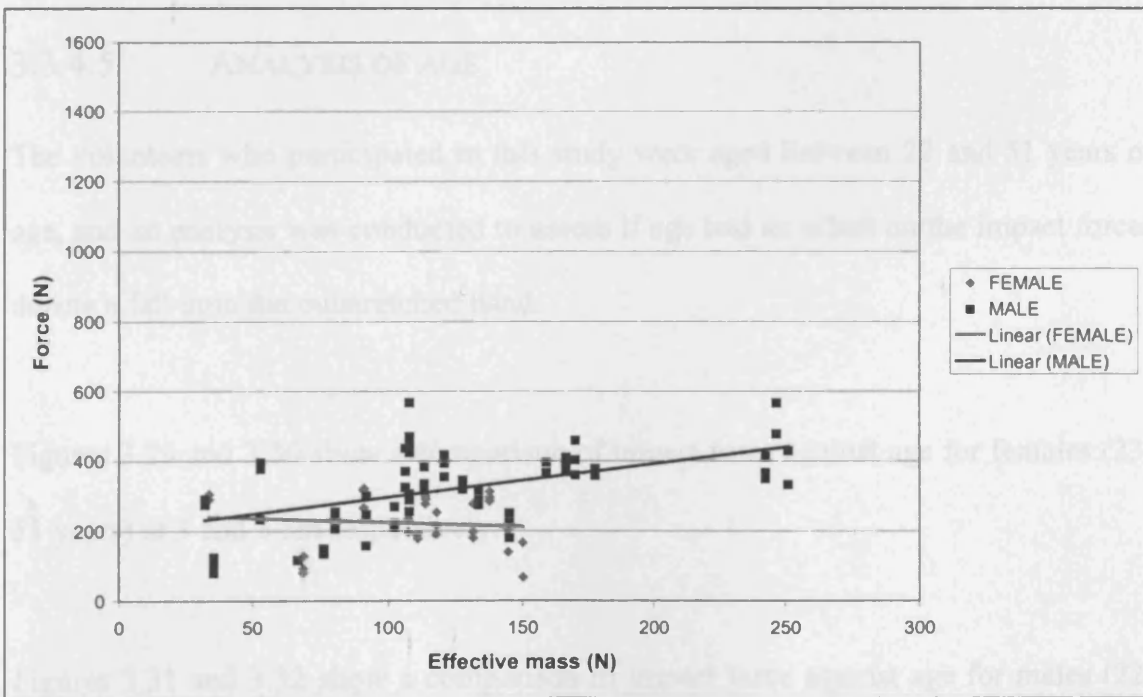


Figure 3.27: Graph showing a comparison of impact force peak F2 against effective mass for females and males at a fall height of 3 cm.

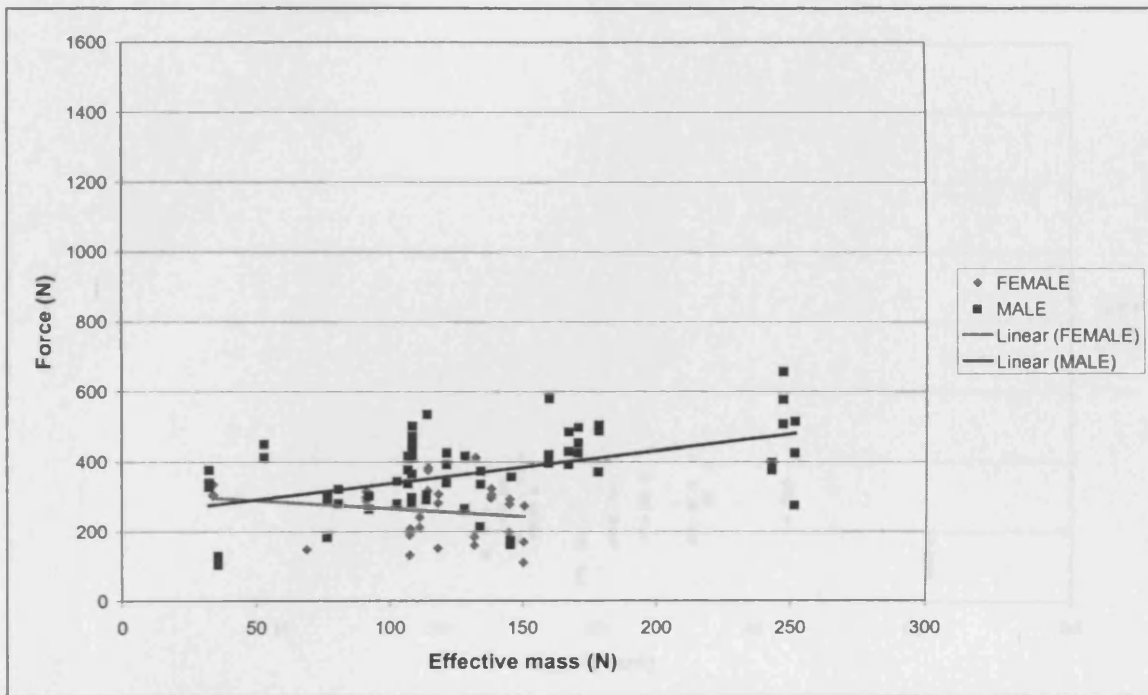


Figure 3.28: Graph showing a comparison of impact force peak F2 against effective mass for females and males at a fall height of 5 cm.

3.3.4.5 ANALYSIS OF AGE

The volunteers who participated in this study were aged between 22 and 51 years of age, and an analysis was conducted to assess if age had an effect on the impact forces during a fall onto the outstretched hand.

Figures 3.29 and 3.30 show a comparison of impact force against age for females (23-51 years) at 3 and 5 cm respectively.

Figures 3.31 and 3.32 show a comparison of impact force against age for males (22-47 years) at 3 and 5 cm respectively.

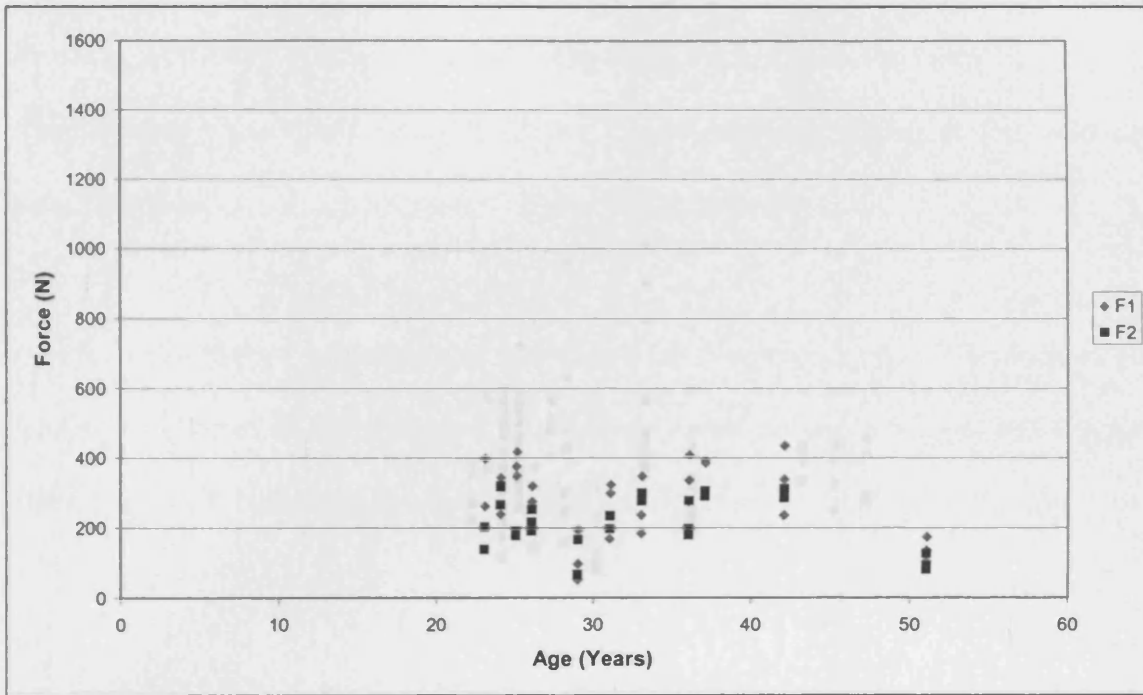


Figure 3.29: Graph showing a comparison of impact force peaks F1 and F2 against age for females at a fall height of 3 cm.

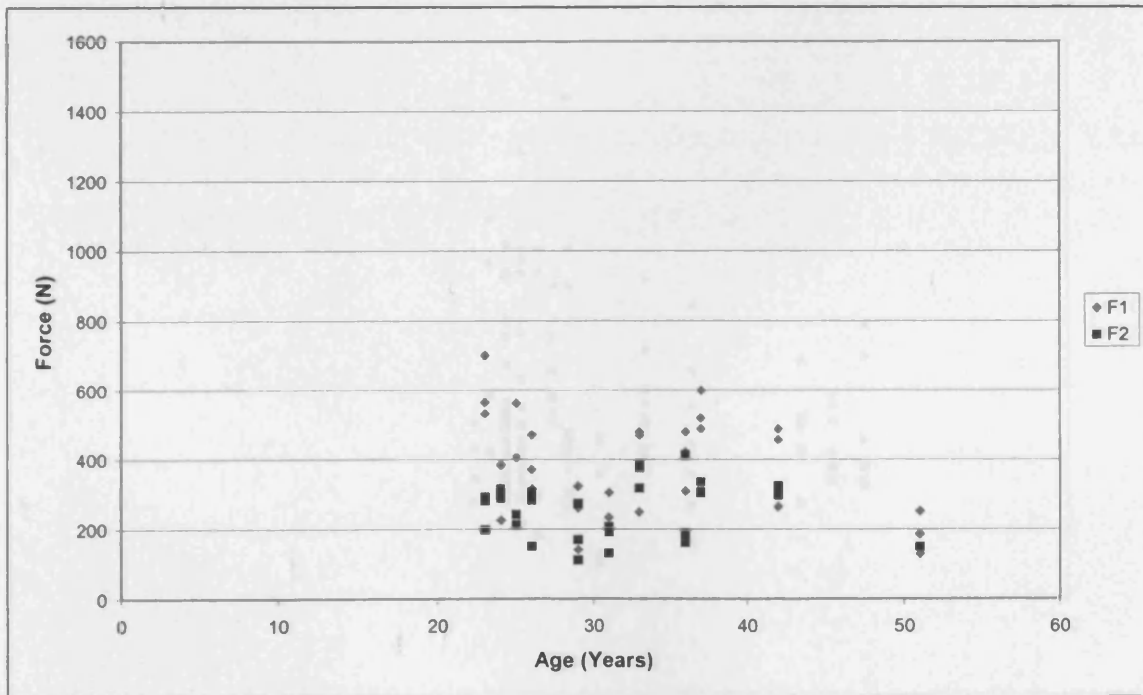


Figure 3.30: Graph showing a comparison of impact force peaks F1 and F2 against age for females at a fall height of 5 cm.

3.4 SURFACE STUDY USING MOTION ANALYSIS

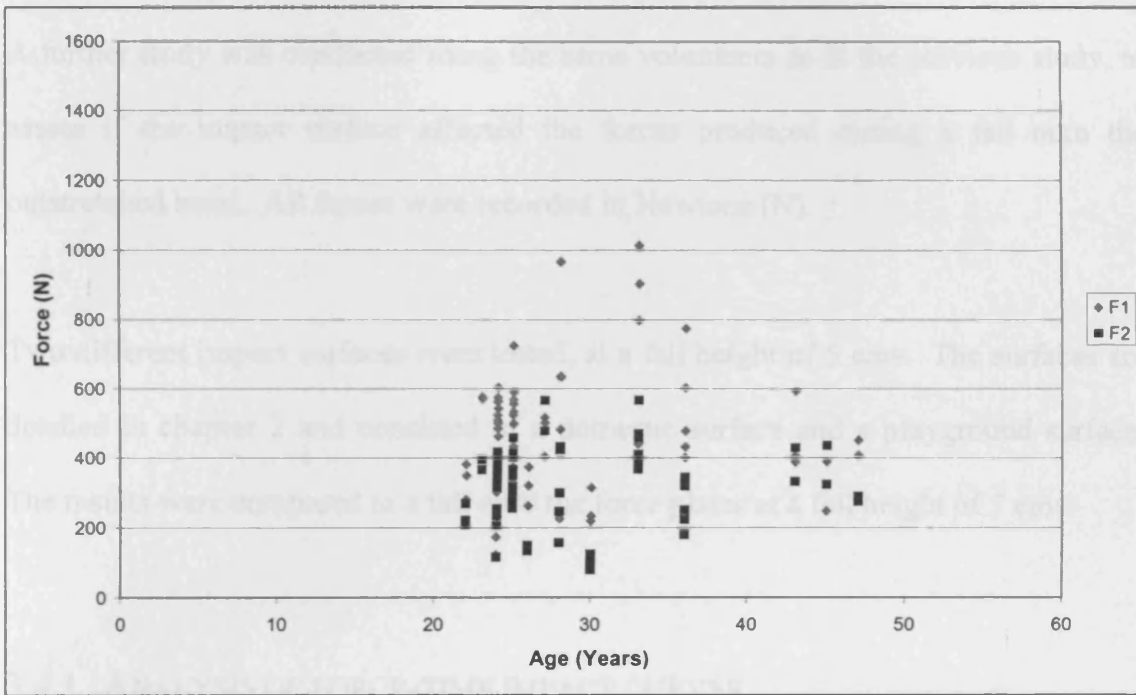


Figure 3.31: Graph showing a comparison of impact force peaks F1 and F2 against age for males at a fall height of 3 cm.

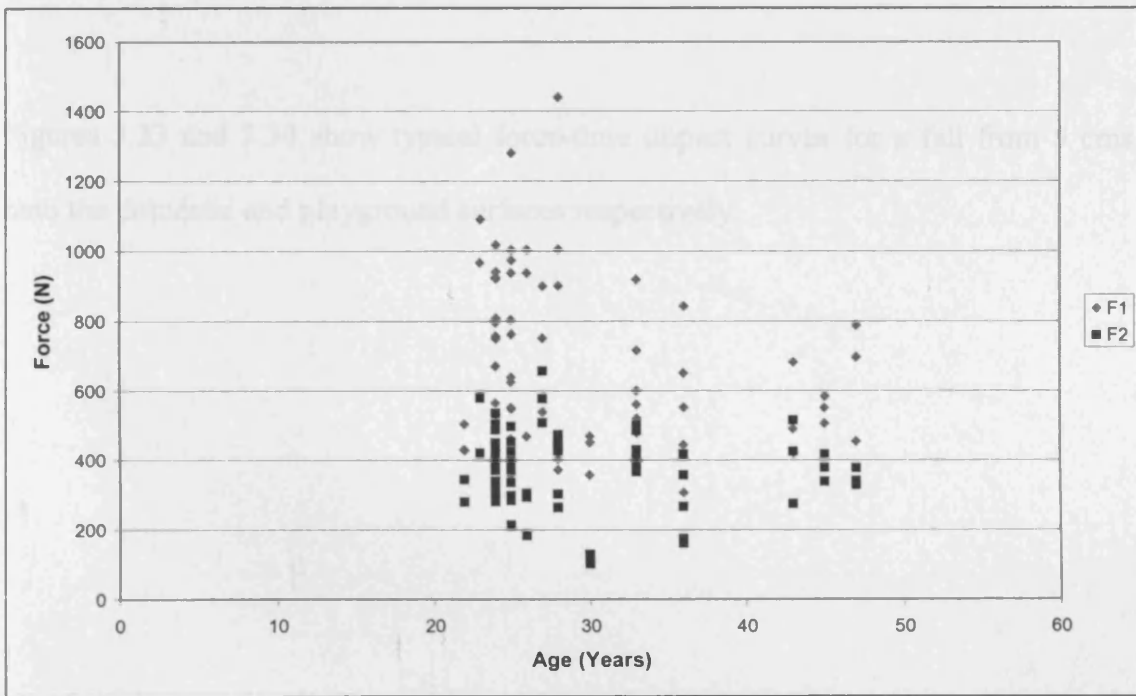


Figure 3.32: Graph showing a comparison of impact force peaks F1 and F2 against age for males at a fall height of 5 cm.

3.4 SURFACE STUDY USING MOTION ANALYSIS

A further study was conducted using the same volunteers as in the previous study, to assess if the impact surface affected the forces produced during a fall onto the outstretched hand. All forces were recorded in Newtons (N).

Two different impact surfaces were tested, at a fall height of 5 cms. The surfaces are detailed in chapter 2 and consisted of a domestic surface and a playground surface. The results were compared to a fall onto the force plates at a fall height of 5 cms.

3.4.1 ANALYSIS OF FORCE-TIME IMPACT CURVES

Falls onto the outstretched hand, from fall heights of 3 and 5 cm, produced force-time impact curves with peak characteristics similar to those found during a fall directly onto the force plates.

Figures 3.33 and 3.34 show typical force-time impact curves for a fall from 5 cms, onto the domestic and playground surfaces respectively.

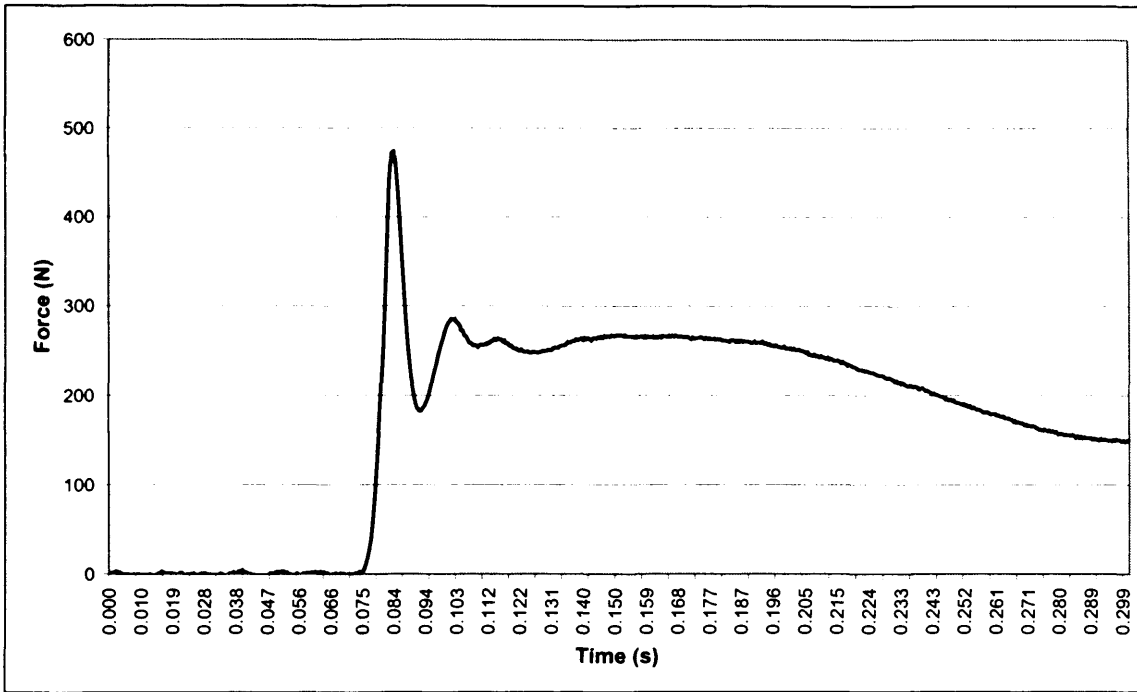


Figure 3.33: Graph showing a typical force-time impact curve at a fall height of 5 cm onto the domestic surface.

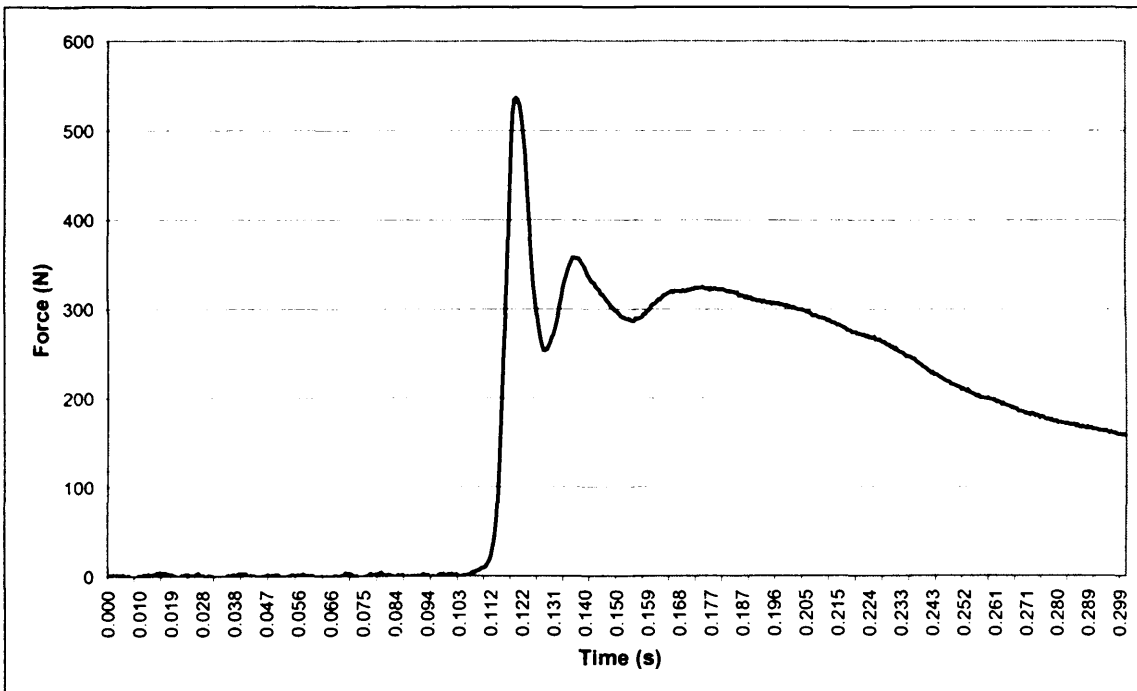


Figure 3.34: Graph showing a typical force-time impact curve at a fall height of 5 cm onto the playground surface.

3.4.2 IMPACT FORCES

An analysis was conducted to assess the magnitude of the impact forces recorded during the falls from the drop rig onto the force plates, domestic surface and playground surface at a fall height of 5 cms.

Figures 3.35 and 3.36 show a comparison of the impact forces, for force peaks F1 and F2, onto the experimental surfaces (force plate (FP), domestic (DS) and playground (PT)) for females and males respectively, from a height of 5 cm. The y-error bars show the maximum and minimum forces recorded for females and males at each force peak.

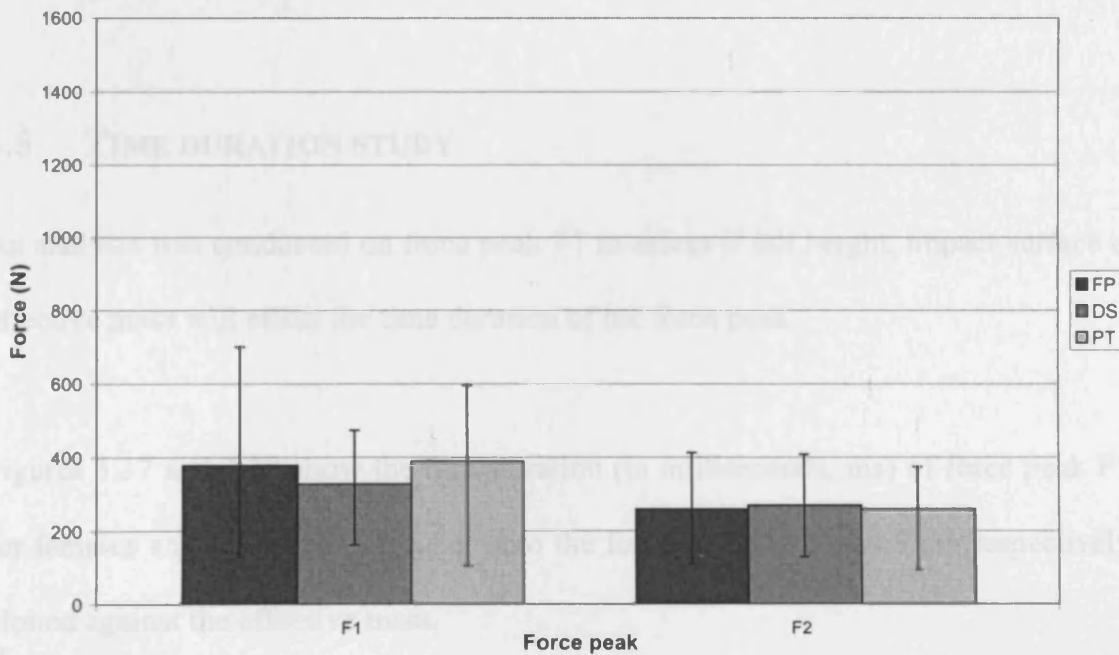


Figure 3.35: Graph showing a comparison of impact force peaks F1 and F2 at different surfaces for females at a fall height of 5 cm.

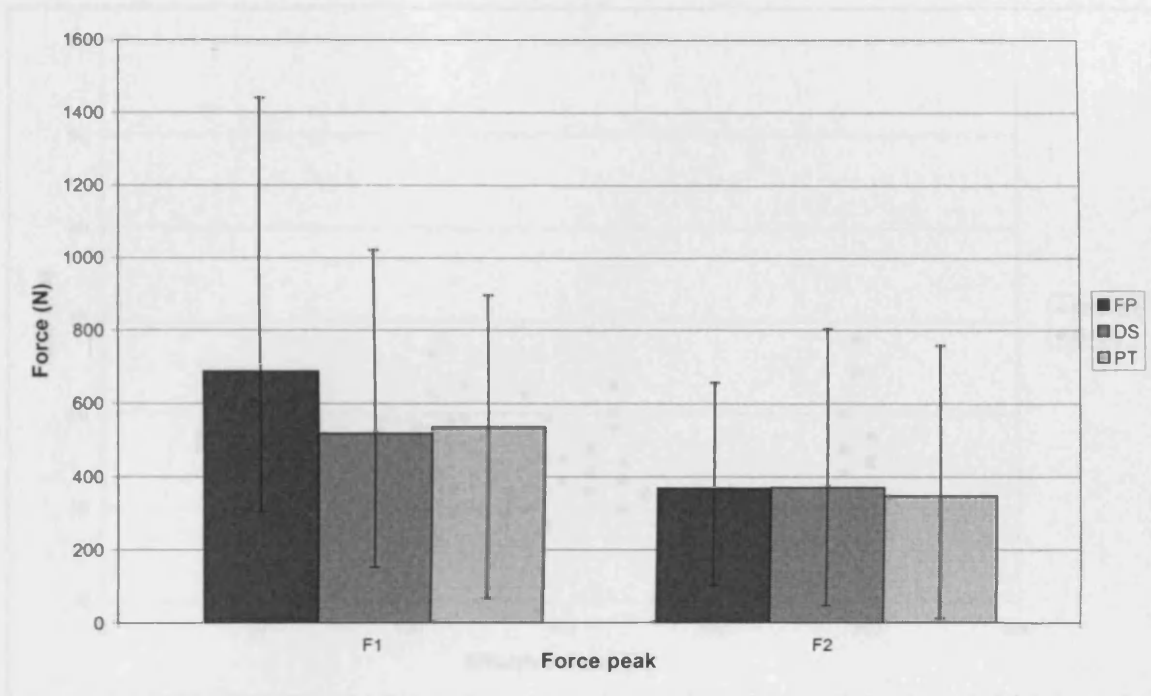


Figure 3.36: Graph showing a comparison of impact force peaks F1 and F2 at different surfaces for males at a fall height of 5 cm.

3.5 TIME DURATION STUDY

An analysis was conducted on force peak F1 to assess if fall height, impact surface or effective mass will effect the time duration of the force peak.

Figures 3.37 and 3.38 show the time duration (in milliseconds, ms) of force peak F1, for females and males, during a fall onto the force plates at 3 and 5 cm respectively, plotted against the effective mass.

Figures 3.39 and 3.40 show the time duration (in ms) of force peak F1, for females and males, during a fall from 5 cm onto the domestic and playground surfaces respectively, plotted against the effective mass.

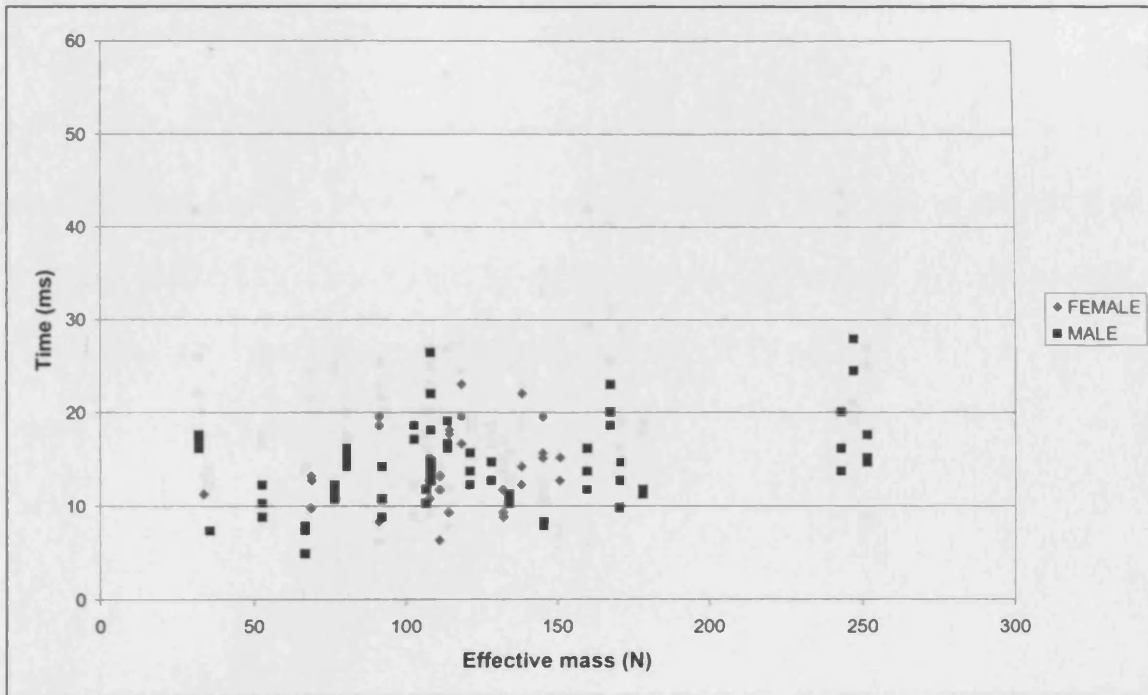


Figure 3.37: Graph showing the time duration of impact force peak F1 for females and males onto force plates at a fall height of 3 cm.

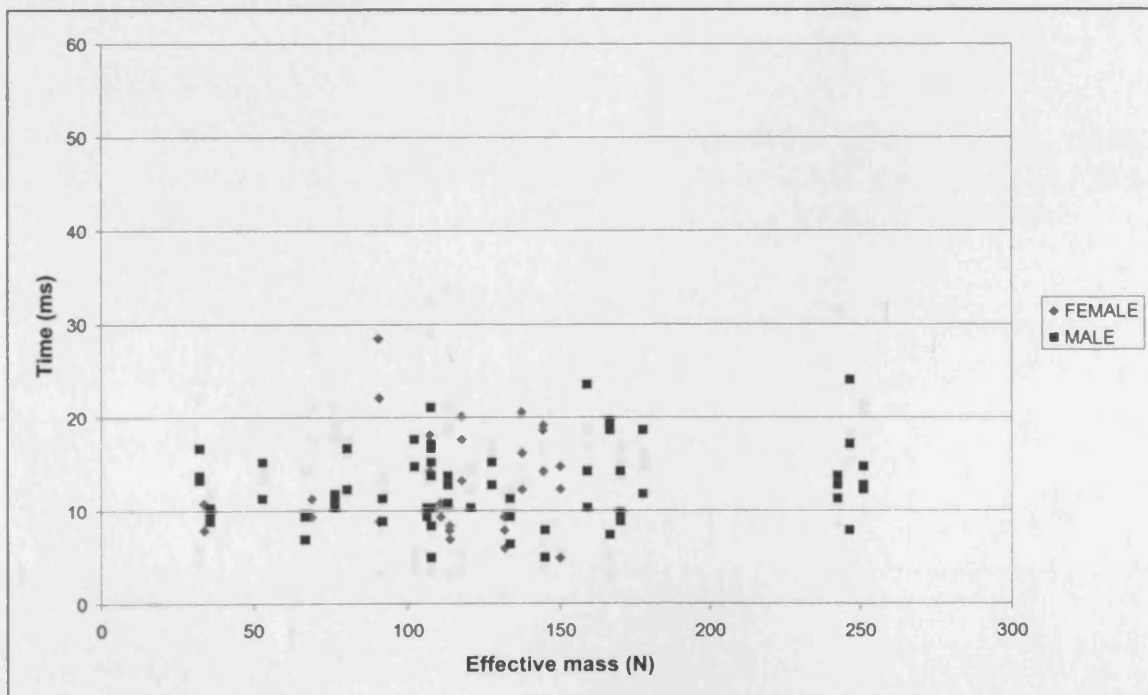


Figure 3.38: Graph showing the time duration of impact force peak F1 for females and males onto force plates at a fall height of 5 cm.

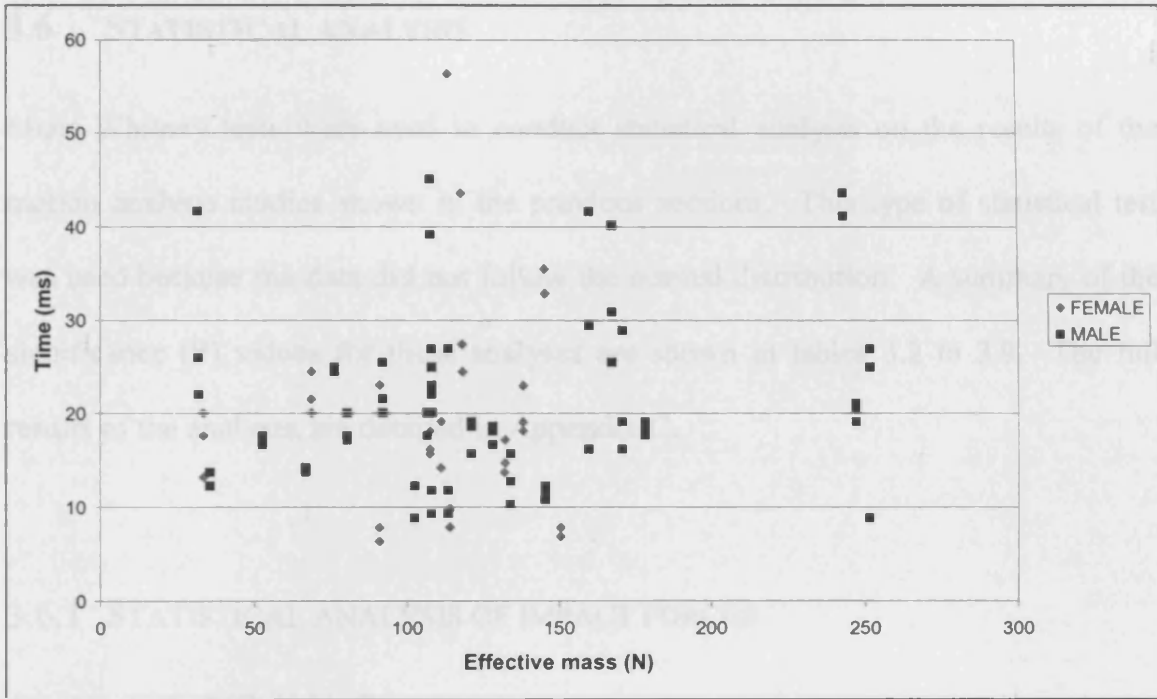


Figure 3.39: Graph showing the time duration of impact force peak F1 for females and males onto the domestic surface at a fall height of 5 cm.

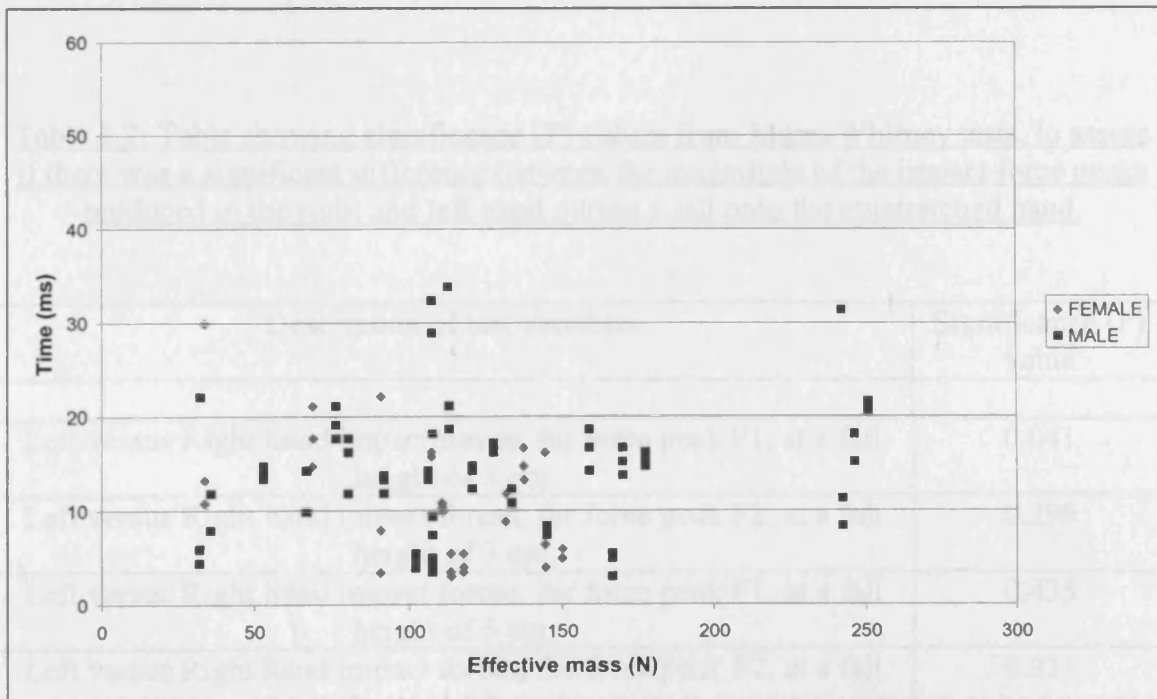


Figure 3.40: Graph showing the time duration of impact force peak F1 for females and males onto the playground surface at a fall height of 5 cm.

3.6 STATISTICAL ANALYSIS

Mann-Whitney tests were used to conduct statistical analysis on the results of the motion analysis studies shown in the previous sections. This type of statistical test was used because the data did not follow the normal distribution. A summary of the significance (P) values for these analyses are shown in tables 3.2 to 3.9. The full results of the analyses are detailed in Appendix C.

3.6.1 STATISTICAL ANALYSIS OF IMPACT FORCES

Statistical analysis was conducted to assess if there was a significant difference between the magnitude of the impact force peaks F1 and F2 produced in each hand and also between the magnitude of the impact force peaks F1, F2 and F3. The summarised results of the analysis are shown in tables 3.2 and 3.3 respectively.

Table 3.2: Table showing significance (P) values from Mann-Whitney tests, to assess if there was a significant difference between the magnitude of the impact force peaks produced in the right and left hand during a fall onto the outstretched hand.

Description of test variables	Significance (P) value
Left versus Right hand impact forces, for force peak F1, at a fall height of 3 cm.	0.041
Left versus Right hand impact forces, for force peak F2, at a fall height of 3 cm.	0.299
Left versus Right hand impact forces, for force peak F1, at a fall height of 5 cm.	0.435
Left versus Right hand impact forces, for force peak F2, at a fall height of 5 cm.	0.931

Table 3.3: Table showing significance (P) values from Mann-Whitney tests, to assess if there was a significant difference between the magnitude of the impact force peaks during a fall onto the outstretched hand.

Description of test variables	Significance (P) value
Force peak F1 versus F2, in females at a fall height of 3 cm.	0.012
Force peak F1 versus F3, in females at a fall height of 3 cm.	0.108
Force peak F2 versus F3, in females at a fall height of 3 cm.	0.507
Force peak F1 versus F2, in females at a fall height of 5 cm.	0.001
Force peak F1 versus F3, in females at a fall height of 5 cm.	0.001
Force peak F2 versus F3, in females at a fall height of 5 cm.	0.178
Force peak F1 versus F2, in males at a fall height of 3 cm.	0.000
Force peak F1 versus F3, in males at a fall height of 3 cm.	0.000
Force peak F2 versus F3, in males at a fall height of 3 cm.	0.859
Force peak F1 versus F2, in males at a fall height of 5 cm.	0.000
Force peak F1 versus F3, in males at a fall height of 5 cm.	0.000
Force peak F2 versus F3, in males at a fall height of 5 cm.	0.194

3.6.2 STATISTICAL ANALYSIS ON THE FACTORS AFFECTING A FALL ONTO THE OUTSTRETCHED HAND

Statistical analysis was conducted to assess if gender, fall height, effective mass, age or impact surface would significantly effect the impact forces found during a fall onto the outstretched hand.

Tables 3.4 to 3.8 show the summary of the significance (P) values for gender, fall height, effective mass, age and impact surface respectively.

Table 3.4: Table showing significance (P) values from Mann Whitney tests, to assess if gender significantly affects the magnitude of the impact force peaks during a fall onto the outstretched hand.

Description of test variables	Significance (P) value
Female versus Male impact forces, for force peak F1, at a fall height of 3 cm.	0.000
Female versus Male impact forces, for force peak F2, at a fall height of 3 cm.	0.000
Female versus Male impact forces, for force peak F1, at a fall height of 5 cm.	0.000
Female versus Male impact forces, for force peak F2, at a fall height of 5 cm.	0.000

Table 3.5: Table showing significance (P) values from Mann Whitney tests, to assess if the fall height significantly affects the magnitude of the impact force peaks during a fall onto the outstretched hand.

Description of test variables	Significance (P) value
Fall height of 3 cm versus 5 cm impact forces, for force peak F1, for females	0.012
Fall height of 3 cm versus 5 cm impact forces, for force peak F2, for females	0.065
Fall height of 3 cm versus 5 cm impact forces, for force peak F1, for males	0.000
Fall height of 3 cm versus 5 cm impact forces, for force peak F2, for males	0.014

Table 3.6: Table showing significance (P) values from Mann Whitney tests, to assess if effective mass significantly affects the magnitude of the impact force peaks during a fall onto the outstretched hand.

Description of test variables	Significance (P) value
Low versus high female effective mass impact forces, for force peak F1, at a fall height of 3 cm.	0.634
Low versus high female effective mass impact forces, for force peak F2, at a fall height of 3 cm.	0.739
Low versus high female effective mass impact forces, for force peak F1, at a fall height of 5 cm.	0.210
Low versus high female effective mass impact forces, for force peak F2, at a fall height of 5 cm.	0.893
Low versus high male effective mass impact forces, for force peak F1, at a fall height of 3 cm.	0.015
Low versus high male effective mass impact forces, for force peak F2, at a fall height of 3 cm.	0.004
Low versus high male effective mass impact forces, for force peak F1, at a fall height of 5 cm.	0.057
Low versus high male effective mass impact forces, for force peak F2, at a fall height of 5 cm.	0.006

Table 3.7: Table showing significance (P) values from Mann Whitney tests, to assess if age significantly affects the magnitude of the impact force peaks during a fall onto the outstretched hand.

Description of test variables	Significance (P) value
Older versus Younger female volunteer impact forces, for force peak F1, at a fall height of 3 cm.	0.451
Older versus Younger female volunteer impact forces, for force peak F2, at a fall height of 3 cm.	0.660
Older versus Younger female volunteer impact forces, for force peak F1, at a fall height of 5 cm.	0.425
Older versus Younger female volunteer impact forces, for force peak F2, at a fall height of 5 cm.	0.803
Older versus Younger male volunteer impact forces, for force peak F1, at a fall height of 3 cm.	0.149
Older versus Younger male volunteer impact forces, for force peak F2, at a fall height of 3 cm.	0.102
Older versus Younger male volunteer impact forces, for force peak F1, at a fall height of 5 cm.	0.003
Older versus Younger male volunteer impact forces, for force peak F2, at a fall height of 5 cm.	0.025

Table 3.8: Table showing significance (P) values from Mann Whitney tests, to assess if the impact surface significantly affects the magnitude of the impact force peaks during a fall onto the outstretched hand.

Description of test variables	Significance (P) value
Force plate versus Domestic surface impact forces, for force peak F1, for females.	0.173
Force plate versus Playground surface impact forces, for force peak F1, for females.	0.687
Domestic surface versus Playground surface impact forces for force peak F1, for females.	0.009
Force plate versus Domestic surface impact forces, for force peak F2, for females.	0.584
Force plate versus Playground surface impact forces, for force peak F2, for females.	0.789
Domestic surface versus Playground surface impact forces for force peak F2, for females.	0.564
Force plate versus Domestic surface impact forces, for force peak F1, for males.	0.000
Force plate versus Playground surface impact forces, for force peak F1, for males.	0.001
Domestic surface versus Playground surface impact forces for force peak F1, for males.	0.457
Force plate versus Domestic surface impact forces, for force peak F2, for males.	0.919
Force plate versus Playground surface impact forces, for force peak F2, for males.	0.317
Domestic surface versus Playground surface impact forces for force peak F2, for males.	0.301

3.6.3 STATISTICAL ANALYSIS ON THE TIME DURATION OF FORCE PEAK F1

A further analysis was conducted to assess if the time duration of force peak F1 would be significantly affected by fall height or impact surface.

Table 3.9 shows the summary of the significance (P) values for the time duration of force peak F1.

Table 3.9: Table showing significance (P) values from Mann Whitney tests, to assess if the time duration of impact force peak F1 is significantly affected by fall height or impact surface during a fall onto the outstretched hand.

Description of test variables	Significance (P) value
Fall height of 3 cm versus 5 cm, for females.	0.138
Force plate versus Domestic surface, at a fall height of 5 cm, for females.	0.005
Force plate versus Playground surface, at a fall height of 5 cm, for females.	0.190
Domestic surface versus Playground surface, at a fall height of 5 cm, for females.	0.000
Fall height of 3 cm versus 5 cm, for males.	0.025
Force plate versus Domestic surface, at a fall height of 5 cm, for males.	0.000
Force plate versus Playground surface, at a fall height of 5 cm, for males.	0.110
Domestic surface versus Playground surface, at a fall height of 5 cm, for males.	0.000

3.6 HIGH-SPEED VIDEO STUDY

A series of experiments were conducted on five volunteers who were dropped from heights of 1 and 5 cm from a drop rig onto two force plates, to assess the mechanisms involved during a fall onto the outstretched hand. One volunteer was then dropped through heights of 10 and 20 cms.

A further series of experiments were conducted assessing falls from standing height using two volunteers, who had previous training in how to fall during combat training.

The study was conducted using high-speed video (HSV) cameras, coupled with an Electromyography (EMG) system. All forces were recorded in Newtons (N).

3.6.1 TYPICAL FORCE-TIME IMPACT CURVES

Falls onto the outstretched hand, from fall heights of 1, 5, 10 and 20 cms from the drop rig, and falls from a standing height, produced force-time impact curves with peak characteristics.

Figures 3.41 to 3.44 show typical force-time impact curves for falls from 1, 5, 10 and 20 cm respectively.

Figure 3.45 shows a typical force time curve for a fall from a standing height.

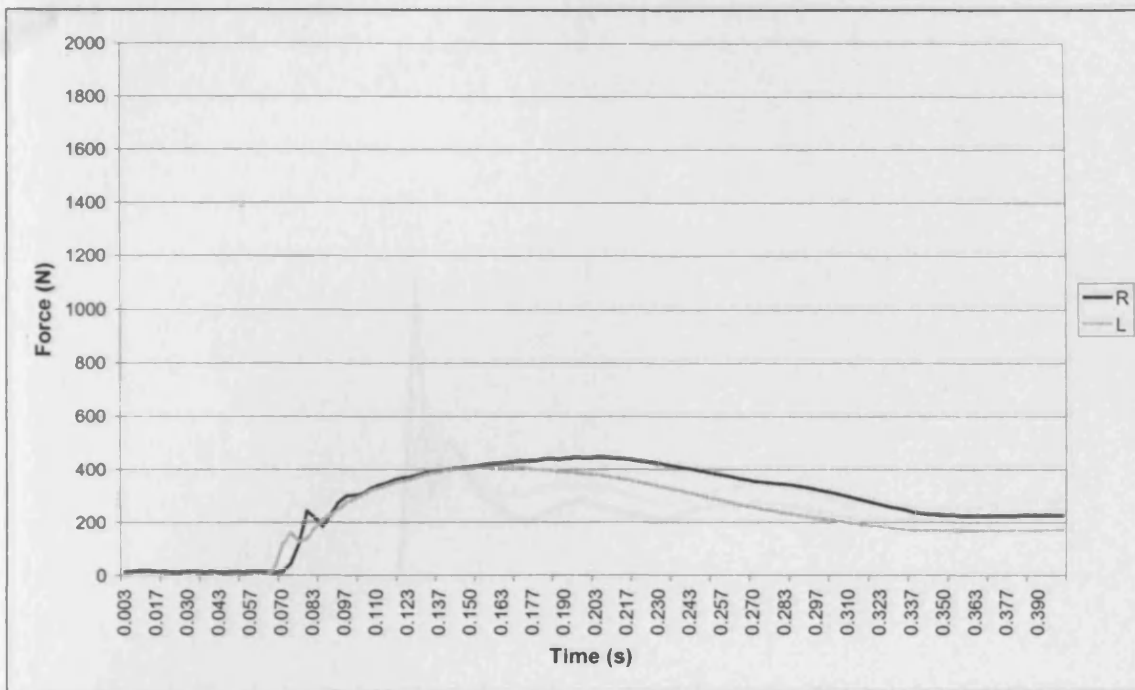


Figure 3.41: Graph showing typical force-time impact curve at a fall height of 1 cm.

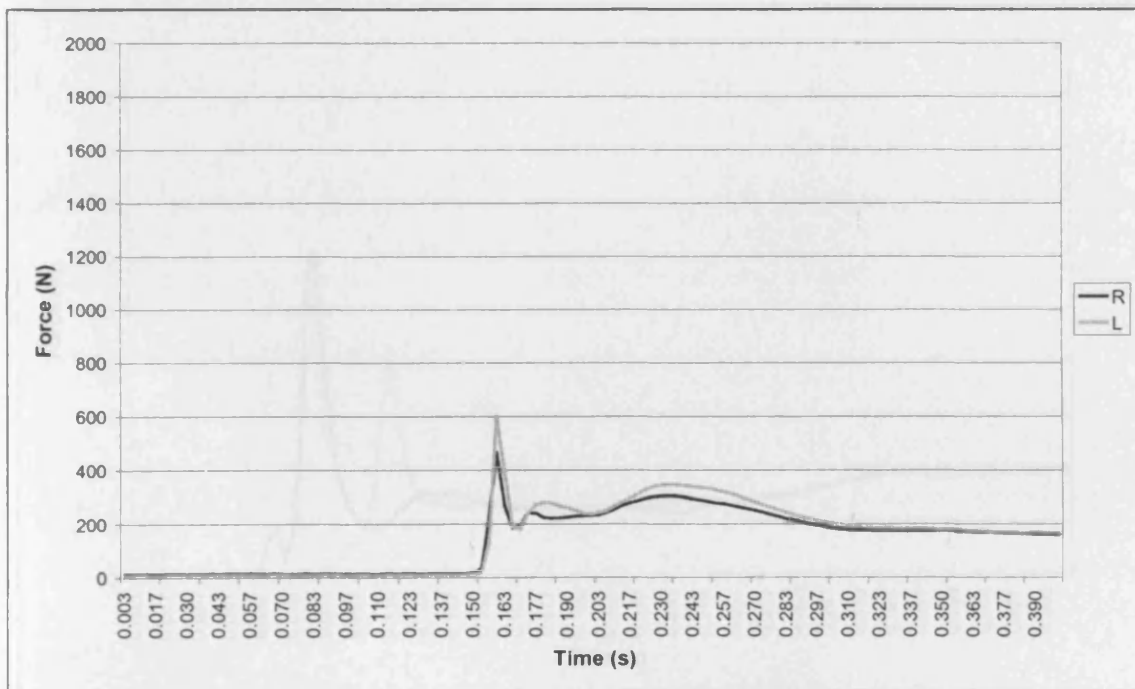


Figure 3.42: Graph showing typical force-time impact curve at a fall height of 5 cm.

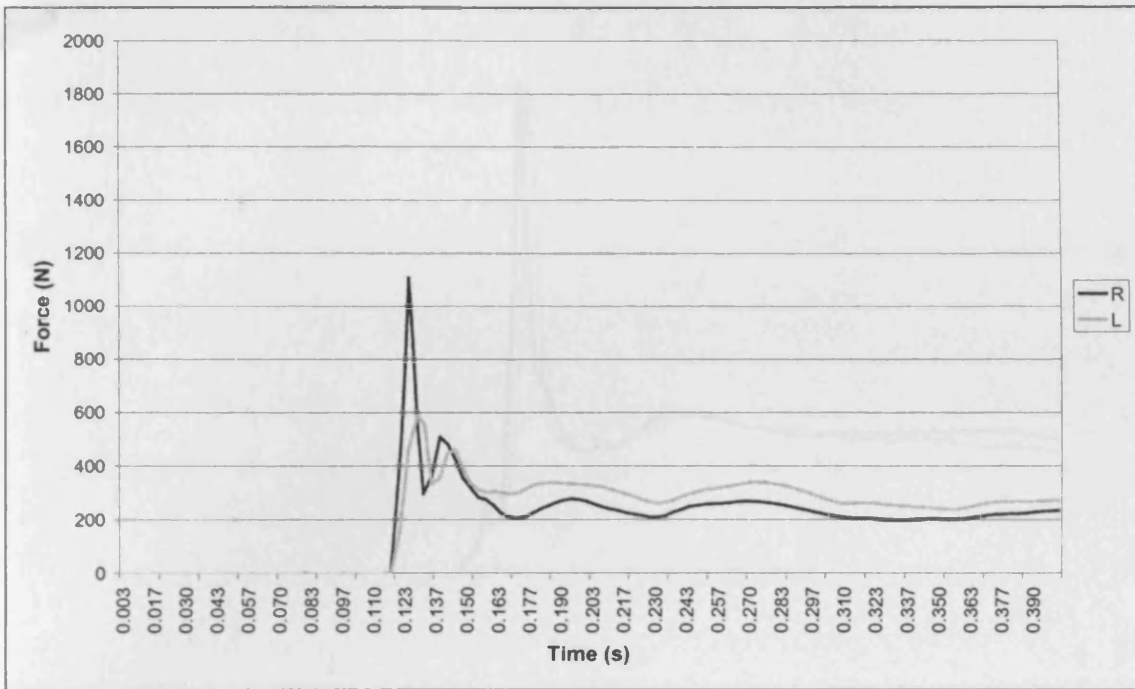


Figure 3.43: Graph showing typical force-time impact curve at a fall height of 10 cm.

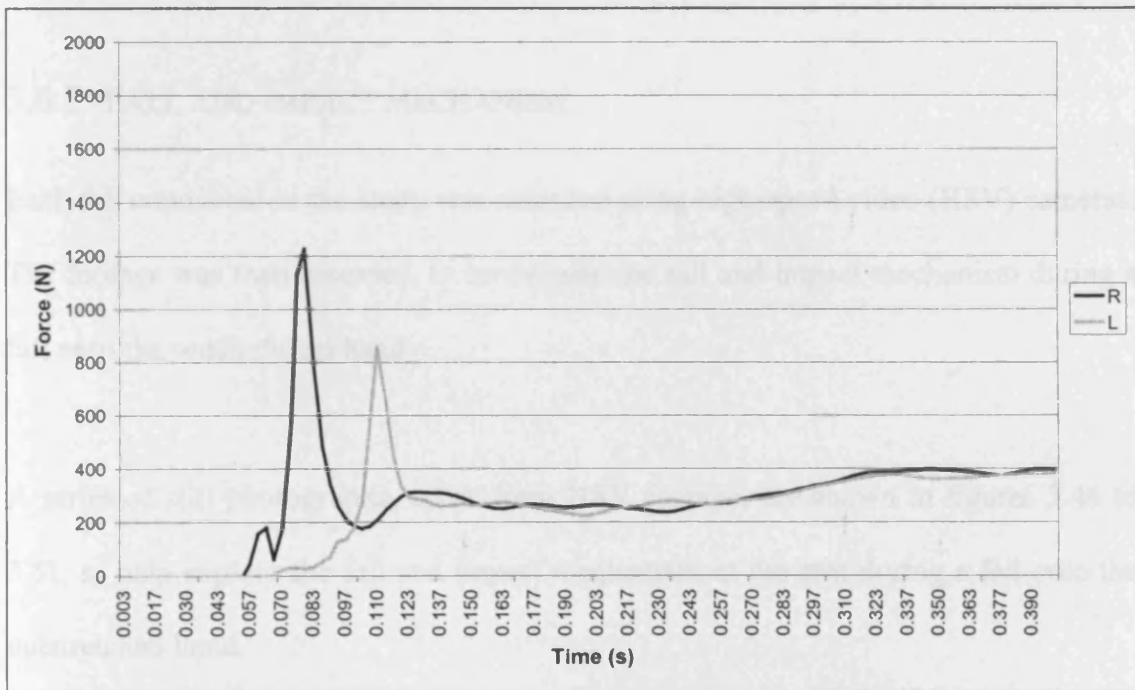


Figure 3.44: Graph showing typical force-time impact curve at a fall height of 20 cm.

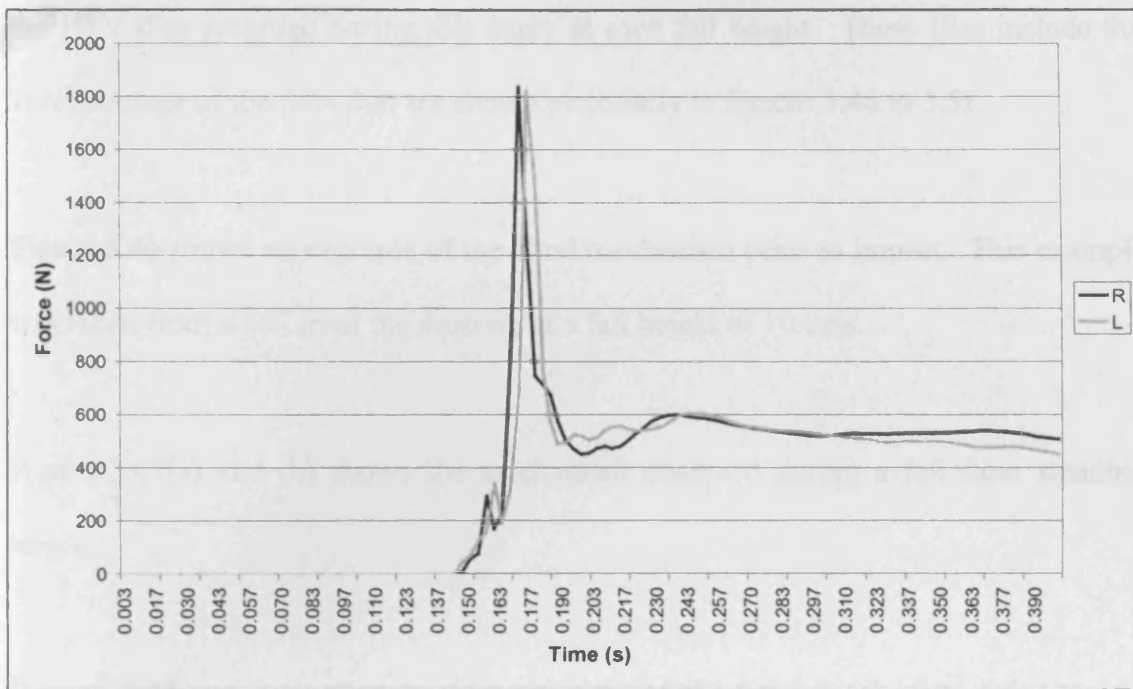


Figure 3.45: Graph showing typical force-time impact curve from a standing fall height.

3.6.2 FALL AND IMPACT MECHANISM

Each fall conducted in the study was recorded using high-speed video (HSV) cameras. The footage was then assessed, to investigate the fall and impact mechanism during a fall onto the outstretched hand.

A series of still photographs, taken from HSV footage, are shown in figures 3.46 to 3.51, to help explain the fall and impact mechanism of the arm during a fall onto the outstretched hand.

Due to the short time duration of the impact event and the high capture rate of the cameras it is difficult to fully appreciate these mechanisms using still photographs.

For this reason, Appendix E contains a Compact Disc (CD) that includes examples of the HSV files recorded during this study at each fall height. These files include the video footage of the falls that are shown pictorially in figures 3.46 to 3.51.

Figure 3.46 shows an example of the hand mechanism prior to impact. This example was taken from a fall from the drop rig at a fall height of 10 cms.

Figure 3.47(a) and (b) shows the mechanism observed during a fall from standing height.

Figures 3.48 and 3.49 show a close up view of the hand mechanism prior to and during impact.

Figure 3.50 show an example of the shock wave that is observed to travel through the arm during impact with the force plate.

Figure 3.51 shows a comparison between the skin and soft tissues of the arm immediately prior to and during impact, from a fall from standing height.



160	Volunteer suspended in rig, hands in natural position to arrest fall.
262	Volunteer released from drop rig, hands immediately start to flex upwards at the wrist combined with flexion of the elbow joint.
282	Wrist now at maximum upward flexion, finger tips above the base of the palm
294	Hands are accelerated towards the floor in a slapping motion combined with extension of the elbow joint
306	Hands impact the floor with both fingers and palm simultaneously

Real image photographs

Time (ms)

Description of fall

Figure 3.46: Series of still photographs taken from high-speed video footage, showing the hand mechanism prior to impact during a fall onto the force plates from a 10 cm fall height

		0	Volunteer at standing height in starting position.
		362	Volunteer initiates the fall; the arms start to move anteriorly away from the side of the body.
		640	The arms are more elevated now and the fingers and wrist start to extend.
		764	The wrist starts to flex slightly causing the fingers to move upward.
Real image photographs	Time (ms)	Description of fall	

Figure 3.47(a): Series of still photographs taken from high-speed video footage, showing a fall onto the force plates from standing height.

		812	The hands show a rapid downward movement, causing the fingertips to make contact with the force plate.
		824	The rest of the hand 'rolls' onto the force plate causing full impact of the hand.
		916	The elbows flex, lowering the body to the floor.
		998	The body impacts with the floor, the elbows are at full flexion. The head has turned completely to the side to protect the head and face.
Real image photographs	Time (ms)	Description of fall	

Figure 3.47(b): Series of still photographs taken from high-speed video footage, showing a fall onto the force plates from standing height.



Real image photograph

240

Hands comes into view of the camera

282

Hands fully extended towards force plate

322

Finger tip touch on right hand

330

All tips touching, hand starts to roll onto force plate

Time (ms)

Description of fall



Real image photograph

340

All fingers are on the force plate, hand is bending at the knuckles

350

Hand fully impacted onto the force plate

418

Body half way to the floor, decrease in elbow angle causes extension of wrist

668

Body impacts floor, wrist at almost right angle, elbow now at acute angle (lower than 45°)

Time (ms)

Description of fall

Figure 3.48: Series of still photographs taken from high-speed video footage, showing a fall onto the force plates from kneeling height (female volunteer).



18

Hands comes into view of the camera

226

Hands fully extended towards force plate, wrist almost straight with arm

260

Finger tip touch on right hand

274

All tips touching, hand starts to roll onto force plate (note fingers touch on left hand)



286

All fingers are on the force plate, hand is bending at the knuckles

312

Hand fully impacted onto the force plate

470

Body half way to the floor, decrease in elbow angle causes extension of wrist

914

Body impacts floor, wrist at almost right angle, elbow now at acute angle (lower than 45°)

Real image photograph Time (ms) Description of fall

Real image photograph Time (ms) Description of fall

Figure 3.49: Series of still photographs taken from high-speed video footage, showing a fall onto the force plates from kneeling height (male volunteer).

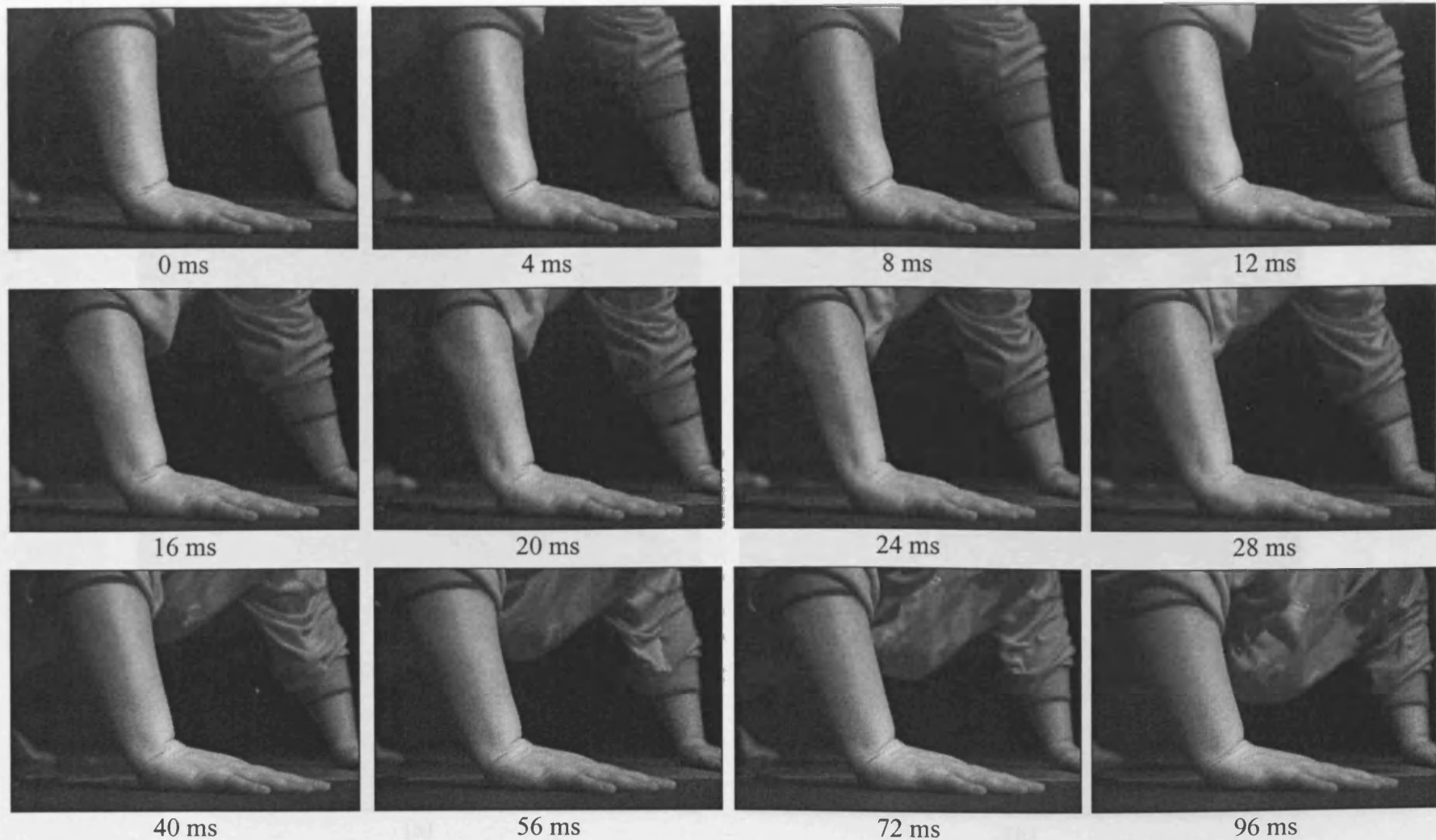
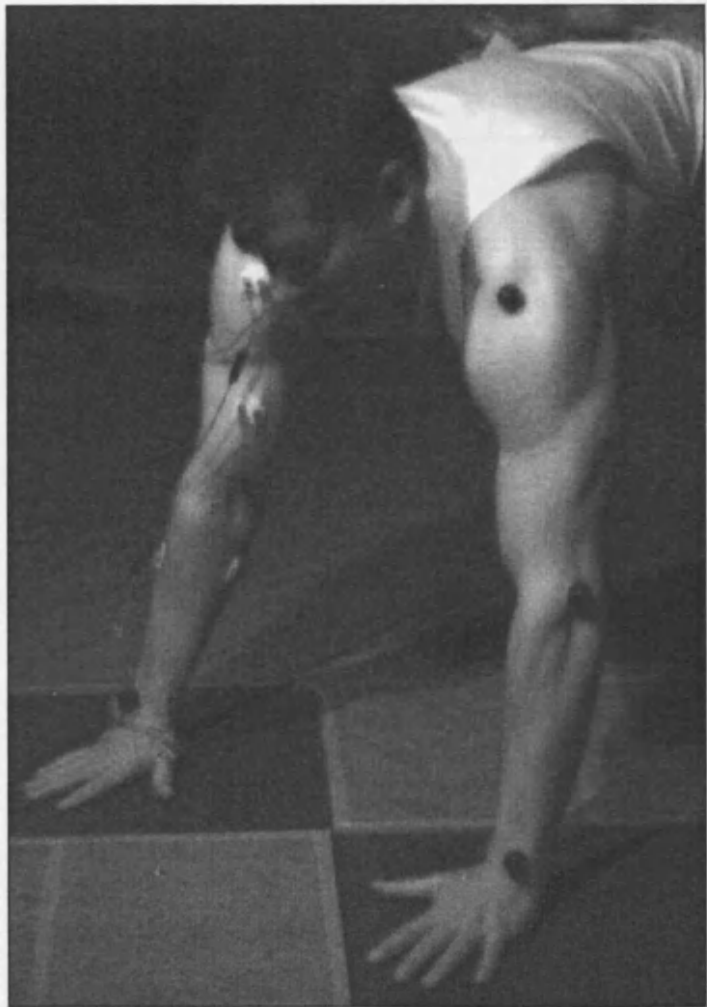


Figure 3.50: Series of still photographs taken from high-speed video footage, showing shock wave travelling up through the lower arm with the associated time, during a fall from kneeling height.



(a)



(b)

Figure 3.51: Still photographs taken from high-speed video footage showing a comparison between skin and soft tissues (a) immediately prior to and (b) during impact with the force plates, from a fall from standing height.

3.6.3 ELECTROMYOGRAPHY RESULTS.

A Bortec 8-channel Electromyography (EMG) system was used with the high-speed video (HSV) equipment in the HSV study to assess the time of muscle activation during a fall onto the outstretched hand. The EMG traces were filtered to remove noise by passing the waveform through a 2nd order low pass filter with cut off at 20 Hz.

Figure 3.52 shows a graph with the original and filtered waveform for the triceps brachii muscle for a fall from 1 cm.

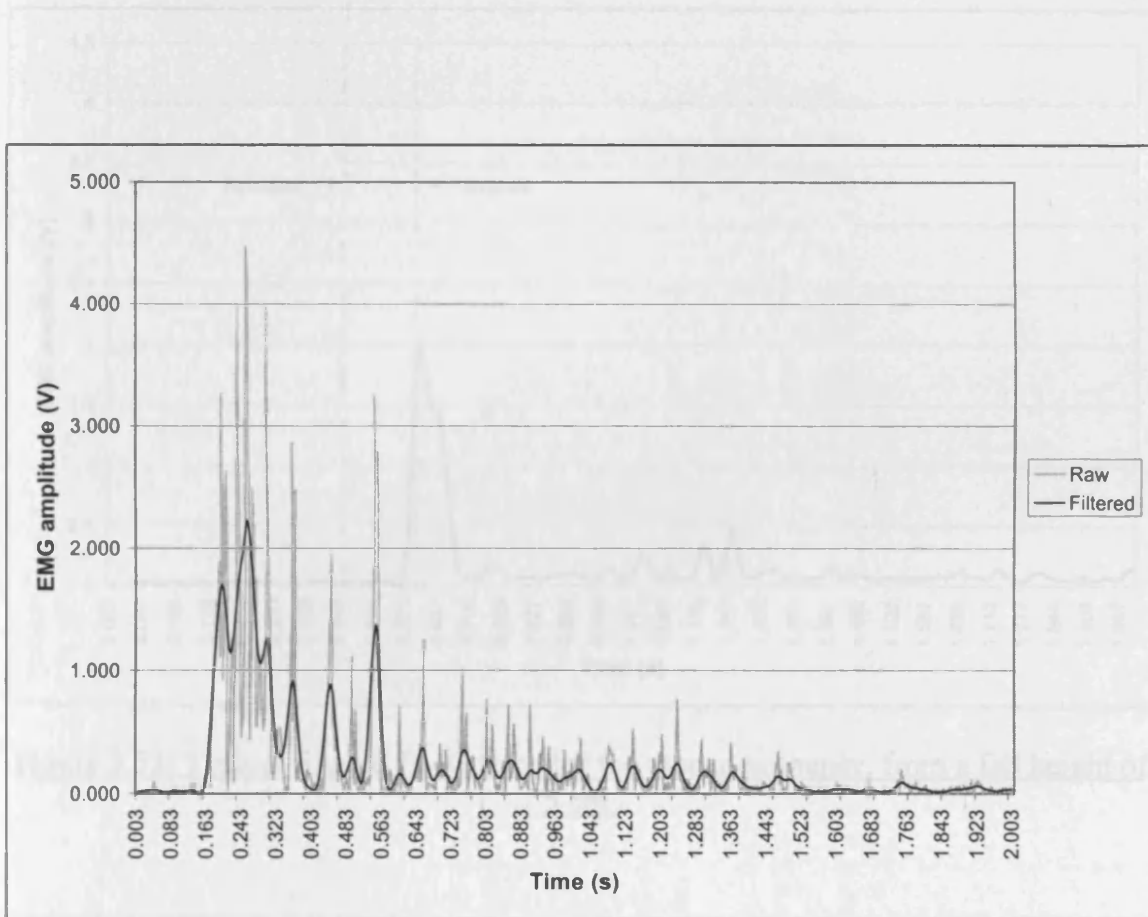


Figure 3.52: Typical EMG trace of the triceps brachii muscle showing the raw and filtered data for a fall height from 1 cm.

The muscles analysed during the EMG study were: 1-the thenar eminence, 2-forearm flexors, 3-forearm extensors, 4-biceps brachii, 5-triceps brachii, 6-anterior deltoid, 7-pectoralis major and 8-trapezius (neck).

Figures 3.53 to 3.60 show typical filtered data for the EMG traces, recorded from falls from the drop rig, from a height of 5 cm, for each muscle group respectively. The graphs also show the time the volunteer was released from the drop rig and the time of impact onto the force plate.

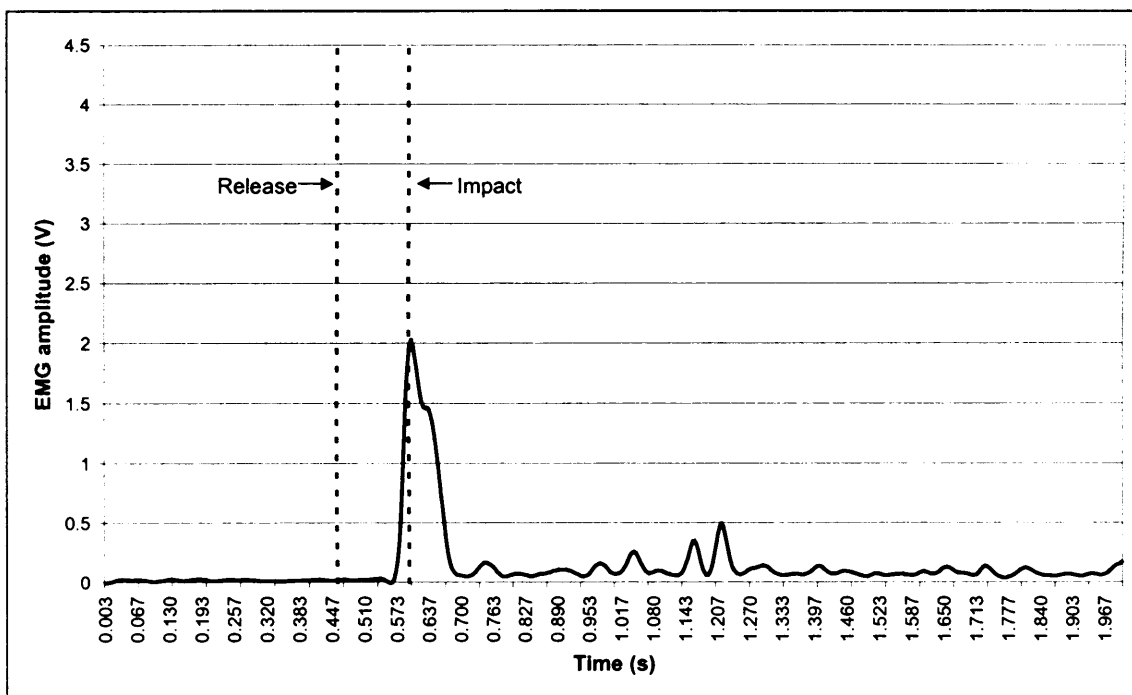


Figure 3.53: Typical filtered EMG trace for the thenar eminence, from a fall height of 5 cm.

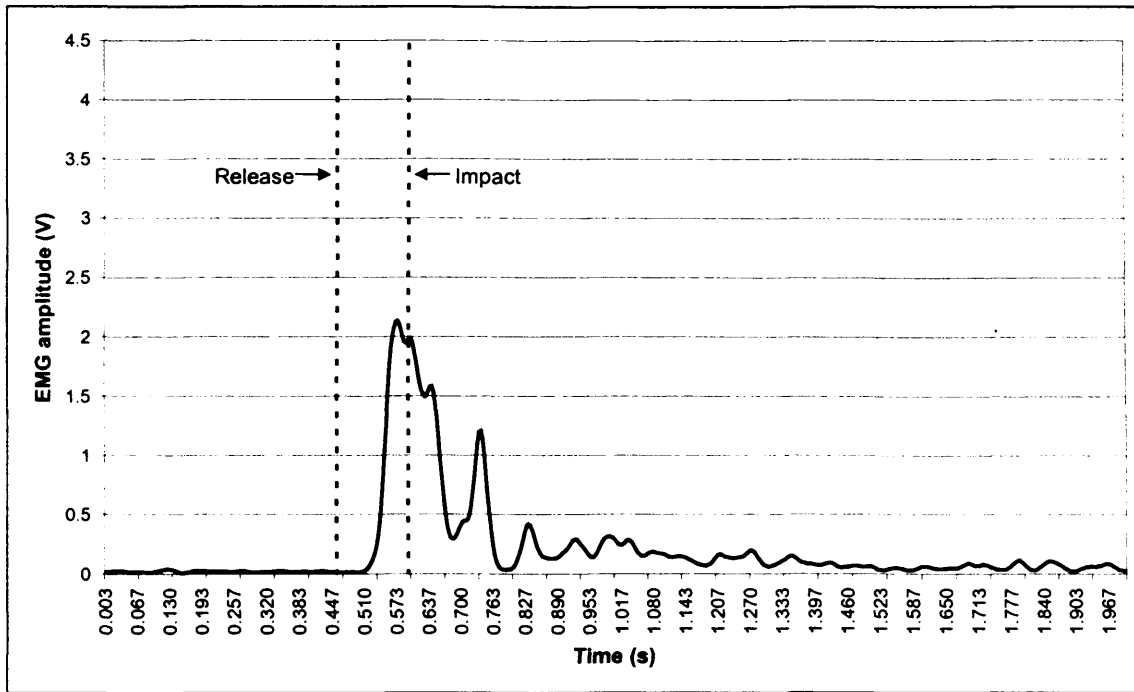


Figure 3.54: Typical filtered EMG trace for the forearm flexors, from a fall height of 5 cm.

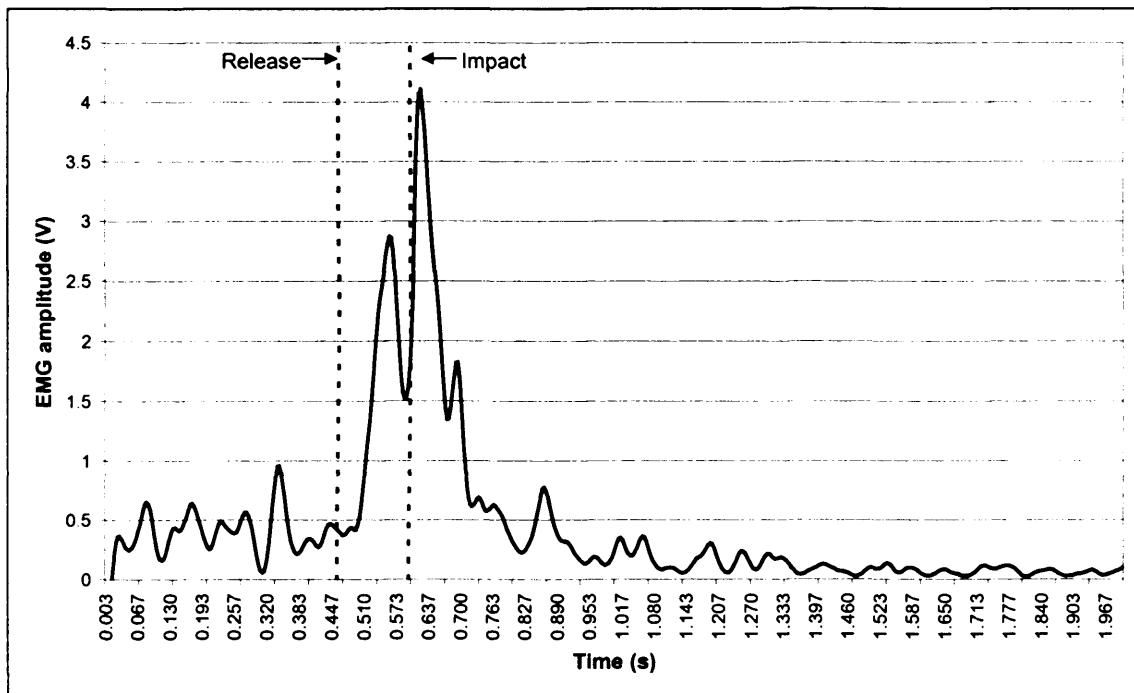


Figure 3.55: Typical filtered EMG trace for the forearm extensors, from a fall height of 5 cm.

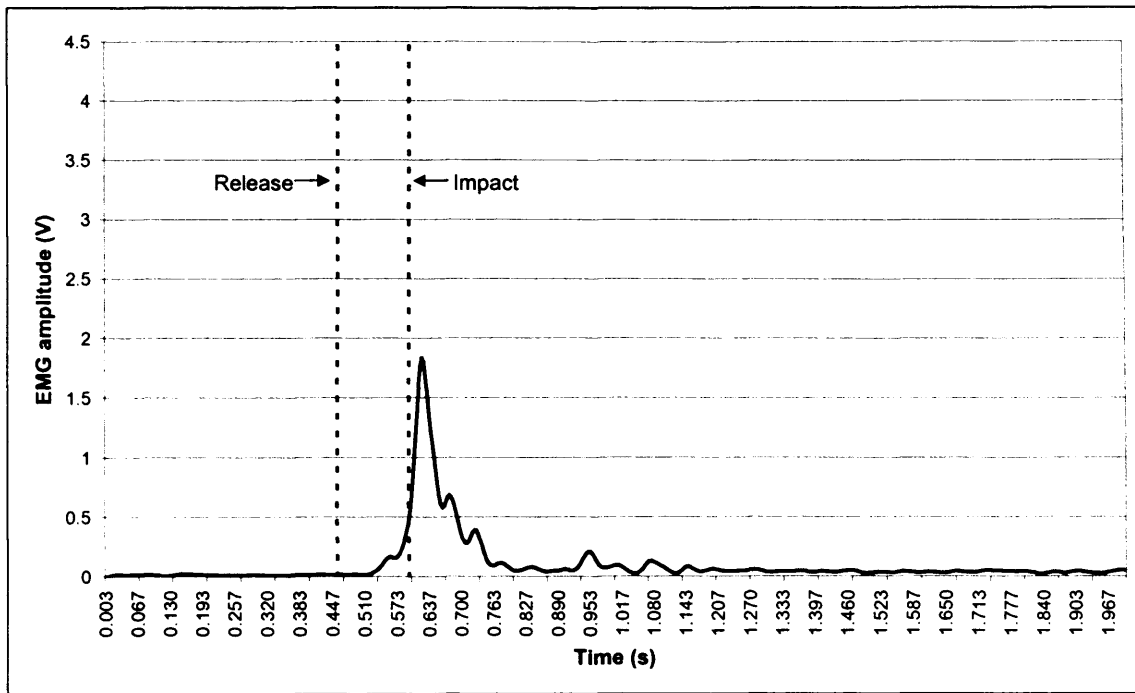


Figure 3.56: Typical filtered EMG trace for the biceps brachii, from a fall height of 5 cm.

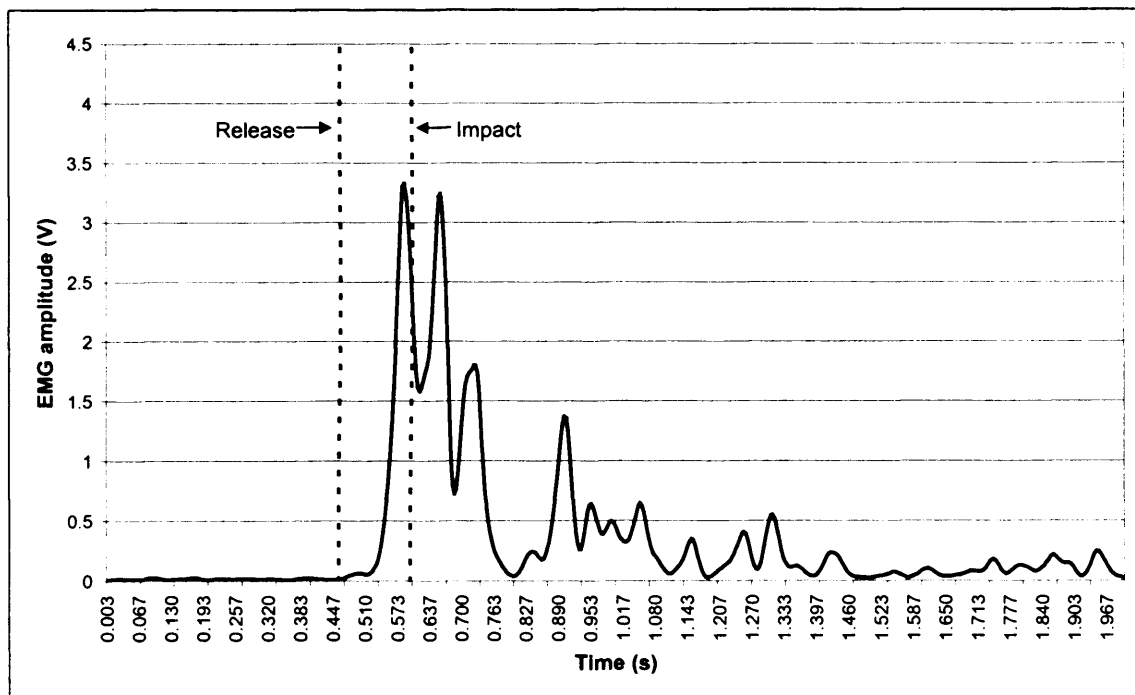


Figure 3.57: Typical filtered EMG trace for the triceps brachii, from a fall height of 5 cm.

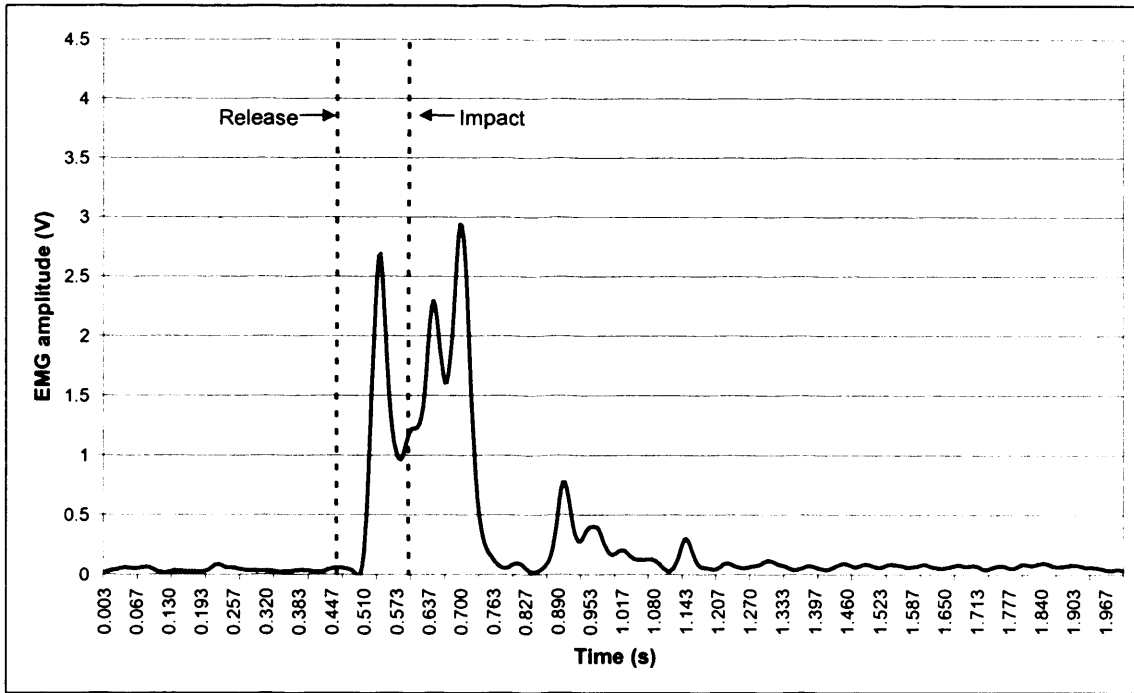


Figure 3.58: Typical filtered EMG trace for the anterior deltoid, from a fall height of 5 cm.

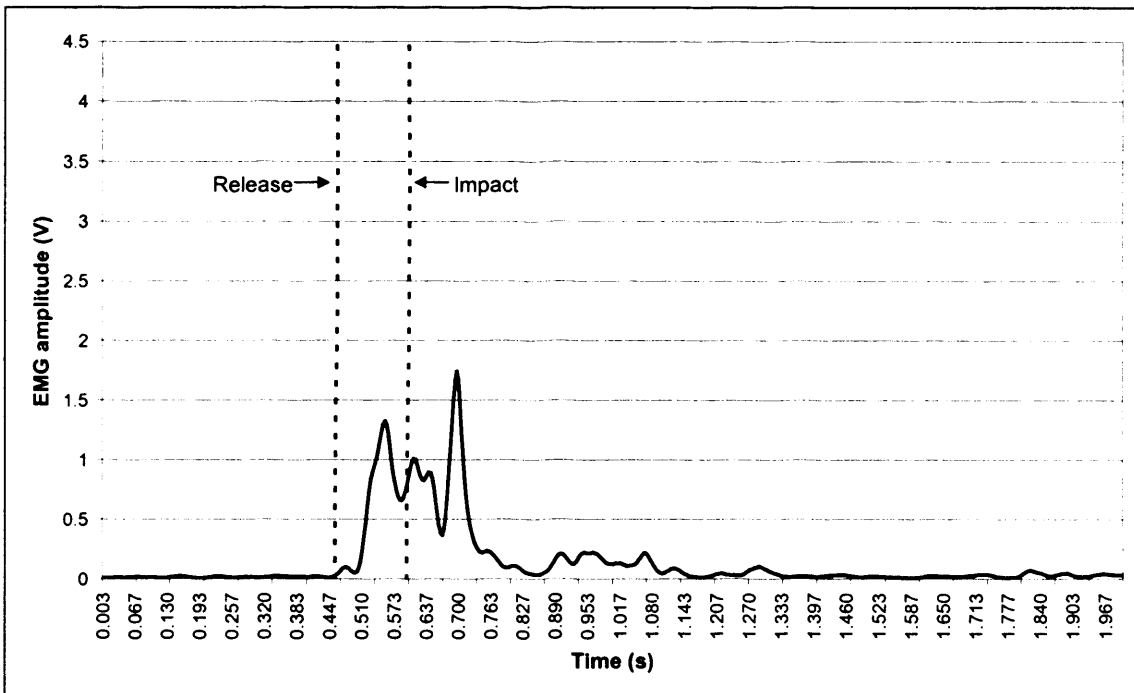


Figure 3.59: Typical filtered EMG trace for the pectoralis major, from a fall height of 5 cm.

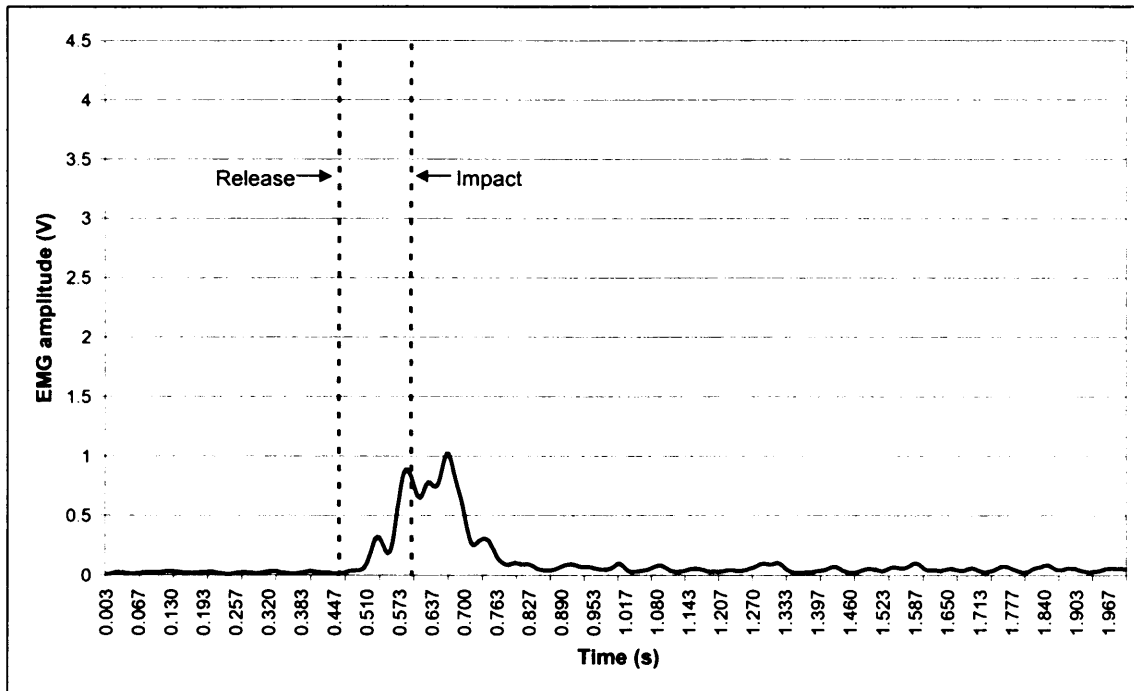


Figure 3.60: Typical filtered EMG trace for the trapezius, from a fall height of 5 cm.

Figures 3.61 to 3.68 show typical filtered data for the EMG traces, recorded from falls from standing height, for each muscle group respectively. The graphs also show the time of impact onto the force plate.

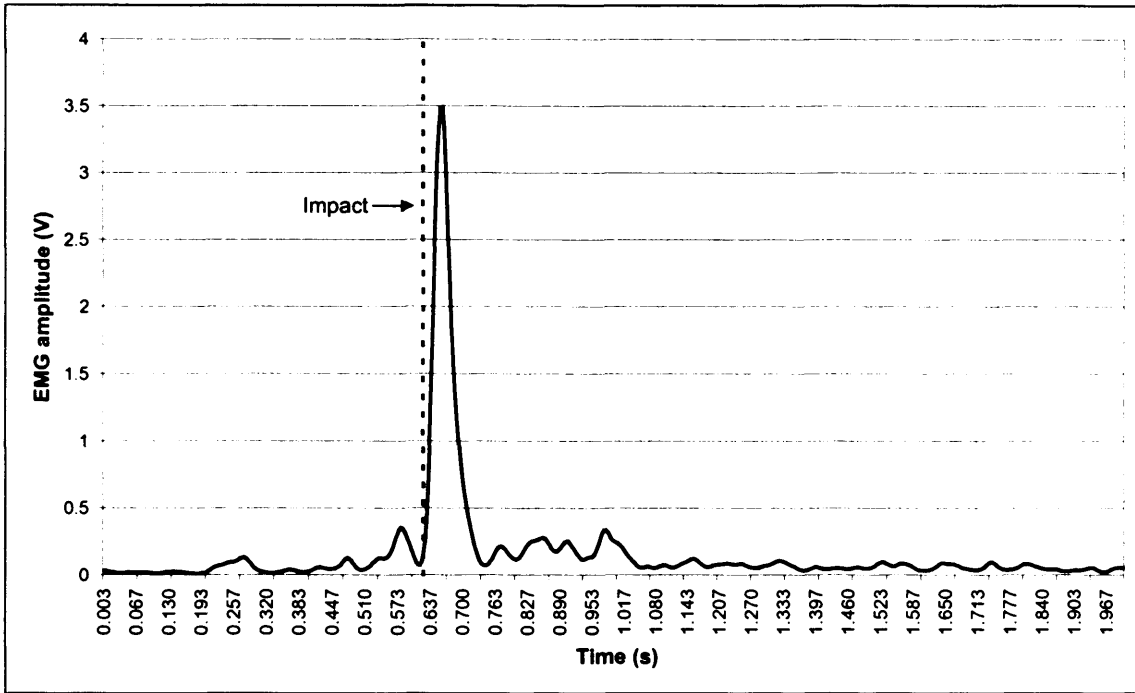


Figure 3.61: Typical filtered EMG trace for the thenar eminence, for a fall from standing height.

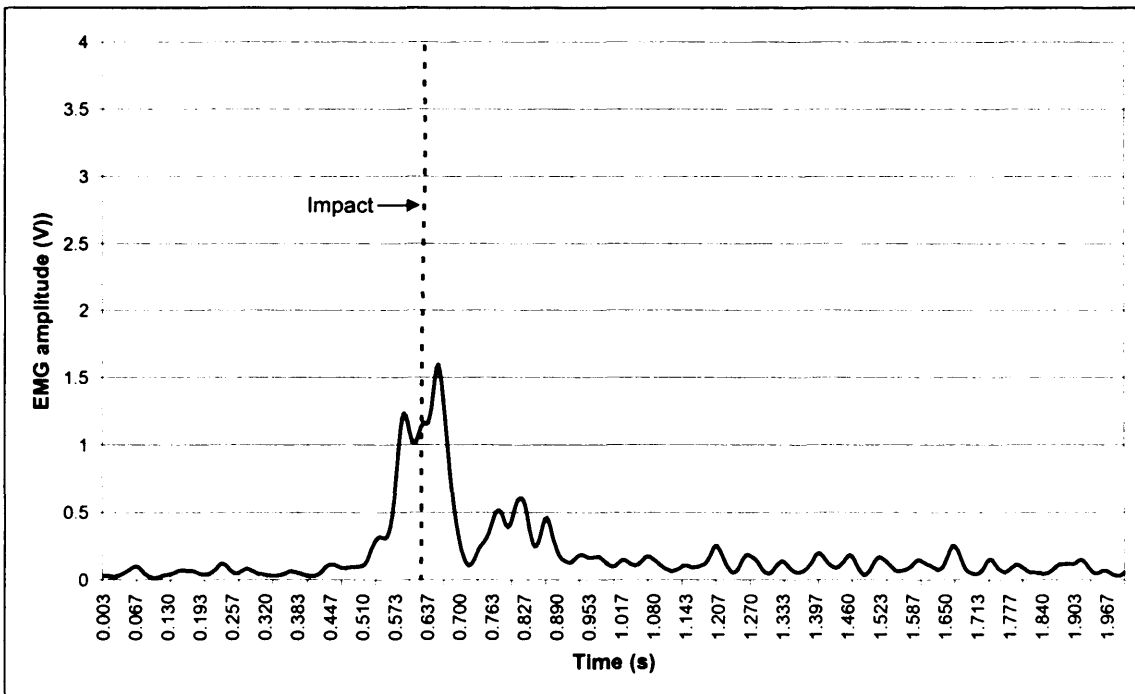


Figure 3.62: Typical filtered EMG trace for the forearm flexors, for a fall from standing height.

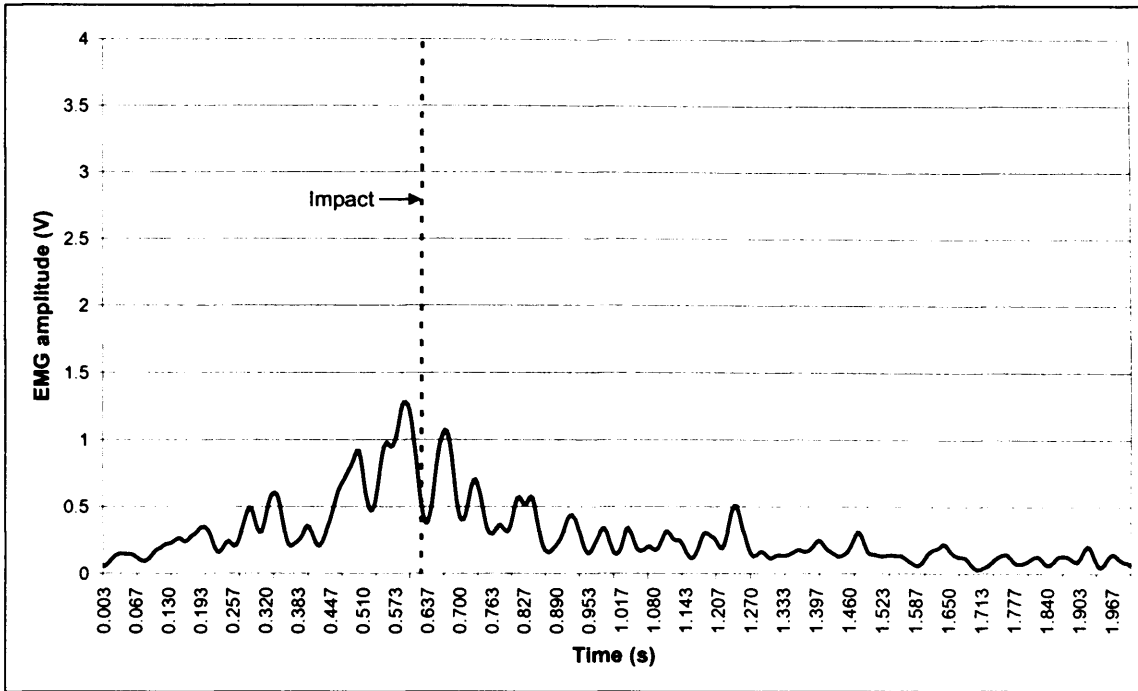


Figure 3.63: Typical filtered EMG trace for the forearm extensors, for a fall from standing height.

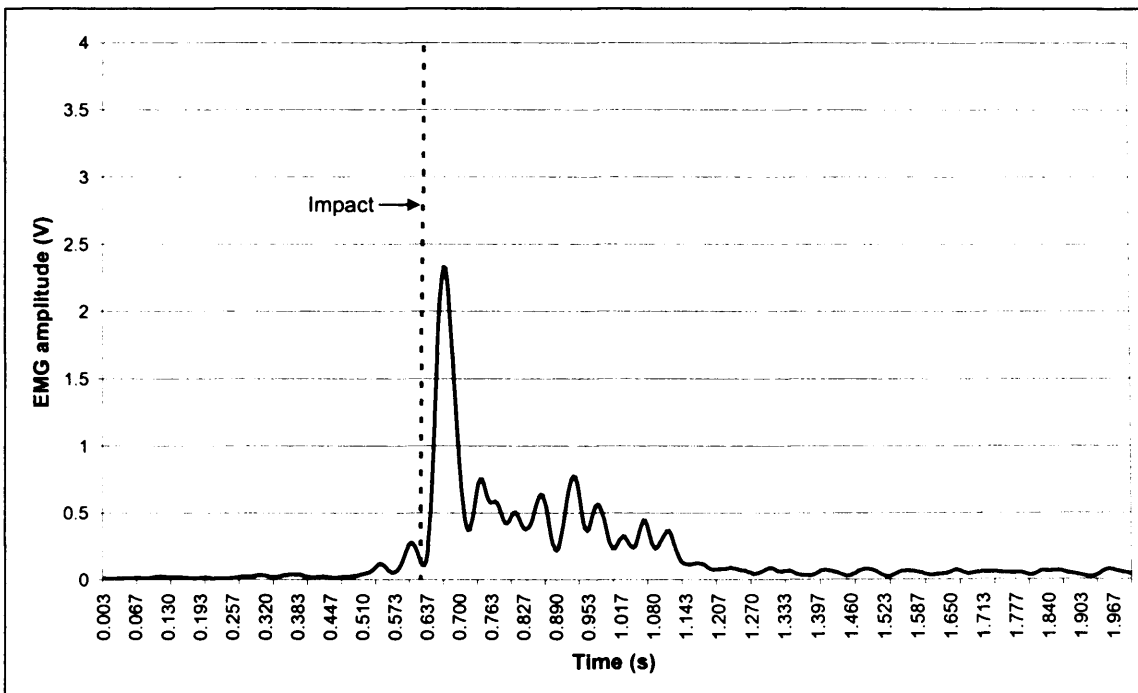


Figure 3.64: Typical filtered EMG trace for the biceps brachii, for a fall from standing height.

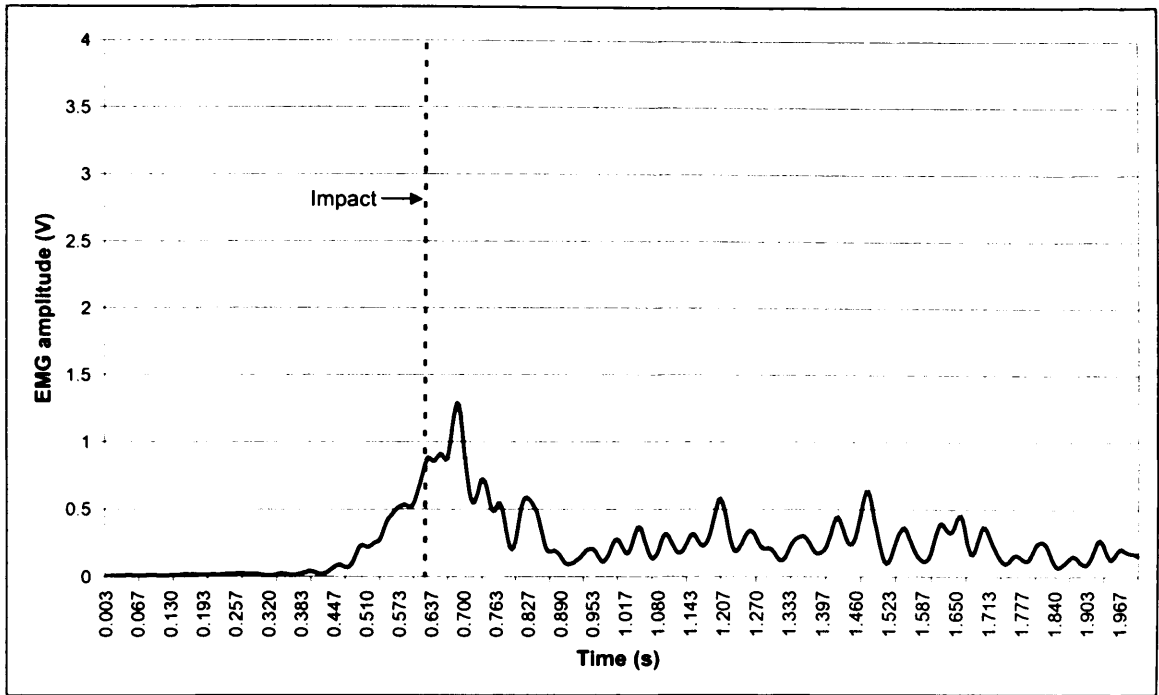


Figure 3.65: Typical filtered EMG trace for the triceps brachii, for a fall from standing height.

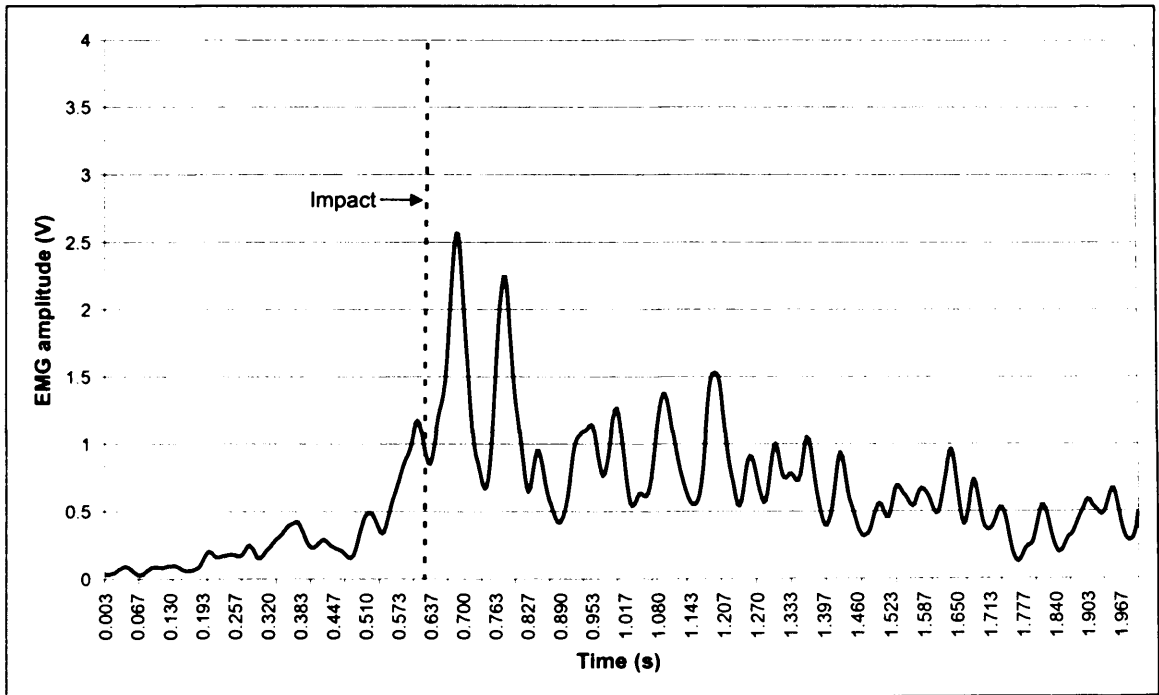


Figure 3.66: Typical filtered EMG trace for the anterior deltoid, for a fall from standing height.

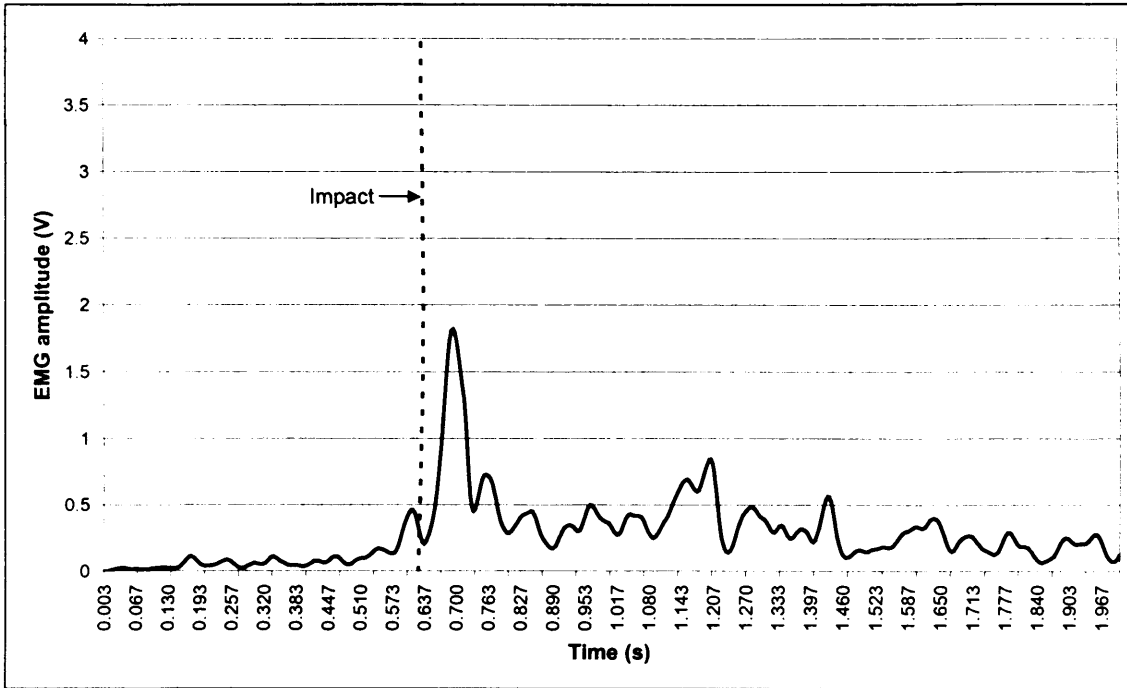


Figure 3.67: Typical filtered EMG trace for the pectoralis major, for a fall from standing height.

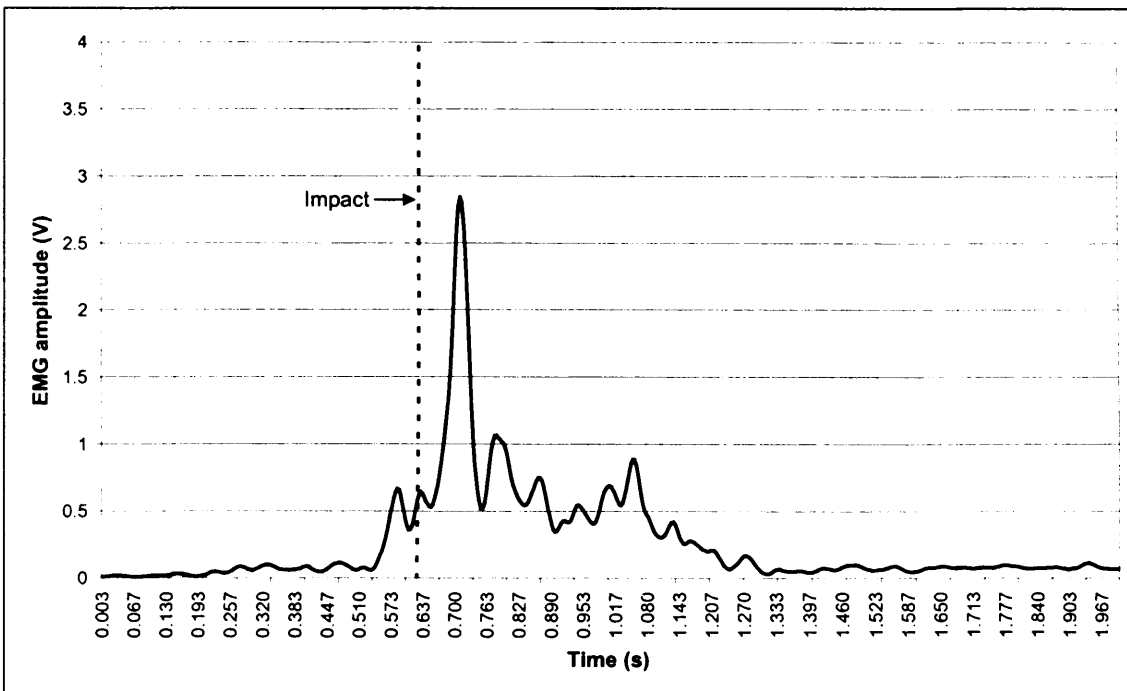


Figure 3.68: Typical filtered EMG trace for the trapezius, for a fall from standing height.

3.7 COMPUTER MODELLING RESULTS

Drop test simulations were conducted on Model 5 to obtain force values at the contact between the hand and floor.

Figure 3.69 shows the results from a simulation conducted at drop heights of 1 cm and 2 cm.

Figure 3.70 shows the results from a simulation conducted with masses of 15 kg and 30 kg from a drop height of 1 cm.

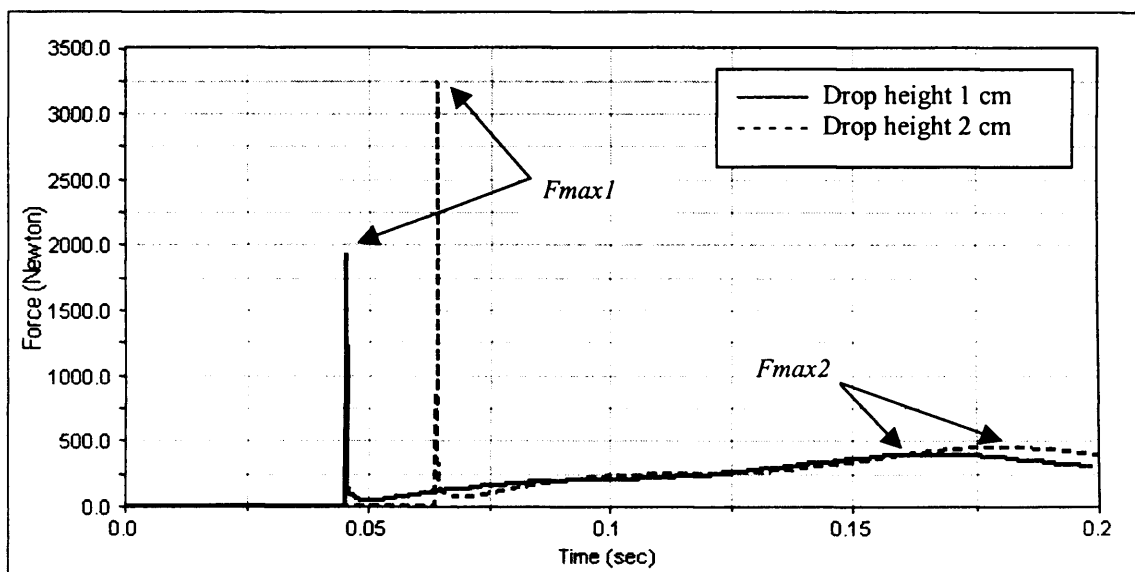


Figure 3.69: Graph showing force-time curve of hand to ground contact of model 5, from a fall height of 1 and 2 cm.

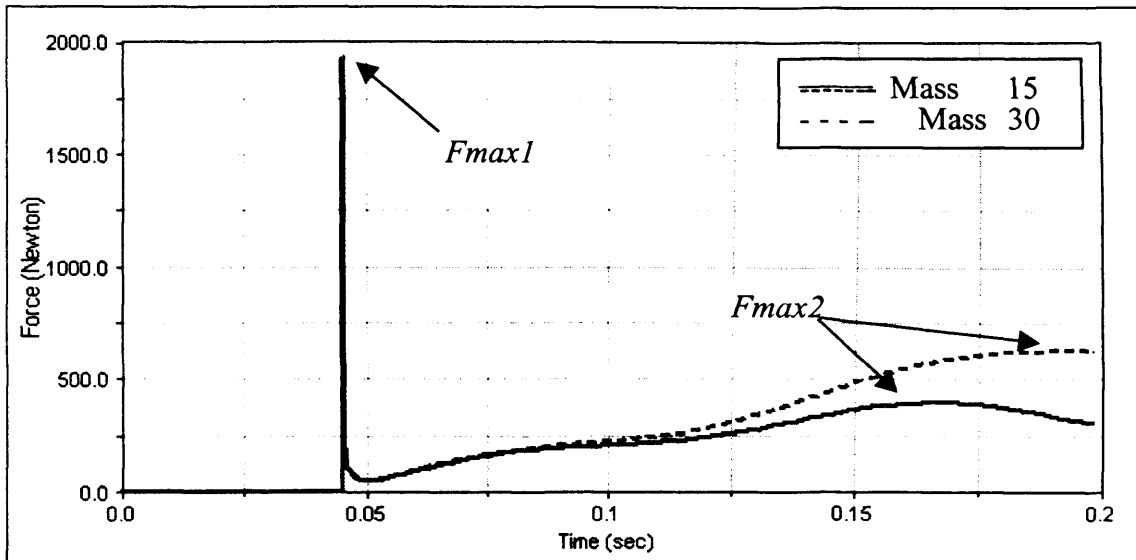


Figure 3.70: Graph showing force-time curve of hand to ground contact of model 5, with masses of 15 and 30 kg.

CHAPTER 4

DISCUSSION

4.1 INTRODUCTION

Playground injuries account for a small proportion of childhood injuries yet, they are important because they account for a large number of hospital admissions (Mott *et al*, 1994, Mowat *et al*, 1998). A series of experiments were conducted to assess the impact of a fall onto the outstretched hand, the methodology of which was detailed in chapter 2.

The objectives of this study were:

- to obtain impact data for a fall from a non-injurious height, using adult volunteers falling onto the outstretched hand
- to assess what factors are influential on the forces produced during the experimental falls. These factors include the fall height, the effective mass, gender and age of the volunteer, the impact surface, and the angle of the elbow prior to and during impact
- to investigate the mechanism of the arm prior to and during impact
- to assess the activation of the muscles in the arm in response to a fall
- to develop a computational arm model to enable falls from higher (injurious) heights to be investigated.

The results of these studies (detailed in chapter 3) will be discussed in this chapter.

4.2 OBSERVATIONAL STUDY

An observational study was conducted to assess the position of the arm, specifically the angle of the elbow, during a fall and subsequent impact with a surface. A volunteer was subjected to a series of experiments involving falls from a standing height, to assess if there was a difference between the reaction and position of the arm during a self initiated fall and an unexpected fall.

Previous studies by Kim et al (1997) and Chou et al (2001) investigated the effect of how elbow flexion affects the impact forces produced at the hand, by dropping subjects onto a surface with a fully extended elbow as one of the test criteria. Chiu and Robinovitch (1996, 1998) used a fully extended arm throughout their studies as a 'worst case falling scenario' but admitted that common experience tells us that this is not typical of actual falls.

This observational study acted as a means of determining if falls do occur onto a fully extended arm or whether the elbow is always slightly flexed. The findings of which were used for further studies.

Figure 3.1 shows a series of photographs, taken from video footage of a standing fall onto a 2.5 cm foam surface, with the corresponding stick figures from Qualysis Track Manager and the associated time of the fall. Table 3.1 shows the angles of the arm at an anatomically relaxed position (taken at standing height immediately before the fall was initiated) and also immediately prior to impact. It can be seen that in none of the fall scenarios did the volunteer attempt to break the fall using a fully extended arm,

instead the arm was flexed slightly during descent and extended marginally prior to impact with the surface.

From this observational study it was decided that falling onto an extended arm in an experimental context would not be consistent with falling in a physiological context and volunteers should therefore be able to assume a natural arm angle, rather than a pre-defined position, prior to falling. The author suggests that if falls onto the outstretched hand do not occur with a fully extended elbow then there is little use in using it as a 'worst case falling scenario'. These findings were used as the methodology for further tests.

4.3 MOTION ANALYSIS STUDY

A second study was conducted on 35 volunteers, who were suspended in a kneeling press-up position from a drop rig, and dropped through heights of 3 and 5 cm onto two Bertec force plates. Figure 3.2 shows a series of photographs, taken from video footage of a 5 cm fall from the drop rig, onto the force plates, with the corresponding stick figures from Qualysis Track Manager and the associated time of the fall.

4.3.1 ANALYSIS OF ARM ANGLES AT 3 AND 5 CM FALL HEIGHTS

To assess the angle of the arm immediately prior to impact, an analysis was conducted from the results of the drop tests at 3 and 5 cm. An initial recording was taken of the arm in a fully extended position and then the angle of the arm was recorded at the initial position in the drop rig, on release from the drop rig and immediately prior to impact with the force plates.

The arm angles were averaged over the three drop tests, at each height and the difference in angle was calculated compared to the fully extended position. The full set of results can be seen in Appendix B. The angle of the arm (from the vertical axis) immediately prior to impact is shown graphically in figure 3.3.

From the results shown in figure 3.3, it can be seen that only 1 person in 35 volunteers showed an almost fully extended arm on impact with the force plate (volunteer with mass 104 kg). Most volunteers demonstrated an arm angle of between 10° and 60° flexion compared to an extended arm. These results emphasise that falls onto the outstretched hand do not commonly occur onto a fully extended elbow and therefore, justify the adoption of a methodology free from physiological constraints.

It is noteworthy, that in 98% of the drop tests both arms were observed to flex in response to being released from the harness. Eighty seven percent of the tests showed a subsequent extension of the arms, immediately prior to impact. Only 1% of the volunteers did not flex or extend their arm during the drop tests.

4.3.2 ANALYSIS OF FALLS AT 3 AND 5 CM FALL HEIGHTS ONTO FORCE PLATES

Figures 3.4 and 3.5 show typical force time curves for impacts at heights of 3 and 5 cm respectively. The graphs indicate that a fall onto the outstretched hand produces an initial force peak (F1), followed by two further force peaks (F2 and F3). These force peaks are highlighted in figure 3.6 and introduce the terminology for describing

the force peaks throughout this study. It should be noted that force time curves with four force peaks were observed in six tests (out of 200), all of which were females and all but one from a height of 5 cm. Since force time curves with four force peaks are relatively rare they are not used in the analysis.

Analysis of these force peaks and the reasons for their occurrence will be discussed in the remainder of this chapter.

4.3.3 HAND DOMINANCE

An analysis was conducted to assess whether hand dominance affected the order in which the hands impacted the force plates. In 200 tests, 57% of volunteers impacted with their left hand first, 37% with their right and 6% impacted with both hands simultaneously (<2 ms between impacts). There was no difference in whether the volunteer was left or right hand dominant, the majority of both categories impacted more with their left hands. There is no reason from these results to suggest that hand dominance influences the order in which the hands impact the floor during a fall.

A comparison was then made between the force magnitude produced in the right and left hand impacts for force peaks F1 and F2. Figures 3.7 and 3.8 show the comparison of force (in Newtons, N) between the right and left hands, categorised by fall height and force peak.

The results showed that the average forces at 3 cm, for peak force F1 were 462.89 N for the right hand and 408.25 N for the left hand. The average forces for force peak F2 were 308.61 N for the right hand and 289.91 N for the left hand.

Falling from 5 cm, the average forces for peak force F1 were 626.32 N for the right hand and 662.88 N for the left hand. The average forces for force peak F2 were 334.89 N for the right hand and 357.39 N for the left hand.

From these results it can be suggested, that there was little significant difference between the forces of the two hands impacting the force plate. Statistical analysis, shown in table 3.2, showed that there was significance ($P < 0.05$) at 3 cm for force peak F1 but there was no significance ($P > 0.05$) for all other tests. Since there was little significant difference between the force magnitude of the force peaks for each hand further analyses used the left hand only for simplicity.

4.3.4 IMPACT FORCES AT 3 AND 5 CM

Figure 3.9 and 3.10 show the impact forces of the force peaks F1, F2 and F3 for all 35 volunteers (in terms of effective mass) at fall heights of 3 and 5 cm respectively. These results suggest that the magnitude of force peak F1 is, generally, always higher than the magnitude of F2 or F3 at both 3 and 5 cm. This difference in magnitude appears greater at a 5 cm fall height than at 3 cm. (There is little difference between the results for force peaks F2 and F3).

Figure 3.11 shows a comparison of impact force peak F1 at 3 and 5 cm. It can be seen that (as suggested from figures 3.9 and 3.10) force peak F1 is greater at a fall height of 5 cm than at 3 cm.

Figure 3.12 shows a comparison of impact force peak F2 at 3 and 5 cm. This graph suggests that although the impact forces for force peak F2 are greater at the higher fall height, the increase is smaller when compared to the same comparison of force peak F1.

During a fall onto the outstretched hand, the experimental results suggest that fall height is a factor in determining the impact force, particularly force peak F1.

The results also suggest that the impact force increases as the effective mass of the volunteer increases. If the trendlines of figures 3.11 and 3.12 were extended back to the y-axis it would show that zero effective mass would not give zero force. This is because the mass at impact is not static (i.e. $1 \text{ kg at } 9.81 \text{ m/s}^2 = 1 \text{ N}$) but, has been dropped through a height and is therefore, subject to a deceleration on impact.

Figure 3.12 suggests that there is a similar rate of increase of force peak F2 with effective mass, for both fall heights. This is suggested from the similar gradients, 0.9510 and 0.9343, of the trendlines for 3 and 5 cm fall heights respectively. The gradients can be found from the trendline equations that are displayed in figure 3.12. Assessment of the trendline equations for force peak F1 (figure 3.11) also show a similar gradient, 0.9157, at a fall height of 5 cm. The gradient of force peak F1 at 3 cm was 0.7256.

The increase of impact force with effective mass, therefore, appears to be consistent for force peaks F1 and F2 at both fall heights, suggesting that there may be a relationship between these two force peaks.

Initial observations from the results suggest, that fall height and effective mass influence the magnitude of the impact forces and that there may be a possible relationship between force peaks F1 and F2. These results, focusing on factors that may affect the impact forces, will be discussed in more detail in the following sections.

4.3.4.1 FORCE PEAKS

Figures 3.13 and 3.14 show graphs comparing the force peaks for females and males (respectively) at both fall heights. The results have been separated into female and male volunteers due to results found in the next section (4.3.4.2) of this chapter.

For females at 3 cm, the average forces (N) for force peaks F1, F2 and F3 are 279.82 N, 221.87 N and 238.21 N respectively. At 5 cm, the average forces for force peaks F1, F2 and F3 are 377.57 N, 259.99 N and 225.35 N respectively.

For males at 3 cm, the average forces for force peaks F1, F2 and F3 are 466.80 N, 320.37 N and 315.82 N respectively. At 5 cm, the average forces for force peaks F1, F2 and F3 are 687.74 N, 366.38 N and 335.23 N respectively.

The results suggest that, on average, force peak F1 is higher than the subsequent force peaks and that although force peak F2 does tend to be generally higher than force peak F3, they are of similar magnitude (largest difference between force peak F2 and F3 is approximately 35 N).

Statistical analysis, shown in table 3.3, indicated significance ($P < 0.05$) between force peaks F1 and F2, and F1 and F3, in females at 3 cm. There is a high significance ($P < 0.01$) between force peaks F1 and F2, and F1 and F3 at 5 cm for females. For the male population, there is a very high significance ($P < 0.001$) between force peaks F1 and F2, and F1 and F3 at both heights. There is no significance ($P > 0.05$) between force peaks F2 and F3 in either females or males at either fall height.

Force peak F3 is not present in all force time curves and it is suggested from these results that when it does occur the magnitude is not significantly different to force peak F2. From these results the analysis of the impact forces will be conducted using only force peaks F1 and F2.

Initial observations in section 4.3.4 suggested that there might be a relationship between force peaks F1 and F2. Figures 3.15 and 3.16 show a comparison of force peak F1 against force peak F2, at 3 and 5 cm respectively, to assess if any relationship is present. The results suggest that there is a positive linear relationship between force peaks F1 and F2 (as F1 increases, F2 increases). The increase of force peak F2 is not as great as the increase of force peak F1, confirming the suggestion that the magnitude of force peak F1 is, generally, always greater than F2.

At a fall height of 3 cm the gradient of the trendline is 1.1091 and at 5 cm the gradient is 1.4251. This increase in gradient with increase in fall height suggests that as the fall height increases, force peak F1 increases at a greater rate than force peak F2. These results concur with a study by Chiu and Robinovitch (1996) who concluded that 'the ratio of Fmax1 [force peak F1] to Fmax2 [force peak F2] increased with increasing fall height'.

4.3.4.2 GENDER

Previous studies assessing falls onto the outstretched hand were conducted using only male volunteers (Dietz *et al*, 1981, Kim *et al*, 1997, Chou *et al*, 2001, DeGoede and Ashton-Miller, 2002, Kim and Ashton-Miller, 2003, Lo *et al*, 2003). A study by Chiu and Robinovitch (1998) did use female as well as male volunteers but did not appear to analyse the results separately. It is therefore, not known if impact forces during a fall onto the outstretched hand are similar in females and males.

Figure 3.17 and 3.18 show a comparison of the impact forces of force peak F1, separated into female and male volunteers at fall heights of 3 and 5 cm respectively, to assess if the magnitude of the force peak is affected by gender. The same comparison for force peak F2 is shown in figures 3.19 and 3.20 for 3 and 5 cm respectively.

The force peak values for females and males are grouped together separately, to allow simple comparisons of gender differences with relation to effective mass. The results suggest that for force peak F1, at 3 and 5 cm, there is a difference in the range of

forces between females and males, the males producing a greater impact force for the equivalent range of effective mass than females.

For force peak F2 the results suggest that the male impact forces tend to be slightly higher than the females, but not to the extent as previously mentioned in force peak F1.

The average forces at 3 cm, for force peak F1, are 279.82 N for females and 466.80 N for males. For force peak F2, the average forces are 221.87 N for females and 320.37 N for males. These results are shown graphically in figure 3.21.

The average forces at 5 cm, for force peak F1, are 377.57 N for females and 687.74 N for males. For force peak F2, the average forces are 259.99 N for females and 368.39 N for males. These results are shown graphically in figure 3.22.

These results suggest an increase in impact force in males, for force peaks F1 and F2, compared to females at both fall heights. (This increase in force is more prevalent in force peak F1 than F2).

Statistical analysis, shown in table 3.4, indicated that gender is very highly significant ($P < 0.001$) for both force peaks (F1 and F2) at both fall heights (3 and 5 cm).

Results from this study therefore, show that there is a noticeable difference between the forces produced during a fall onto the outstretched hand in females when compared to males.

No previous literature has been found that reported a reduction in impact force in females, compared to males, during a fall onto the outstretched hand. Reasons for these differences in females and males could be contributed to neuromuscular and/or musculo-skeletal physiological differences, producing a difference in fall arrest strategy or alternatively that females may simply not have the strength to arrest a fall in an effective way to avoid fracture.

It is worth noting however, that fracture forces for forearms, found in cadaver studies, seem to show slight variations between females and males, the female fracture forces generally being slightly lower than the males. This may be attributable to post menopausal demineralisation since the sample group by implication will be from aged cadavers.

However, if we assume that higher peak impact forces are more likely to produce a fracture, and that females generally produce a lower impact force, this would imply that females are less likely to fracture their arms during a fall.

The number of accidents involving fractures of the lower arm has been collected by the Home Accident Surveillance System and the Leisure Accident Surveillance System (HASS/LASS, 2005) split by gender and age. (The results of which can be seen in Appendix D). The data, taken between 1996 and 2002, shows that little difference is present in the number of arm fractures between female and male children aged 0 to 10 years. Similarly, little difference is seen between adults of 25 to 40 years. Between 10 and 25 years, however, the number of arm fractures is greater in

males than females. Above 40 years, the number of arm fractures is greater in females than in males.

Therefore, applying the assumptions made in the 25 to 40 years age range, to the volunteers used in this study (22 to 51 years), there is no evidence to suggest that females are less likely to fracture their arms than males. This would imply that, as the impact forces for females were lower than the male impact forces in this study, and that fractures occur equally between females and males, the force to fracture a female arm is lower than the force required to fracture a male arm.

It should be noted, however, that the study (HASS/LASS, 2005) makes no reference to associated injuries or the accident type, which would possibly show female/male differences. It should also be noted that the experimental results are for adults falling from low fall heights. If the study was repeated using adults falling from higher fall heights the results may be different.

From these results the author suggests that any studies using both female and male volunteers, falling onto the outstretched hand, should be analysed separately and assumptions made for one gender population cannot be assumed for the other, particularly for force peak F1. From these findings, further analysis of this study will be conducted separating the results for females and males accordingly.

4.3.4.3 HEIGHT

Volunteers were dropped through two heights of 3 and 5 cm to assess if fall height affected the magnitude of the impact force. Figures 3.23 and 3.24 show a comparison

of impact forces for females and males, for force peaks F1 and F2, at fall heights of 3 and 5 cms respectively.

The results show that for force peak F1 in females, the average forces are 279.82 N for 3 cm and 377.57 N for 5 cm. For males, the average forces are 466.80 N for 3 cm and 687.74 N for 5 cm.

For force peak F2 in females, the average forces are 221.87 N for 3 cm and 259.99 N for 5 cm. For males, the average forces are 320.37 N for 3 cm and 368.39 N for 5 cm.

These results suggest a definite increase in force due to an increase in fall height in both females and males. The increase is greater between fall heights for force peak F1 than for F2.

Statistical analysis (shown in table 3.5) indicated that, for force peak F1, the fall height is very highly significant ($P < 0.001$) in males and significant ($P < 0.05$) for females. For force peak F2, height was found to be significant ($P < 0.05$) in males but not significant ($P > 0.05$) for females.

These results suggest that fall height is an important indicator of force peak magnitude, particularly force peak F1, when assessing falls onto the outstretched hand. These results correlate well with a previous study (Chiu and Robinovitch, 1998), that found force peak F1 to be influenced greatly by fall height.

4.3.4.4 EFFECTIVE MASS

Analysis of the impact forces from figures 3.11 and 3.12 in section 4.3.4 suggested that as the effective mass of the volunteers increase, the impact force increases.

Due to the position of the body during impact, it was important that the *effective* mass and not the *total* mass of the volunteers be considered. During the fall experiments, the knees of the volunteer remained in contact with the floor at all times and therefore, by implication the total mass of the volunteer did not act through the arms during impact. The effective mass was calculated by taking a static force value of the volunteers when in a kneeling press-up position on the force plates. Chiu and Robinovitch (1996 and 1998) used a similar method of calculating the effective mass during a fall onto the outstretched hand, whilst in a kneeling position.

Figure 3.25 and 3.26 show the impact forces of force peak F1, for females and males, at heights of 3 and 5 cm respectively, plotted against effective mass. The impact forces for force peak F2 for females and males at 3 and 5 cm are shown in figures 3.27 and 3.28.

The results in figures 3.25 to 3.28 suggest that in males, an increase in the effective mass causes an increase in the impact forces for both force peaks, F1 and F2. This effect appears more prevalent in force peak F2 than F1. In females however, the effective mass appears to have little effect on the impact forces.

Statistical analysis, shown in table 3.6, indicated that the effective mass was highly significant ($P < 0.01$) in males in force peak F2 at both 3 and 5 cm and significant

($P < 0.05$) at 3 cm for force peak F1. The effective mass was not significant ($P > 0.05$) in males at 5 cm for force peak F1 or for females at any height for either force peak.

Similar results were found in Chiu and Robinovitch (1998) who reported that an increase in effective mass caused an increase in impact force peak F2 at all heights and in force peak F1 at 1 and 3 cm, but not at 5 cm. These results however, were taken from a study using only eight females and eight males and the results were analysed grouping both genders together. If the results from this thesis were grouped with both genders they would show similar results. It has however, already been stated previously that gender differences are highly significant when assessing falls onto the outstretched hand (section 4.3.4.2) and therefore this would not be an accurate way of representing the results.

This study would therefore, suggest that in males, the effective mass affects the impact force magnitude of force peak F2, but only influences force peak F1 at small fall heights (< 5 cm). The effective mass does not appear to affect the impact forces in females. Reasons for these differences in females and males could be due to neuromuscular and/or musculo-skeletal physiological differences producing a difference in fall arrest strategy.

4.3.4.5 AGE

Previous researchers (DeGoede *et al*, 2001, DeGoede and Ashton-Miller, 2003, Kim and Ashton-Miller, 2003) have attempted to assess if age is an influencing factor on the impact forces produced during a fall onto the outstretched hand. Due to safety considerations, it was neither ethical nor desirable to drop elderly volunteers onto

force plates, as it is not known whether even falls from small heights may cause fracture.

The previous studies that have been attempted have used other methods (Arresting an oncoming pendulum whilst in a seated position - DeGoede and Ashton-Miller, 2003, Falls onto vertically positioned force plates – Kim and Ashton-Miller, 2003) to assess the reaction time of elderly volunteers compared to young volunteers and then used the results to make assumptions about any age effects on the impact forces. The conclusions of these studies show that although reaction time may decrease with age, it was not to such an extent that would affect the arms getting into position to arrest a fall.

To further investigate age considerations, this study used a range of volunteers aged between 22 and 51 years of age, thus employing a greater range of ages than previous fall studies, to enable the effect of age on the impact forces to be assessed.

Figures 3.29 and 3.30 show a comparison of impact force against age for females (23-51 years) at 3 and 5 cm respectively and figures 3.31 and 3.32 show the same comparisons in males (22-47 years) at 3 and 5 cm respectively.

The results suggest, from figures 3.29 and 3.30 for female data, that there is no noticeable trend when assessing impact force compared to age. The force may appear to decrease in age due to the data for the 51-year-old volunteer however, if these results alone were removed the trend may even appear to increase. In the male data, figures 3.31 and 3.32, there also seems to be no noticeable trend in results.

These results suggest that within our experimental age range, age is not a significant factor when assessing the forces in the arm during a fall.

Statistical analysis, shown in table 3.7, was conducted by splitting the data into lower and upper age groups within the female and male data using the median of the ages as a cut off point. It can be seen in the female data that age was not a significant factor ($P>0.05$) at either height for either F1 or F2. In the male data there was no significance ($P>0.05$) at 3 cm for either F1 or F2 but there was a high significance ($P<0.01$) at 5 cm for F1 and significance ($P<0.05$) at 5 cm for F2.

The implication is that within the experimental series, although there is no significance for females regarding age, there may be significance within the male population at higher fall heights.

It should be noted that, in this study, even the oldest female and male volunteers are still relatively young (51 and 47 years respectively). Using volunteers that are 65 and over would give a better appreciation of the effect age has on the impact forces produced during a fall onto the outstretched hand. However, it was previously discussed that conducting fall studies on older adults is not possible due to safety reasons and this study has gone further than most to try and assess any age differences that may be present.

4.4 SURFACE STUDY USING MOTION ANALYSIS

A third study was conducted, using the same volunteers as the previous study, to assess the effect that impact surface had on the magnitude of the impact forces, produced during a fall onto the outstretched hand. Two different surfaces (a carpet tile used in domestic surfacing and a wet pour playground tile) were placed over the force plates and the volunteers were dropped through a height of 5 cm onto each surface.

4.4.1 FORCE TIME CURVES ONTO SURFACES

Figures 3.33 and 3.34 show typical force-time impact curves for a fall from 5 cms, onto the domestic and playground surfaces respectively. It can be seen from the results depicted in figures 3.33 and 3.34 that falls onto the experimental impact surfaces produce the same range of force peaks as the falls directly onto the force plate (an initial force peak, F1, followed by subsequent force peaks, F2 and F3) as seen previously in figures 3.4 and 3.5.

Since the force time curves were similar to the previous study, the analysis was conducted using force peaks F1 and F2, onto the left hand and separating female and male volunteers. The results from falls onto the force plates at a fall height of 5 cm were used to compare the affect the impact surfaces have, if any, on the impact forces.

4.4.2 IMPACT FORCES

Figures 3.35 and 3.36 show a comparison of the impact forces onto the experimental surfaces (force plate (FP), domestic (DS) and playground (PT)) for females and males respectively, from a fall height of 5 cm.

For females, the average forces (N) for force peak F1 were 377.57 N for FP, 328.47 N for DS and 388.84 N for PT. For force peak F2 the average forces were 259.99 N for FP, 270.23 N for DS and 259.21 N for PT

For males, the average forces for force peak F1 were 687.74 N for FP, 518.23 N for DS and 535.73 N for PT. For force peak F2 the average forces were 368.39 N for FP, 370.71 N for DS and 347.60 N for PT.

At this low fall height the results from this study suggest that there is little difference in the impact forces produced during a fall onto the force plate, when compared to the domestic and playground surfaces, at both force peaks F1 and F2. The only noticeable difference is the larger impact force for force peak F1 in males (figure 3.36), compared to the other surfaces.

Statistical analysis, shown in table 3.8, indicates that in females there is a high significance ($P < 0.01$) for force peak F1 between the domestic and playground surface, but no significance for any other surfaces at force peak F1 or F2.

In males there is very high significance ($P < 0.001$) for force peak F1 between the force plate and domestic surface, and high significance ($P < 0.01$) between the force plate

and the playground surfaces. There was no significance ($P>0.05$) between the domestic and playground surfaces at force peak F1 or any of the surfaces at force peak F2.

These results suggest that there may be some differences in impact forces at force peak F1, but that the impact surface does not change the impact forces of force peak F2. These results are similar to that of Robinovitch and Chiu (1998) who stated that practical decreases in surface stiffness attenuate force peak F1 but not F2.

It is acknowledged that the fall heights used in this study are relatively low (3 and 5 cm) and that the impact forces may well be attenuated by the surfaces at a higher fall height. This confirms the need for a computer/mechanical arm model to be developed to test the forces produced in the arm due to a fall from higher fall heights.

4.5 ANALYSIS OF TIME DURATION OF FORCE PEAK F1

An analysis was conducted on force peak F1 to assess if any factors, which are suggested to effect the magnitude of the force peak (fall height, impact surface or effective mass), will effect the time duration of the peak.

Figures 3.37 to 3.40 show the time duration (in milliseconds, ms) of force peak F1, for falls from a height of 3 and 5 cm onto force plates and at 5 cm onto the domestic and playground surfaces (respectively). This is plotted against the effective mass for each volunteer.

The range of peak time duration at a fall height of 3 cm is 6.37-23.03 ms for females and 4.90-27.93 ms for males. For a fall height of 5 cm the range of peak time duration is 4.90-28.42 ms for females and 4.90-24.01 ms for males. (At the 3 cm fall height a point with time duration of 109 milliseconds was disregarded as an anomaly, because it fell well above the other results).

The range of peak time duration for the domestic surface is 6.37-56.36 ms for females and 8.82-45.08 ms for males. For the playground surface the range of peak time duration is 2.94-29.89 ms for females and 2.94-33.81 ms for males.

Chiu and Robinovitch (1998) reported peak time duration of 20 ms for F1. This value however, was averaged from falls at 1, 3 and 5 cm fall heights. They do not separate the time duration for the individual fall heights.

Kim *et al* (1997) found the mean time duration to be 34 ms, this result was averaged for falls with and without elbow flexion during standing falls onto an inclined force plate 10° to the vertical.

Kim and Ashton-Miller (2003) also conducted standing falls onto an inclined force plate 10° to the vertical and found the time duration of force peak F1 to be less than 60 ms. This result was found using young and older adult male volunteers.

The results from this study suggest that there seems to be little difference when assessing the time duration of falls from 3 cm compared to falls from 5 cm onto the

force plates (figures 3.37 and 3.38), suggesting that fall height does not alter the time duration of force peak F1.

Assessment of falls onto the other surfaces, when compared to falls of the same height, seem to suggest that there may be some differences, particularly when assessing the falls onto the domestic surface (figure 3.39), compared to falls onto the force plate from the same height (figure 3.38).

Statistical analysis, shown in table 3.9, showed that fall height (3 cm versus 5 cm) is significant ($P < 0.05$) in males but not significant ($P > 0.05$) in females, when assessing the time duration of force peak F1. When comparing the falls onto the force plate from 5 cm with falls onto the domestic surface, the time duration of force peak F1 was found to be highly significant ($P < 0.01$) in females and very highly significant ($P < 0.001$) in males.

There was no significance ($P > 0.05$) when comparing falls from 5 cm onto the force plates with falls onto the playground surface in either females or males, but when comparing the domestic surface with the playground surface, the time duration was found to be very highly significant ($P < 0.001$) in both females and males.

The results suggest that fall height may be significant in males but not in females. It is noteworthy, that these falls were from low fall heights and the difference of time duration from higher fall heights may be more significant.

It appears, that the time duration of force peak F1 was affected during a fall onto the domestic surface with, on average, a longer time duration than that of a fall onto the force plate or playground surface from the same fall height. However, the time duration of force peak F1 during a fall onto the playground surface did not seem to be much different to a fall onto the force plate.

As far as the author is aware, this is the first study to investigate the effects of fall height and impact surface on the time duration of the impact force peak F1. The previous studies that did assess the time duration (Robinovitch and Chiu, 1998, Kim *et al*, 1997 and Kim and Ashton-Miller, 2003) discussed above, did not distinguish between different falls from different heights and none of them used different impact surfaces. Although the results from this study are not as clear as one would have hoped, it does show that these two factors (fall height and impact surface) may affect the time duration of force peak F1.

4.6 SUMMARY OF MAIN RESULTS AND DISCUSSION FROM MOTION ANALYSIS STUDIES

- Falls onto the outstretched hand do not generally occur onto a fully extended arm, most volunteers demonstrate an arm angle of between 10° and 60° flexion.
- Falls onto the outstretched hand produce an impact force characterised by an initial force peak, F1, followed by two further force peaks, F2 and F3. Force peak F1 was found to be generally higher than the subsequent force peaks F2 and F3. Force peak F3 is not present in all force time curves and it is suggested from the results that when it does occur it is not significantly different to force peak F2.

- A positive linear relationship was found between force peaks F1 and F2 (as F1 increases, F2 increases). The increase of force peak F2 is not as great as the increase of force peak F1, confirming the suggestion that the magnitude of force peak F1 is generally greater than F2.
- There was no evidence from the results to suggest that hand dominance influences the order in which the hands impact the floor during a fall. Furthermore, there was little significant difference between the forces of the two hands impacting the force plate.
- Male volunteers produced higher impact forces at force peaks F1 and F2 compared to the female volunteers. This increase in force for male volunteers was more prevalent for force peak F1 than F2.
- An increase in fall height produced an increase in impact force in both females and males. The increase was greater between fall heights for force peak F1 than for F2. This suggests that as the fall height increases, force peak F1 increases at a greater rate than force peak F2. Height is therefore, an important indicator of force peak magnitude, particularly force peak F1, when assessing falls onto the outstretched hand.
- This study suggests that, in males, the effective mass influences the impact force magnitude of force peak F2 but only influences force peak F1 at small fall heights (< 5 cm). The effective mass does not appear to affect the impact forces in females.
- Although age was not a significant factor of impact force for females, the results suggest that it may be of significance within the male population. It is unclear from the results whether or not age was a contributing factor to the impact force

during a fall onto the outstretched hand and this effect would need to be investigated with a greater age range to draw any valid conclusions.

- Falls onto different impact surfaces (a domestic surface and a playground safety surface) were found to produce impact forces with similar characteristics as falls directly onto the force plates (an initial force peak, F1, followed by subsequent force peaks, F2 and F3).
- The results suggest that there may be some differences in impact forces at force peak F1 but that the impact surface does not change the impact forces of force peak F2.
- The results of the time duration of F1 suggest that fall height may be significant factor in males but not in females. It is noteworthy, that these falls were from low fall heights and the difference of time duration from higher fall heights may be more noticeable.
- It appears that the time duration of force peak F1 was affected during a fall onto the domestic surface with, on average, a longer time duration than that of a fall onto the force plate or playground surface from the same fall height. However, the time duration of force peak F1 during a fall onto the playground surface did not seem to be significantly different to a fall onto the force plate.

4.7 HIGH-SPEED VIDEO (HSV) STUDY

The factors affecting the impact force from a fall onto the outstretched hand have been discussed above, the main points of which were that gender, height and effective mass are all influencing factors on the force peak magnitude. Age, impact surface and

hand dominance were found, to either not effect the impact force, or there was inconclusive evidence to suggest either way.

To understand the impact force involved in a fall onto the outstretched hand, it is important to understand the mechanism of the fall and what happens at the point of impact. This has not been previously discussed in detail, however, previous studies have assessed the effect of fall arrest strategies using elbow flexion (refs). It is noteworthy, that these fall arrest strategies may provide some detail of how to reduce the force at impact, but do not explain the mechanism of the arm prior to and during impact with a surface.

A detailed study was conducted using high-speed video (HSV) cameras, coupled with an Electromyography (EMG) system to investigate the mechanics of the arm and hand immediately prior to and during impact.

Five volunteers (a female and male each weighing 105 kg, a female and male weighing 60 kg and a male who weighed 80 kg) were suspended in a kneeling press-up position from a drop rig, and dropped through heights of 1 and 5 cm onto two Bertec force plates. The lowest fall height was reduced from the 3 cm, used in the motion analysis studies, to 1 cm, to provide a greater difference in the two fall heights to enable a better comparison.

Since fall height was found to be an influencing factor, when assessing impact forces of falls onto the outstretched hands, some further tests were conducted at greater fall heights. One volunteer was dropped through heights of 10 and 20 cm from the drop

rig (the methodology for falls at 1 and 5 cm was used) and two volunteers, who had previous training in how to fall during combat training, were subjected to a series of falls from standing height, onto the force plates.

4.7.1 FORCE TIME CURVES FOR FALLS AT 1, 5, 10 AND 20 CM FALL HEIGHTS

Figures 3.41 to 3.44 show force time curves for falls from 1, 5, 10 and 20 cm respectively. It can be seen from the results depicted in these graphs that these falls produced the same range of force peaks as reported in the motion analysis study (an initial force peak, F1, followed by subsequent force peaks, F2 and F3).

It is noteworthy, that the average impact forces for falls from 1 and 5 cm, for females, were 298.70 N and 569.69 N for F1 respectively, and 357.40 N and 456.30 N for F2 respectively.

The average impact forces for falls from 1, 5, 10 and 20 cm, for males were 131.59 N, 640.22 N, 1119.55 N and 1284.43 N for F1 respectively, and 310.30 N, 305.59 N, 529.02 N and 324.22 N for F2 respectively.

4.7.2 FORCE TIME CURVES FROM STANDING HEIGHT

Figure 3.45 shows a typical force time curve for a fall from a standing height. This graph similarly shows an impact force with initial force peak F1 followed by subsequent force peaks, F2 and F3.

The average impact force for a fall from standing height was 1827.16 N for force peak F1, and 748.37 N for force peak F2. These results are for male volunteers, as there were no female volunteers who fell from a standing height.

These forces are slightly higher than those reported in a previous study (Dietz *et al*, 1981) that conducted falls onto the outstretched hand from standing height. Dietz *et al* (1981) found impact forces for force peak F1 to be approximately 1300 to 1400 N.

The impact forces reported in section 4.9.1 and 4.9.2 further confirm the findings from the previous study using motion analysis, that an increase in fall height produces an increase in impact force in both females and males. Force peak F1 increasing at a greater rate than F2.

It is noteworthy, that during the falls from 20 cm and standing height, there appears to be a small force peak before force peak F1, or two-stage increase in force peak F1. This can be seen in figures 3.44 and 3.45 for the falls from 20 cm and standing height respectively. This effect was due to the mechanism of the hand impacting the force plate and will be discussed in section 4.7.3.4.

4.7.3 FALL AND IMPACT MECHANISM

The mechanism prior to impact was assessed by investigating the high-speed video recording for each fall and assessing:

- the motion of the arm and hands during descent, immediately prior to and during impact with the surface,
- which part of the hand first impacts the force plate, and
- any other movements that may contribute to the fall (head, body etc.).

A pattern was observed in the fall mechanism that appeared to be fall height dependent. The pattern is discussed below according to fall height.

4.7.3.1 FALLS FROM 1 CM

Shortly after release from the drop rig, at a height of 1 cm, three of the five volunteers exhibited finger motion in an upward direction (due to extension of the wrist) concomitant with flexion at the elbow. In these volunteers it appeared that the upward motion was part of a 'slapping' motion of the hand. This is assumed to be due to the start of a rapid downward hand movement seen just prior to impact. The palm of the hand impacted the force plate before the 'slapping' motion could be fully executed.

Assessment of the other two volunteers showed no movement in the hand or fingers at all during the fall, although one volunteer exhibited elbow flexion. One volunteer impacted with the palm and the other volunteer with both palm and fingers.

It is noteworthy, that due to the short time duration of the impact event and the high capture rate of the cameras, the falls from low fall heights could not be portrayed pictorially. A video file showing an example of a fall from 1 cm can be seen in Appendix E (1cm.avi).

4.7.3.2 FALLS FROM 5 CM

Ten further drop tests were conducted from a fall height of 5 cm, during which the volunteers demonstrated a clearly definable upward motion of the fingers, due to extension of the wrist, with concomitant elbow flexion. This movement was followed by a 'slapping' motion of the hand onto the force plates. Variation was observed in the hand impacts that appeared to be during the 'slapping' phase. Those volunteers who carried out a full slapping motion impacted either with their fingers, or both fingers and palm simultaneously. The other volunteers, who did not perform a full 'slap' impacted with their palm first.

As noted previously in section 4.7.3.1, due to the short time duration of the impact event and the high capture rate of the cameras, the falls from low fall heights could not be portrayed pictorially. The video file showing an example of a fall from 5 cm can be seen however, in Appendix E (5cm.avi).

4.7.3.3 FALLS FROM 10 AND 20 CM

A further series of falls were conducted from 10 and 20 cm fall heights. During the falls, the hand and arm demonstrated a similar upward finger motion, elbow flexion and 'slapping' motion of the hand onto the force plate to that reported at fall heights of 1 and 5 cm. This movement, at a fall height of 10 cm, is demonstrated in a series of still photographs taken from high-speed video footage shown in figure 3.46. The full fall can be seen in video format in Appendix E (10cm.avi).

The 'slapping' motion of the hand from 10 cm is suggested (as was previously at 1 and 5 cm) to be due to the rapid downward hand motion immediately prior to impact. At this fall height however, there is no doubt that the fingers impact the force plate first, followed by the rest of the hand. The fall from 20 cm demonstrated the same mechanism that was observed in the 10 cm fall experiment.

At the 20 cm fall height, movement of the head was also observed. After the hands had impacted with the force plate, the volunteer turned his head to one side. The video of this fall can be seen in Appendix E (20cm.avi). This action is presumed to be a protective reflex, used to prevent impact occurring to the front of the head and face, should attempts to fully arrest the fall with the upper limbs fail.

The reason this head movement was not used by volunteers at the lower fall heights could be due to the volunteer having more time at the higher height, in which to carry out this movement. Falls from the lower fall heights may not have been sufficient to trigger the response or it could be that at the lower fall height the volunteer did not feel that there was a risk of the head impacting with the floor.

4.7.3.4 FALLS FROM A STANDING HEIGHT

A series of falls were conducted from a standing height, using two volunteers (males) who had previous training in how to fall during combat training.

Figure 3.47(a) and (b) shows a series of photographs taken from high-speed video footage for a fall from standing height. Unlike the previous falls, in which the

volunteer was released without warning from a drop rig, the falls from standing height were self initiated. The full video footage can be seen in Appendix E (standing.avi).

Initially, before the onset of the fall was commenced, the arms were in an anatomically relaxed position by the side of the volunteer. As the fall was initiated the arms were flexed anteriorly at the shoulder joint, with a pronated forearm, into an outstretched position. The wrist and fingers were both extended, causing the arm and hand to be in an almost straight line with each other (the elbow remained slightly flexed).

Immediately prior to impact, the wrist hyperextended slightly, causing the fingers to move upwards, before a rapid downward movement of the wrist (flexion). This upward movement of the fingers was not as pronounced as previously reported in the falls from the drop rig.

Impact on the force plate occurred sequentially at the fingertips, followed by the knuckles at the palmer aspect of the hand (metacarpophalanx joint) and then the palm; in effect the hand 'rolled' onto the force plate. (For further explanation of this hand impact see section 4.7.3.4.1 below).

This sequential impacting of the fingertips, knuckles and palm provides insight into the change that occurred in the rise of force peak F1 during the falls from 20 cm and standing height that was briefly discussed in section 4.7.2.

At the lower fall heights the hand impacts 'as one' and so there is a quick rise in the force peak (F1). At these higher heights however, the impact occurs in stages, which subsequently affects the way in which force peak F1 occurs. If the impact onto the different sections of the hand is relatively smooth, then this will produce a two-stage increase in force peak F1. (This was also observed to happen in a study by Dietz *et al* (1981) previously discussed in chapter 1). If however, the impact is not smooth then the impact force produced will show a smaller impact force peak for the knuckle impact, followed by force peak F1 where the full hand impacts.

Immediately after the hand fully impacted the force plate, flexion of the elbow occurred, allowing the body to be lowered to the ground in a controlled manner. During all standing falls, the head was turned to the side at impact, protecting the front of the head and face from impacting with the force plate.

4.7.3.4.1 OBSERVATIONAL STUDY

An observational study was conducted using two volunteers from the previous study (one male and one female, both with mass of 105 kg). Macro lenses were attached to the HSV cameras to enable close up views of the hands at impact to be investigated. The subjects fell from a kneeling height, impacting the force plates by adopting a natural physiological response to arrest the fall. This fall height was chosen because it was the lowest fall height from which a standing fall height arrest strategy was observed, but which minimised the impact forces occurring to the hand and wrist.

Figures 3.48 and 3.49 show a series of photographs taken from HSV footage of the falls from kneeling height for the female and male volunteers respectively. The

mechanism of the fingertip impact followed by the hand 'rolling' onto the force plate (as explained briefly in the previous section 4.7.3.5) can be seen pictorially, with an explanation of the event next to the photographs. It can be noted that the time of the impact, from fingertips to full hand, is 28 ms for the female volunteer and 52 ms for the male volunteer.

4.7.4 SHOCK WAVE

Assessment of the HSV study suggests, that when the hand impacts with the force plate, a shock wave is visible in the arm. This shock wave was not visible in the motion analysis study due to the slower capture rate of the equipment. (HSV capture rate - 500 fps, Digital Video camera capture rate - 60 fps).

Each fall was assessed to investigate the position of the shock wave in the arm and whether a pattern could be seen. When the HSV footage was played back, at 60 fps the shock wave was clearly visible, but in time lapse it was difficult to observe so this next section attempts to describe the shock wave verbally. (The shock wave can be observed during all the falls included as video files in Appendix E).

Figure 3.50 shows a series of photographs, taken from high-speed video footage of the observational study discussed in 4.7.3.4.1, showing the impact of an arm from a fall from kneeling height (the video file of which can be seen in Appendix E, kneeling.avi). The series of photographs are a representation of the shock wave, visible in the arm, during impact with the force plates. The associated time from

impact (0 ms) for each photograph is given, showing the shock wave in the forearm to last just 96 ms.

Assessment of the first four photographs in the sequence ($t=0$ to $t=112$ ms) show that the muscles and soft tissues in the arm initially move downwards, causing the tissues to bunch at the wrist. This is due to the arm coming to an abrupt halt, due to the impact, but the muscle and soft tissues, having potential energy, continue to move down.

A second set of four photographs, shown in figure 3.50, starting at 16 ms after impact, show a shock wave travelling up through the lower arm. The left-hand side of the forearm shows a dark shadow where the arm almost appears concave, this is the shock wave travelling up the arm. A dimple also appears at the wrist at 16 ms and this develops into two and then three (one above each other) by 24 ms. This is where the skin and soft tissues are moving upwards away from the wrist and are forced to move around the underlying ulna bone.

The final set of four photographs show the skin and soft tissues moving back down the arm into their original position.

The shock wave was observed to travel the entire length of the arm. Figure 3.51 shows two photographs, the first showing the arm just prior to impact from a fall from standing height, and the second showing the arm after impact. Comparing the two photographs it can be seen that the second photograph clearly shows a disturbance on

the surface of the skin. This is the shock wave travelling up through the entire arm, causing movement of the skin and soft tissues that was discussed above.

4.7.4.1 RELATIONSHIP BETWEEN SHOCK WAVE AND FORCE TIME CURVES

The shock waves discussed in the previous section were analysed, to compare their occurrence in the arm, in relation to the force peaks on the associated force time curves. This was conducted for all the force time curves produced at the force plates, for all volunteers at heights of 1, 5, 10 and 20 cm from the drop rig and from falls from standing height (figures 3.41 to 3.45 respectively).

It was not possible in all volunteers to clearly define a relationship between the position of the shock wave in the arm and the force peaks of the impact force. This is due to the direction of travel of the shock wave, the lighting and the camera angles.

General observations showed that the shock wave appeared in the lower arm, around the elbow joint and in the upper arm, but not necessarily as separate entities. Sometimes it was clear that the shock wave was in the lower arm and the elbow at the same time. It also did not appear in all three arm segments for every fall, sometimes only showing in just one segment. There was only one test (out of 21) where there was no visible shock wave.

Assessing the shock wave by fall height or mass showed no similarities at all when compared to the associated force time curves. When assessing the shock waves for individual volunteers there were more similarities.

The individual shock wave patterns changed between fall heights of 1 and 5 cm and showed similarities when comparing the 5 cm fall responses. The similarities were mainly during the onset of the shock wave and where it disappears. For example, assessing the standing height falls for one volunteer, the onset for most of the shock waves were seen at the rise of force peak F2 in the lower arm and elbow and continued through the arm into the upper arm right until the fall of force peak F3. The pattern in individuals was also slightly different in each arm.

It is clear that the mechanism of the shock wave in the arm, caused by an impact, is different between individuals and is not purely a factor of height or mass. It is suggested that the shock wave is a result of a number of factors such as the height fallen, the effective mass of the individual, the structural composition of the arm (muscular and soft tissue), skin movement, the orientation of the arm and the way in which the fall is arrested.

4.8 ELECTROMYOGRAPHY STUDY

A Bortec 8-channel Electromyography (EMG) system was used with the high-speed video (HSV) equipment to record the electrical activity of specific muscles during a fall onto the outstretched hand. The muscles analysed were: the thenar eminence,

forearm flexors, forearm extensors, biceps brachii, triceps brachii, anterior deltoid, pectoralis major and the trapezius in the neck.

The EMG traces were filtered to remove noise by passing the waveform through a 2nd order low pass filter with cut off at 20 Hz. Figure 3.52 shows a graph with the original and filtered EMG waveform for comparison.

The filtered EMG waveforms were analysed, to assess the onset of muscle activation before impact occurred. The time of the initial activation of the muscle after the volunteer was released from the drop rig was compared between volunteers to assess if there was any patterns in the order in which the muscles fired. This was to assess the reflexive action of the arm in response to a fall. (This study was not concerned with the amplitude of the EMG traces).

4.8.1 ANALYSIS OF EMG DATA DURING FALLS FROM THE DROP RIG, FROM HEIGHTS OF 1, 5, 10 AND 20 CM

Figures 3.53 to 3.60 show typical filtered data for the EMG traces, recorded from falls from the drop rig, from a height of 5 cm, for each muscle group respectively. The maximum time found from activation of the first muscle compared to the last was 164 ms and the minimum time between first and last was 40 ms.

Individual volunteer response, or fall height, made little difference to the onset of muscle activation. These findings were also observed in a study by Dietz *et al* (1981). There was however, some similarity in the order in which muscles fired.

The forearm extensors were found to have fired either as the first or second muscle in 13 out of 17 tests. The pectoralis major fired first or second in 11 out of 17 tests. It is no surprise perhaps to note, that these two muscles are the earliest to fire. The extensor muscles would be responsible for lifting the fingers up to enable the volunteer to fall onto the outstretched hand. The pectoralis major muscle would enable the volunteer to stabilise their arms at a position in which to effectively arrest their fall. Both of these muscles may well have been partially activated before release from the drop rig, as would other muscles, to position the arms to arrest the oncoming fall.

The other muscle that showed some similar results between volunteers was the thenar eminence. This was the last or second to last muscle to fire in 15 out of 16 tests. This muscle group would be partly responsible for stabilising the hand during impact.

From the results it suggests that there seems to be no relationship between the neurological initiation of the muscles in comparison to the fall mechanism before impact. This would suggest that the neurological initiation of the muscles during this study, was due to motor vestibular reflexes reacting to the fall and not an intentional cerebral decision as to when it is best to arrest the fall.

4.8.2 ANALYSIS OF EMG DATA DURING FALLS FROM STANDING HEIGHT

Figures 3.61 to 3.68 show typical filtered data for the EMG traces, recorded from falls from standing height, for each muscle group respectively. The maximum time found from activation of the first muscle compared to the last was 95 ms and the minimum time between first and last was 60 ms.

Unfortunately, there were only 3 tests available for EMG analysis during falls from standing height, but similar results were found when compared to the results from the falls from the drop rig, discussed in the previous section.

There was little similarity observed between the onset of muscle activation between the volunteers, but there were similarities in the order in which the muscles fired. The thenar eminence was the last muscle to fire in all three tests and the forearm extensors were the last muscle to fire in two out of three of the tests.

Since the fall response for falls from a standing height and falls from the drop rig show a similar muscle-firing pattern, the falls from the drop rig show a good representation of a fall from standing height and are therefore, a good analogue for investigating falls onto the outstretched hand.

4.9 SUMMARY OF MAIN RESULTS AND DISCUSSION FROM HSV AND EMG STUDIES

- Force time curves for falls from 1, 5, 10 and 20 cm produced the same range of force peaks as reported in the motion analysis study (an initial force peak, F1, followed by subsequent force peaks, F2 and F3).
- Falls from a standing height similarly showed an impact force with initial force peak F1, followed by subsequent force peaks, F2 and F3.
- The impact forces found in the HSV study confirmed the findings from the previous study using motion analysis, that an increase in fall height produces an increase in impact force in both females and males. Force peak F1 increasing at a greater rate than F2.
- Volunteers falling from the drop rig were observed to have a similar fall arrest response regardless of the fall height. This involved the upward motion of the fingers, due to extension of the wrist, with concomitant elbow flexion. This movement was followed by a 'slapping' motion of the hand onto the force plates, due to a rapid downward hand motion immediately prior to impact.
- Impact occurred to the palm, at smaller fall heights (1 and 5 cm), and onto the fingertips, followed by the palm, as the fall height increased (10 and 20 cm).
- In the 20 cm fall, after the hands had impacted with the force plate, the volunteer was observed to turn his head to one side. This action is presumed to be a protective reflex used to prevent impact occurring to the front of the head and face, should attempts to fully arrest the fall with the upper limbs fail. The reason this head movement was not used by volunteers at the lower fall heights could be due to the volunteer having more time at the higher height, in which to carry out this movement. Falls from the lower fall heights may not have been sufficient to

trigger the response or it could be that at the lower fall height the volunteer did not feel that there was a risk of the head impacting with the floor.

- Falls from a standing height were also observed to involve similar fall arrest strategies. Initially, before the onset of the fall was commenced, the arms were in an anatomically relaxed position, by the side of the volunteer. As the fall was initiated the arms were flexed anteriorly at the shoulder joint, with a pronated forearm, into an outstretched position. The wrist and fingers were both extended, causing the arm and hand to be in an almost straight line with each other (the elbow remained slightly flexed). Immediately prior to impact the wrist hyperextended slightly, causing the fingers to move upwards, before a rapid downward movement of the wrist (flexion). Impact on the force plate occurred sequentially at the fingertips, followed by the knuckles at the palmer aspect of the hand (metacarpophalanx joint) and then the palm; in effect the hand 'rolled' onto the force plate. Immediately after the hand fully impacted the force plate, flexion of the elbow occurred, allowing the body to be lowered to the ground in a controlled manner.
- During all standing falls, the head was turned to the side at impact (as was observed at the 20 cm fall height), protecting the front of the head and face from impacting with the force plate.
- The sequential impacting of the fingertips, knuckles and palm produced a change in the rise of force peak F1. At the lower fall heights the hand impacts 'as one' and so there is a quick rise in the force peak (F1). At these higher heights however, the impact occurs in stages, which subsequently affects the way in which force peak F1 occurs. If the impact onto the different sections of the hand is relatively smooth, then this will produce a two-stage increase in force peak F1.

If however, the impact is not smooth then the impact force produced will show a smaller impact force peak for the knuckle impact, followed by force peak F1 where the full hand impacts.

- On impact, a shock wave was observed to travel the entire length of the arm. General observations showed that the shock wave appeared in the lower arm, around the elbow joint and in the upper arm, but not necessarily as separate entities.
- Assessing the shock wave by fall height or mass showed no similarities at all when compared to the associated force time curves. When assessing the shock waves for individual volunteers there were more similarities. The similarities were mainly during the onset of the shock wave and where it disappears.
- It was found that the mechanism of the shock wave in the arm is different between individuals and is not purely a factor of height or mass. It is suggested that the shock wave is a result of a number of factors such as the height fallen, the effective mass of the individual, the structural composition of the arm (muscular and soft tissue), skin movement, the orientation of the arm and the way in which the fall is arrested.
- EMG analysis showed little similarity could be found between the onset of muscle activation in individual volunteer responses or from falls from different heights. There was however, some similarity in the order in which muscles fired with the forearm extensors and pectoralis major predominantly firing before the other muscles and the thenar eminence predominately one of the last muscles to fire.
- The results suggested that the neurological initiation of the arm, chest and shoulder muscles during this study, was due to motor vestibular reflexes reacting

to the fall and not an intentional cerebral decision as to when is best to arrest the fall.

- Since the fall response for falls from a standing height and falls from the drop rig show a similar muscle-firing pattern, the falls from the drop rig show a good representation of a fall from standing height and are therefore, a good analogue for investigating falls onto the outstretched hand.

4.10 COMPUTER MODELLING

4.10.1 INTRODUCTION

The majority of falls conducted during the motion analysis and high-speed studies were from low fall heights (1, 3 and 5 cm). It was not possible to conduct a full study from higher fall heights because of the risk of arm fracture. All falls that were conducted from higher heights used volunteers who had received training in how to fall during combat training.

It is therefore, important to develop a method for investigating falls onto the outstretched arm from higher fall heights, without the injury risks involved using volunteers. To do this a computer model was developed using the ADAMS[®] (Automatic Dynamic Analysis of Mechanical Systems) software package.

4.10.2 PROGRESSION OF MODELS

A preliminary model was developed (figure 3.25: Model 1), which provided an opportunity to become familiar with the ADAMS[®] software package and provided a

model that could be subjectively compared with real-life experience. Parameters such as the mass of the body and the spring characteristics were adjusted to develop a life-like (biofidelic) model.

An initial mass of 15 kg was used throughout the models to represent the effective mass of the body.

Further considering Model 1, the links representing the upper and lower arm, were not considered suitable because in ADAMS[®] links do not carry any mass and cannot contain contacts. The contacts in Model 1 were instead added to the joints. Due to the limitations of using links, Model 2 was constructed using cylinders for the upper and lower arms.

Model 2 (figure 3.26) was the first to be raised off the floor, as in a drop simulation, so a cylinder was added to represent the hand and contacts were added between the floor and the hand to assess the effect this would have on the model. The model was observed to fall under gravity at first, but when the hand made contact with the floor it bounced back up towards the lower arm, even though friction was added at the contact point. Due to the bouncing of the hand, the arm did not respond in the way which was expected as the elbow angle did not decrease, as it would do during a fall arrest. After the hand had bounced, the contact point across the whole hand was reduced to one point at the wrist. This resulted in the hand sliding across the floor instead of staying in a static position.

It was thought that the model should be altered to a two handed model to assess how the effective body mass and the added friction of two hands would change the model dynamics. Model 3 (figure 3.27) was developed using this concept. Initially the arms and contacts replicated those of Model 2, so it was decided that the problem was not the contact surface, but the way in which the hand behaved when it did make contact.

In a fall situation, as observed during the fall studies, our reflexes react in the wrists and arms to enable the person to break their fall by landing on the outstretched hand. Landing on the back of the hand would seriously increase the risk of fracture compared to that of the outstretched hand. To replicate this in modeling terms meant having to constrain the wrist so it bent in a 'normal' way. A *primitive joint* was added to the hand with a parallel axis to the floor. This joint ensured that the hand could only ever be parallel to the floor throughout the simulation, effectively enabling the model to only fall onto the outstretched hand.

Although this parallel joint was added, the hands still bounced off the floor, but not to the extent as in the previous models. The author decided after evaluating this model, that it would be an improved simulation to use the one-arm models, as this would be more representative of a fall.

The short duration of the contact of hand to ground during a fall makes it extremely unlikely that both hands would hit the floor simultaneously. In fact, it was found from the motion analysis study that only 6% of the volunteers impacted with both hands simultaneously (<2 ms between impacts) and that there was little difference between the impact forces in both hands.

It was also noted that although there is a spring damper system representing the elbow resistance to the fall there would also be damping in the actual arm through the bones, connective tissue, soft tissue and muscles so the next model, Model 4, incorporates this.

Both the upper and lower arms in Model 4 (figure 3.28) are composed of two sections of cylinders that contain a translational joint and a spring damper. This enables the arm to effectively contract and expand like a bone or muscle being compressed and released. It was decided that this model would remain static and so the hand was locked to the floor.

Model 5 (figure 3.28) was a combination of different features of the other models and has, as such, an increasing level of biofidelity. It was also raised off the floor to simulate a fall and a measure function was created to record the impact force on the ground in terms of Newtons.

4.10.3 SIMULATED RESPONSE

Simulations were conducted on Model 5 using a mass of 15 kg from fall heights of 1 cm and 2 cm and with masses of 15 kg and 30 kg at 1 cm. Fall height and effective mass were found to influence the force peaks of F1 and F2 respectively from results found in the fall studies and it was decided that these factors would be a useful tool in validating the biomechanical model.

Observations from the fall studies showed that force peak F1 occurred between approximately 5 and 28 ms during falls onto the force plates and that the overall time of the complete impact (shown in the force time curves) did not exceed 200 ms. The simulations therefore were performed for 200 ms.

It can be seen from figures 3.69 and 3.70 that the graphs are similar to those found from the fall studies in that there is a high frequency peak (F1) followed by a lower frequency peak (F2). These two peaks occurred regardless of the changes in drop height or mass. It can be seen from figure 3.69 that impact forces were found to be 1933 N for force peak F1, and 395 N for force peak F2, from a height of 1 cm. The impact forces were found to be 3231 N for force peak F1 and 448 N for force peak F2, from a height of 2 cm.

These results correlate well with the findings of the fall studies in that an increase in fall height produces an increase in force peak F1. There was also an increase in force peak F2, but not to as great an extent as F1, a finding that was also observed during the fall studies. However, the biomechanical model appears to have overestimated the magnitude of force peak F1. This is due to the stiffness and damping values used to simulate those found in the bones and joints of the arm. Also the material properties used to represent the hand and ground were harder than those of the skin and palmer tissues. These harder surface properties would produce a greater impact force.

Results from figure 3.70 show that when the simulation was conducted, using different masses (from a drop height of 1 cm), the graph showed different peak

characteristics than were seen during a change in fall height. Force peak F2 increased from 395 N to 624 N, for 15 and 30 kg respectively, but force peak F1 did not increase at all giving 1933 N for both masses.

These results also correlate well with the findings from the fall studies in that the effective mass was found to influence force peak F2 but not F1.

Further tests from higher fall heights were unable to be completed due to time constraints, however it should be noted that this is the only known computer model for the investigation of falls onto the outstretched hand that includes elbow flexion.

DeGoede *et al* (2002) constructed a model in ADAMS[®] that took into account elbow flexion, but the model was locked to the ground and did not therefore, assess the effect of fall height. Other computer models of the arm by Chiu and Robinovitch (1996, 1998) and Davidson *et al* (2004, 2005) were developed using a fully extended arm.

4.11 DISCUSSION OF FALL STUDIES AND COMPUTER SIMULATIONS

The computer model was found to correlate well with the results found from the motion analysis and high-speed video (HSV) studies in that fall height had an influence on force peak F1 and effective mass had an influence on force peak F2 (in male volunteers).

However, the magnitude of the forces for force peak F1 were greatly over estimated. Force peak F1 showed much greater forces, 1933 N from the biomechanical model compared to 288.70 N for females and 131.59 N for males, from the falls in the HSV study, at a fall height of 1 cm. This was attributed to the values used to simulate the stiffness and damping properties of the arm.

The results indicate that the computer model developed in this study is a good initial model to simulate falls onto the outstretched hand.

4.12 PROBLEMS AND LIMITATIONS OF STUDY

Many of the problems and limitations of this study were mentioned in the relevant sections of this chapter. Other problems that have not been discussed previously are detailed below:

- During the fall experiments from the drop rig, the main problem encountered was ensuring that all the volunteers fell from the same fall height. Two blocks of wood (3 and 5 cm thick) were placed under the volunteers hands, whilst they were suspended in the rig, to enable the volunteers to be raised to the correct test fall height. The volunteers were informed not to move from their position once the blocks had been removed but, in the short time between removing the block of wood and dropping the volunteer, some volunteers did move slightly. This was only discovered when the results were analysed. The consequence of this problem is that occasionally the volunteer did not fall from the height specified. In all

cases where this occurred, the volunteer fell from a slightly lower height, up to approximately 1 cm below the test height, rather than from a greater fall height.

- The effective mass of the volunteer was recorded by positioning the volunteer with each hand on a force plate, whilst laying on the floor. The volunteer was asked to perform a press-up, with their knees remaining on the floor, and hold the position so that a recording could be made of the force transmitted to the force plates by each hand. The values at each force plate were then calculated and averaged to give the effective mass in each arm for each volunteer. This position was used as it best replicated the position in which the volunteer would arrest their fall onto the force plate. However, when the volunteers were raised up to the correct fall height, the knees often moved towards the hands to enable them to remain on the floor. The implication of this is that the volunteers may not have been in the same position during the fall arrest, as they were when their effective mass was calculated. In hindsight, it would have been better to calculate the effective mass of the volunteer using the magnitude of the force time curve after the immediate impact had subsided.

CHAPTER 5

CONCLUSIONS

5.1 INTRODUCTION

The shock absorbing properties of Impact Absorbing Playground Surfaces (IAPS) are currently tested using a British Standard head impact testing device, for their ability to prevent serious head injury.

Research has shown that the installation of IAPS in the play areas of Cardiff has indeed reduced the amount of serious head injuries, however, even though head injuries have been greatly reduced in severity, arm fractures have not reduced in severity or frequency.

Therefore, the current strategies for the assessment and prevention of head injury potential have been shown to be highly successful, yet totally ineffective for preventing upper limb fractures. A need therefore exists to develop a method for the assessment of playground surfaces for their ability to alleviate arm fractures and subsequently to assist in the development of 'arm friendly' surfaces.

The aims of this study were to investigate the forces that are produced in the arm, during a fall onto the outstretched hand, at a non-injurious level, and to further utilize the data to aid in the development of a mechanical arm fracture model that could be used, alongside the head form, to test IAPS for their ability to alleviate arm fractures.

The objectives of this study were:

- to obtain impact data for a fall from a non-injurious height using adult volunteers falling onto the outstretched hand

- to assess what factors are influential on the forces produced during the experimental falls. These factors include the fall height, the effective mass, gender and age of the volunteer, the impact surface, and the angle of the elbow prior to and during impact
- to investigate the mechanism of the arm prior to and during impact
- to assess the activation of the muscles in the arm in response to a fall
- to develop a computational arm model to enable falls from higher (injurious) heights to be investigated.

A study was conducted, using motion analysis equipment, to investigate the forces produced during a fall onto the outstretched hand. Volunteers were dropped through a height of 3 and 5 cm onto force plates and from 5 cm onto a domestic surface and a playground surface.

A further study was conducted to assess the mechanism of the arm prior to and during impact using high-speed video (HSV) equipment. Electromyography (EMG) equipment was also used to record the activation of certain muscles throughout the falls. These tests were completed with five volunteers at heights of 1 and 5 cm onto force plates, and further tests were conducted on one volunteer at heights of 10 and 20 cm, and two volunteers from standing height.

5.2. CONCLUSIONS

5.2.1 GENERAL CONCLUSIONS

This study showed that falls onto the outstretched hand produce an impact force characterised by an initial force peak, F1, followed by two further force peaks, F2 and F3. The magnitude of force peak F1 was found to be generally higher than the subsequent force peaks F2 and F3. Force peak F3 was not present in all force time curves and it was suggested from the results that when it did occur it was not significantly different to force peak F2.

A positive linear relationship was found between force peaks F1 and F2 (as F1 increases, F2 increases). The increase of force peak F2 was not as great as the increase of force peak F1, confirming the suggestion that the magnitude of force peak F1 is generally greater than force peak F2.

5.2.2 FACTORS AFFECTING THE IMPACT FORCES

Gender was found to significantly affect the impact forces, with male volunteers producing higher impact forces at force peaks F1 and F2 compared to the female volunteers. This increase in force for male volunteers was more prevalent for force peak F1 than F2.

Fall height was found to be an important indicator of force peak magnitude, particularly force peak F1. An increase in fall height produced an increase in impact force in both females and males. The lowest impact force for force peak F1 was

70.31 N for a fall from 1 cm and the highest was 1904.83 N for a fall from standing height. Although the magnitude of force peak F2 also increased with fall height, it was not as great as the increase of force peak F1. These results suggest that as the fall height increases, force peak F1 increases at a greater rate than force peak F2.

In male volunteers only, the effective mass was found to influence the impact force magnitude of force peak F2 at all fall heights but only influence force peak F1 at small fall heights (< 5 cm). The effective mass did not appear to affect the impact forces in females.

5.2.3 MECHANISM OF FALL ARREST AND IMPACT

It was found that falls did not generally occur onto a fully extended elbow. Instead, volunteers demonstrated an arm angle of between 10° and 60° flexion.

Volunteers falling from the drop rig were observed to have a similar fall arrest response regardless of the fall height. This involved the upward motion of the fingers, due to extension of the wrist, with concomitant elbow flexion. This movement was followed by a 'slapping' motion of the hand onto the force plates, due to a rapid downward hand motion immediately prior to impact. The impact occurred to the palm at smaller fall heights (1 and 5 cm), and onto the fingertips, followed by the palm, as the fall height increased (5, 10 and 20 cm). At 5 cms, some of the volunteers were observed to impact with their palm first, whilst other were observed to impact onto their fingertips, followed by the palm.

Falls from a standing height were also observed to involve similar fall arrest strategies. Initially, before the onset of the fall was commenced, the arms were in an anatomically relaxed position, by the side of the volunteer. As the fall was initiated the arms were flexed anteriorly at the shoulder joint, with a pronated forearm, into an outstretched position. The wrist and fingers were both extended, causing the arm and hand to be in an almost straight line with each other (the elbow remained slightly flexed). Immediately prior to impact the wrist hyperextended slightly, causing the fingers to move upwards, before a rapid downward movement of the wrist (flexion).

Impact onto the force plate occurred sequentially at the fingertips, followed by the knuckles at the palmer aspect of the hand (metacarpophalanx joint) and then the palm; in effect the hand 'rolled' onto the force plate. Immediately after the hand fully impacted the force plate, flexion of the elbow occurred, allowing the body to be lowered to the ground in a controlled manner.

In all falls from 20 cm and above, the volunteers were observed to turn their head to the side to protect the head and face from impacting with the force plate.

The sequential impacting of the fingertips, knuckles and palm produced a change in the rise of force peak F1. At the lower fall heights the hand impacted 'as one' and so there was a quick rise in the force peak (F1). At these higher heights however, the impact occurred in stages, which subsequently affected the way in which force peak F1 occurred. If the impact onto the different sections of the hand was relatively smooth, then this would produce a two-stage increase in force peak F1. If however, the impact was not smooth then the impact force produced would show a smaller

impact force peak for the knuckle impact, followed by force peak F1 where the full hand impacted.

On impact, a shock wave was observed to travel the entire length of the arm. General observations showed that the shock wave appeared in the lower arm, around the elbow joint and in the upper arm, but not necessarily as separate entities. The mechanism of the shock wave was found to be different in individuals due to a combination of factors that included the height fallen, the effective mass of the individual, the structural composition of the arm (muscular and soft tissue), skin movement, the orientation of the arm and fall arrest strategy.

Results from the EMG study suggest that the neurological initiation of arm, chest and shoulder muscles in response to the fall was due to motor vestibular reflexes and not an intentional cerebral decision as to when was best to arrest the fall.

5.2.4 COMPUTER MODELLING

A computer model was developed to enable falls from a higher height, such as those that occur during a playground fall, to be investigated. The model was simulated to fall from a height of 1 and 2 cm using a mass of 15 kg and from a height of 1 cm using masses of 15 and 30 kg.

Despite the overestimation of the magnitude of force peak F1, the computer model was found to correlate well with the results found from the experimental studies in that force peak F1 was influenced by fall height and force peak F2 was influenced by

effective mass (shown experimentally in male volunteers). The overestimation of force peak F1 was due to the stiffness and damping values used to simulate those found in the bones and joints of the arm and the material properties used to represent the hand and ground.

5.3 SUMMARY OF CONCLUSIONS

- Falls onto the outstretched hand produce an impact force characterised by an initial force peak, F1, followed by two further force peaks, F2 and F3. The magnitude of force peak F1 was found to be generally higher than the subsequent force peaks F2 and F3. Force peak F3 was not present in all force time curves and it was suggested from the results that when it did occur it was not significantly different to force peak F2.
- A positive linear relationship was found between force peaks F1 and F2 (as F1 increases, F2 increases). The increase of force peak F2 was not as great as the increase of force peak F1, confirming the suggestion that the magnitude of force peak F1 is generally greater than F2.
- Gender, fall height and effective mass were found to be important factors when assessing the impact forces found during a fall onto the outstretched hand.
- Falls did not generally occur onto a fully extended elbow.

- The fall arrest strategy prior to and during impact was found to be similar regardless of the fall height.
- At higher fall heights, 20 cm and above, the volunteers were observed to turn their head to the side to protect the head and face from impacting with the force plate.
- On impact, a shock wave was observed to travel the entire length of the arm. It is suggested that the shock wave is a result of a number of factors such as, the height fallen, the effective mass of the individual, the structural composition of the arm (muscular and soft tissue), skin movement, the orientation of the arm and the way in which the fall is arrested.
- The neurological initiation of arm, chest and shoulder muscles in response to the fall was due to motor vestibular reflexes and not an intentional cerebral decision as to when was best to arrest the fall.
- Despite the overestimation of the magnitude of force peak F1, the computer model was found to correlate well with the results found from the experimental studies in that force peak F1 was influenced by fall height and force peak F2 was influenced by effective mass (in male volunteers).

CHAPTER 6

FURTHER WORK

6.1 INTRODUCTION

Impact Absorbing Playground Surfaces (IAPS), have been shown to be highly effective at reducing serious head injury, due to falls from playground equipment, but totally ineffective at alleviating arm fractures (Mott *et al*, 1994, Mott *et al*, 1997, Norton *et al*, 2004). The methods for testing IAPS should therefore be reassessed, with a view to designing new surfaces that would alleviate arm fractures, whilst still reducing the number of serious head injuries.

The main shortcoming of this idea, at present, is the lack of quantitative impact data available for the forces produced in the arm during a fall, particularly in children. The literature review in chapter 1 highlighted areas of research that have begun to assess falls onto the outstretched hand in adults. This study was conducted to further investigate the forces produced during a fall onto the outstretched hand, taking into account the shortcomings and limitations of previous work. The results of which showed that falls onto the outstretched hand, in adults, produce an impact force with characteristic peaks. The magnitude of these peaks were shown to be significantly affected by fall height, gender and effective mass (in male volunteers). A similar fall arrest strategy was also observed regardless of individual volunteers or fall height. However, further work is required to increase the accuracy of the results and therefore, the validity of the conclusions discussed in the previous chapter. This chapter discusses some of the methods that could be utilised to further improve on the work in this study.

6.2 FALL EXPERIMENTS

- It has been mentioned previously that gender was an important factor in determining the magnitude of the impact forces produced during a fall onto the outstretched hand. This has not been reported in any previous literature and the methodology for this study perhaps reflects this as in the volunteer sample of 35, only 11 volunteers were female. However, the volunteers were selected randomly within an engineering department so it is no surprise that males were more heavily represented. It would therefore, be of interest to specifically design a study to further assess gender differences. If possible female and male volunteers should be matched in height, weight and age to eliminate any other factors that may affect the results. The volunteers could then be dropped using the same methodology detailed in this study. The results of the study may give further insight into any differences that are present between the impact forces produced in females compared to males, during a fall onto the outstretched hand.
- The age of volunteers in this study ranged from 22 to 51 years, thus employing a wider range of ages than previous reported fall studies. The results of the study showed that age was not a significant factor in females but suggested significance in males at higher fall heights. Previous studies by DeGoede *et al*, 2001 and DeGoede *et al*, 2002 investigated age effects by studying young (25 ± 3 years) and older (70 ± 3 years) adults. They also found that age was not a significant factor but it was noted that the older adults were all healthy and may not represent the typical older adult and the methodology of the study was not an accurate representation of a fall. Due to moral and ethical reasons, no research has been conducted to experimentally investigate falls in children. However, a study could

be conducted to assess if the fall arrest strategy in children differs greatly to that of an adult by dropping children onto heavily padded surfaces. An initial study could use children who are used to falling, such as gymnasts or those who study martial arts, as this would reduce the risk of injury. If the fall arrest strategy is found to be similar, a further study could then be conducted to drop other children onto surfaces and eventually onto padded force plates to assess the range of forces produced. To gain impact force data from children falling onto the outstretched hand would be invaluable to designing an arm fracture testing device and the development of new playground surfaces.

- Two different impact surfaces were tested in this study, as well as falls directly onto the force plate, to assess if they made any difference to the impact forces produced. The results did not provide enough detail from which to draw any valid conclusions. A further study should be conducted to drop volunteers onto a wider variety of playground and domestic surfaces to assess if a difference can be observed. A good starting point would be to use the selection of surface mixtures in Cory (1998) that were used to assess the effect impact surfaces had on head impacts. Epidemiology has already been shown that the IAPS currently available do not prevent arm fractures from occurring but it is not known if the impact surfaces make any differences at all to the impact forces produced during a fall onto the outstretched hand. Results from the study could then be used to assist in the development of new surfaces.

6.3 MODELLING

- A computer model was developed using ADAMS[®] software that, when simulated to fall from heights of 1 and 2 cm, correlated well with the impact peak characteristics found from the experimental studies. However, due to the estimations made for the stiffness and damping properties of the joints and bones, and the material properties used to represent the arm, the model was found to greatly overestimate the impact force. Development of this model should be given further consideration to enable a computer model that better replicates the response of the arm, due to falls from low heights. Simulations should be performed on the developed model at all the heights used in the experimental study (1, 3, 5, 10 and 20 cm) to validate it and then further simulations can be performed to predict impact forces from higher fall heights. Variations should also be made in the value used to represent the effective mass. Values from the experimental drop tests could again be utilised as an initial starting point of the range of effective masses in adults.
- MADYMO (MAtheMatical DYnamic MOdelling) is a computer program, developed by TNO automotive, to simulate the crash test dummies and standard crash tests that all vehicles are required to go through in the automotive industry. The MADYMO software is continually updated and developed, as more research data becomes available. Until 1998 the range of models available to MADYMO users were limited to the Anthropometric Test Devices (ATDs), better known as crash test dummies, required for the testing stipulations in crash test standards. The dummies are measuring devices, which are robust and can be crashed repeatedly without damage, unlike a real human. In response TNO have recently

utilised the data direct from human, animal and cadaver studies to define the response of the human body under mechanical loading to design a suite of highly biofidelic computer generated models. The dummies that are now available range from a 12-month-old child to a 95th percentile male, with varying levels of biofidelity. Simulations could therefore, be performed on these dummies, initially starting with the adult dummies, to further investigate falls onto the outstretched hand. Using computer simulations would enable the collection of impact data for falls from a higher height. The material properties of the simulated impact surface could also be changed to replicate current surfaces and to aid in the development of new surfaces.

- The aim of this study was to develop an arm fracture model to use alongside the British Standards head impact testing device, to test Impact Absorbing Playground Surfaces for their ability to alleviate arm fractures and subsequently to assist in the development of 'arm friendly' surfaces. Researchers at the Cardiff University, School of Medicine, have undertaken one of the largest playground injury studies in the world. Data from the experimental falls conducted in this study, and future data from the computer simulations performed in ADAMS and MADYMO, along with data from the playground injury study can be used to validate a mechanical arm fracture model for falls from playground equipment. It is hoped that an arm fracture criterion will be developed with threshold data for the impact forces likely to produce arm fracture during falls. This validated model could be applied not only to investigate playground injuries but also for application to domestic falls and non-accidental injury investigation for a range of ages.

REFERENCES

Altman, A., Ashby, K., Stathakis, V. 1996. Childhood injuries from playground equipment. Victorian Injury Surveillance System. Hazard, Edition 29.

Ashby, A., Corbo, M. 2000. Child fall injuries: an overview. Victorian Injury Surveillance System. Hazard, Edition 44.

ASTM (American Standards for Testing Materials), Standard Test Method for Shock Absorbing Properties of Playground Surface Systems and Materials, ANSI/ASTM, 1978, F 355-78 in Cory, C.Z. 1998. Assessing the severity of child head impacts onto various domestic surface mixtures. Master of Philosophy Thesis. University of Wales, Cardiff, UK.

Boon, R. 2003. Sensory-Motor Integration and Learning. [WWW]: <URL <http://home.iprimus.com.au/rboon/SensoryIntegration.htm>> [Accessed September 2005]

Bond, M.T., Peck, M.G. 1993. The risk of childhood injury on Boston's playground equipment and surfaces. American journal of public health, Vol 83 (5), 731-733.

British Standard Institution (BSI), BS 7188: Methods of Test for Impact Absorbing Playground Surfaces, 1989.

Carola, R., Harley, J.P., Noback, R. 1990. Human anatomy and physiology. International edition. McGraw-Hill. ISBN 0-07-100686-9.

Chalmers, D.J., Marshall, S.W., Langley, J.D., Evans, M.J., Brunton, C.R., Kelly, A.-M., Pickering, A.F. 1996. Height and surfacing as risk factors for injury in falls from playground equipment: a case control study. *Injury Prevention* 2, 98-104.5

Chiu, J., Robinovitch, S.N. 1996. Transient Impact response of the body during a fall on the outstretched hand. *ASME BED* 33, 269-270.

Chiu, J., Robinovitch, S.N. 1998. Prediction of upper extremity impact forces during falls on the outstretched hand. *Journal of Biomechanics* 31, 1169-1176.

Chou, P.-H., Chou, Y.-L., Lin, C.-J., Su, F.-C., Lou, S.-Z., Lin, C.-F., Huang, G.-F. 2001. Effect of elbow flexion on upper extremity impact forces during a fall. *Clinical Biomechanics* 16, 888-894.

Clapperton, A., Cassell, E., Wallace, A.M. 2003. Injury to children aged 5-15 years at school. *Victorian Injury Surveillance System. Hazard, Edition 53.*

Cory, C.Z. 1998. Assessing the severity of child head impacts onto various domestic surface mixtures. *Master of Philosophy Thesis. University of Wales, Cardiff, UK.*

Davidson, P.L., Chalmers, D.J., Wilson, B.D. 2004. Stochastic-rheological simulation of free-fall arm impact in children: Application to playground injuries. *Computer Methods in Biomechanics and Biomedical Engineering* 7, 63-71.

Davidson, P.L., Chalmers, D.J., Stephenson, S.C. 2005. Prediction of distal radius fracture in children, using a biomechanical impact model and case-control data on playground free falls. *Journal of Biomechanics*, article in press, corrected proof, available online 23 February 2005.

DeGoede, K.M., Ashton-Miller, J.A., Liao, J.M., Alexander, N.B. 2001. How quickly can healthy adults move their hands to intercept an approaching object? Age and gender effects. *Journal of Gerontology* 56A, No. 9, M584-M588.

DeGoede, K.M., Ashton-Miller, J.A., Schultz, A.B., Alexander, N.B. 2002. Biomechanical Factors affecting the peak hand reaction force during the bimanual arrest of a moving mass. *Journal of Biomechanical Engineering* 124, 107-112.

DeGoede, K.M., Ashton-Miller, J.A. 2002. Fall arrest strategy affects peak hand impact force in a forward fall. *Journal of Biomechanics* 35, 843-848.

DeGoede, K.M., Ashton-Miller, J.A. 2002. Biomechanical simulations of forward fall arrests: effects of upper extremity arrest strategy, gender and aging-related declines in muscle strength. *Journal of Biomechanics* 36, 413-420.

DeGoede, K.M., Ashton-Miller, J.A., Shultz, A.B. 2003. Fall related upper body injuries in the older adult: a review of the biomechanical issues. *Journal of Biomechanics* 36, 1043-1053.

Dietz, V., Noth, J. 1978. Pre-innervation and stretch responses of triceps brachii in man falling with and without visual control. *Brain Research* 142, 576-579.

Dietz, V., Noth, J., Schmidtbleicher, D. 1981. Interaction between pre-activity and stretch reflex in human triceps brachii during landing from forward falls. *Journal of Physiology* 311, 113-115.

Frykman, C. 1967. Fracture of the distal radius including sequelae - shoulder-hand-finger syndrome, disturbance in the distal radio-ulnar joint and impairment of nerve function. *Acta Orthopaedica Scandinavica* S108, 1-153.

Goss, S. 1992. School Injuries. Victorian Injury Surveillance System. Hazard, Edition 10.

Goulding *et al*, 1998 in Davidson, P.L., Chalmers, D.J., Stephenson, S.C. 2005. Prediction of distal radius fracture in children, using a biomechanical impact model and case-control data on playground free falls. *Journal of Biomechanics*, article in press, corrected proof, available online 23 February 2005.

Guyton, A.C. 1991. Textbook of medical physiology. Eighth edition. W.B. Saunders Company. ISBN 0-7216-3087-1.

Hamill, J., Knutzen, K.M. 2003. Biomechanical basis of human movement. Second edition. Lippincott Williams and Wilkins. ISBN 0-7817-3405-3.

HASS/LASS data. (Home Accident Surveillance System and the Leisure Accident Surveillance System). Home and Lesuire accident statistics. Collected by the DTI, provided by RoSPA. [WWW]

<URL <http://www.hassandlass.org.uk/query/index.htm>> [Accessed September 2005]

Hayes, W.C., 1991, *in* Davidson, P.L., Chalmers, D.J., Stephenson, S.C. 2005. Prediction of distal radius fracture in children, using a biomechanical impact model and case-control data on playground free falls. *Journal of Biomechanics*, article in press, corrected proof, available online 23 February 2005.

Horsman, A., Currey, J.D. 1983. Estimation of mechanical properties of the distal radius from bone mineral content and cortical width. *Clinical Orthopaedics* 176, 298-304.

Hsiao, E.T., Robinovitch, S.N. 1998. Common protective movements govern unexpected falls from standing height. *Journal of Biomechanics* 31, 1-9.

Illingworth, C., Brennan, P., Jay, A., Al-Rawi, F., Collick, M. 1975. 200 injuries caused by playground equipment. *British Medical Journal* 4, 332-334.

Kim, K.-J., Schultz, A.B., Ashton-Miller, J.A., Alexander, N.B. 1997. Impact characteristics of an outstretched arm when arresting a forward fall. *ASME BED* 35, 331-332.

Kim, K.-J., Ashton-Miller, J.A. 2003. Biomechanics of fall arrest using the upper extremity: age differences. *Clinical Biomechanics* 18, 311-318.

King, K.L., Ball, D.J. 1991. Playground Injuries: A Scientific Appraisal of Popular Concerns. *Journal of the Royal Society of Health*, 134-137.

Kreighbaum, E., Barthels, K.M. 1996. *Biomechanics, A qualitative approach to studying human movement*, fourth edition. Allyn and Bacon. ISBN 0-205-18651-3.

Kroonenburg, A.J., van den, Hayes, W.C., McMahon, T.A. 1996. Hip impact velocities and body configurations for voluntary falls from standing height. *Journal of Biomechanics* 29, 807-811.

Levine, R. Chapter in Nahum, A.M., Melvin, J.W. (eds). 1993. *Accidental Injury: Biomechanics and Prevention*, pp 460-491. Springer-Verlag. ISBN 0-387-97881.

Lo, J., McCabe, G.N., DeGoede, K.M., Okuizumi, H., Ashton-Miller, J.A. 2003. On reducing hand impact force in forward falls: results of a brief intervention in young males. *Clinical Biomechanics* 18, 730-736.

Macarthur, C., Hu, X., Wesson, D.E., Parkin, P.C. 2000. Risk factors associated with falls from playground equipment. *Accident Analysis and Prevention* 32, 377-382.

Maki, B.E., Fernie, G.R. 1990. Impact attenuation of floor coverings in simulated falling accidents. *Applied Ergonomics* 21.2, 107-114.

Melvin, J.W., Evans, F.G. 1985 in Maki, B.E., Fernie, G.R. 1990. Impact attenuation of floor coverings in simulated falling accidents. *Applied Ergonomics* 21.2, 107-114..

Moore, K.L. and Agur, A.M.R. 1995. *Essential Clinical Anatomy*. Lippincott Williams and Wilkins. ISBN 0-683-06128-3.

Mott, A., Evans, R., Rolfe, K., Potter, D., Kemp, K.W., Sibert, J.R. 1994. Patterns of injuries to children on public playgrounds. *Archives of Disease in Childhood* 71, 328-330.

Mott, A., Rolfe, K., James, R., Evans, R., Kemp, A., Dunstan, F., Kemp, K., Sibert, J. 1997. Safety of surfaces and equipment for children in playgrounds. *Lancet* 349, 1874-1876.

Mowat, D.L., Wang, F., Pickett, W., Brison, R.J. 1998. A case-control study of risk factors for playground injuries among children in Kingston and area. *Injury Prevention* 4, 39-43.

Myers, E.R., Sebeny, E.A., Hecker, A.T., Corcoran, T.A., Hipp, J.A., Greenspan, S.L., Hayes, W.C. 1991. Correlations between photon absorption properties and failure load of the distal radius *in vitro*. *Calcified Tissue International* 49, 292-297.

Myers, E.R., Hecker, A.T., Rooks, D.S., Hipp, J.A., Hayes, W.C. 1993. Geometric variables from DXA of the radius predict forearm fracture load *in vitro*. *Calcified Tissue International* 52, 199-204.

Norton, C., Rolfe, K., Morris, S., Evans, R., James, R., Jones, M.D., Cory, C., Dunstan, F., Sibert, J.R. 2004. Head injury and limb fracture in modern playgrounds. *Archives of Disease in Childhood*, 89 (2), 152-153.

Ozanne-Smith, J. 2001. Prevention of hospital-treated child fall injuries. *Victorian Injury Surveillance System. Hazard, Edition 48*.

Panjabi, M.M., White, A.A. 2001. *Biomechanics in the musculoskeletal system*. Churchill Livingstone. ISBN 0-443-06585-3.

Paton, D.F. 1992. *Fractures and orthopaedics*. Second edition. Churchill Livingstone. ISBN 0-443-04707-3.

Robinovitch, S.N., Chiu, J. 1998. Surface stiffness affects impact force during a fall on the outstretched hand. *Journal of Orthopaedic Research* 16, 309-313.

Routley, V. 1993. Injuries in child care settings. *Victorian Injury Surveillance System. Hazard, Edition 16*.

Sabick, M.B., Hay, J.G., Goel, V.K., Banks, S.A. 1999. Active responses decrease impact forces at the hip and shoulder in falls to the side. *Journal of Biomechanics* 32, 993-998.

Sherker, S., Ozanne-Smith, J., Rachnitzer, G., Grzebieta, R. 2003. Development of a multidisciplinary method to determine risk factors for arm fracture in falls from playground equipment. *Injury Prevention* 9, 279-283.

Sherker, S., Ozanne-Smith, J., Rachnitzer, G., Grzebieta, R. 2005. Out on a limb: risk factors for arm fracture in playground equipment falls. *Injury Prevention* 11, 120-124.

Smeesters, C., Hayes, W.C., McMahon, T.A. 2001. The threshold trip duration for which recovery is no longer possible is associated with strength and reaction time. *Journal of Biomechanics* 34, 589-595.

Spadaro J.A., Werner, F.W., Brenner, R.A., Fortino, M.D., Fay, L.A., Edwards, W.T. 1994. Cortical and trabecular bone contribute strength to the osteopenic distal radius. *Journal of Orthopaedic Research* 12, 211-218.

Stathakis, V., 1999 in Ozanne-Smith, J. 2001. Prevention of hospital-treated child fall injuries. *Victorian Injury Surveillance System. Hazard, Edition 48.*

APPENDIX A

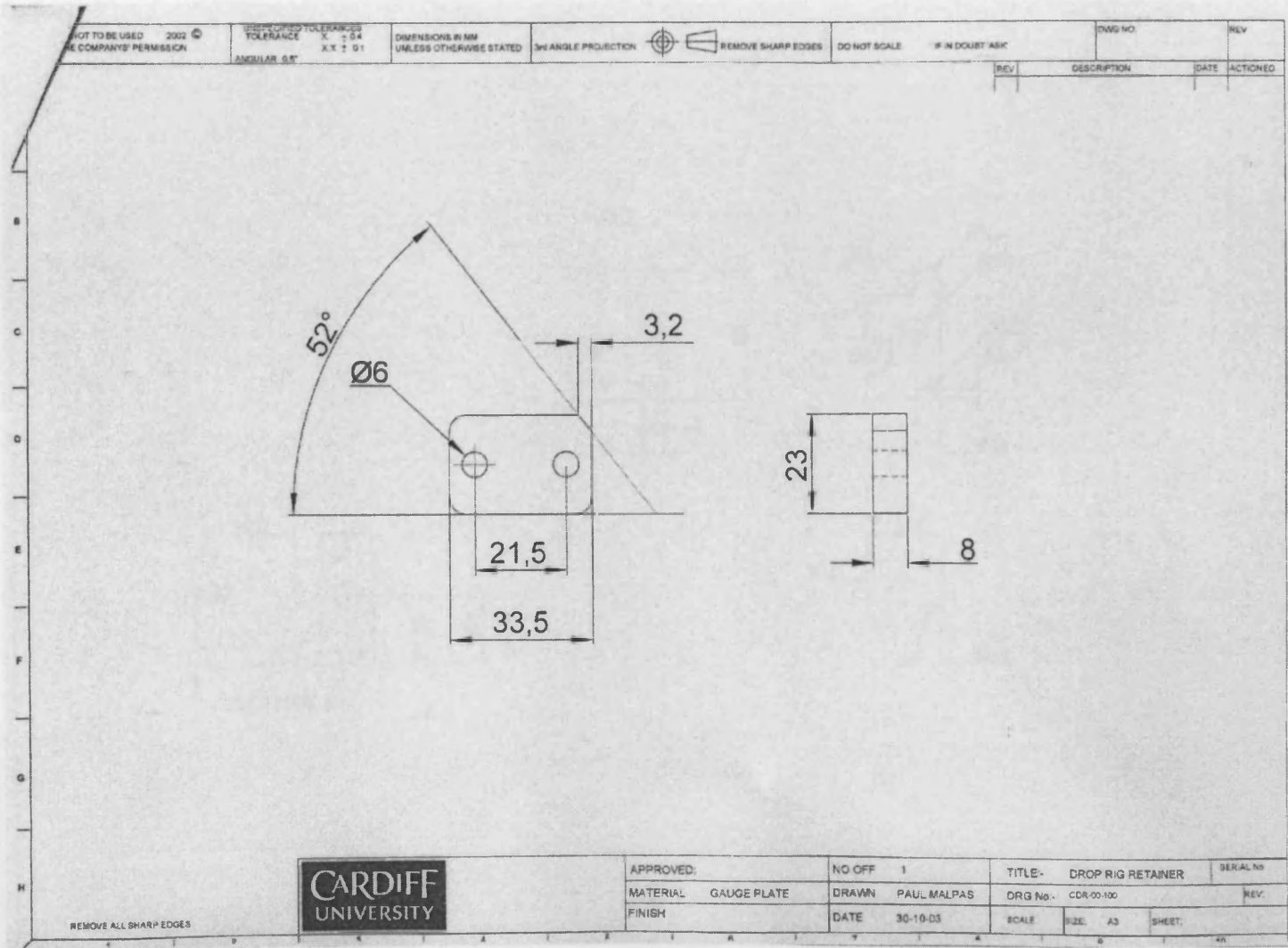


Figure A1: Technical drawing for the drop rig retainer

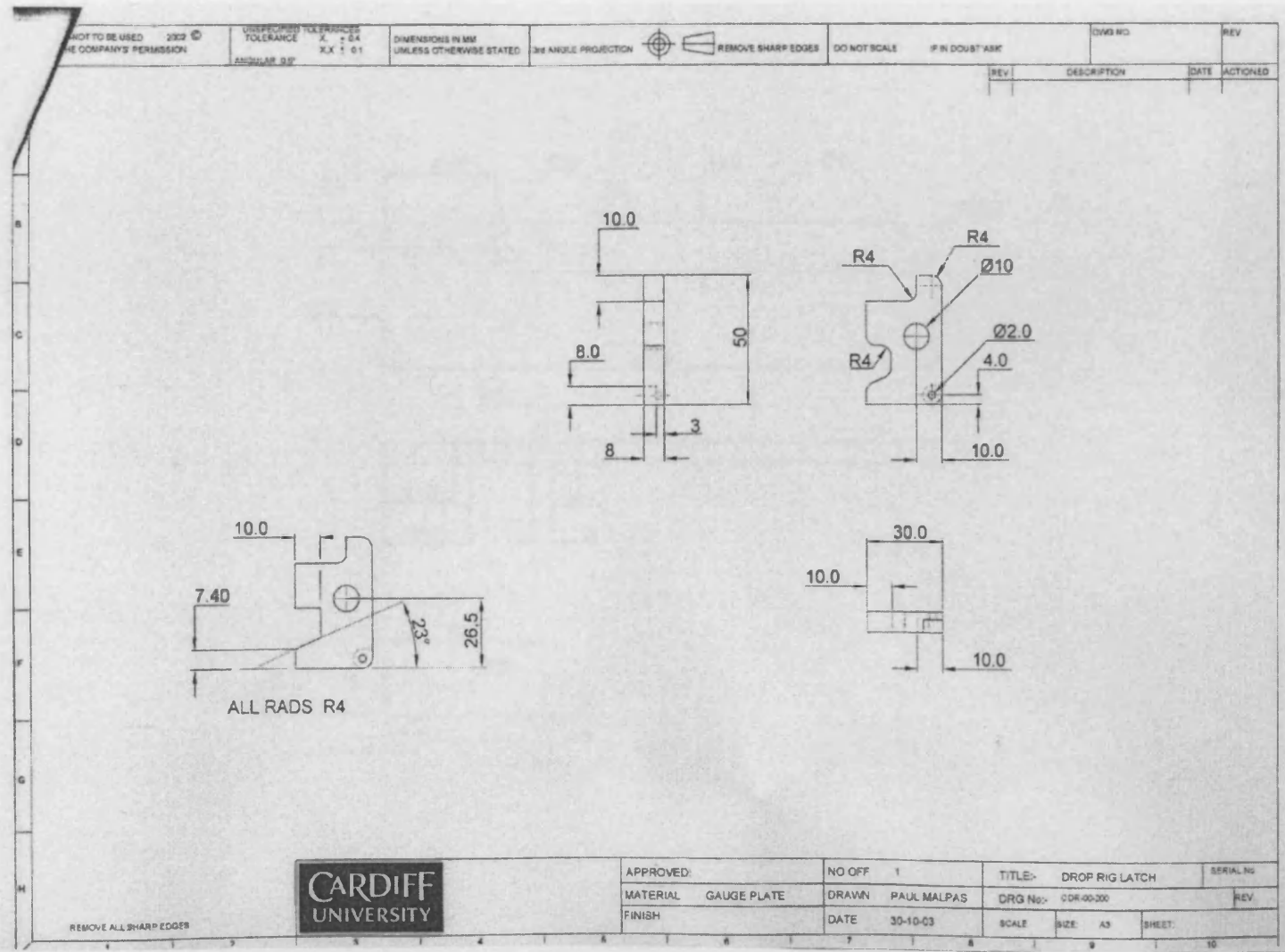


Figure A2: Technical drawing for the drop rig latch

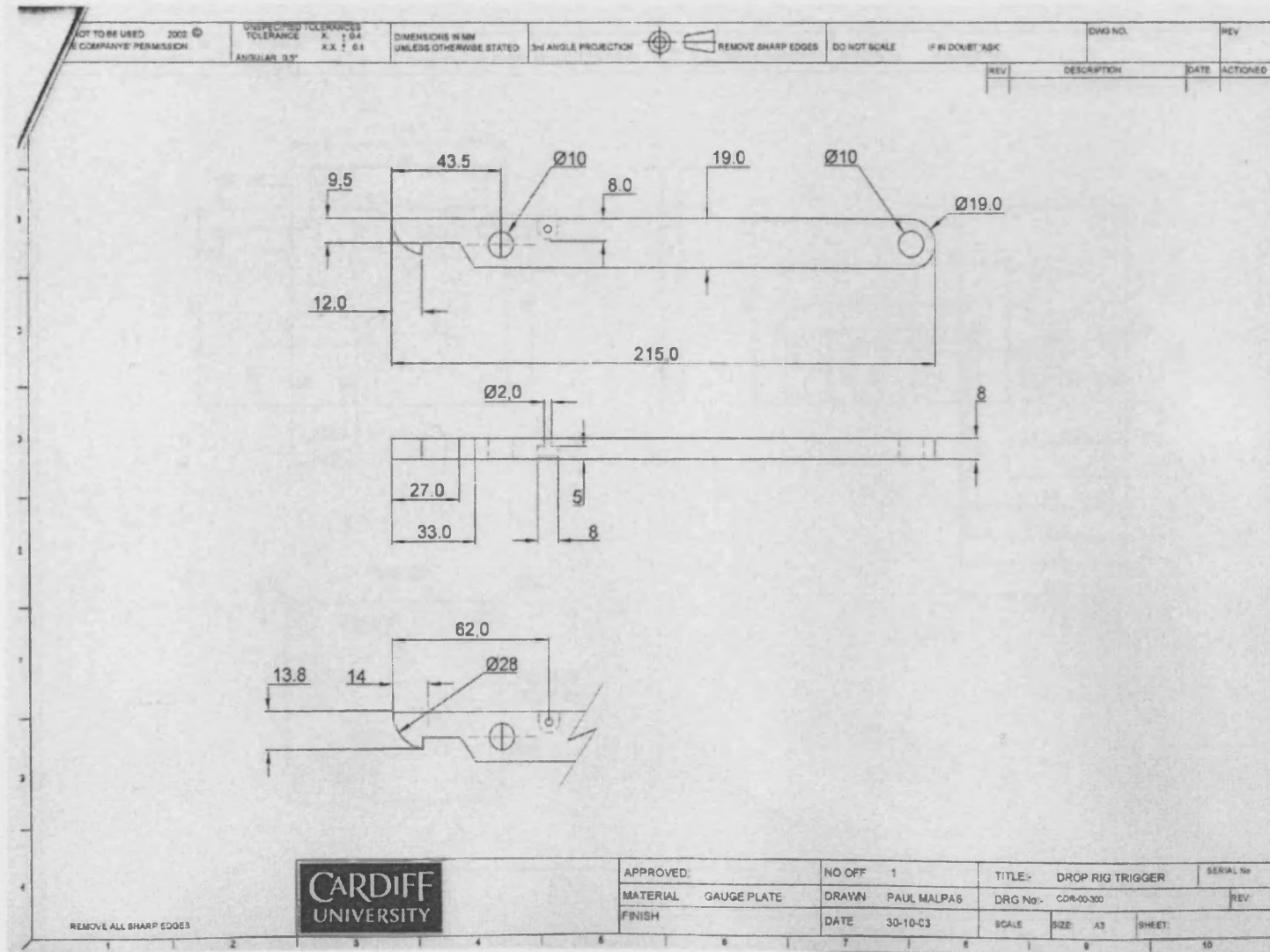


Figure A3: Technical drawing for the drop rig trigger

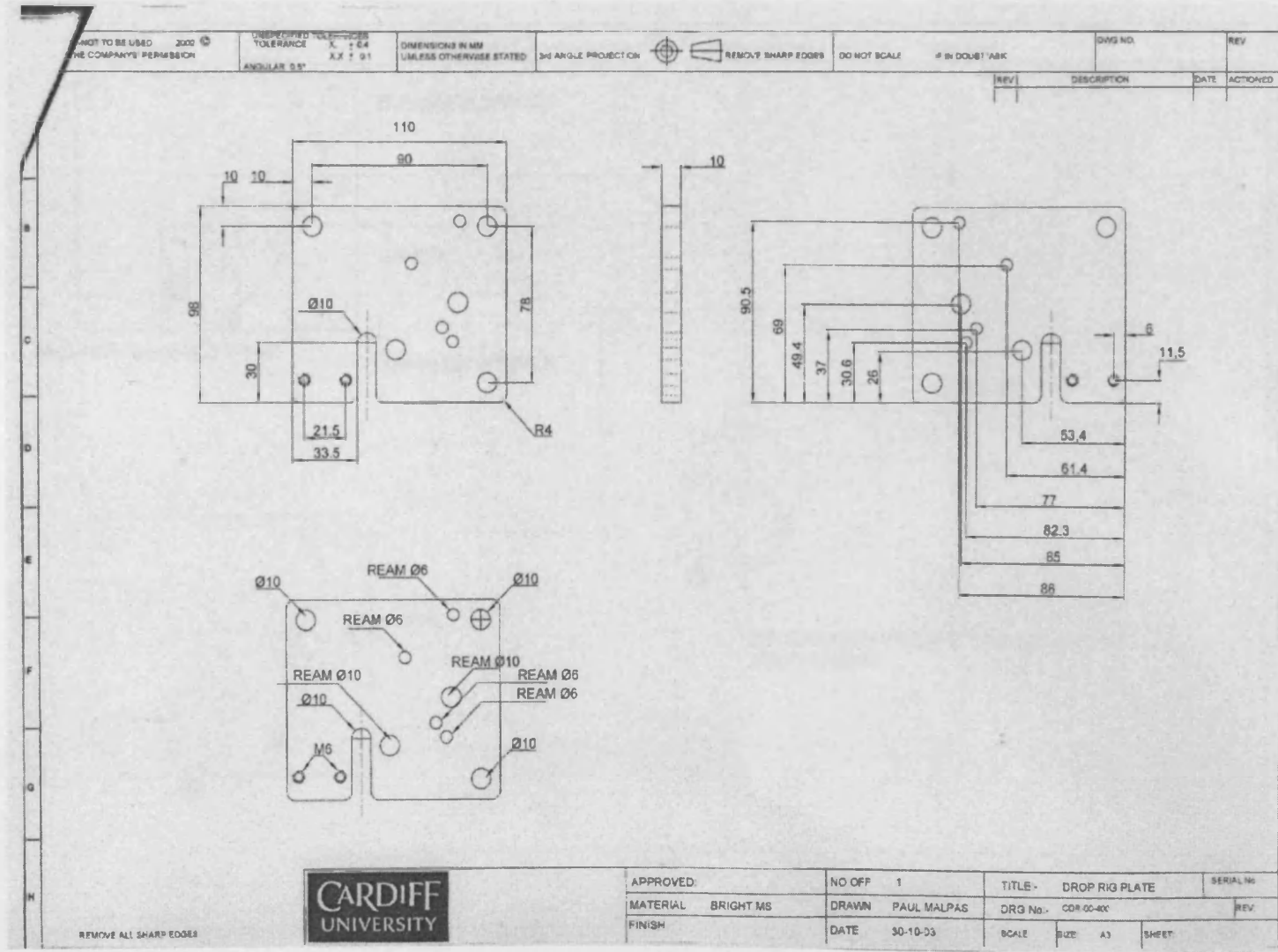


Figure A4: Technical drawing for the drop rig plate

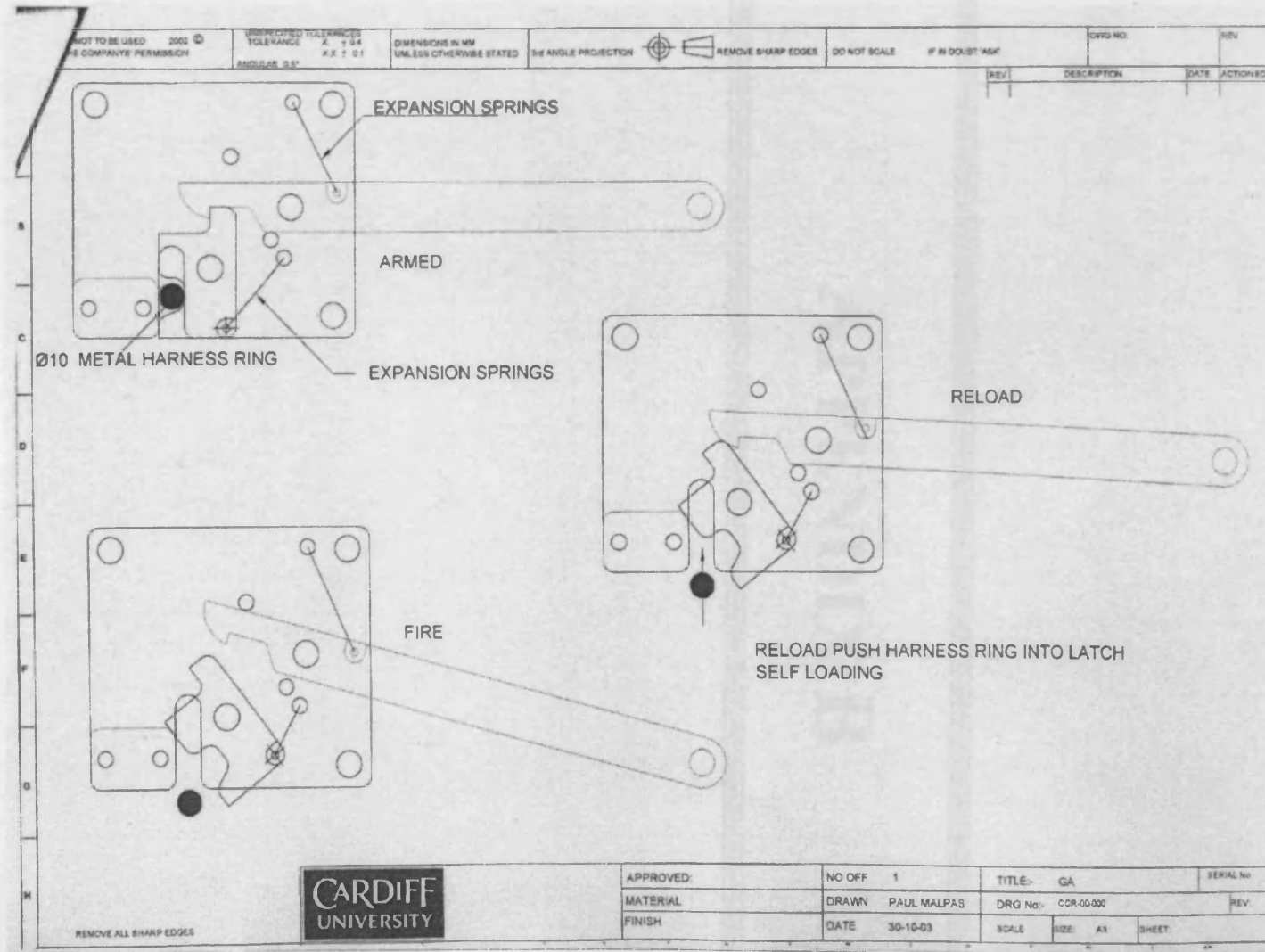


Figure A5: Assembly drawing for drop rig mechanism

APPENDIX B

Table B1: Table showing the arm angles for the left arm from a fall height of 3 cm.

Test details			Raw data				Average data			Arm angle (from vertical axis)		
Name	Number	Mass (kg)	Extended	Initial	Release	Prior to impact	Initial	Release	Prior to impact	Initial	Release	Prior to impact
AB3	1	55	157	120	120	133	125.33	125.33	131.00	31.67	31.67	26.00
	2	55		125	125	128						
	3	55		131	131	132						
SC3	1	56	154	105	102	100	107.00	102.67	101.00	47.00	51.33	53.00
	2	56		109	105	101						
	3	56		107	101	102						
LJ3	1	57	149	142	142	143	141.67	141.67	142.67	7.33	7.33	6.33
	2	57		141	141	141						
	3	57		142	142	144						
JH3	1	59	152	96	93	100	96.67	93.67	101.33	55.33	58.33	50.67
	2	59		100	96	103						
	3	59		94	92	101						
JC3	1	63	156	139	136	139	140.33	137.33	140.67	15.67	18.67	15.33
	2	63		142	139	145						
	3	63		140	137	138						
DO3	1	63	159	109	107	116	97.00	96.00	102.67	62.00	63.00	56.33
	2	63		94	93	98						
	3	63		88	88	94						
TS3	1	64	155	131	128	134	129.33	126.33	135.33	25.67	28.67	19.67
	2	64		122	120	133						
	3	64		135	131	139						
DG3	1	65	157	75	71	79	76.00	72.00	79.00	81.00	85.00	78.00

	2	65		80	75	82						
	3	65		73	70	76						
DE3	1	66	157	134	131	135	132.00	130.33	131.33	25.00	26.67	25.67
	2	66		129	130	128						
	3	66		133	130	131						
KH3	1	66	156	127	125	122	126.33	122.67	121.33	29.67	33.33	34.67
	2	66		128	121	122						
	3	66		124	122	120						
WS3	1	66	153	117	115	112	113.67	110.67	107.67	39.33	42.33	45.33
	2	66		111	108	104						
	3	66		113	109	107						
PK3	1	68	162	128	126	136	126.00	122.67	128.33	36.00	39.33	33.67
	2	68		124	119	121						
	3	68		126	123	128						
LN3	1	68	156	118	113	118	120.33	116.00	121.33	35.67	40.00	34.67
	2	68		123	119	125						
	3	68		120	116	121						
CF3	1	73	151	111	107	112	111.00	108.00	113.00	40.00	43.00	38.00
	2	73		111	109	114						
SJ3	1	73	154	138	136	133	138.67	136.67	135.00	15.33	17.33	19.00
	2	73		136	134	133						
	3	73		142	140	139						
RM3	1	74	152	86	84	86	98.67	97.00	99.00	53.33	55.00	53.00
	2	74		101	100	106						
	3	74		109	107	105						
IS3	1	74	159	87	83	88	91.67	87.33	91.67	67.33	71.67	67.33
	2	74		93	89	93						
	3	74		95	90	94						

SE3	2	74	162	133	133	132	134.00	133.50	132.00	28.00	28.50	30.00
	3	74		135	134	132						
IP3	1	76	161	93	86	89	85.33	80.00	83.33	75.67	81.00	77.67
	2	76		88	83	85						
	3	76		75	71	76						
MB3	1	76	150	96	93	96	99.33	95.67	97.33	50.67	54.33	52.67
	2	76		100	96	97						
	3	76		102	98	99						
LT3	1	77	160	140	138	139	142.33	141.00	140.67	17.67	19.00	19.33
	2	77		142	141	140						
	3	77		145	144	143						
RIP3	1	79	154	130	128	126	135.00	131.33	131.00	19.00	22.67	23.00
	2	79		128	123	124						
	3	79		147	143	143						
TW3	1	79	158	118	116	114	119.00	115.67	115.00	39.00	42.33	43.00
	2	79		126	124	121						
	3	79		113	107	110						
RE3	1	80	157	123	119	120	116.33	112.00	116.00	40.67	45.00	41.00
	2	80		108	104	111						
	3	80		118	113	117						
GS3	1	80	140	101	97	108	101.00	97.00	106.67	39.00	43.00	33.33
	2	80		100	96	109						
	3	80		102	98	103						
KO3	2	81	170	-	-	-	-	-	-	-	-	-
	3	81		-	-	-						
	4	81		-	-	-						
MS3	1	84	152	117	114	121	114.67	111.33	120.67	37.33	40.67	31.33
	2	84		117	114	125						

	3	84		110	106	116						
DS3	1	84	165	91	87	88	97.67	91.67	92.33	67.33	73.33	72.67
	2	84		102	95	96						
	3	84		100	93	93						
TOM3	1	85	164	118	114	117	124.00	120.33	121.00	40.00	43.67	43.00
	2	85		129	127	125						
	3	85		125	120	121						
ME3	1	86	152	133	131	135	135.00	132.67	136.00	17.00	19.33	16.00
	2	86		135	132	136						
	3	86		137	135	137						
TG3	1	95	157	136	133	136	140.00	137.00	141.33	17.00	20.00	15.67
	2	95		140	137	140						
	3	95		144	141	148						
MR3	1	102	158	143	141	142	136.33	135.00	133.67	21.67	23.00	24.33
	2	102		138	136	137						
	3	102		128	128	122						
MJ3	1	104	147	118	112	114	119.33	109.67	111.00	27.67	37.33	36.00
	2	104		123	106	107						
	3	104		117	111	112						
RP3	1	104	150	148	145	155	146.33	143.33	151.33	3.67	6.67	-1.33
	2	104		147	144	149						
	3	104		144	141	150						
TO3	1	106	159	117	114	112	103.00	100.00	99.33	56.00	59.00	59.67
	2	106		96	92	95						
	3	106		96	94	91						

Table B2: Table showing the arm angles for the right arm from a fall height of 3 cm.

Test details			Raw data				Average data			Arm angle (from vertical axis)		
Name	Number	Mass (kg)	Extended	Initial	Release	Prior to impact	Initial	Release	Prior to impact	Initial	Release	Prior to impact
AB3	1	55	154.6	112	112	121	120.00	118.67	123.00	34.60	35.93	31.60
	2	55		123	121	124						
	3	55		125	123	124						
SC3	1	56	152	100	97	102	98.33	95.00	101.33	53.67	57.00	50.67
	2	56		93	90	98						
	3	56		102	98	104						
LJ3	1	57	147	133	133	135	135.67	135.67	136.67	11.33	11.33	10.33
	2	57		135	136	136						
	3	57		139	138	139						
JH3	1	59	143	94	92	97	93.00	90.67	95.00	50.00	52.33	48.00
	2	59		94	91	96						
	3	59		91	89	92						
JC3	1	63	153	138	137	135	138.33	136.67	135.00	14.67	16.33	18.00
	2	63		142	143	139						
	3	63		135	130	131						
DO3	1	63	-	106	103	109	101.00	98.33	102.33	-	-	-
	2	63		97	95	98						
	3	63		100	97	100						
TS3	1	64	151	128	123	128	129.00	124.33	129.33	22.00	26.67	21.67
	2	64		131	127	132						
	3	64		128	123	128						

DG3	1	65	156	91	87	92	87.67	83.33	87.00	68.33	72.67	69.00
	2	65		91	85	87						
	3	65		81	78	82						
DE3	1	66	160	127	126	125	134.67	132.33	131.33	25.33	27.67	28.67
	2	66		138	137	134						
	3	66		139	134	135						
KH3	1	66	153	134	132	130	130.00	127.33	126.67	23.00	25.67	26.33
	2	66		127	121	123						
	3	66		129	129	127						
WS3	1	66	149	116	111	112	113.00	108.33	106.33	36.00	40.67	42.67
	2	66		110	105	100						
	3	66		113	109	107						
PK3	1	68	160	130	129	129	127.67	126.00	126.00	32.33	34.00	34.00
	2	68		124	122	121						
	3	68		129	127	128						
LN3	1	68	152	126	122	125	128.00	123.67	128.00	24.00	28.33	24.00
	2	68		130	126	131						
	3	68		128	123	128						
CF3	1	73	147	113	107	108	114.50	109.50	111.50	32.50	37.50	35.50
	2	73		116	112	115						
SJ3	1	73	161	150	151	151	145.00	144.67	144.00	16.00	16.33	17.00
	2	73		141	140	139						
	3	73		144	143	142						
RM3	1	74	151	78	76	80	90.67	88.67	93.33	60.33	62.33	57.67
	2	74		94	93	101						
	3	74		100	97	99						
IS3	1	74	152	89	83	87	94.00	87.67	93.33	58.00	64.33	58.67
	2	74		93	87	94						

	3	74		100	93	99						
SE3	2	74	158	132	132	132	131.00	130.50	130.00	27.00	27.50	28.00
	3	74		130	129	128						
IP3	1	76	168	105	99	101	98.00	93.33	97.00	70.00	74.67	71.00
	2	76		101	97	100						
	3	76		88	84	90						
MB3	1	76	149	100	94	96	102.33	93.67	94.67	46.67	55.33	54.33
	2	76		103	89	90						
	3	76		104	98	98						
LT3	1	77	152	131	126	127	131.00	126.67	127.00	21.00	25.33	25.00
	2	77		129	124	125						
	3	77		133	130	129						
RIP3	1	79	157	145	143	142	141.67	139.00	137.33	15.33	18.00	19.67
	2	79		144	142	140						
	3	79		136	132	130						
TW3	1	79	155	121	119	116	119.67	115.33	114.67	35.33	39.67	40.33
	2	79		125	119	123						
	3	79		113	108	105						
RE3	1	80	155	122	119	121	118.67	114.67	120.33	36.33	40.33	34.67
	2	80		112	108	117						
	3	80		122	117	123						
GS3	1	80	144	113	109	121	112.33	108.00	119.67	31.67	36.00	24.33
	2	80		112	108	121						
	3	80		112	107	117						
KO3	2	81	158	68	68	67	85.50	84.00	85.50	72.50	74.00	72.50
	3	81		103	100	104						
	4	81		64	64	65						
MS3	1	84	156	143	140	146	139.00	135.33	142.67	17.00	20.67	13.33

	2	84		138	135	146						
	3	84		136	131	136						
DS3	1	84	158	87	83	86	94.33	88.67	91.67	63.67	69.33	66.33
	2	84		102	95	98						
	3	84		94	88	91						
TOM3	1	85	163	121	116	119	125.67	121.67	122.67	37.33	41.33	40.33
	2	85		129	127	125						
	3	85		127	122	124						
ME3	1	86	149	132	130	131	133.00	130.67	132.00	16.00	18.33	17.00
	2	86		134	131	133						
	3	86		133	131	132						
TG3	1	95	154	139	136	137	144.00	141.00	143.67	10.00	13.00	10.33
	2	95		144	141	143						
	3	95		149	146	151						
MR3	1	102	162	147	145	148	143.33	141.00	143.00	18.67	21.00	19.00
	2	102		147	145	147						
	3	102		136	133	134						
MJ3	1	104	147	123	120	120	121.33	114.33	115.33	25.67	32.67	31.67
	2	104		120	106	107						
	3	104		121	117	119						
RP3	1	104	144	145	139	144	143.33	138.00	144.00	0.67	6.00	0.00
	2	104		148	143	147						
	3	104		137	132	141						
TO3	1	106	169	115	113	110	106.67	103.67	103.33	62.33	65.33	65.67
	2	106		102	99	100						
	3	106		103	99	100						

Table B3: Table showing the arm angles for the left arm from a fall height of 5 cm.

Test details			Raw data				Average data			Arm angle (from vertical axis)		
Name	Number	Mass (kg)	Extended	Initial	Release	Prior to impact	Initial	Release	Prior to impact	Initial	Release	Prior to impact
AB5	1	55	157	128	127	131	133.00	132.33	137.33	24.00	24.67	19.67
	2	55		131	131	136						
	3	55		140	139	145						
SC5	1	56	154	110	105	106	111.33	105.33	106.67	42.67	48.67	47.33
	2	56		108	100	102						
	3	56		116	111	112						
LJ5	1	57	149	142	137	132	140.00	138.33	137.33	9.00	10.67	11.67
	2	57		138	138	139						
	3	57		140	140	141						
JH5	1	59	152	105	101	115	102.50	99.00	112.00	49.50	53.00	40.00
	3	59		100	97	109						
JC5	1	63	156	145	144	147	142.33	140.33	143.67	13.67	15.67	12.33
	2	63		141	139	138						
	3	63		141	138	146						
DO5	1	63	159	89	87	95	99.67	97.67	107.67	59.33	61.33	51.33
	2	63		100	97	104						
	3	63		110	109	124						
TS5	1	64	155	136	131	140	135.33	131.33	143.00	19.67	23.67	12.00
	2	64		138	134	147						
	3	64		132	129	142						
DG5	1	65	157	101	95	98	90.50	85.50	94.00	66.50	71.50	63.00

	3	65		80	76	90						
DE5	1	66	157	124	121	136	127.67	126.00	133.33	29.33	31.00	23.67
	2	66		127	126	128						
	3	66		132	131	136						
KH5	1	66	156	126	118	118	131.33	126.67	125.67	24.67	29.33	30.33
	2	66		137	133	131						
	3	66		131	129	128						
WS5	1	66	153	123	115	113	125.33	121.33	118.67	27.67	31.67	34.33
	2	66		121	119	115						
	3	66		132	130	128						
PK5	1	68	162	123	119	124	121.67	118.00	126.33	40.33	44.00	35.67
	2	68		119	115	123						
	3	68		123	120	132						
LN5	1	68	156	114	108	119	119.67	114.33	124.33	36.33	41.67	31.67
	2	68		124	119	125						
	3	68		121	116	129						
CF5	1	73	151	121	115	125	110.33	107.00	116.33	40.67	44.00	34.67
	2	73		105	102	109						
	3	73		105	104	115						
SJ5	1	73	154	141	127	129	140.33	130.67	137.67	13.67	23.33	16.33
	2	73		139	132	139						
	3	73		141	133	145						
RM5	1	74	152	90	88	93	97.33	94.33	98.33	54.67	57.67	53.67
	2	74		98	94	98						
	3	74		104	101	104						
IS5	1	74	159	122	115	117	119.00	113.00	115.67	40.00	46.00	43.33
	2	74		127	122	123						
	3	74		108	102	107						

SE5	2	74	162	137	136	136	138.00	137.00	136.50	24.00	25.00	25.50
	3	74		139	138	137						
IP5	1	76	161	100	93	95	98.67	92.00	97.67	62.33	69.00	63.33
	2	76		101	93	100						
	3	76		95	90	98						
MB5	1	76	150	93	89	92	99.00	95.67	100.33	51.00	54.33	49.67
	2	76		101	98	100						
	3	76		103	100	109						
LT5	1	77	160	134	129	134	139.33	135.67	140.67	20.67	24.33	19.33
	2	77		143	141	139						
	3	77		141	137	149						
RIP5	1	79	154	127	119	123	133.00	128.00	127.33	21.00	26.00	26.67
	2	79		134	130	126						
	3	79		138	135	133						
TW5	1	79	158	98	92	96	119.33	113.67	117.33	38.67	44.33	40.67
	2	79		124	119	124						
	3	79		136	130	132						
RE5	1	80	157	133	115	116	135.00	123.50	126.00	22.00	33.50	31.00
	2	80		137	132	136						
GS5	1	80	140	78	74	87	92.33	87.67	100.33	47.67	52.33	39.67
	2	80		74	70	87						
	3	80		125	119	127						
KO5	1	81	170	90	88	91	87.33	86.00	90.00	82.67	84.00	80.00
	2	81		82	81	85						
	3	81		90	89	94						
MS5	1	84	152	127	121	121	121.33	117.00	122.67	30.67	35.00	29.33
	2	84		120	116	121						
	3	84		117	114	126						

DS5	1	84	165	119	116	120	110.33	106.00	111.67	54.67	59.00	53.33
	3	84		102	97	104						
	4	84		110	105	111						
TOM5	1	85	164	117	111	117	124.00	118.67	126.33	40.00	45.33	37.67
	2	85		131	126	132						
	3	85		124	119	130						
ME5	1	86	152	140	141	137	138.00	137.00	140.33	14.00	15.00	11.67
	2	86		136	134	140						
	3	86		138	136	144						
TG5	1	95	157	144	140	141	141.67	138.33	143.67	15.33	18.67	13.33
	2	95		138	134	139						
	3	95		143	141	151						
MR5	1	102	158	128	125	128	137.33	135.33	139.33	20.67	22.67	18.67
	2	102		141	140	146						
	3	102		143	141	144						
MJ5	1	104	147	125	120	121	116.67	109.67	111.00	30.33	37.33	36.00
	2	104		112	107	110						
	3	104		113	102	102						
RP5	1	104	150	149	145	148	149.00	146.00	153.00	1.00	4.00	-3.00
	2	104		149	147	155						
	3	104		149	146	156						
TO5	1	106	159	97	91	92	106.00	100.00	101.00	53.00	59.00	58.00
	2	106		111	105	105						
	3	106		110	104	106						

Table B4: Table showing the arm angles for the right arm from a fall height of 5 cm.

Test details			Raw data				Average data			Arm angle (from vertical axis)		
Name	Number	Mass (kg)	Extended	Initial	Release	Prior to impact	Initial	Release	Prior to impact	Initial	Release	Prior to impact
AB5	1	55	154.6	121	118	124	125.33	123.00	128.00	29.27	31.60	26.60
	2	55		120	118	125						
	3	55		135	133	135						
SC5	1	56	152	109	104	109	112.67	108.00	113.00	39.33	44.00	39.00
	2	56		108	103	112						
	3	56		121	117	118						
LJ5	1	57	147	139	125	120	135.67	130.33	128.33	11.33	16.67	18.67
	2	57		134	132	130						
	3	57		134	134	135						
JH5	1	59	143	102	99	107	100.50	97.50	105.00	42.50	45.50	38.00
	3	59		99	96	103						
JC5	1	63	153	141	140	140	142.33	140.67	141.67	10.67	12.33	11.33
	2	63		143	143	145						
	3	63		143	139	140						
DO5	1	63	-	99	94	99	101.33	98.67	106.67	-	-	-
	2	63		94	92	99						
	3	63		111	110	122						
TS5	1	64	151	129	121	128	131.00	126.33	133.00	20.00	24.67	18.00
	2	64		134	132	136						
	3	64		130	126	135						
DG5	1	65	156	112	104	105	107.00	99.50	105.00	49.00	56.50	51.00

	3	65		102	95	105						
DE5	1	66	160	128	121	134	131.33	126.33	132.67	28.67	33.67	27.33
	2	66		130	126	130						
	3	66		136	132	134						
KH5	1	66	153	126	120	124	131.00	127.67	129.00	22.00	25.33	24.00
	2	66		135	132	133						
	3	66		132	131	130						
WS5	1	66	149	131	127	125	136.67	134.33	132.00	12.33	14.67	17.00
	2	66		133	131	129						
	3	66		146	145	142						
PK5	1	68	160	123	120	120	122.67	119.33	122.00	37.33	40.67	38.00
	2	68		120	115	120						
	3	68		125	123	126						
LN5	1	68	152	119	112	122	123.67	117.67	123.33	28.33	34.33	28.67
	2	68		126	119	124						
	3	68		126	122	124						
CF5	1	73	147	120	113	113	113.33	105.67	108.00	33.67	41.33	39.00
	2	73		110	98	100						
	3	73		110	106	111						
SJ5	1	73	161	149	151	146	150.00	152.00	146.67	11.00	9.00	14.33
	2	73		149	151	145						
	3	73		152	154	149						
RM5	1	74	151	80	77	85	87.67	85.00	93.00	63.33	66.00	58.00
	2	74		89	87	99						
	3	74		94	91	95						
IS5	1	74	152	118	109	115	116.33	107.67	112.67	35.67	44.33	39.33
	2	74		122	113	116						
	3	74		109	101	107						

SE5	2	74	158	131	129	128	131.50	128.50	128.50	26.50	29.50	29.50
	3	74		132	128	129						
IP5	1	76	168	110	103	105	114.67	107.67	113.33	53.33	60.33	54.67
	2	76		118	110	117						
	3	76		116	110	118						
MB5	1	76	149	91	85	89	101.00	95.00	100.33	48.00	54.00	48.67
	2	76		105	99	101						
	3	76		107	101	111						
LT5	1	77	152	125	118	128	131.67	126.00	132.33	20.33	26.00	19.67
	2	77		137	132	133						
	3	77		133	128	136						
RIP5	1	79	157	138	131	132	140.33	136.67	136.67	16.67	20.33	20.33
	2	79		138	136	134						
	3	79		145	143	144						
TW5	1	79	155	95	88	101	117.00	110.33	123.33	38.00	44.67	31.67
	2	79		121	116	129						
	3	79		135	127	140						
RE5	1	80	155	138	123	124	138.00	128.50	132.50	17.00	26.50	22.50
	2	80		138	134	141						
GS5	1	80	144	90	85	96	98.33	94.33	107.00	45.67	49.67	37.00
	2	80		78	74	92						
	3	80		127	124	133						
KO5	1	81	158	83	81	85	82.67	81.67	87.67	75.33	76.33	70.33
	2	81		78	78	85						
	3	81		87	86	93						
MS5	1	84	156	142	140	139	139.00	136.33	140.67	17.00	19.67	15.33
	2	84		145	142	144						
	3	84		130	127	139						

DS5	1	84	158	113	110	116	104.67	101.33	108.00	53.33	56.67	50.00
	3	84		96	92	100						
	4	84		105	102	108						
TOM5	1	85	163	125	118	119	127.67	122.33	127.00	35.33	40.67	36.00
	2	85		131	126	131						
	3	85		127	123	131						
ME5	1	86	149	140	138	136	137.33	135.67	139.67	11.67	13.33	9.33
	2	86		134	132	140						
	3	86		138	137	143						
TG5	1	95	154	149	148	155	147.00	143.67	150.67	7.00	10.33	3.33
	2	95		144	140	144						
	3	95		148	143	153						
MR5	1	102	162	137	135	140	142.33	140.33	146.67	19.67	21.67	15.33
	2	102		146	144	150						
	3	102		144	142	150						
MJ5	1	104	147	127	124	127	119.67	116.00	118.00	27.33	31.00	29.00
	2	104		117	114	117						
	3	104		115	110	110						
RP5	1	104	144	143	137	138	144.00	139.33	144.67	0.00	4.67	-0.67
	2	104		143	139	146						
	3	104		146	142	150						
TO5	1	106	169	97	94	96	105.67	101.67	103.33	63.33	67.33	65.67
	2	106		109	105	108						
	3	106		111	106	106						

APPENDIX C

Table C1: Mann-Whitney Test - Left versus Right hand impact forces, for force peak F1, at a fall height of 3 cm.

Ranks

	HAND	N	Mean Rank	Sum of Ranks
LvR F1	1	98	107.33	10518.00
3cm	2	99	90.76	8985.00
	Total	197		

Test Statistics^a

	LvR F1 3cm
Mann-Whitney U	4035.000
Wilcoxon W	8985.000
Z	-2.039
Asymp. Sig. (2-tailed)	.041

a. Grouping Variable: HAND

Table C2: Mann-Whitney Test - Left versus Right hand impact forces, for force peak F2, at a fall height of 3 cm.

Ranks

	HAND	N	Mean Rank	Sum of Ranks
LvR F2	1	96	101.20	9715.00
3cm	2	97	92.85	9006.00
	Total	193		

Test Statistics^a

	LvR F2 3cm
Mann-Whitney U	4253.000
Wilcoxon W	9006.000
Z	-1.039
Asymp. Sig. (2-tailed)	.299

a. Grouping Variable: HAND

Table C3: Mann-Whitney Test - Left versus Right hand impact forces, for force peak F1, at a fall height of 5 cm.

Ranks

	HAND	N	Mean Rank	Sum of Ranks
LvR F1	1	98	100.61	9860.00
5cm	2	96	94.32	9055.00
	Total	194		

Test Statistics^a

	LvR F1 5cm
Mann-Whitney U	4399.000
Wilcoxon W	9055.000
Z	-.780
Asymp. Sig. (2-tailed)	.435

a. Grouping Variable: HAND

Table C4: Mann-Whitney Test - Left versus Right hand impact forces, for force peak F2, at a fall height of 5 cm.

Ranks

	HAND	N	Mean Rank	Sum of Ranks
LvR F2	1	93	94.34	8774.00
5cm	2	94	93.66	8804.00
	Total	187		

Test Statistics^a

	LvR F2 5cm
Mann-Whitney U	4339.000
Wilcoxon W	8804.000
Z	-.086
Asymp. Sig. (2-tailed)	.931

a. Grouping Variable: HAND

Table C5: Mann-Whitney Test - Force peak F1 versus F2, in females at a fall height of 3 cm.

Ranks

	GROUP	N	Mean Rank	Sum of Ranks
F3	1	31	36.65	1136.00
	2	30	25.17	755.00
	Total	61		

Test Statistics^a

	F3
Mann-Whitney U	290.000
Wilcoxon W	755.000
Z	-2.525
Asymp. Sig. (2-tailed)	.012

a. Grouping Variable: GROUP

Table C6: Mann-Whitney Test - Force peak F1 versus F3, in females at a fall height of 3 cm.

Ranks

	GROUP	N	Mean Rank	Sum of Ranks
F3	1	31	26.90	834.00
	3	17	20.12	342.00
	Total	48		

Test Statistics^a

	F3
Mann-Whitney U	189.000
Wilcoxon W	342.000
Z	-1.606
Asymp. Sig. (2-tailed)	.108

a. Grouping Variable: GROUP

Table C7: Mann-Whitney Test - Force peak F2 versus F3, in females at a fall height of 3 cm.

Ranks

	GROUP	N	Mean Rank	Sum of Ranks
F3	2	30	23.00	690.00
	3	17	25.76	438.00
	Total	47		

Test Statistics^a

	F3
Mann-Whitney U	225.000
Wilcoxon W	690.000
Z	-.664
Asymp. Sig. (2-tailed)	.507

a. Grouping Variable: GROUP

Table C8: Mann-Whitney Test - Force peak F1 versus F2, in females at a fall height of 5 cm.

Ranks

	GROUPS	N	Mean Rank	Sum of Ranks
F5	1	32	38.56	1234.00
	2	30	23.97	719.00
	Total	62		

Test Statistics^a

	F5
Mann-Whitney U	254.000
Wilcoxon W	719.000
Z	-3.183
Asymp. Sig. (2-tailed)	.001

a. Grouping Variable: GROUPS

Table C9: Mann-Whitney Test - Force peak F1 versus F3, in females at a fall height of 5 cm.

Ranks

	GROUPS	N	Mean Rank	Sum of Ranks
F5	1	32	28.53	913.00
	3	15	14.33	215.00
	Total	47		

Test Statistics^a

	F5
Mann-Whitney U	95.000
Wilcoxon W	215.000
Z	-3.309
Asymp. Sig. (2-tailed)	.001

a. Grouping Variable: GROUPS

Table C10: Mann-Whitney Test - Force peak F2 versus F3, in females at a fall height of 5 cm.

Ranks

	GROUPS	N	Mean Rank	Sum of Ranks
F5	2	30	24.87	746.00
	3	15	19.27	289.00
	Total	45		

Test Statistics^a

	F5
Mann-Whitney U	169.000
Wilcoxon W	289.000
Z	-1.348
Asymp. Sig. (2-tailed)	.178

a. Grouping Variable: GROUPS

Table C11: Mann-Whitney Test - Force peak F1 versus F2, in males at a fall height of 3 cm.

Ranks

	SGROUP	N	Mean Rank	Sum of Ranks
M3	1	67	84.93	5690.00
	2	66	48.80	3221.00
	Total	133		

Test Statistics^a

	M3
Mann-Whitney U	1010.000
Wilcoxon W	3221.000
Z	-5.405
Asymp. Sig. (2-tailed)	.000

a. Grouping Variable: SGROUP

Table C12: Mann-Whitney Test - Force peak F1 versus F3, in males at a fall height of 3 cm.

Ranks

	SGROUP	N	Mean Rank	Sum of Ranks
M3	1	67	54.96	3682.00
	3	27	29.00	783.00
	Total	94		

Test Statistics^a

	M3
Mann-Whitney U	405.000
Wilcoxon W	783.000
Z	-4.174
Asymp. Sig. (2-tailed)	.000

a. Grouping Variable: SGROUP

Table C13: Mann-Whitney Test - Force peak F2 versus F3, in males at a fall height of 3 cm.

Ranks

	SGROUP	N	Mean Rank	Sum of Ranks
M3	2	66	47.32	3123.00
	3	27	46.22	1248.00
	Total	93		

Test Statistics^a

	M3
Mann-Whitney U	870.000
Wilcoxon W	1248.000
Z	-.178
Asymp. Sig. (2-tailed)	.859

a. Grouping Variable: SGROUP

Table C14: Mann-Whitney Test - Force peak F1 versus F2, in males at a fall height of 5 cm.

Ranks

	SGROUPS	N	Mean Rank	Sum of Ranks
M5	1	64	90.45	5789.00
	2	64	38.55	2467.00
	Total	128		

Test Statistics^a

	M5
Mann-Whitney U	387.000
Wilcoxon W	2467.000
Z	-7.916
Asymp. Sig. (2-tailed)	.000

a. Grouping Variable: SGROUPS

Table C15: Mann-Whitney Test - Force peak F1 versus F3, in males at a fall height of 5 cm.

Ranks

	SGROUPS	N	Mean Rank	Sum of Ranks
M5	1	64	49.25	3152.00
	3	18	13.94	251.00
	Total	82		

Test Statistics^a

	M5
Mann-Whitney U	80.000
Wilcoxon W	251.000
Z	-5.557
Asymp. Sig. (2-tailed)	.000

a. Grouping Variable: SGROUPS

Table C16: Mann-Whitney Test - Force peak F2 versus F3, in males at a fall height of 5 cm.

Ranks

	SGROUPS	N	Mean Rank	Sum of Ranks
M5	2	64	43.31	2772.00
	3	18	35.06	631.00
	Total	82		

Test Statistics^a

	M5
Mann-Whitney U	460.000
Wilcoxon W	631.000
Z	-1.300
Asymp. Sig. (2-tailed)	.194

a. Grouping Variable: SGROUPS

Table C17: Mann-Whitney Test - Female versus Male impact forces, for force peak F1, at a fall height of 3 cm.

Ranks				
	GROUP	N	Mean Rank	Sum of Ranks
GF1THREE	1	31	27.11	840.50
	2	67	59.86	4010.50
	Total	98		

Test Statistics ^a	
	GF1THREE
Mann-Whitney U	344.500
Wilcoxon W	840.500
Z	-5.302
Asymp. Sig. (2-tailed)	.000

a. Grouping Variable: GROUP

Table C18: Mann-Whitney Test - Female versus Male impact forces, for force peak F2, at a fall height of 3 cm.

Ranks				
	GROUPS	N	Mean Rank	Sum of Ranks
GF2THREE	1	30	30.50	915.00
	2	66	56.68	3741.00
	Total	96		

Test Statistics ^a	
	GF2THREE
Mann-Whitney U	450.000
Wilcoxon W	915.000
Z	-4.268
Asymp. Sig. (2-tailed)	.000

a. Grouping Variable: GROUPS

Table C19: Mann-Whitney Test - Female versus Male impact forces, for force peak F1, at a fall height of 5 cm.

Ranks				
	SGROUP	N	Mean Rank	Sum of Ranks
GF1FIVE	1	32	25.50	816.00
	2	64	60.00	3840.00
	Total	96		

Test Statistics ^a	
	GF1FIVE
Mann-Whitney U	288.000
Wilcoxon W	816.000
Z	-5.720
Asymp. Sig. (2-tailed)	.000

a. Grouping Variable: SGROUP

Table C20: Mann-Whitney Test - Female versus Male impact forces, for force peak F2, at a fall height of 5 cm.

Ranks				
	SGROUPS	N	Mean Rank	Sum of Ranks
GF2FIVE	1	30	29.40	882.00
	2	64	55.98	3583.00
	Total	94		

Test Statistics ^a	
	GF2FIVE
Mann-Whitney U	417.000
Wilcoxon W	882.000
Z	-4.404
Asymp. Sig. (2-tailed)	.000

a. Grouping Variable: SGROUPS

Table C21: Mann-Whitney Test – Fall height of 3 cm versus 5 cm impact forces,
for force peak F1, for females

Ranks			
	SGROUP	N	Sum of Ranks
FF1	1	31	810.00
	2	32	1206.00
	Total	63	

Test Statistics ^a	
	FF1
Mann-Whitney U	314.000
Wilcoxon W	810.000
Z	-2.502
Asymp. Sig. (2-tailed)	.012

a. Grouping Variable: SGROUP

Table C22: Mann-Whitney Test – Fall height of 3 cm versus 5 cm impact forces,
for force peak F2, for females

Ranks			
	SGROUPS	N	Sum of Ranks
FF2	1	30	790.00
	2	30	1040.00
	Total	60	

Test Statistics ^a	
	FF2
Mann-Whitney U	325.000
Wilcoxon W	790.000
Z	-1.848
Asymp. Sig. (2-tailed)	.065

a. Grouping Variable: SGROUPS

Table C23: Mann-Whitney Test – Fall height of 3 cm versus 5 cm impact forces,
for force peak F1, for males

Ranks				
	GROUP	N	Mean Rank	Sum of Ranks
MF1	1	67	49.03	3285.00
	2	64	83.77	5361.00
	Total	131		

Test Statistics ^a	
	MF1
Mann-Whitney U	1007.000
Wilcoxon W	3285.000
Z	-5.235
Asymp. Sig. (2-tailed)	.000

a. Grouping Variable: GROUP

Table C24: Mann-Whitney Test – Fall height of 3 cm versus 5 cm impact forces,
for force peak F2, for males

Ranks				
	GROUPS	N	Mean Rank	Sum of Ranks
MF2	1	66	57.55	3798.00
	2	64	73.70	4717.00
	Total	130		

Test Statistics ^a	
	MF2
Mann-Whitney U	1587.000
Wilcoxon W	3798.000
Z	-2.445
Asymp. Sig. (2-tailed)	.014

a. Grouping Variable: GROUPS

Table C25: Mann-Whitney Test - Low versus high female effective mass impact forces, for force peak F1, at a fall height of 3 cm.

Ranks

	GROUP	N	Mean Rank	Sum of Ranks
F3CM1	1	14	16.86	236.00
	2	17	15.29	260.00
	Total	31		

Test Statistics^b

	F3CM1
Mann-Whitney U	107.000
Wilcoxon W	260.000
Z	-.476
Asymp. Sig. (2-tailed)	.634
Exact Sig. [2*(1-tailed Sig.)]	.653 ^a

a. Not corrected for ties.

b. Grouping Variable: GROUP

Table C26: Mann-Whitney Test - Low versus high female effective mass impact forces, for force peak F2, at a fall height of 3 cm.

Ranks

	GROUPS	N	Mean Rank	Sum of Ranks
F3CM2	1	14	14.93	209.00
	2	16	16.00	256.00
	Total	30		

Test Statistics^b

	F3CM2
Mann-Whitney U	104.000
Wilcoxon W	209.000
Z	-.333
Asymp. Sig. (2-tailed)	.739
Exact Sig. [2*(1-tailed Sig.)]	.759 ^a

a. Not corrected for ties.

b. Grouping Variable: GROUPS

Table C27: Mann-Whitney Test - Low versus high female effective mass impact forces, for force peak F1, at a fall height of 5 cm.

Ranks				
	SGROUP	N	Mean Rank	Sum of Ranks
F5CM1	1	14	14.14	198.00
	2	18	18.33	330.00
	Total	32		

Test Statistics ^b	
	F5CM1
Mann-Whitney U	93.000
Wilcoxon W	198.000
Z	-1.254
Asymp. Sig. (2-tailed)	.210
Exact Sig. [2*(1-tailed Sig.)]	.220 ^a

a. Not corrected for ties.

b. Grouping Variable: SGROUP

Table C28: Mann-Whitney Test - Low versus high female effective mass impact forces, for force peak F2, at a fall height of 5 cm.

Ranks				
	SGROUPS	N	Mean Rank	Sum of Ranks
F5CM2	1	11	14.73	162.00
	2	18	15.17	273.00
	Total	29		

Test Statistics ^b	
	F5CM2
Mann-Whitney U	96.000
Wilcoxon W	162.000
Z	-.135
Asymp. Sig. (2-tailed)	.893
Exact Sig. [2*(1-tailed Sig.)]	.912 ^a

a. Not corrected for ties.

b. Grouping Variable: SGROUPS

Table C29: Mann-Whitney Test - Low versus high male effective mass impact forces, for force peak F1, at a fall height of 3 cm.

	GROUP	N	Mean Rank	Sum of Ranks
M3CM1	1	36	28.64	1031.00
	2	31	40.23	1247.00
	Total	67		

	M3CM1
Mann-Whitney U	365.000
Wilcoxon W	1031.000
Z	-2.427
Asymp. Sig. (2-tailed)	.015

a. Grouping Variable: GROUP

Table C30: Mann-Whitney Test - Low versus high male effective mass impact forces, for force peak F2, at a fall height of 3 cm.

	GROUPS	N	Mean Rank	Sum of Ranks
M3CM2	1	36	27.31	983.00
	2	30	40.93	1228.00
	Total	66		

	M3CM2
Mann-Whitney U	317.000
Wilcoxon W	983.000
Z	-2.872
Asymp. Sig. (2-tailed)	.004

a. Grouping Variable: GROUPS

Table C31: Mann-Whitney Test - Low versus high male effective mass impact forces, for force peak F1, at a fall height of 5 cm.

Ranks				
	SGROUP	N	Mean Rank	Sum of Ranks
M5CM1	1	32	28.06	898.00
	2	32	36.94	1182.00
	Total	64		

Test Statistics ^a	
	M5CM1
Mann-Whitney U	370.000
Wilcoxon W	898.000
Z	-1.907
Asymp. Sig. (2-tailed)	.057

a. Grouping Variable: SGROUP

Table C32: Mann-Whitney Test - Low versus high male effective mass impact forces, for force peak F2, at a fall height of 5 cm.

Ranks				
	SGROUPS	N	Mean Rank	Sum of Ranks
M5CM2	1	32	26.09	835.00
	2	32	38.91	1245.00
	Total	64		

Test Statistics ^a	
	M5CM2
Mann-Whitney U	307.000
Wilcoxon W	835.000
Z	-2.753
Asymp. Sig. (2-tailed)	.006

a. Grouping Variable: SGROUPS

Table C33: Mann-Whitney Test - Older versus Younger female volunteer impact forces, for force peak F1, at a fall height of 3 cm.

Ranks				
	AGE	N	Mean Rank	Sum of Ranks
FORCEF	1	14	17.36	243.00
	2	17	14.88	253.00
	Total	31		

Test Statistics ^b	
	FORCEF
Mann-Whitney U	100.000
Wilcoxon W	253.000
Z	-.754
Asymp. Sig. (2-tailed)	.451
Exact Sig. [2*(1-tailed Sig.)]	.468 ^a

a. Not corrected for ties.

b. Grouping Variable: AGE

Table C34: Mann-Whitney Test - Older versus Younger female volunteer impact forces, for force peak F2, at a fall height of 3 cm.

Ranks				
	AGES	N	Mean Rank	Sum of Ranks
FORCES	1	13	14.69	191.00
	2	17	16.12	274.00
	Total	30		

Test Statistics ^b	
	FORCES
Mann-Whitney U	100.000
Wilcoxon W	191.000
Z	-.439
Asymp. Sig. (2-tailed)	.660
Exact Sig. [2*(1-tailed Sig.)]	.680 ^a

a. Not corrected for ties.

b. Grouping Variable: AGES

Table C35: Mann-Whitney Test - Older versus Younger female volunteer impact forces, for force peak F1, at a fall height of 5 cm.

Ranks				
	SAGE	N	Mean Rank	Sum of Ranks
FORCEHF	1	14	18.00	252.00
	2	18	15.33	276.00
	Total	32		

Test Statistics ^b	
	FORCEHF
Mann-Whitney U	105.000
Wilcoxon W	276.000
Z	-.798
Asymp. Sig. (2-tailed)	.425
Exact Sig. [2*(1-tailed Sig.)]	.442 ^a

a. Not corrected for ties.

b. Grouping Variable: SAGE

Table C36: Mann-Whitney Test - Older versus Younger female volunteer impact forces, for force peak F2, at a fall height of 5 cm.

Ranks				
	SAGES	N	Mean Rank	Sum of Ranks
FORCEHS	1	14	15.93	223.00
	2	16	15.13	242.00
	Total	30		

Test Statistics ^b	
	FORCEHS
Mann-Whitney U	106.000
Wilcoxon W	242.000
Z	-.249
Asymp. Sig. (2-tailed)	.803
Exact Sig. [2*(1-tailed Sig.)]	.822 ^a

a. Not corrected for ties.

b. Grouping Variable: SAGES

Table C37: Mann-Whitney Test - Older versus Younger male volunteer impact forces, for force peak F1, at a fall height of 3 cm.

	AGE	N	Mean Rank	Sum of Ranks
FORCEF	1	33	37.48	1237.00
	2	34	30.62	1041.00
	Total	67		

	FORCEF
Mann-Whitney U	446.000
Wilcoxon W	1041.000
Z	-1.442
Asymp. Sig. (2-tailed)	.149

a. Grouping Variable: AGE

Table C38: Mann-Whitney Test - Older versus Younger male volunteer impact forces, for force peak F2, at a fall height of 3 cm.

	AGES	N	Mean Rank	Sum of Ranks
FORCES	1	33	37.36	1233.00
	2	33	29.64	978.00
	Total	66		

	FORCES
Mann-Whitney U	417.000
Wilcoxon W	978.000
Z	-1.635
Asymp. Sig. (2-tailed)	.102

a. Grouping Variable: AGES

Table C39: Mann-Whitney Test - Older versus Younger male volunteer impact forces, for force peak F1, at a fall height of 5 cm.

Ranks				
	SAGE	N	Mean Rank	Sum of Ranks
FORCEHF	1	30	39.83	1195.00
	2	34	26.03	885.00
	Total	64		

Test Statistics ^a	
	FORCEHF
Mann-Whitney U	290.000
Wilcoxon W	885.000
Z	-2.960
Asymp. Sig. (2-tailed)	.003

a. Grouping Variable: SAGE

Table C40: Mann-Whitney Test - Older versus Younger male volunteer impact forces, for force peak F2, at a fall height of 5 cm.

Ranks				
	SAGES	N	Mean Rank	Sum of Ranks
FORCEHS	1	30	38.07	1142.00
	2	34	27.59	938.00
	Total	64		

Test Statistics ^a	
	FORCEHS
Mann-Whitney U	343.000
Wilcoxon W	938.000
Z	-2.247
Asymp. Sig. (2-tailed)	.025

a. Grouping Variable: SAGES

Table C41: Mann-Whitney Test - Force plate versus Domestic surface impact forces, for force peak F1, for females.

Ranks			
GROUP	N	Mean Rank	Sum of Ranks
FSUR1 1	32	31.56	1010.00
2	32	33.44	1070.00
Total	64		

Test Statistics ^a	
	FSUR1
Mann-Whitney U	482.000
Wilcoxon W	1010.000
Z	-.403
Asymp. Sig. (2-tailed)	.687

a. Grouping Variable: GROUP

Table C42: Mann-Whitney Test - Force plate versus Playground surface impact forces, for force peak F1, for females.

Ranks			
GROUP	N	Mean Rank	Sum of Ranks
FSUR1 1	32	35.09	1123.00
3	31	28.81	893.00
Total	63		

Test Statistics ^a	
	FSUR1
Mann-Whitney U	397.000
Wilcoxon W	893.000
Z	-1.361
Asymp. Sig. (2-tailed)	.173

a. Grouping Variable: GROUP

Table C43: Mann-Whitney Test - Domestic surface versus Playground surface impact forces, for force peak F1, for females.

Ranks

	GROUP	N	Mean Rank	Sum of Ranks
FSUR1	2	32	37.94	1214.00
	3	31	25.87	802.00
	Total	63		

Test Statistics^a

	FSUR1
Mann-Whitney U	306.000
Wilcoxon W	802.000
Z	-2.612
Asymp. Sig. (2-tailed)	.009

a. Grouping Variable: GROUP

Table C44: Mann-Whitney Test - Force plate versus Domestic surface impact forces, for force peak F2, for females.

Ranks

	GROUPS	N	Mean Rank	Sum of Ranks
FSUR2	1	30	32.13	964.00
	2	32	30.91	989.00
	Total	62		

Test Statistics^a

	FSUR2
Mann-Whitney U	461.000
Wilcoxon W	989.000
Z	-.268
Asymp. Sig. (2-tailed)	.789

a. Grouping Variable: GROUPS

Table C45: Mann-Whitney Test - Force plate versus Playground surface impact forces, for force peak F2, for females.

Ranks

	GROUPS	N	Mean Rank	Sum of Ranks
FSUR2	1	30	29.73	892.00
	3	31	32.23	999.00
	Total	61		

Test Statistics^a

	FSUR2
Mann-Whitney U	427.000
Wilcoxon W	892.000
Z	-.548
Asymp. Sig. (2-tailed)	.584

a. Grouping Variable: GROUPS

Table C46: Mann-Whitney Test - Domestic surface versus Playground surface impact forces for force peak F2, for females.

Ranks

	GROUPS	N	Mean Rank	Sum of Ranks
FSUR2	2	32	30.69	982.00
	3	31	33.35	1034.00
	Total	63		

Test Statistics^a

	FSUR2
Mann-Whitney U	454.000
Wilcoxon W	982.000
Z	-.577
Asymp. Sig. (2-tailed)	.564

a. Grouping Variable: GROUPS

Table C47: Mann-Whitney Test - Force plate versus Domestic surface impact forces, for force peak F1, for males.

Ranks				
	SGROUP	N	Mean Rank	Sum of Ranks
MSUR1	1	64	76.81	4916.00
	2	66	54.53	3599.00
	Total	130		

Test Statistics ^a	
	MSUR1
Mann-Whitney U	1388.000
Wilcoxon W	3599.000
Z	-3.372
Asymp. Sig. (2-tailed)	.001

a. Grouping Variable: SGROUP

Table C48: Mann-Whitney Test - Force plate versus Playground surface impact forces, for force peak F1, for males.

Ranks				
	SGROUP	N	Mean Rank	Sum of Ranks
MSUR1	1	64	80.33	5141.00
	3	69	54.64	3770.00
	Total	133		

Test Statistics ^a	
	MSUR1
Mann-Whitney U	1355.000
Wilcoxon W	3770.000
Z	-3.841
Asymp. Sig. (2-tailed)	.000

a. Grouping Variable: SGROUP

Table C49: Mann-Whitney Test - Domestic surface versus Playground surface impact forces for force peak F1, for males.

Ranks				
	SGROUP	N	Mean Rank	Sum of Ranks
MSUR1	2	66	70.56	4657.00
	3	69	65.55	4523.00
	Total	135		

Test Statistics ^a	
	MSUR1
Mann-Whitney U	2108.000
Wilcoxon W	4523.000
Z	-.744
Asymp. Sig. (2-tailed)	.457

a. Grouping Variable: SGROUP

Table C50: Mann-Whitney Test - Force plate versus Domestic surface impact forces, for force peak F2, for males.

Ranks				
	SGROUPS	N	Mean Rank	Sum of Ranks
MSUR2	1	64	68.86	4407.00
	2	66	62.24	4108.00
	Total	130		

Test Statistics ^a	
	MSUR2
Mann-Whitney U	1897.000
Wilcoxon W	4108.000
Z	-1.001
Asymp. Sig. (2-tailed)	.317

a. Grouping Variable: SGROUPS

Table C51: Mann-Whitney Test - Force plate versus Playground surface impact forces, for force peak F2, for males.

	SGROUPS	N	Mean Rank	Sum of Ranks
MSUR2	1	64	66.65	4265.50
	3	69	67.33	4645.50
	Total	133		

	MSUR2
Mann-Whitney U	2185.500
Wilcoxon W	4265.500
Z	-.101
Asymp. Sig. (2-tailed)	.919

a. Grouping Variable: SGROUPS

Table C52: Mann-Whitney Test - Domestic surface versus Playground surface impact forces for force peak F2, for males.

	SGROUPS	N	Mean Rank	Sum of Ranks
MSUR2	2	66	64.44	4253.00
	3	69	71.41	4927.00
	Total	135		

	MSUR2
Mann-Whitney U	2042.000
Wilcoxon W	4253.000
Z	-1.034
Asymp. Sig. (2-tailed)	.301

a. Grouping Variable: SGROUPS

Table C53: Mann-Whitney Test - Time duration of force peak F1, fall height of 3 cm versus 5 cm, for females.

Ranks

	GROUP	N	Mean Rank	Sum of Ranks
FEMALE	1	32	35.95	1150.50
	2	32	29.05	929.50
	Total	64		

Test Statistics^a

	FEMALE
Mann-Whitney U	401.500
Wilcoxon W	929.500
Z	-1.485
Asymp. Sig. (2-tailed)	.138

a. Grouping Variable: GROUP

Table C54: Mann-Whitney Test - Time duration of force peak F1, force plate versus Domestic surface, at a fall height of 5 cm, for females.

Ranks

	GROUP	N	Mean Rank	Sum of Ranks
FEMALE	2	32	25.64	820.50
	3	31	38.56	1195.50
	Total	63		

Test Statistics^a

	FEMALE
Mann-Whitney U	292.500
Wilcoxon W	820.500
Z	-2.801
Asymp. Sig. (2-tailed)	.005

a. Grouping Variable: GROUP

Table C55: Mann-Whitney Test - Time duration of force peak F1,
force plate versus Playground surface, at a fall height of 5 cm, for females.

Ranks				
	GROUP	N	Mean Rank	Sum of Ranks
FEMALE	2	32	35.55	1137.50
	4	32	29.45	942.50
	Total	64		

Test Statistics ^a	
	FEMALE
Mann-Whitney U	414.500
Wilcoxon W	942.500
Z	-1.310
Asymp. Sig. (2-tailed)	.190

a. Grouping Variable: GROUP

Table C56: Mann-Whitney Test - Time duration of force peak F1,
Domestic surface versus Playground surface, at a fall height of 5 cm, for females.

Ranks				
	GROUP	N	Mean Rank	Sum of Ranks
FEMALE	3	31	40.68	1261.00
	4	32	23.59	755.00
	Total	63		

Test Statistics ^a	
	FEMALE
Mann-Whitney U	227.000
Wilcoxon W	755.000
Z	-3.700
Asymp. Sig. (2-tailed)	.000

a. Grouping Variable: GROUP

Table C57: Mann-Whitney Test - Time duration of force peak F1, fall height of 3 cm versus 5 cm, for males.

Ranks

	GROUPS	N	Mean Rank	Sum of Ranks
MALE	1	70	77.04	5392.50
	2	68	61.74	4198.50
	Total	138		

Test Statistics^a

	MALE
Mann-Whitney U	1852.500
Wilcoxon W	4198.500
Z	-2.249
Asymp. Sig. (2-tailed)	.025

a. Grouping Variable: GROUPS

Table C58: Mann-Whitney Test - Time duration of force peak F1, Force plate versus Domestic surface, at a fall height of 5 cm, for males.

Ranks

	GROUPS	N	Mean Rank	Sum of Ranks
MALE	2	68	46.18	3140.00
	3	69	91.49	6313.00
	Total	137		

Test Statistics^a

	MALE
Mann-Whitney U	794.000
Wilcoxon W	3140.000
Z	-6.685
Asymp. Sig. (2-tailed)	.000

a. Grouping Variable: GROUPS

Table C59: Mann-Whitney Test - Time duration of force peak F1,
Force plate versus Playground surface, at a fall height of 5 cm, for males.

Ranks				
	GROUPS	N	Mean Rank	Sum of Ranks
MALE	2	68	62.23	4231.50
	4	66	72.93	4813.50
	Total	134		

Test Statistics ^a	
	MALE
Mann-Whitney U	1885.500
Wilcoxon W	4231.500
Z	-1.596
Asymp. Sig. (2-tailed)	.110

a. Grouping Variable: GROUPS

Table C60: Mann-Whitney Test - Time duration of force peak F1,
Domestic surface versus Playground surface, at a fall height of 5 cm, for males.

Ranks				
	GROUPS	N	Mean Rank	Sum of Ranks
MALE	3	69	84.13	5805.00
	4	66	51.14	3375.00
	Total	135		

Test Statistics ^a	
	MALE
Mann-Whitney U	1164.000
Wilcoxon W	3375.000
Z	-4.901
Asymp. Sig. (2-tailed)	.000

a. Grouping Variable: GROUPS

APPENDIX D

Tables showing victims of home and leisure accidents.

Involving falls and fractures to lower arm:radius/ulna, 1996-2002

Data taken from a sample of 16-18 UK hospitals.

The National Estimates are for the UK, based on the sample figures.

Table D1: HASS/LASS 0-15 years

AGE:	0 < 5	0 < 5	5 < 10	5 < 10	10 < 15	10 < 15
YEAR:	FEMALE	MALE	FEMALE	MALE	FEMALE	MALE
1996	145	177	335	345	225	395
1997	166	218	331	389	267	446
1998	159	186	313	321	216	371
1999	199	187	369	437	284	469
2000	186	234	409	465	294	516
2001	192	196	382	461	309	541
2002	172	201	319	416	272	523

Table D2: HASS/LASS 15-30 years

AGE:	15 < 20	15 < 20	20 < 25	20 < 25	25 < 30	25 < 30
YEAR:	FEMALE	MALE	FEMALE	MALE	FEMALE	MALE
1996	38	105	24	34	35	37
1997	44	112	26	41	33	49
1998	36	123	28	35	28	30
1999	47	107	34	40	35	36
2000	49	132	25	49	33	37
2001	39	129	34	40	27	47
2002	38	145	37	48	40	37

Table D3: HASS/LASS 30-45 years

AGE:	30 < 35	30 < 35	35 < 40	35 < 40	40 < 45	40 < 45
YEAR:	FEMALE	MALE	FEMALE	MALE	FEMALE	MALE
1996	23	38	27	28	30	14
1997	42	45	37	27	35	16
1998	29	36	24	27	31	24
1999	35	34	32	36	45	27
2000	44	45	40	37	40	42
2001	34	28	42	36	43	31
2002	41	54	44	42	38	28

Table D4: HASS/LASS 45-60 years

AGE:	45 < 50	45 < 50	50 < 55	50 < 55	55 < 60	55 < 60
YEAR:	FEMALE	MALE	FEMALE	MALE	FEMALE	MALE
1996	26	16	50	18	65	21
1997	29	26	47	17	48	19
1998	14	22	41	21	44	20
1999	35	27	57	24	73	17
2000	48	32	70	32	73	27
2001	29	34	69	27	60	20
2002	40	19	53	25	73	22

Table D5: HASS/LASS 60-75 years

AGE:	60 < 65	60 < 65	65 < 70	65 < 70	70 < 75	70 < 75
YEAR:	FEMALE	MALE	FEMALE	MALE	FEMALE	MALE
1996	55	20	69	10	70	22
1997	75	13	64	14	91	12
1998	71	15	65	22	96	12
1999	91	18	90	21	108	17
2000	92	23	115	21	124	26
2001	83	20	89	22	121	12
2002	75	29	107	18	128	22

Table D6: HASS/LASS 75-90 years

AGE:	75 < 80	75 < 80	80 < 85	80 < 85	85 < 90	85 < 90
YEAR:	FEMALE	MALE	FEMALE	MALE	FEMALE	MALE
1996	68	15	73	15	39	8
1997	75	19	67	7	42	4
1998	101	12	64	10	45	5
1999	109	21	63	11	55	10
2000	133	26	106	20	66	9
2001	153	23	121	15	86	9
2002	128	23	118	5	76	6

Table D7: HASS/LASS 90-100 years and total and national estimates

AGE:	90 < 95	90 < 95	95 < 100	95 < 100	TOTALS	NATIONAL ESTIMATES
YEAR:	FEMALE	MALE	FEMALE	MALE		
1996	19	1	9	0	1,622	31,159
1997	26	1	8	0	1,817	35,813
1998	28	6	7	3	1,566	30,584
1999	36	3	10	1	1,945	35,574
2000	27	12	9	0	2,104	37,325
2001	38	5	10	1	2,081	37,146
2002	38	5	4	0	1,903	39,012

APPENDIX E

CD containing examples of high-speed video files. These files will play on any computer that has Windows Media Player installed.

Files:

1cm.avi

5cm.avi

10cm.avi

20cm.avi

standing.avi

kneeling.avi

